UNIVERSITY OF GENOVA

Polytechnic School

Doctoral Program in Science and Technology for Electronic and Telecommunication Engineering (XXXII cycle)

Distributed Sensing and Stimulation Systems Towards Sense of Touch Restoration in Prosthetics

Hoda Fares

***

Supervisor: Prof. Maurizio Valle

A thesis submitted for the degree of
Doctor of Philosophy

February 2020

Acknowledgments

This thesis, like any other work I have attempted in my life, wouldn't have been possible without the sustenance of certain people around me. It is my genuine intent to acknowledge their efforts and contributions through my journey to earn my Ph.D. which has been an indeed life-changing experience.

My sincerest thanks are directed to Prof. Maurizio Valle, Prof. Strahinja Dosen, Prof. Ali Ibrahim, and Prof. Lucia Seminara for all the guidance and encouragement I received from their side at every step of the way. Their refined advice and the echo of their words sketched a well-lit path leading the way to substantial achievements and successes for me as an individual and for the team as a whole.

I hand my appreciation to my colleagues for their assistance whether through teamwork to bring the best of us in a professional environment or through the nurture of new friendships on the personal level. Their presence added a tasteful joy to this experience.

Furthermore, one cannot but recognize the support I received from the University of Genova in Italy and the University of Aalborg in Denmark. Their staff showed the highest level of dedication to foster a positive working environment for me and my colleagues.

My ultimate and deepest gratitude goes to my family and friends, without whom I wouldn't have made it this far. Their unconditional care proved to have the most influential role not only through my Ph.D. journey but rather through my whole life. I am indebted to forever cherish all their endeavors to back me up through the downs and rejoice with me through the ups.

Paint me grateful for all your contributions. You have enriched my soul.

Hoda Fares

Abstract

Modern prostheses aim at restoring the functional and aesthetic characteristics of the lost limb. To foster prosthesis embodiment and functionality, it is necessary to restitute both volitional control and sensory feedback. Contemporary feedback interfaces presented in research use few sensors and stimulation units to feedback at most two discrete feedback variables (e.g. grasping force and aperture), whereas the human sense of touch relies on a distributed network of mechanoreceptors providing high-fidelity spatial information. To provide this type of feedback in prosthetics, it is necessary to sense tactile information from artificial skin placed on the prosthesis and transmit tactile feedback above the amputation in order to map the interaction between the prosthesis and the environment. This thesis proposes the integration of distributed sensing systems (e-skin) to acquire tactile sensation, and non-invasive multichannel electrotactile feedback and virtual reality to deliver high-bandwidth information to the user. Its core focus addresses the development and testing of close-loop sensory feedback human-machine interface, based on the latest distributed sensing and stimulation techniques for restoring the sense of touch in prosthetics. To this end, the thesis is comprised of two introductory chapters that describe the state of art in the field, the objectives and the used methodology and contributions; as well as three studies distributed over stimulation system level and sensing system level.

The first study presents the development of a close-loop compensatory tracking system to evaluate the usability and effectiveness of electrotactile sensory feedback in enabling real-time closed-loop control in prosthetics. It examines and compares the subject's adaptive performance and tolerance to random latencies while performing the dynamic control task (i.e. position control) and simultaneously receiving either visual feedback or electrotactile feedback for communicating the momentary tracking error. Moreover, it reported the minimum time delay needed for an abrupt impairment of users' performance. The experimental results have shown that electrotactile feedback performance is less prone to changes with longer delays. However, visual feedback drops faster than electrotactile with increased time delays. This is a good indication for the effectiveness of electrotactile feedback in enabling closed-loop control in prosthetics since some delays are inevitable.

The second study describes the development of a novel non-invasive compact multichannel interface for electrotactile feedback, containing 24 pads electrode matrix, with a fully programmable stimulation unit, that investigates the ability of able-bodied human subjects to localize the electrotactile stimulus delivered through the electrode matrix. Furthermore, it designed a novel dual parameter -modulation (interleaved frequency and intensity) and compared it to conventional stimulation (same frequency for all pads). In addition and for the first time, it compared the electrotactile stimulation to mechanical stimulation. More, it exposes the integration of virtual prosthesis with the developed system in order to achieve better user experience and object manipulation through mapping the acquired real-time collected tactile data and feedback it simultaneously to the user. The experimental results demonstrated that the proposed interleaved coding substantially improved the spatial localization compared to same-frequency stimulation. Furthermore, it showed that testing subjects using same-frequency stimulation (i.e. conventional stimulation at 50Hz) was equivalent to mechanical stimulation, whereas the performance with dual-parameter modulation (i.e. proposed interleaved stimulation at 10 Hz and 400Hz) was significantly better.

The third study presents the realization of a novel, flexible, screen- printed e-skin based on P(VDF-TrFE) piezoelectric polymers, that would cover the fingertips and the palm of the prosthetic hand (particularly the Michelangelo hand by Ottobock) and an assistive sensorized glove for stroke patients. Moreover, it developed a new validation methodology to examine the sensors' behavior while being solicited. The characterization results showed compatibility between the expected (modeled) behavior of the electrical response of each sensor to measured mechanical (normal) force at the skin surface, which in turn proved the combination of both fabrication and assembly processes was successful. This paves the way to define a practical, simplified and reproducible characterization protocol for e-skin patches

In conclusion, by adopting innovative methodologies in sensing and stimulation systems, this thesis advances the overall development of closed-loop sensory feedback human-machine interface used for the restoration of sense of touch in prosthetics. Moreover, this research could lead to high-bandwidth high-fidelity transmission of tactile information for modern dexterous prostheses that could ameliorate the end-user experience and facilitate its acceptance in daily life.

Keywords: *Closed-Loop Control, Sensory Feedback, Sensory Substitution, Electronic Skin, Sense of Touch, Distributed Tactile Sensing, Electrotactile Feedback, Distributed Non-Invasive Electrotactile Stimulation, Myoelectric Prosthetics, Screen Printed Sensory Arrays.*

Contents

Acknowledgements ..... **ii**

Abstract ..... **iii**

Contents ..... **v**

List of Figures ..... **viii**

List of Tables ..... **xiii**

Chapter 1 Introduction **14**

1.1 Motivation for going beyond state of art 19

1.2 Principle contributions 19

1.2.1 At the stimulation interface level 19

1.2.2 At the tactile sensing system level 21

1.3 Thesis Outline 22

Chapter 2 Somatosensory Feedback Restoration in Prosthetics **25**

2.1 Introduction 25

2.2 Background 25

2.2.1 State of Art on Prosthetics 25

2.2.2 Human – Machine Interface in Myoelectric Prostheses 27

2.2.3 Invasive Sensory Feedback Systems 37

2.2.4 Non-Invasive Sensory Feedback Systems 40

2.3 Distributed Simulation Interface 45

2.4 Conclusion 48

Chapter 3 Compensatory Tracking Delay Tractability in Close-Loop Dynamic Task based on Visual and Electrotactile Feedback **50**

3.1 Introduction 50

3.2 Methods 53

3.2.1 Modeling Human Operator in the Closed – Control System (CLS) 53

3.2.2 Compensatory Tracking Close – Loop System 54

3.2.3 Participants 56

3.2.4 Study Design 57

3.2.5 Experimental Setup 59

3.3 Experimental Procedure 60

3.4 Data Analysis 64

3.5 Results Summary 66
3.6 Discussion 68
3.7 Conclusion 68
Chapter 4 Multichannel Electrotactile Stimulation System for Restoration of Sensory Information 69
4.1 Introduction 69
4.2 Materials and Methods 71
4.2.1 Simulation Setup 71
4.2.2 Participants 74
4.2.3 Study Design 75
4.2.4 Subject Preparation and Electrode Mounting 76
4.3 Experimental Procedure 77
4.3.1 Testing Protocol 78
4.4 Data Analysis 83
4.5 Results 84
4.6 Discussion 86
4.7 On the use of virtual prosthesis in the sensory feedback interface system 91
4.7.1 System description 92
4.7.2 Mapping Protocol and stimulation patterns 94
4.8 Conclusion 96
Chapter 5 Artificial Tactile Sensing and E-Skins In Prosthetics 97
5.1 Introduction 97
5.2 Sense of Touch 98
5.3 Physiology of the Human Skin 99
5.4 Artificial Skins: Concept and Evolution 101
5.5 E-Skin System 105
5.5.1 Tactile Sensing Systems 106
5.5.2 Embedded Electronic System 112
5.6 Conclusion 116
Chapter 6 Screen – Printed Electronic Skin Based on Piezoelectric Polymer Sensors 118
6.1 Introduction 118
6.2 Materials and Methods 120
6.2.1 Electronic Skin Design and Technology 120
6.2.2 Experimental setup 126
6.2.3 Reference skin structure and model 128
6.3 Results 132
6.3.1 Morphology of the Sensing Patches: Issues 132

6.3.2 Experimental tests 134
6.3.3 Data Analysis 137
6.4 Discussion 148
6.5 Conclusion 151
Chapter 7 Outlook and Futurework 154
7.1 At the Stimulation System 155
7.2 At the sensing System 157
References 159
Appendix A - Case Report 170
Appendix B - Information Notes To The Participant 180
Appendix C - Curriculum Vitae 188

List of Figures

Figure 1.1 The control feedforward loop and the sensory feedback loop in the myoelectric prosthetics 16

Figure 1.2 Proposed Sensory feedback system for restoring the sense of touch in prosthetic hands using electrotactile stimulation..... 18

Figure 2.1 Overview of different types of prostheses: (a) Transradial cosmetic prosthesis (b) Body-powered prosthesis with the harness (c) Commercially available myoelectric prostheses: Left: RSL Steeper Bebionic , middle: Multi-finger articulated i-limb ultra (Touch Bionics Inc., UK), Right: Michelangelo Hand with an active wrist and two-grip patterns (Otto Bock HealthCare GmbH, Germany). 26

Figure 2.2 Existing sensory feedback loops while using non-invasive stimulation interfaces 28

Figure 2.3 The control feedforward loop and the sensory feedback loop 29

Figure 2.4 Comparisons among different control strategies used with myoelectric prosthesis. From top to bottom: (a) on/off control (one electrode used to provide binary control), (b) proportional control (two electrodes used for opposite actions), and (c) pattern recognition control (multi-channel electrodes used, the signals are classified into different movement patterns and given in a sequential decisions as control output), (d) regression control (the extracted information extracted from the EMG signals are mapped into continuous kinematics and used as control signals for the prosthesis)..... 30

Figure 2.5 Summary of the most clinically advanced myoelectric approaches classification (pattern recognition) regression algorithms, and hybrid systems. Recent post-processing steps have provided classification systems means for proportional and simultaneous control, which is directly generated by regression-based systems. Sensory fusion and computer vision have also been combined with these approaches to improve their performance [reprinted]..... 31

Figure 2.6 General architecture for providing sensory feedback. The input stage, namely sensing transduction, converts physical stimuli (sensory inputs) from one form of energy (typically mechanical) to another form of energy (converted inputs, typically electrical) that is more appropriate for processing. Then, a decoding algorithm identifies important sensory events/states (e.g., contact or angular position of a joint), and an encoding algorithm transforms them into output signals that can be interpreted by the CNS as if they were a substitute of the sensory input. The output stage – that is, actuating transduction – converts the output signals into the appropriate form of energy to be applied on body sensory systems (output stimuli) either invasively or noninvasively (reprinted from [2])..... 33

Figure 2.7 Possible pathways for feedback information to prosthesis. Different colors correspond to different pathways (A, B, C). Pathway A is related to sensory information that is directly fed back to the CNS (e.g., visual and auditory feedback); Pathway B to the information that is conveyed to functional sensory motor systems invasively or noninvasively; Pathway C is related to the intrinsic feedback. Image adapted from [2]. 35

Figure 2.8 Block diagram for sensory feedback methods 36

Figure 2.9 Targeted re innervation (source Ottobock courtesy)..... 38

Figure 2.10 Peripheral nerve stimulation (source 77), Different illustrations of different approaches to restore the sense of touch through PNS interfaces.(A) Regenerative electrodes. B) Extra-fascicular electrodes. C) Intra-fascicular electrodes. D) Dorsal root ganglion implant and E) Targeted sensory reinnervation)..... 39

Figure 2.11 Central nervous system (CNS) stimulation: a) Close loop of somatosensory neuroprosthesis (source brian lee 2018), b) source Bensmaia 2015 40

Figure 2.12 Mechanotactile stimulation examples: a) Pressure feedback cuff (source [8]) b) Silicon Bulb Mechanical Feedback and Mechanical Pressure Feedback device (source [8]) 41

Figure 2.13 Examples of vibrators used in vibrotactile feedback. (source [8]) 42

Figure 2.14 Examples of electrotactile feedback. source [8] and [13]..... 43

Figure 3.1 The general structure of the closed loop system. 53

Figure 3.2 Illustration of manual – control task (compensatory tracking task). Left: the controller uses the joystick to compensate the error which the difference between the target and the controlled trajectory, Right: The black box represents the PC screen, two graphical indicators, the red is fixed and the green is the controlled, the error is the distance between the two indicators..... 54

Figure 3.3 Block diagram of the one-dimensional compensatory tracking system 54

Figure 3.4 Illustration of the frequency response. Top: the amplitude ratio, Bottom: the phase shift. The position control or zero-order control is represented for (a) Controlled process, (b) Human operator and (c) the close-loop system..... 56

Figure 3.5 Compensatory tracking experimental setup with in-set latency in a closed loop system with either electrotactile feedback or visual feedback. The reference trajectory is r(t), y(t) is the generated trajectory, e(t) is the tracking error and u(t) is the control signal. The error was transmitted either using visual feedback or electrical feedback. The stimulator provided electrotactile stimulation through the electrodes placed in the forearm, while the monitor display provided the visual feedback. The joystick acts as controller and it transmits the commands to compensate the tracking error. 58

Figure 3.6 Experimental setup elements and electrode mounting for electrotactile stimulation 59

Figure 3.7 Summed-sine forcing function. We used nine sine waves, each with a different phase 61

Figure 3.8 Block diagram of the experimental setup. Depending on the testing scenario, the subjects were provided either by visual feedback displayed on the monitor in front of them or by electrotactile feedback delivered via two electrodes mounted on the dominant hand in which the subject is controlling the joystick. The visual feedback consisted of a green rhombus displaying the tracking error. It moved on the horizontal axis in a defined range. The red circle is placed at the zero point to clearly indicate the area where the green rhombus should optimally be (i.e. where the tracking error is smaller than 5%). The electrotactile feedback consisted of two electrodes placed on the dorsal and volar sides of the forearm to track both positive and negative tracking error respectively. 62

Figure 3.9 Subject performing the compensatory tracking with electrotactile feedback: a) during the training phase with hybrid feedback (i.e. while receiving both visual and electrotactile at the same time), b) during the testing phase only with electrotactile feedback (no visual feedback at all)..... 64

Figure 3.10 Testing protocol summary..... 65

Figure 3.11 Two exemplary representative performance at time delay t= 0sec of one subject. The blue dashed line and the solid red line represents the reference trajectory and the generated trajectory respectively. a) Top: Compensatory tracking with visual feedback (CORR=91.45, RMSE = 0.2), b) Compensatory tracking with electrotactile feedback (CORR= 91, RMSE=0.24) 66

Figure 3.12 The overall average correlation across the subjects for different in-set latency time delays (t1 =0 sec, t2 =0.2 sec, t3 =0.4 sec, t4 = 0.8 sec and t5 =1.2 sec). The red line represents the compensation using electrotactile feedback and the blue line represents the compensation using visual feedback. 67

Figure 3.13 The overall average RMSE across the subjects for different introduced time delays (t1 =0 sec, t2 =0.2 sec, t3 =0.4 sec, t4 = 0.8 sec and t5 =1.2 sec). The red line represents the compensation using electrotactile feedback and the blue line represents the compensation using visual feedback. 67

Figure 4.1 Testing setup of the stimulator and generated waveform. a) Block diagram of the testing setup, b) Real photo of the issued signals from the stimulator, c) Typical stimulation waveform. Notation: A – pulse amplitude; w – pulse width; d – inter-pulse delay; T – inter-pulse interval (pulse rate = frequency = 1/T). 72

Figure 4.2 Testing chain of the stimulator 73

Figure 4.3 Experimental Stimulation setup: a) The indenter is used for mechanical stimulation, while all other elements are used for electrotactile stimulation experiments, b) illustration of the electrode matrix with dimensions. 74

Figure 4.4 Electrode mounting. The reference position for electrode matrix is indicated by a black dot, it corresponds to the intersection between two superficial flexors, i.e. the palmaris longus and the flexor carpi ulnaris muscles. Reference pad for that position is number 22. 77

Figure 4.5 Testing phases: a) Phase 0, Phase 1: subject preparation and intensity adjustment, The spatial correspondence between the matrix electrode and the geometrical arrangement of the pads in the sketch is preserved, Right: Relaxation arm position b) Left : phase 2: Training , Right: Electrostimulation tests: a sketch of the matrix electrode (4 columns, 6 rows) is placed on the table next to the forearm. 81

Figure 4.6 Experiments with mechanical stimulation. A screen is placed between the participant's forearm and the sketch of the matrix electrode. (b) Top view. (b) Side view. 82

Figure 4.7 Testing Protocol 82

Figure 4.8 The results for individual subjects (P1-P8). Reported percentages are associated to identifying the right pad (light blue), missing the pad but addressing the right column (orange), missing the pad and the column (grey), no answer (yellow). 84

Figure 4.9 The summary results for all subjects (Sample size n = tested subjects = 8) Bars and stars indicated statistical significance (*, $p<0.05$, **, $p<0.01$, ***, $p<0.001$). The bars show the success rates (mean ± standard deviation) : a) in identifying the right pad ,b) pointing to the right pad or first neighbors (F.N.) within the same column , c) pointing to the right pad or any pad belonging to the same column , d) and pointing to the right pad or any of its first neighbors, regardless of the column 86

Figure 4.10 Success rates for the identification of each pad. The scheme reported in (a) illustrates the orientation of the matrix electrode with respect to the forearm. 87

Figure 4.11 Block Diagram of the virtual reality simulation system and the electrotactile stimulation feedback system. The Virtual prosthesis simulated on the Laptop PC is controlled through a graphical interface developed in MAT LAB. The tactile Feedback resulting from

different object manipulations with the virtual prosthesis is presented to the user in the form of electrotactile stimulation provided by the IntFES-ver2 stimulator. 93

Figure 4.12 MLP Sensor configuration of the virtual prosthesis 94

Figure 4.13 Implemented Grasp classification to retrieve tactile sensory information and mapped to the user through the stimulation interface 95

Figure 4.14 Stimulation Map from tactile simulated sensors to stimulation active pads .The color tactile feedback map from the simulated touch sensors prosthesis (18 touch sensors) into the flexible stimulation electrode (24 pads). 95

Figure 5.1 Schematic illustration of the distribution and classification of the mechanoreceptors in the human skin. 100

Figure 5.2 The time life for evolution of tactile e-skin 104

Figure 5.3 Application scenario for restoring the sense of touch in prosthetics 105

Figure 5.4 Illustration of the E-skin general structure 106

Figure 5.5 Functional block diagram for the embedded electronic system. 1st route: Raw Tactile Data, 2nd route: Classification, 3rd route: Extracting general contact Features, 4th route: Classification based on feature extraction 113

Figure 6.1 Illustration of fabrication process flow of printed ferroelectric sensor arrays based on P(VDF-TrFE) repeated units (reprinted with permission from JNR). 122

Figure 6.2 (a) Cross sectional view of a single sensor unit: sketch with indicative thicknesses of various layers, (b) Reprinted microscopic photo of the sensing element Sketch of the sensing patch, (c) Sketch of the sensing patch, & (d) Picture of a real sample 123

Figure 6.3 Design of Different Sensing Patches. (a) Sample A-Palm right 2 - 4x2 array = 8 taxels, Taxel diameter = 2mm, center-to-center pitch = 1 cm, total sensing area = 2.1 x 1.1 cm2. (b) Sample B- Palm left 2 – 4x2 array = 8 taxels, Taxel diameter = 2mm, pitch = 1.1 cm, total sensing area = 2.1 x 1.1 cm2. (c) Sample C-Michelangelo palm -12 taxels, taxel diameter = 2mm. (d) Sample E- Michelangelo little -4 taxels, taxel diameter = 1mm, total sensing area: square side =1.1 cm (e) Sample D- Palm right 1 – two 4x2 arrays -16 taxels, Taxel diameter = 2mm, center-to-center pitch =0.9cm, total sensing area = 0.9 x 2.7 cm2. 125

Figure 6.4 Experimental setup. Top: Block Diagram, Bottom: Pictures of the setup. The blue dotted line shows the alignment of the testing elements. 127

Figure 6.5 The applied coupling scenario 128

Figure 6.6 Sketch of the general working mechanism of the (PVDF-TrFE) sensor. The Hertzian input force (with contact radius a) is transmitted to the sensor (with radius rT) through the elastomer layer of thickness h. With the presupposition that the sensor works solely in compressive mode, it directly converts the received normal stress T3 into electrical displacement D3, through a characterizing piezoelectric coefficient, namely the d33 (1). A charge amplifier is used to convert the total sensor charge into voltage. 129

Figure 6.7 Results for the numerical COMSOL simulations for the finite case. The proportionality coefficient σ between average normal stress on the sensor and overall (Hertzian) contact force F3 (2) is plotted versus the imprint radius a (contact size) scaled by the elastomer thickness h. Note that the applied force is centered on the sensor. The two curves are associated to two different sensor sizes: = 1mm (sensors on the palm), = 0.5mm (sensors on the fingertip) 131

Figure 6.8 (a) Normal sensor, (b) Fault in the sensor top electrode (pole), (c) Cut in the sensor tracks, due to short circuits during the poling procedure, (d) Shortcuts between sensor tracks. 133

Figure 6.9 The heat map of the deposition substrate (DIN A3) prone to shrinkage .. 134

Figure 6.10 Example of the frequency behavior of both the real and imaginary part of the d33 piezoelectric coefficient. The scale for the Im (d33) (= d'') is on the right y-axis..... 136

Figure 6.11 Compared categories (CAT1, CAT2, CAT3, and CAT 4) and heat map on the A3 fabrication substrate. 137

Figure 6.12 (a) Cloud distribution of working palm sensors .(b) Statistical study: one way balanced anova, average d33 vs. preload 138

Figure 6.13 Average d33 vs Preload () for four different categories: (a) Category 1 (palm left 2). (b) Category 2 (palm right 2). (c) Category 3 (palm right 1). (d) Category 4 (Michelangelo palm). One-way anova has been applied for statistical analysis 140

Figure 6.14 Average d33 vs patches at PL=1N, 2N, and 3N arranged respectively as (a), (b) and (c). The four categories and all corresponding patches can be distinguished on the x-axis. 142

Figure 6.15 Average d33 vs preload. Sensors belonging to categories 1 and 4, only. To avoid dot superposition, values associated with the same preload are plotted such that dots do not lie on the same vertical line 144

Figure 6.16 Average d33 for each sensor at PL=1N (top), 2N (middle), 3N (bottom)145

Figure 6.17 Average d33 vs preload for the three analyzed patches belonging to category 1: Palm left 2.2. (top), Palm left 2.3 (middle), Palm left 2.4 (bottom). 146

Figure 6.18 Average d33 vs preload for the two samples of Michelangelo little: ML.1 and ML.2. Statistical study: unbalanced one-Way ANOVA. 148

Figure 6.19 Sensor electrodes have been severely damaged after coupling with adhesive tape all over the skin patch. 150

List of Tables

Table 2.1 Summary of available sensory feedback systems 45

Table 2.2 Comparison between main sensory substitution feedback methods 46

Table 3.1 Basic Participants Characteristics 57

Table 3.2 Study Design Overview 58

Table 4.1 Basic Participants Characteristics 75

Table 4.2 Study Design Overview 75

Table 5.1 Characteristics of different tactile sensors used for e-skin fabrication 110

Table 5.2 Design requirements for tactile sensing system in prosthetics 111

Table 6.1 Palm patches categories (Data set 1, palm sensors) 138

Table 6.2 Statistical Study variables (Data set 1, palm sensors) 139

Table 6.3 Statistical Study variables: a) CAT 1 (palm left 2), b) Category 2 (palm right 2), c) Category 3 (palm right 1), and d) Category 4 (Michelangelo palm) 140

Table 6.4 Statistical Study variables for all patches tested at three different preloads 143

Table 6.5 Statistical Study variables 147

Table 6.6 Statistical Study variables 148

Table 6.7 Illustration of Different coupling methods 151

Chapter 1 Introduction

Losing an upper limb is devastating as person's hands are their tools for daily interaction, expressive communication, and environment exploration. Every year in Europe there is around 50 to 270 newly recorded upper limb amputations, with an estimated population of approximately 1900 with traumatic amputation and around 9400 with complete upper-limb loss. This loss can significantly reduce the quality of life of an amputee, leaving him/her less capable and more dependent. Upper limb prosthesis could be used as a substitute for the missing limb to reproduce the body appearance and the hand capabilities for amputees [1][2].

An ideal prosthetic hand should deliver the functionality of grasp or manipulation; nonetheless, it should also provide tactile sensation to explore surrounding objects in human-centered environments. However, the current prosthetic systems (i.e. components and interfaces) are still a long way from realizing this goal and few could provide efficient tactile feedback to the users. There has been an impressive development of prosthesis technology during the last decades, yet the rejection rates of hand prostheses are still relatively high (between 19% and 35%) and the users still think of it to be a tool rather than a limb replacement. According to a survey done in 2013, amputees indicated that the two critical elements that would optimize the functional recovery are 1) enhanced intuitive motor control and 2) ability to feel their prosthesis [3].

Currently, the majority of prosthetic hands merely focus on improving the mechanical structure and control strategies to obtain better performance, while in the other flip none of it (i.e. commercial or research hands) could ensure comprehensive feedback. Taking top commercial myoelectric hands such as Bebionic by steeper [4] and Michelangelo hand by OttoBock [5], and i-limb Ultra-revolution by Ossur [6], enable users to perform basic daily tasks, yet none of them could provide tactile information without visual feedback. Apart, only VINCENT evolution 3, has a stimulation system for tactile feedback, the grasping force applied by the prosthesis is translated into vibration levels using a single vibration motor [7] and still, no reports confirmed its effectiveness. Clinically wise, SensorHand (OttoBock) contains a three-

dimensional force sensor, which measures the shear force to automatically change the grip force to prevent slipping of grasped objects.

Providing sensory feedback to prosthesis allows the users to "feel" his/her bionic limb. The feedback might reinforce the user's motor control during dexterous activities such as manipulation and grasping, and decrease the cognitive load. Moreover, it could increase the acceptance rates of prosthetics. Furthermore, it can facilitate prosthesis incorporation in the body schema and may yield a better psychological experience that in turn elevates the sense of embodiment and reduces phantom limb pain [8][9].

Myoelectric prostheses are controlled by recording electrical muscle activity (i.e. EMG electromyography signals) from the residual limb of the amputee to decode his/her movement intentions Therefore, they can be used in the restoration of lost motor functions after hand amputation. Nevertheless, this restoration is only partial with the absence of tactile sensation feedback [10]. Myoelectric prostheses users perceive sensory information from the prosthesis, they can feel motor vibrations from the socket, and they get proprioceptive information from the muscles used for myoelectric control [11]. Such incidental feedback may be inadequate, and it is a great challenge to implement sensory feedback in prosthesis [9].

A major limitation in upper limb prosthetics is the poor information transfer from the user to the prosthesis (control) and vice-versa (sensory feedback). Recently, several research groups are working on providing natural sensations to hand prostheses via invasive feedback stimulation interfaces such as direct electrical stimulation to the peripheral nervous system (PNS), central nervous system (CNS) at the motor cortex and spinal cord. However, some users might not be willing to undergo the risks associated with surgical intervention and therefore, they might prefer non-invasive stimulation feedback methods [8][9]. The most common non-invasive methods employed to elicit sensory feedback in prosthetics are sensory substitutions methods that rely on vibrotactile, mechanotactile, electrotactile stimulation, etc [2]. In addition to the stimulation interfaces that are used to deliver tactile information, there is an extensive focus in the literature on developing tactile sensing systems in order to detect and measure sensory signals of contact location, object properties such as texture, stiffness, and temperature through touch. This is conventionally performed by integrating tactile sensors such as force, pressure, temperature sensors or artificial skins (i.e. e-skin) to the fingertips or palm of prosthetic hands [12]. Nevertheless, few examples of distributed sensing systems have been used in human-machine interfacing for prosthetics [13].

Achieving closed-loop control in prosthetics requires a dynamic interplay between motor output and sensory input [14] [15] [16]. Figure 1.1 illustrates both the sensory feedback and the feedforward control loops for the myoelectric prosthesis. The restoration and implementation of sensory feedback is a long-standing challenge [17]. To this aim, the information from prosthesis sensors is transmitted to the user by stimulating the skin of the residual limb using electro, vibro, or mechano-tactile stimuli to activate the tactile sense. There have been many investigations on the nature of these artificial sensory methods yet all of the developed systems have been limited by a small information transfer bandwidth. The human sense of touch relies on a dense network of mechanoreceptors to provide spatially distributed information (e.g., pressure distribution). To provide high-resolution tactile information mimicking the human sense of touch, this information first needs to be measured by adequate artificial systems integrating a high-density network of sensing units. Typically, a single stimulation unit is used to convey a prosthesis variable, which is often the grasping force. In some cases, multichannel interfaces have been used to encode up to two discrete variables (e.g., grasping force and aperture) [18].

For transmitting the tactile information to the user, the spatial distribution of sensed forces should be mapped into a homologous spatial distribution of tactile stimulators that provide sensation to the user. While distributed sensing system technologies are now mature in

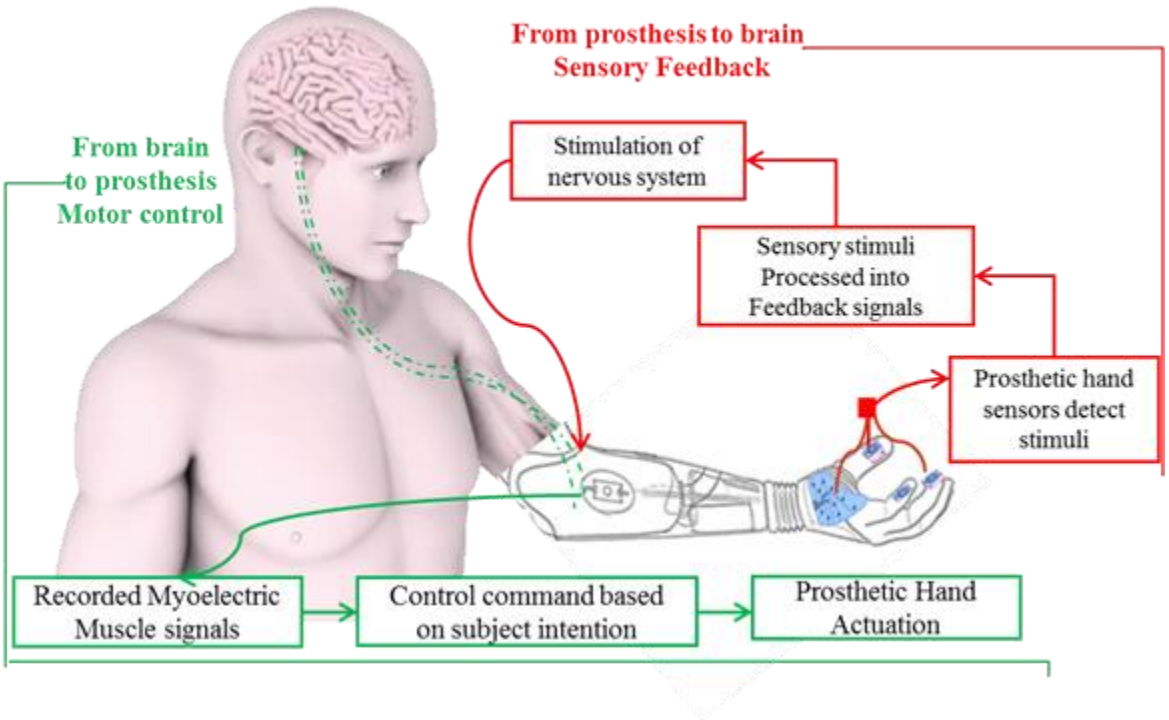

Figure 1.1 The control feedforward loop and the sensory feedback loop in the myoelectric prosthetics

the autonomous robotic domain, only a few examples of these systems integrated into man-machine interfacing for prosthetics have been reported [19][20][21].

In this context, looking to fill the addressed gap between the control loop (i.e. information transfer from the user to the prosthesis) and the sensory feedback (i.e. information transfer from the prosthesis to the user). Our collaborates and we - the Cosmic lab group at University of Genova- Italy (http://www.cosmiclab.diten.unige.it/) have been working on developing a closed-loop sensory feedback interface system that would restore the sense of touch to the prosthetic users. The proposed system would comprise:

1) An electronic skin (e-skin) based on dense piezoelectric sensory arrays (taxels) to mimic the tactile receptors and cover the prosthesis.

2) An embedded electronic system integrating signal conditioning, data acquisition, and tactile data processing inside the prosthesis pocket.

3) A non-invasive electrotactile based stimulation system to transmit and translate the captured information into feedback signals through electrode matrices attached to the residual limb and encapsulated within the prosthetic socket.

Figure 1.2 presents a close-up image of the proposed system for the restoration of sensory feedback in prosthetics.

Primarily, a bench prototype e-skin based on Piezoelectric polymer films of Polyvinylidene Fluoride (PVDF) has been used to measure sensing information, which meets the requirements of mechanical flexibility, high sensitivity, detectability of dynamic contact events, wide dynamics (light/strong touch), low cost, lightweight and robustness. In a consecutive realization, an e-skin based on screen-printing technologies has been used for ad-hoc e-skin design, optimizing taxel size and sensor pitch according to application requirements. Moreover, a protective layer based on PDMS elastomer layer has been integrated on top for stress transmission and sensor protection. This late realization of the screen-printed e-skin and characterization is considered one of the basic corners of this thesis's achievements and contributions.

Secondary, the embedded electronic system that has to acquire the tactile data, process and extract structured information, a dedicated real-time hardware implementation of tactile data processing algorithms have been studied. The first studies have highlighted that

special attention must be given to the features of this system, such as power consumption, complexity, and delay. The requirements related to the development of embedded data processing units for e-skin are still far from being achieved. Therefore, new methods and techniques to reduce hardware complexity and power consumption of the embedded electronic system have been investigated.

Thirdly, the electrotactile stimulation delivering low-level electrical current pulses to the skin to depolarize skin afferents, thereby eliciting tactile sensations has been studied and tested. Several methods have been developed to interpret tactile data in real-time and retrieve touch information such as contact location area, and duration and to efficiently deliver artificial tactile information (recorded by artificial skin) to the prosthesis user through multichannel electrocutaneous stimulation. The realization of novel methods to decode and transmit high-fidelity tactile data to the users through testing the effectiveness of the novel multichannel electrotactile stimulation system. Moreover, the verification of the feasibility of using sensory – substitution techniques (i.e. comparison between electrotactile feedback vs. visual feedback) has been the second and third side corners in the triangle of achievements and contributions of this thesis.

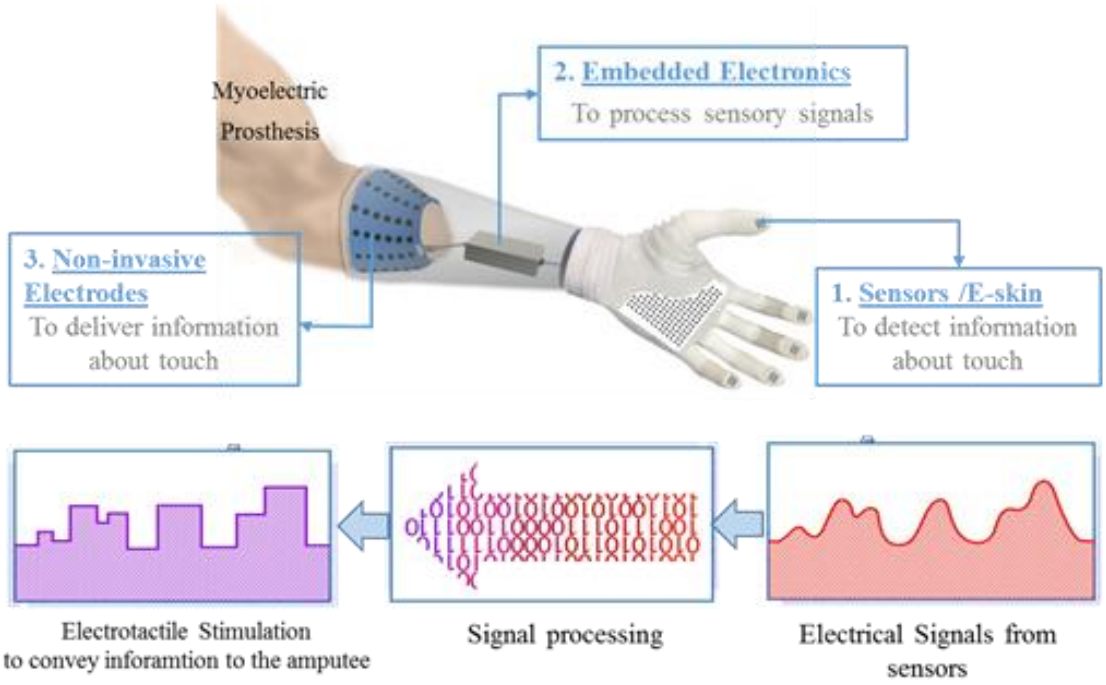

Figure 1.2 Proposed Sensory feedback system for restoring the sense of touch in prosthetic hands using electrotactile stimulation

1.1 Motivation for going beyond the state of art

With the advancement of the technologies for high-density tactile sensing and electrotactile stimulation, the salient goal of providing comprehensive feedback from the prosthesis to the user becomes reachable. Remarkable research efforts had been done, however, it still required addressing the challenges. Our pivotal goal is a prosthetic system covered with a dense network of tactile sensors to restore the feeling of touch over the whole surface of the prosthesis (whole hand and maybe even a forearm/socket). Such a prosthesis would provide a completely new experience to an amputee, improving utility and facilitating the feeling of embodiment to the level that is far beyond the conventional systems based on discrete sensing and stimulation.

The main objective of this thesis is developing a closed-loop sensory feedback interface that would restore the sense of touch in prosthetics, using a piezoelectric polymer sensory arrays acting as artificial skin system to measure tactile information and an electrotactile stimulation system to convey the acquired tactile information to the prosthetic users (amputees). This thesis proposed the idea of embedding artificial distributed tactile sensing and stimulation systems in prosthetic to provide high-fidelity, high-bandwidth tactile feedback to the prosthesis users. This idea has been established on one hand by developing artificial tactile sensing arrays (e-skin) for prosthetics that mimic human skin features and test its reliability and efficient functionality. On the other hand, by developing optimized methods/tools (such as coding, parameter modulation, electrode configuration) for the transmission of sensory feedback acquired from the artificial skin through non-invasive multichannel electrotactile stimulation and test its effectiveness on promoting the embodiment and utility of the prosthetic system.

1.2 Principle contributions

Within the addressed project of our group, the following thesis merely focuses on the tactile feedback system, and its principal contributions fall into two main parts of the application: the sensing system and the stimulation interface.

1.2.1 At the stimulation interface level

Two studies were conducted aiming to prove the feasibility of our proposed approach in providing high-bandwidth tactile information through distributed simulation interfaces. The

former study was conducted at the AAU University of Aalborg – Denmark, while the latter study was conducted at the University of Genova-Italy.

- **Study 1:** Compensatory tracking delay tractability in Close –loop dynamic task based on visual and electrotactile feedback

    i. Development of a compensatory tracking close-loop control system in order to prove the usability of electrotactile feedback through assessing the tractable time delay and the responsive ability of subjects while receiving electrotactile feedback.

    ii. Investigation and Comparison of the performance quality of human manual control through close loop compensatory tracking system while providing two feedback schemes (i.e. visual and electrotactile feedback).

    iii. Designing the experimental setup, experimental protocol and developing the software to test the subjects' tolerance for different time delays while performing a compensatory dynamic control task.

    iv. Designing and running pilot tests and an experimental camping on 14 healthy subjects.

    v. Data management and analysis.

- **Study 2:** Dual-parameter modulation improves localization in multichannel electrotactile stimulation.

    i. Development of a novel non-invasive interface for multichannel electrotactile feedback, comprising a matrix of 24 fields (6 x 4) and then assess the feasibility of this stimulation interface to convey information to the prosthetic use.

    ii. Investigation and comparison of three stimulation schemes that implement different modulation of stimulation parameters, conventional stimulation (uniform frequency modulation), dual parameter stimulation (frequency and intensity modulation) and mechanical stimulation.

iii. Designing the experimental setup, experimental protocol and developing the software to evaluate the ability of able-bodied human subject's identification rate to localize the electrotactile stimulus delivered through the matrix.

iv. Designing and running pilot tests and experimental camping on 10 healthy subjects.

v. Data management and analysis.

vi. Integration of Virtual Reality with the developed multichannel electrotactile feedback stimulation system.

1.2.2 At the tactile sensing system level

In the follow-up procedure of realizing a novel PVDF based screen-printed e-skin that could mimic the human skin properties. Study 3 was conducted to validate the functionality of the novel designed and fabricated screen-printed sensory arrays that would cover the fingertips and the palm of the prosthetic hand (specifically the Michelangelo hand by Ottobock) and the ongoing developed assistive sensorized glove for stroke patients.

- **Study 3:** Validation of screen-printed e-skin based on piezoelectric polymer sensors

  i. Developing and designing a testing methodology to validate the functionality of the novel screen-printed tactile sensory arrays while being embedded into an elastic protective layer and working in thickness mode.

  ii. Optimization of the experimental setup system, mapping

  iii. Testing and characterizing two batches designed for fingerprints and hand palm, through examining the charge response in time and frequency domains to various applied preloads.

  iv. Experimental testing with conditioner and electronic interface.

  v. Data management and analysis.

1.3 Thesis Outline

The thesis contains six chapters spread into two parts. The first three chapters deal with the stimulation system, while the next two chapters lie in the sensing system.

Chapter 2 presents a broad nature review of recent advancements in the myoelectric prosthesis. Then, it introduces the concept of closed-loop human-machine interface in prosthetics and its elements. The feedforward control techniques are presented shortly, and then the variant systems and techniques for restoring somatosensory feedback in prosthetics are described with an intensive focus on the non-invasive sensory feedback interfaces. Afterward, an inter-comparison between sensory- substitution techniques has been presented, addressing their features, advantages, and disadvantages. Moreover, it explains the need for sensory and why it is a key element in upper limb prosthetics. Finally, it introduces the motivation of our approach of using non-invasive electrotactile distributed stimulation interfaces to deliver high bandwidth tactile information and to obtain comprehensive feedback.

Chapter 3 addresses the first study about compensatory tracking delay tractability in a closed-loop dynamic task that has been conducted in the AAU university- Aalborg Denmark. This chapter demonstrates the usability of electrotactile feedback in enabling closed-loop control in prosthetics. It presents an assessment and evaluation of the subject's tolerance for different in-set latencies while performing a dynamic control task. More specifically, it compares the performance quality of human manual control through a closed-loop compensatory tracking system while using two sensory feedback schemes (i.e. visual vs. electrotactile feedback). This, in turn, reflects the tractable and responsive ability of electrotactile feedback in closed-loop control- feedback control. Moreover, it examines the adaptive behavior of the subjects "human operators" to different timing latencies when electrotactile and/ or visual sensory feedback is provided. A description of the methods, study design, experimental setup, procedure, and testing protocol is presented, along with summarized results and discussion.

Chapter 4 presents the second conducted study, which assesses the reliability of information transmission while using non-invasive interfaces (i.e. electrotactile stimulation) with many stimulation points or what called distributed stimulation interfaces. A novel non-invasive interface for multichannel electrotactile feedback, comprising a matrix of 24 pads is presented. Moreover, a novel dual-parameter modulation (intensity and frequency) is developed and tested to assist the subject identification rates in correctly identifying an active stimulation pad within

the matrix. Additionally, it demonstrates the improvement of the quality of localization by exploiting parameter modulation flexibility provided by the electrotactile interface. Furthermore, and for the first time, the performance of a distributed electrotactile interface is compared to that of the natural skin being mechanically stimulated over analogous contact areas. Moreover, the chapter discusses and presents the integration of virtual reality with the developed multichannel electrotractile system aiming at achieving a real-time mapping of tactile information captured from the virtual prostheses to the user for better user experience.

Chapter 5 introduces the system approach for an artificial skin implementation in prosthetics. It starts with the explanation of why the human skin plays an important role in the human life and why researchers are trying to reproduce an artificial skin, an overview of the human sense of touch and of the physiology of human skin, and then the concept and the evolution of the artificial skins are introduced. Then, It provided a literature study about the main compartments of the e-skin system (i.e. tactile sensing, interface electronic and the embedded electronic system) starting from the state of art and how to get inspired of what have been implemented on the robotic field, to pave the way of achieving an e-skin compatible to prosthetics application requirements.

Chapter 6 presents the third study conducted in the tactile sensing part. It presents the validation of the recently developed fully screen-printed tactile sensing arrays based on P(VDF-TrFE) piezoelectric polymers for prosthetic applications. Two sets of tactile e-skin patches have been designed and fabricated to be mounted on the fingertips and the palm of Michelangelo prosthetic Hand by Ottobock and assistive sensorized glove for stroke patients. Moreover, this chapter describes the experimental setup and procedures used for the characterization of sensors behavior while being embedded by the protective layer. Moreover, several coupling scenarios developed which lead to a new methodology of testing e-skin patches (i.e. validation protocol for e-skin). Finally, the results, discussion, and conclusive remarks are provided.

Chapter 7 summarizes the thesis in a general outlook. It discusses the impact of the results and methods used in this thesis that would pave the way for the restoration of sense of touch in prosthetics. Finally, recommendations and future work are reported.

Chapter 2 Somatosensory Feedback Restoration in Prosthetics

2.1 Introduction

Prosthetics have made significant progress to enable tetraplegic patients or amputees to restore some of the original body functions and appearance thus reintegrate effectively in the society. Providing sensory feedback to enable closed-loop control in the prosthesis, is necessary to develop a prosthetic system that not only responds to the control signals but also transmits information about the current state of the system back to the user. This chapter presents a brief survey on the state of art myoelectric prostheses. It introduces the concept of closed-loop human-machine interface in prosthetics and its elements. The feedforward control techniques are presented shortly, and then the variant systems and techniques for restoring somatosensory feedback in prosthetics are described with an intensive focus on the non-invasive sensory feedback systems. Moreover, it explains the need for sensory and why it is a key element in upper limb prosthetics. Finally, it provides the motivation of our approach of using non-invasive electrotactile distributed stimulation interfaces to deliver high bandwidth tactile information and to obtain comprehensive feedback.

2.2 Background

This section gives a general outlook on the available myoelectric prostheses in the state of art. Moreover, it explains the human-machine interfaces in prostheses and the closed-loop control and somatosensory loop.

2.2.1 State of Art on Prosthetics

Losing a limb loss can significantly reduce the quality of life of an amputee, leaving him/her feeling less capable and more dependent. However, with technological advances, it has

become possible to create more articulated and controllable prostheses that could restore the appearance and functions of the missing limb. Upper limb prostheses broadly divided into two main categories: passive and active prostheses as shown in Figure. 2.1. The passive prostheses or so-called cosmetic prostheses usually designed for aesthetical reasons and have a high natural appearance. Despite their limited equipment that does not allow the amputee to control it actively, they can still provide some functionality by holding objects and thereby supporting the remaining hand. The advantages of passive prostheses are their lightweight and easy maintenance.

Active prostheses consist of two main sections body-powered and externally powered prostheses. They consist of a socket, which connects the residual stump to the prosthesis and a terminal device. Depending on the amputation, the prosthesis includes one or more joints [22].

The body-powered prosthesis is directly controlled by the amputee (i.e. body activation). It enables functional hand movements that are controlled by voluntary movements of the shoulder and stump muscles. The amputee wears a harness with cables that are connected to the elbow or terminal device. Since the harness is relatively tight, specific movements of the shoulder change the tension on each of the one to three cables that control different parts of the prosthesis. Thereby, the amputee can for example open or close the terminal device. In relation to the

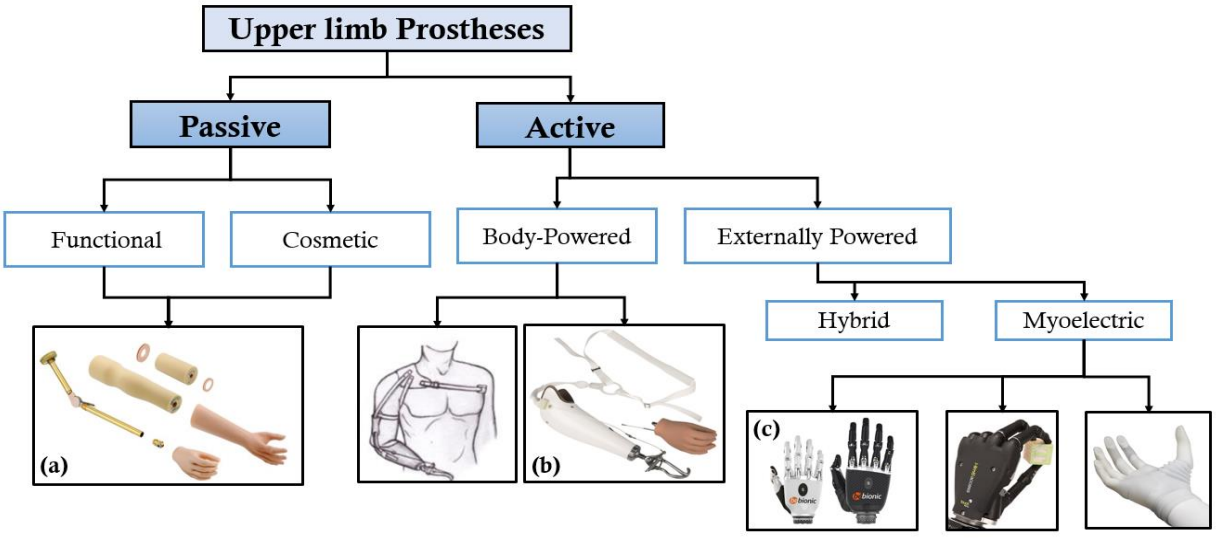

Figure 2.1 Overview of different types of prostheses: (a) Transradial cosmetic prosthesis (b) Body-powered prosthesis with the harness (c) Commercially available myoelectric prostheses: Left: RSL Steeper Bebionic , middle: Multi-finger articulated i-limb ultra (Touch Bionics Inc., UK), Right: Michelangelo Hand with an active wrist and two-grip patterns (Otto Bock HealthCare GmbH, Germany).

sensory feedback, the amputee could receive some of it through the harness and this, in turn, offers the possibility of controlling the prosthesis intuitively. It is a lighter than externally powered prostheses. Forbye, they are cheaper and easier to maintain, which is decisive for amputee that has no health insurance [23].

Externally powered prostheses are controlled yet not powered by the amputee. Generally, a battery acts as an external power supply (i.e. electrical activation). The current rate that is provided by the battery to the motor of the prostheses is controlled by the amputee through the level of muscle contraction. Muscles produce a light current when contracting which can be read out by electrodes placed on the skin surface. These signals are processed and passed to the motor where they serve as a control signal. Myoelectric prostheses offer an advantage in eliminating the donning and wearing a harness. In addition, they provide a higher grip force and allow a wider range of motions around the user's body without affecting the function of the contralateral limb, which is a common problem in body-powered prostheses. Furthermore, they help in reducing the appearance of phantom limb [16] [8] [9].

2.2.2 Human – Machine Interface in Myoelectric Prostheses

Technologically, myoelectric prostheses present the most complex solution for replacing the lost limb offering a wide range of functionalities, ranging from simple grippers to highly dexterous movements (i.e. multi-DOF). As they are designed to replace the lost functionality, they could not be extrapolated by the traditional human-machine interface (HMI) which ensures the interaction between the user and the prosthetic system. In order to ensure an efficient interaction and better manipulation of the surrounding, both the feedforward and feedback pathways need to be restored [24]. Figure 2.2 shows the different loops of interaction between the prosthesis and the user[25]. Figure 2.3 shows the feed-forward control loop and the sensory feedback loop [8].

2.2.2.1 Feedforward Control Interfaces

The feedforward control interface is based on the capture of electromyographic signals (EMGs) from the electrical activity of the excitable cells of the muscles either invasively by implanting the electrodes directly into the muscles or non-invasively by electrodes attached to the skin. The electric signals that the muscles produce upon contraction are the result of a neural

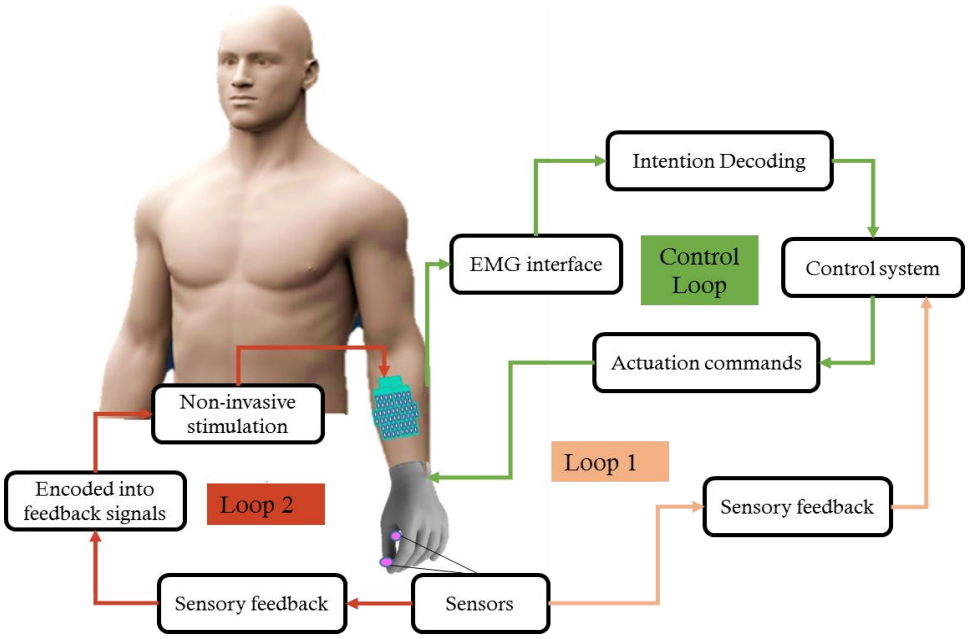

Figure 2.2 Existing sensory feedback loops while using non-invasive stimulation interfaces

command coming from the central nervous system. In order to contract a muscle, motor neurons descending from the primary motor cortex send an activation signal to the respective muscle, which in turn depolarizes the membrane that moves along the motor neuron's axon. This depolarization accumulates at the junction between the motor neuron and its targets, the muscle fibers that are the smallest units of a muscle. When the accumulated potentials reach a certain threshold, series of electric potentials travel along the muscle fibers' outer membrane and result in their contraction. During a muscle contraction, electric potentials of adjacent muscle fibers sum up and generate extracellular field potentials, also called electromyogram (EMG), which can be measured on the skin surface. Therefore, the surface EMG (sEMG) is the electrical signal that represents the contraction level of a muscle. The strength of the signal depends on the number of motor neurons that are active, the number of muscle fibers they recruit and their discharge rate [26].

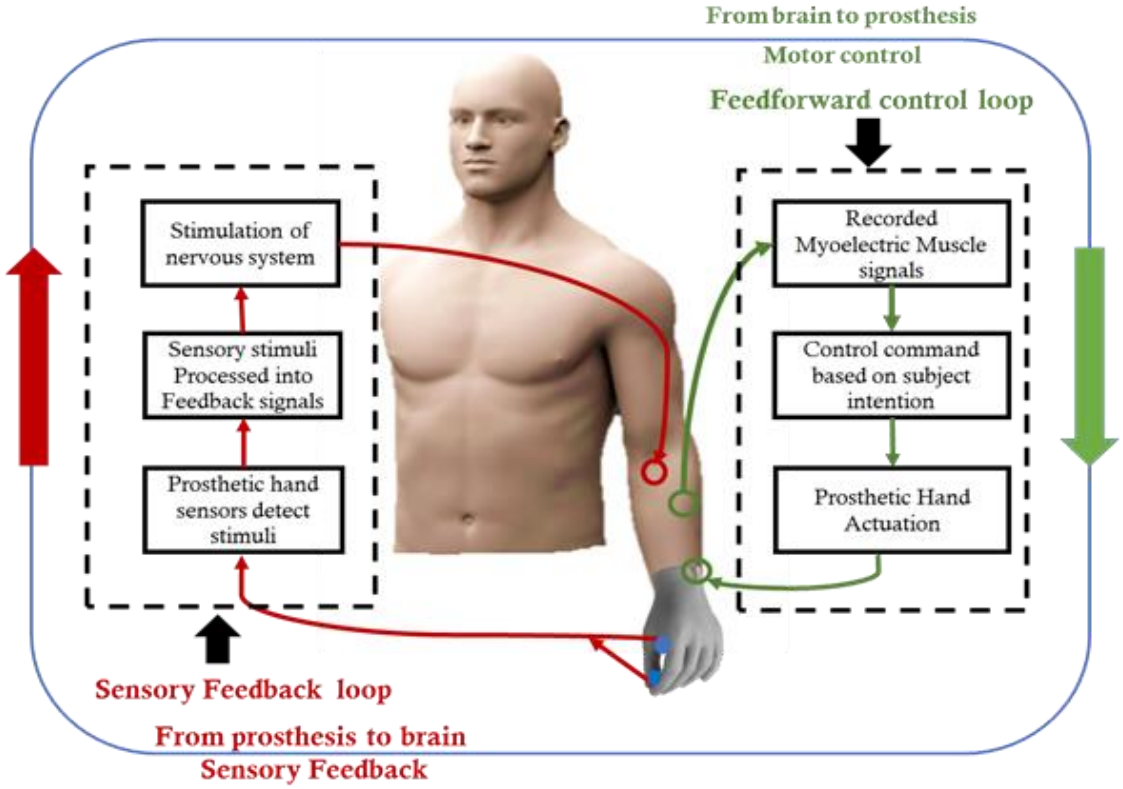

Figure 2.3 The control feedforward loop and the sensory feedback loop

Myoelectric prostheses typically support the control by estimating the electrical muscle activity (i.e. EMG electromyography signals) from the residual limb of the amputee and decoding his movement intentions. Figure 2.4 shows an illustration of different control strategies used with myoelectric. Traditional approaches that are commonly used in commercial myoelectric interfaces depend on a two-side electrode system in order to implement direct proportional control. It usually maps their amplitude to the force or speed of different prosthetic movements (prosthesis degrees of freedom, DOFs). The two electrodes record the activity of the two antagonistic muscles (i.e. the flexor and the extensor) above the amputation. The extensor group of the forearm could be used to control the hand opening while the flexor group activates the hand closing, in such manner, it mimics the natural movement of the limb and allows the user to control it intuitively. It is important to note that the sEMG signals cannot directly be used for the motor control of the prosthesis, it needs first to be preconditioned and sampled as they have low magnitude around (~1 mV) and furthermore they are contaminated by noise signals coming from the near electromagnetic fields. This paradigm has been extended to map

the muscle's activity into multiple DOFs based on switching approaches, such as co-contraction or physical buttons [11] [27].

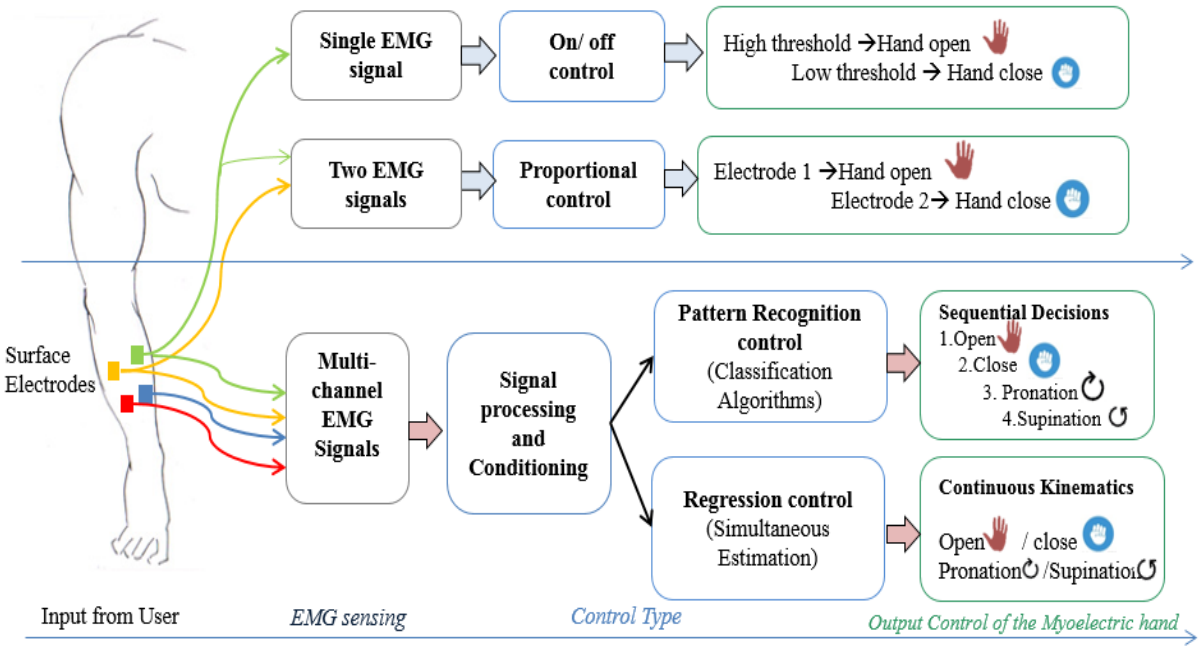

Figure 2.4 Comparisons among different control strategies used with myoelectric prosthesis. From top to bottom: (a) on/off control (one electrode used to provide binary control), (b) proportional control (two electrodes used for opposite actions), and (c) pattern recognition control (multi-channel electrodes used, the signals are classified into different movement patterns and given in a sequential decisions as control output), (d) regression control (the extracted information extracted from the EMG signals are mapped into continuous kinematics and used as control signals for the prosthesis).

In a more advanced step, pattern recognition and other machine-learning algorithms have been applied lately to provide more natural transitions between movements over multiple degrees of freedom, by extracting the useful features present within the electromyographic (EMG) signal. The pattern recognition approach presumes that each hand motion produces a distinct and repeatable activity pattern which could be recorded by multi-electrodes. Depending on these recognized patterns, the system sequentially detects a discrete movement from a predefined set. Moreover, it could execute simultaneous movements through including combined movements in the training set or using parallel architectures

In the same context, regression-basedd algorithms for example linear regression (LR) and Nonnegative Matrix Factorization (NMF), evince a simple and promising strategy to provide proportional and simultaneous control of multiple DOFs [28]. These algorithms establish a continuous mapping between the signals' amplitude and the control of different DOFs as shown in Figure 2.5.

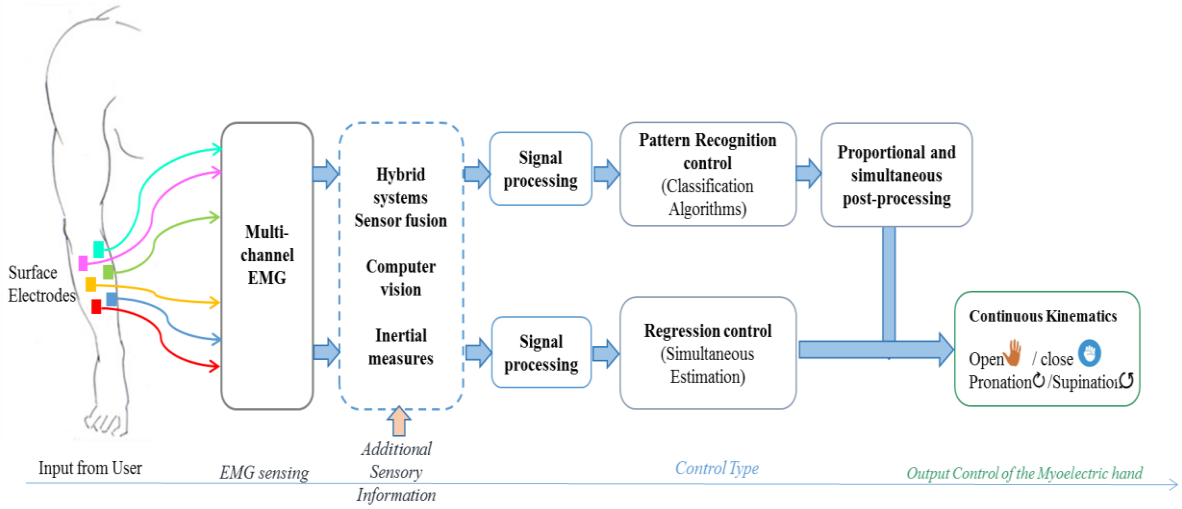

Figure 2.5 Summary of the most clinically advanced myoelectric approaches classification (pattern recognition) regression algorithms, and hybrid systems. Recent post-processing steps have provided classification systems means for proportional and simultaneous control, which is directly generated by regression-based systems. Sensory fusion and computer vision have also been combined with these approaches to improve their performance [reprinted]

2.2.2.2 Sensory Feedback Interfaces

In the recent years, the market has presented several advanced prosthetic hands with wider range of movements and high dexterity of fingers, such as Be-bionic-hand by RSL Steeper [4], UK and Myo-hand and Michelangelo hand by Otto Bock Healthcare Products GmbH, i-limb Ultra-revolution by Ossur, the iLimb Hand (Touch Bionics, UK) [6], VINCENT evolution 3 by Vincent systems [7], LUKE arm (Mobius Bionics LLC, US and cleared by US FDA) [29]. These developments manifest the improvement in the feedforward control strategies and the mechanical structure, which in turn enhance their manipulation performance. However, on the other flip, they still do not provide satisfactory sensory feedback and they are unable to make the users aware of the tactile information without visual feedback. VINCENT evolution 3 might be the only myoelectric prosthesis that features force feedback. The grasping force applied by the prosthesis is translated into vibration levels using a single vibration motor. A research team funded by DARPA's Hand Proprioception and Touch Interfaces (HAPTIX) is working on

advancing the LUKE arm by providing naturalistic touch sensations and motion by stimulating peripheral nerves with electrical pulses sent from a stimulator, which in turn receives signals from pressure sensors placed on the prosthesis. The clinically used SenorHand from Ottobock contains three-dimensional force sensors, which measures the shear force and automatically change the grip force to prevent slipping of grasped objects [30].

Some of the commercially transradial myoelectric prosthesis such as the bebionic [4] and Michelangelo Hand [31] feature sensors, for example, barometric pressure sensors, Force Sensitive Resistors (FSR) [32] or other type of tactile sensors that can be placed on the tips of the digits for achieving grip force control feedback. Using the values these sensors provide, control strategies can be used to adjust grip force and avoid the slipping of objects, or to provide haptic feedback to the user [33]. Yet, it still excludes the users from getting feedback on the grasping and touching [34] [35].

In a parallel line, various sensors integrated for artificial lab hands. For example, For example, force and/ or pressure sensors and torque sensors are used in DLR II hand[36], Southampton Hand [37] LUKE hand [38] and Cyerhand [39] for slip prevention and finger position feedback. In addition, temperature sensors are integrated in Southampton Hand. Besides, micro-vibration sensors are optional on Shadow hand. However, the tactile information acquired by sensors is only fed back to prostheses themselves to pursue a stable control performance, instead of providing tactile feedback to users. Encouragingly, an invasive tactile system was recently tested on self-controlled prostheses users to provide limited tactile feedback [40]. Although preliminary success has been achieved, restoration of tactile sensation for hand prostheses is still a great challenge.

Enabling sensory feedback in prostheses allows the users to "feel" his/her bionic limb. It is of great importance for reinforcing the user's control (increasing the success rate of applying correct grasping), objects manipulation, and decreasing the cognitive load (reducing the reliance on vision). Furthermore, the tactile sensation can facilitate prosthesis incorporation in the body schema to create a better body image and may yield better psychological experience. In rubber hand experiment done on amputees, by synchronous touching of the rubber hand and the stump the rubber hand elicits a feeling of belonging to own body [1]. In addition, sensory feedback in hand prostheses has been reported also the sense of embodiment and phantom limb pain [41].

The Somatic receptors in the upper limb are divided in cutaneous and subcutaneous mechanoreceptors, muscle and skeletal mechanoreceptors, nociceptors and thermal receptors. This complex sensory system encodes and transmits, to the CNS, information about four major modalities: touch, proprioception, pain and temperature. Proprioceptors detect the movement of the muscles or joints and the exteroceptive sensors detect information from the surroundings. Figure 2.6 shows the general architecture of information transduction.

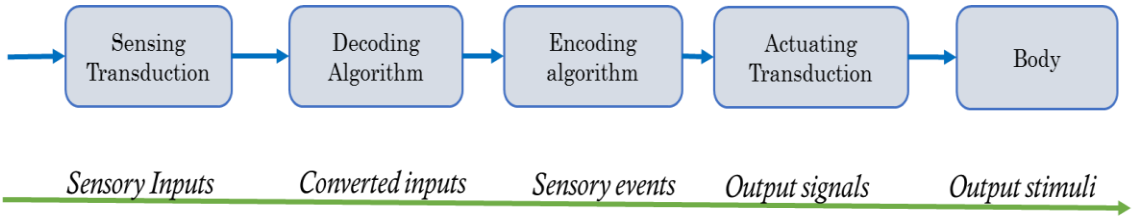

Figure 2.6 General architecture for providing sensory feedback. The input stage, namely sensing transduction, converts physical stimuli (sensory inputs) from one form of energy (typically mechanical) to another form of energy (converted inputs, typically electrical) that is more appropriate for processing. Then, a decoding algorithm identifies important sensory events/states (e.g., contact or angular position of a joint), and an encoding algorithm transforms them into output signals that can be interpreted by the CNS as if they were a substitute of the sensory input. The output stage – that is, actuating transduction – converts the output signals into the appropriate form of energy to be applied on body sensory systems (output stimuli) either invasively or noninvasively (reprinted from [2])

After amputation, a loss of the receptors and interruption of the physiological channels occurs; two potential ways could be used to elicit sensory feedback:

a) Invasively, by interfacing directly with physiologically relevant neural structures in the peripheral nervous system (PNS) or the central nervous system (CNS).

b) Noninvasively, by providing feedback to intact sensory systems (e.g., tactile stimuli on the residual limb, chest, etc.) using temperature, mechanical pressure and augmented reality.

In both cases, the subject should be trained to associate stimuli to physical events occurring at the prosthesis (exteroception) or to states of the prosthesis (proprioception). Proprioceptive information (of the position of the fingers and hand) and tactile information from the glabrous skin gives a vast amount of sensory information to the receiver [28].

Childress et al. [42] proposed the division of the sensory information pathways between the user and the prosthesis depending on which type and where the stimulus is provided, it is summarized in Figure 2.7.

1) ***Pathway A:*** It corresponds to visual or auditory feedback. This sensory information is intrinsic to the user except for blind or deaf people and consequently exists in all prosthetic devices. The visual information acquired from the environment either by looking to the terminal (i.e. Prosthesis) while grasping to roughly regulate the grip strength, sounds produced from the prosthesis such as sound when the hook touches the objects or the motor sound in battery-powered prosthetics while grasping an object, and usually, it is exploited in the control. It is perceived and processed in the central nervous system (CNS).

2) ***Pathway B***: It is related to somatic sensory signals (e.g. tactile, vibration, temperature, and proprioception). This information can be transmitted through the skin, using electrical, vibrotactile stimulation, or directly stimulating peripheral afferent nerves. Non-intentional sensory feedback information transmitted through the socket of the prosthesis is included.

3) ***Pathway C***: It is the feedback inherent to the prosthesis control (e.g. using sensors to adjust grip force automatically and avoid slippage of objects) [2]. The information is processed by the prosthesis, without the intervention of the user.

Sensory feedback for prosthetics can be delivered by associating different sensations with the stimuli detected by the hand and applying it to different body locations. A primary classification for the sensory feedback methods divides them into invasive and non-invasive techniques. Alternatively, the sensory feedback could be classified into somatotopically matched, modality-matched and sensory substitution methods depending on how the sensory information is transmitted to the user. In Somatotopical matching methods, the feedback signal is perceived as being anatomically matched in location to where the stimulus has being applied

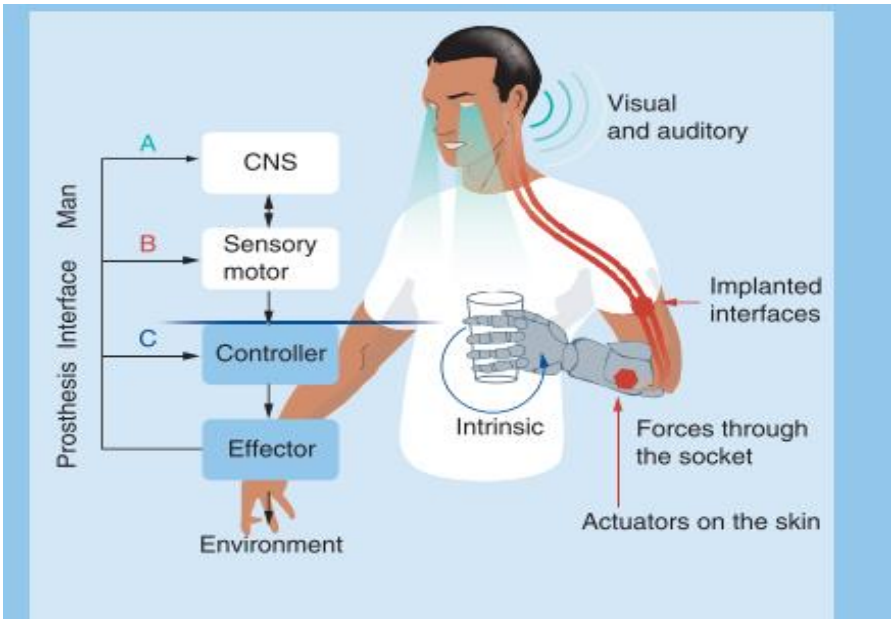

Figure 2.7 Possible pathways for feedback information to prosthesis. Different colors correspond to different pathways (A, B, C). Pathway A is related to sensory information that is directly fed back to the CNS (e.g., visual and auditory feedback); Pathway B to the information that is conveyed to functional sensory motor systems invasively or noninvasively; Pathway C is related to the intrinsic feedback. Image adapted from [2].

to the prosthesis (i.e. invasive methods or sensory feedback applied to phantom mapping). In modality matching methods, the feedback signal that is congruent to the external stimulus detected by the prosthetic sensor; however, the feedback signal could be applied to a physiologically different location representative of the hand or limb [8] [9][43].

Sensory substitution represents a non-modality matched method where the feedback signal that is not matched in modality to the stimulus occurring at the prosthesis. Furthermore, the feedback signal is presented to a location that, physiologically, will not be perceived to the user as in the same corresponding location on their missing limb. The success of the approach depends on the user's ability to interpret the type and location of the stimulus and associate it with the prosthesis. The most common methodology has been to translate tactile information from the prosthesis to the amputee using vibration, electrocutaneous or auditory stimuli. The classification map is shown in Figure 2.8.

Although the primary results with direct neural stimulation were promising more extensive studies are needed to understand how to safely stimulate afferent pathways of the human nervous system to provide effective sensory feedback. Instead, such approaches are invasive and usually require a surgical procedure, which may strongly decrease their acceptance by the prosthesis users [1] [44].

Non-invasive sensory feedback systems could prove to be an interesting alternative to invasive solutions. The implied assumption is that it might not be necessary for an artificial system to exactly restore the biological information transmission, provided that an intuitive communication between the prosthetic device and the human brain is established through a non-invasive interface

In addition to the sensory modality (what is fed back), another crucial aspect is the timing of sensory feedback (when it is fed back). The latency between variations of the output stimulus corresponding to a sensory input variation should be as short as possible to achieve the effective use of such information. In the human sensory system, tactile stimuli take 14-28 ms to reach the cutaneous nucleus [45] Therefore, it is reasonable to believe that to avoid increasing this value significantly, artificial sensory feedback should be delivered to the individual in a fraction of that time (e.g. 3-5 ms). Short latencies are also important for the brain to develop a sense of embodiment (body ownership) of the prosthesis. Indeed, the attribution of a visible hand to the self depends on a match between the afferent somatic signals and visual (and eventually audio) feedback from the hand [46]. Self-attribution occurs with temporal delays up to 300 ms, as reported by Shimada et al. in [47].

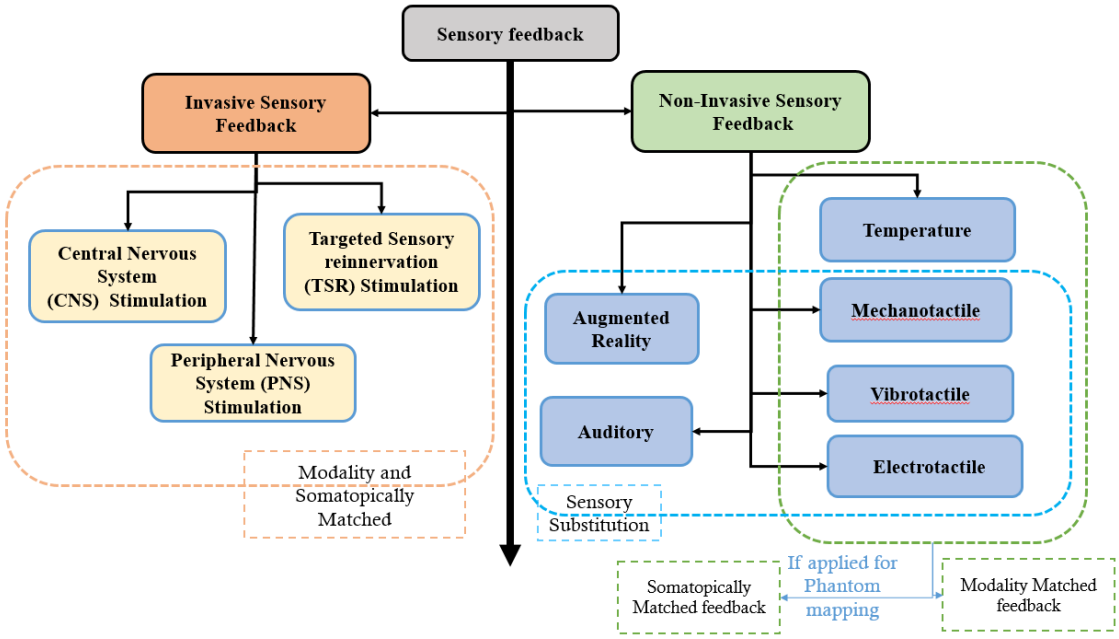

Figure 2.8 Block diagram for sensory feedback methods

Johansson and Birznieks wrote that both friction between the object and the fingertips and the shape of grasped surfaces, recognized by tactile mechanisms, are reflected in the applied fingertip forces within ~100 ms of initial contact [48]. Besides, they claimed that accidental slips

and unexpected perturbations of a grasped object elicit responses in tactile afferent triggering specific behavioral consequences even faster (~65 ms). To conclude, peripheral nerve conduction times and muscular force generation delays account for ~45 ms of the delay and at least 15 ms is required for central processing.

The prevalence of stimulation, i.e. how continuous sensory feedback would be provided is still a debating point within the field. Traditionally, researchers have implemented systems that presented the sensory feedback in a continuous fashion. However, continuous feedback yields to adaptation, meaning that the stimulation is no longer or just barely perceived by the individual after a short while.

2.2.3 Invasive Sensory Feedback Systems

This section describes the different invasive sensory feedback systems presented in the literature review.

2.2.3.1 Targeted Sensory Reinnervation (TSR)

Targeted reinnervation is a reconstructive technique in which the nerves that previously innervated the amputated limb is transferred to another more proximal site that was unaffected by the amputation through a surgical procedure. Therefore, it provides new EMG signals to control myoelectric prosthesis and allows the transfer of sensations in an intuitive manner. It was found that redirected sensory afferents also reinnervate the overlying skin. Which in turn creates an expression of the hand map such that when touched, the amputees feel as if they are being touched on the missing limb. Even though this technology seems to be promising, it is still in an early phase of development and further research needs to be elaborated [49] [50]. Some examples are shown in Figure 2.9.

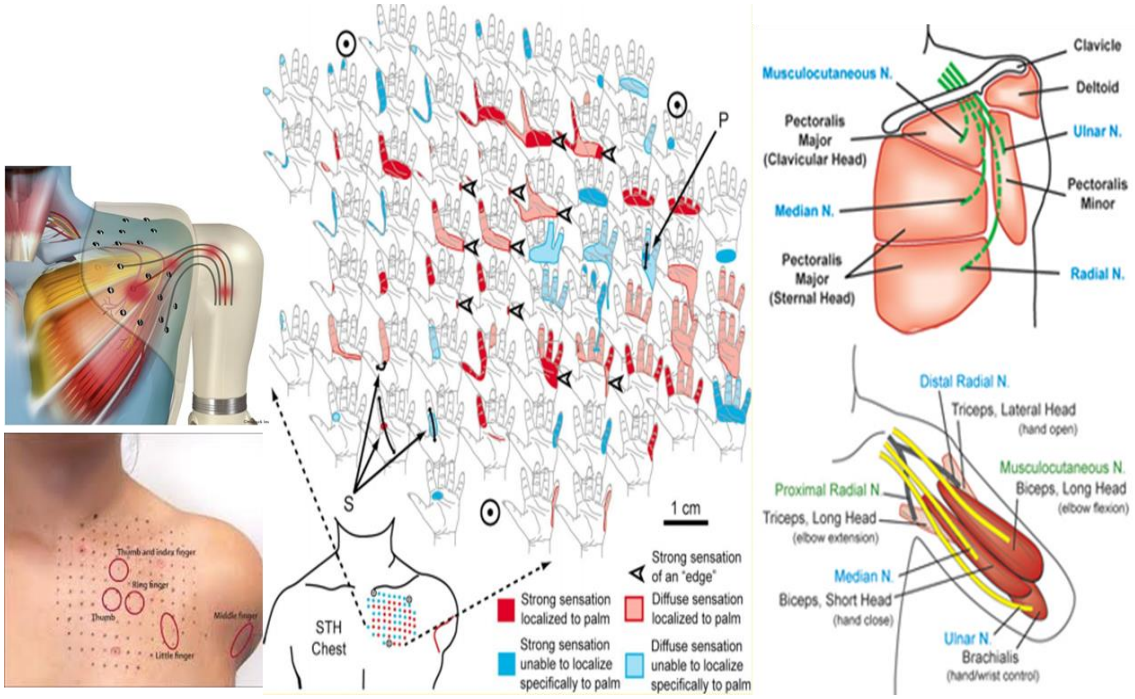

Figure 2.9 Targeted re innervation (source Ottobock courtesy)

2.2.3.2 Peripheral Nervous System (PNS) Stimulation

The peripheral nervous system stimulation is a technique where electric currents are passed through the afferent nerves of the residual limb through implanted electrodes, in order to evoke sensations. The electrodes vary in their degree of invasiveness, for example, extraneral electrodes or Cuffs are wrapped around the nerve, intraneural electrodes like intrafascicular multichannel electrodes are inserted in the nerve itself, and regenerative electrodes such as sieve electrodes which are the most invasive electrodes [51]. Ortiz-Catalan and colleagues [52] presented a solution with bidirectional communication between the prosthetic arm and the wearer through an implanted neuromuscular interface and an Osseo-integrated screw in the humerus. The tactile perception was chronically reproduced still after 11 months through direct electrical stimulation of the peripheral nerves using cuff electrodes. Oddo et al. presents an artificial fingertip with implemented MEMS sensors where the signals were converted to neural spikes to be sent through transverse intra-fascicular multichannel electrodes to stimulate the nerve with the artificial finger. As a technique for sensory feedback, PNS stimulation demands less cognitive requirements, consequently less training and conscious attention. However, the experimental studies demonstrated that recovery of somatic sensory information is still far from being achieved as it holds inherent technological limitations in terms of selectivity, naturalness in elicited sensations and long-term stability. The available neural interfaces activate multiple

afferents at the same time, as a result the spatial resolutions of referred sensations are often large, encompassing entire fingers or areas as large as the palm [53], [54] rather than precise positions and timing conditions. Although participants do report tactile sensations, they are frequently accompanied by foreign sensations resembling vibration, paresthesia, taping or fluttering on the skin [2] [53]. PNS is still in an early stage of development with limited numbers of labor oratory testing for subjects taken; hence it is not ready for real-life application. In addition, at present there remains a reluctance within prosthetic users to undergo surgery [55]. See Figure 2.10.

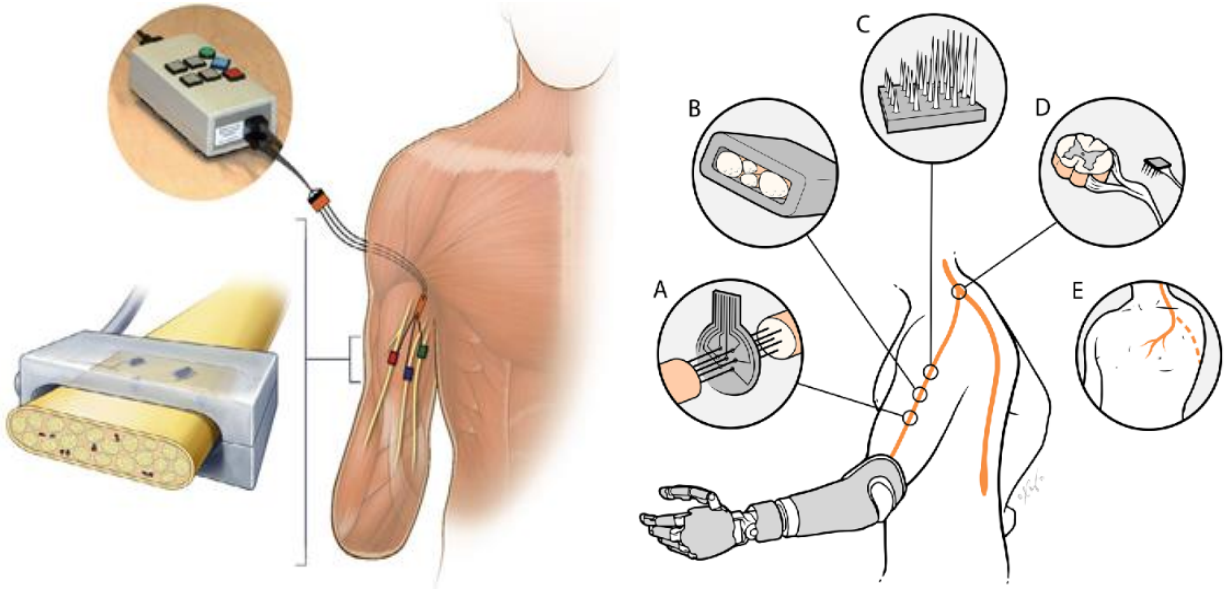

Figure 2.10 Peripheral nerve stimulation (source 77), Different illustrations of different approaches to restore the sense of touch through PNS interfaces.(A) Regenerative electrodes. B) Extra-fascicular electrodes. C) Intra-fascicular electrodes. D) Dorsal root ganglion implant and E) Targeted sensory reinnervation)

2.2.3.3 Central Nervous System (CNS) Stimulation

The central nervous system (CNS) stimulation is a technique in which the somatosensory parts of the brain are electrically stimulated (i.e. intracortical stimulation) in order to elicit tactile or proprioceptive sensations. It primates on non-human by using "brain-machine interfaces", the studies done on monkeys shows the brain-controlled virtual arm. Control of a high-performance prosthetic limb with ten degrees of freedom has been shown by a person with tetraplegia using cortical neural interface implanted in the motor cortex [56]. Moreover, microstimulation in the somatosensory cortex in the hand area has shown promising results, the evoked tactile sensation covered distal parts of the fingers on the palmar side (except for the thumb). The different level stimulations were perceived in different intensities, however, the

feeling was more like pushing not touching. The authors believe that further developments are required to refine this method. See Figure 2.11.

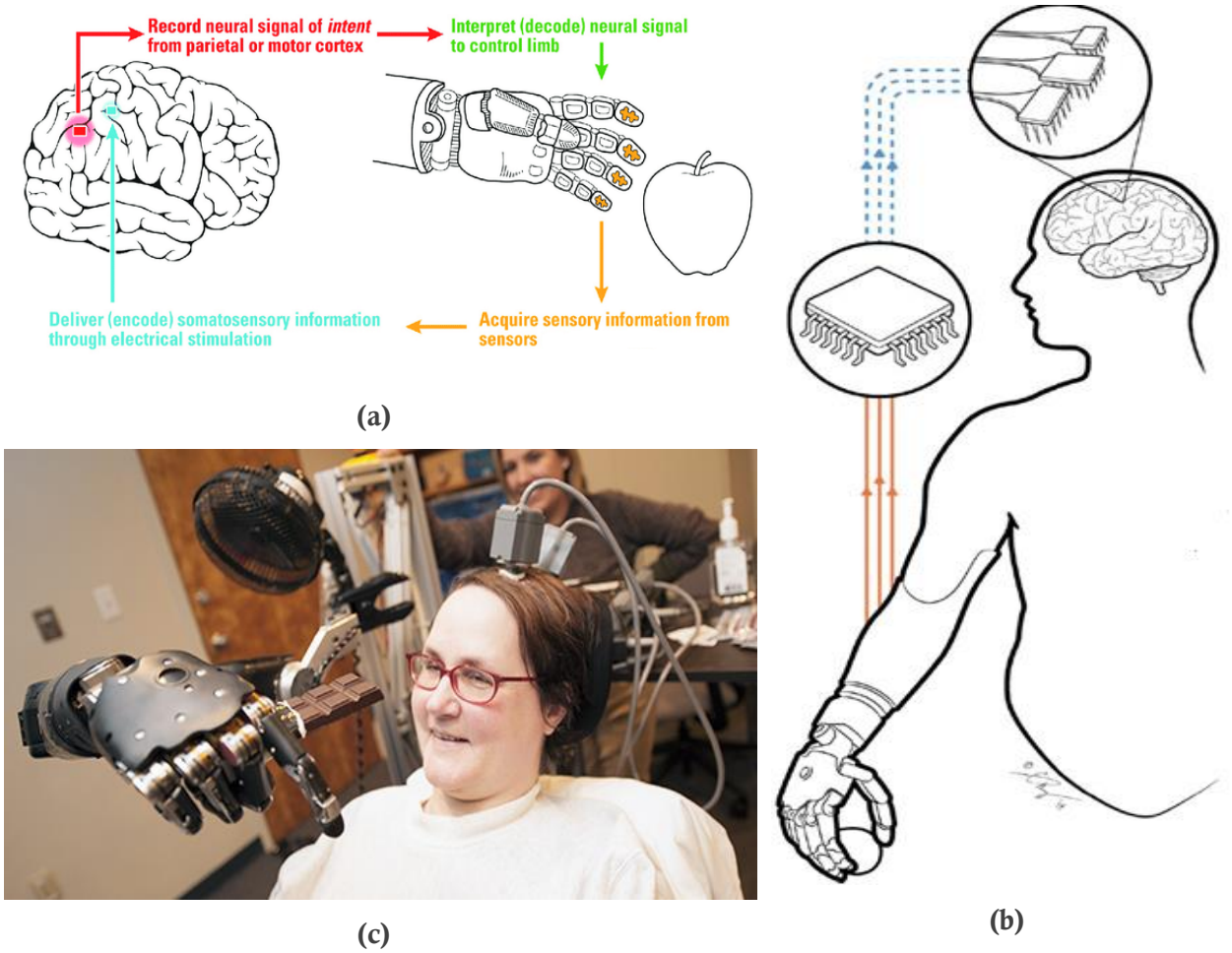

Figure 2.11 Central nervous system (CNS) stimulation: a) Close loop of somatosensory neuroprosthesis (source brian lee 2018), b) source Bensmaia 2015

2.2.4 Non-Invasive Sensory Feedback Systems

In this section, we will preview the different methods deployed to provide non-invasive sensory feedback in upper limb prosthetics specifically prosthetic hands and their recent developments, challenges, and opportunities associated with the non-invasive stimulation methods.

2.2.4.1 Mechanotactile Feedback

Mechanotactile feedback is a modality-matched sensory feedback. It elicits sensory information by applying force to the residual limb. It is commonly used to ensure position or force/ pressure feedback to the amputee during prostheses movement. A wearable mechanotactile stimulator is demonstrated to provide pressure and skin stretch information to

the subject's residual limb as shown in Figure 2.12. Casini et al. [57] demonstrated the application of distributed haptic force to help a user determine an object as hard, medium or soft. A combination of pressure and skin stretch on the bicep was used as the feedback mechanism for the subject. It has a high user acceptance despite its large weight, bulky size and high-energy consumption since it is able to provide the user with a natural feeling of force and pressure unlike electrotactile and vibrotactile stimulation methods [8] [18].

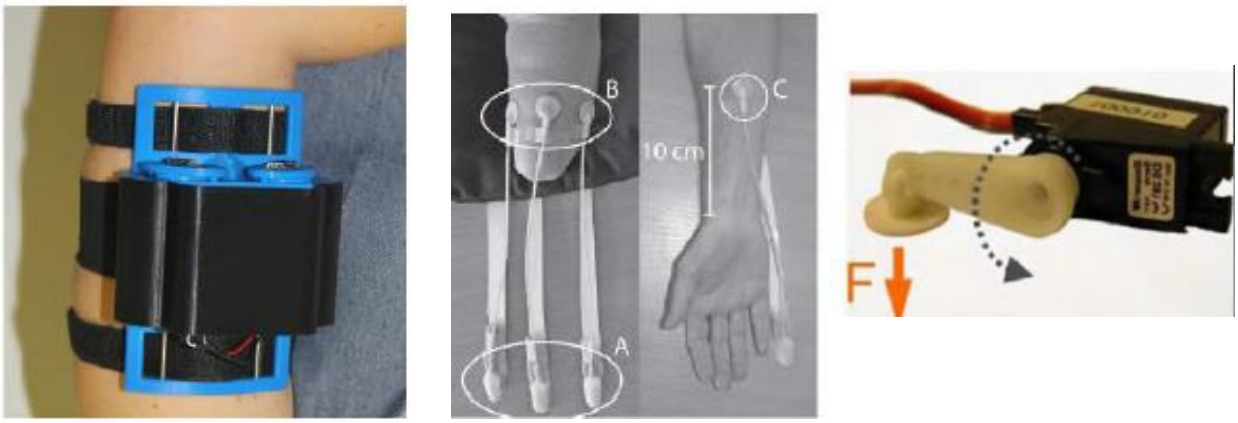

(a) (b)

Figure 2.12 Mechanotactile stimulation examples: a) Pressure feedback cuff (source [8]) b) Silicon Bulb Mechanical Feedback and Mechanical Pressure Feedback device (source [8])

2.2.4.2 Vibrotactile Feedback

Vibrotactile stimulation evokes tactile sensations using mechanical vibration of the skin, typically at frequency ranges from 10Hz to 500 Hz [58]. Vibrotactile stimulation is provoked by mechanical vibration applied to the skin surface to deliver sensory information, especially tactile information. The frequency (10Hz-500Hz), amplitude, location and duration of the vibration can be modulated to determine the type of information to be conveyed. It activates two types of mechanoreceptors in the skin: Pacinian corpuscles which react best to frequencies between 200 and 300 Hz, and Meissner corpuscles which are best activated by frequencies around 50 Hz [59].

The vibrotactile stimulation applied in prosthetic since 1953 [Colzeman et al [20] and it has been implemented to establish proprioceptive communication between the user and prosthesis. It has been explored due to its higher acceptance compared to electrotactile stimulation. It is suitable for myoelectric prostheses and EEG- based prostheses (e.g. i-Limb myoelectric prostheses Ottobock [31], Cyber [39], MANUS [60], Fluid [61]and Smart [62]hands) since no interference with electrical signals. Today's vibrotactile stimulators have low

Figure 2.13 Examples of vibrators used in vibrotactile feedback. (source [8])

power consumption and can be embedded within sockets. Generally, vibrotactile feedback ameliorates user performance by decreasing task execution time and providing better control [8]. Its incorporation reduces cognitive load required to pick up objects compared to using visual feedback alone, however, this was not consistent across all subjects. One limitation is the delay in stimulation as it can decrease embodiment [8] [18].

2.2.4.3 Electrotactile Sensory Substitution Feedback

Electrotactile (or electrocutaneous) stimulation elicit tactile sensations within the skin by passing local electric current to stimulate afferent nerve endings in the PNS [58]. The electric pulses delivered through surface electrodes. The major features of the stimulation that could be modulated to transmit electrotactile feedback information include electrical components i.e. current amplitude (1-20mA), pulse waveform (monophasic/biphasic, rectangular/sinusoidal), frequency (1Hz-5KHz), pulse width, duration of pulse bursts, electrode properties i.e. size(small/large), conducting material; and skin characteristics i.e. location, thickness[8], which leads to a higher bandwidth being available. Electrotactile stimulators can be either current or voltage regulated. The voltage- regulated stimulators decreases skin burns that could appear from high current intensity stimulation, on the other hand, current-regulated stimulation; the current is not affected by changes in the tissue load and impedance at the electrode interface [58] [8].

Electrocutaneous stimulation can evoke a range of sensations that have been qualitatively described by participants as a tingling, itch, vibration, buzz, touch, pressure, pinch and sharp or burning pain[63] depending on the stimulating voltage, current and waveform, as well as on the electrode size, material and contact force, and the skin location, hydration, and thickness[8]. Electrodes with a small area are required when only a limited area is available, even though larger electrodes provide a more comfortable sensation [18]. Hence, a trade-off between electrode size and skin area should be identified when performing multi-site stimulation.

Since there are no moving mechanical parts, the electrotactile systems consume less power, have low weight, produce less noise, and respond faster compared to other tactile feedback systems. On the other hand, it has relatively low acceptability due to uncomfortable and unexpected feelings like skin redness and burning pain. However, the main issue with electrotactile stimulation is the interference among electrical signals, EMG and EEG signals.

It has several applications in the field of rehabilitation e.g. FES field electrical stimulation for motor recovery and muscle actuation of the residual limb. Also in prosthetics, it has been investigated to deliver position information, and transmit somatosensory information to generate natural tactile perception thus enhancing the sense of embodiment. Strbac et al. [13]demonstrated a different electrode design that enabled users to distinguish up to 16 stimulation locations, with up to five different frequencies at once, to provide multiple levels of feedback. Test results from a small number of able-bodied and amputee subjects demonstrated that the subjects could identify six electrodes with four different frequency signals with more than 90% accuracy after minimal training [13].

Electrotactile feedback shows high potential as an easy, quick and controllable method of sensory feedback to deliver multiple information over multiple sites at once. Furthermore, the minimum sensation threshold and pain threshold changes with the position of the electrodes (even with 1mm movement) therefore, the perception of tactile information changes. Re-calibration of thresholds is always required even the stimulation parameters need to be adjusted each time. In a prosthetic context, sensory feedback devices should have long-term stability and consistency of the prosthetic-to-user communication channel. Without stability in the elicited sensations, the user may face substantial challenges in learning to interpret feedback [8].

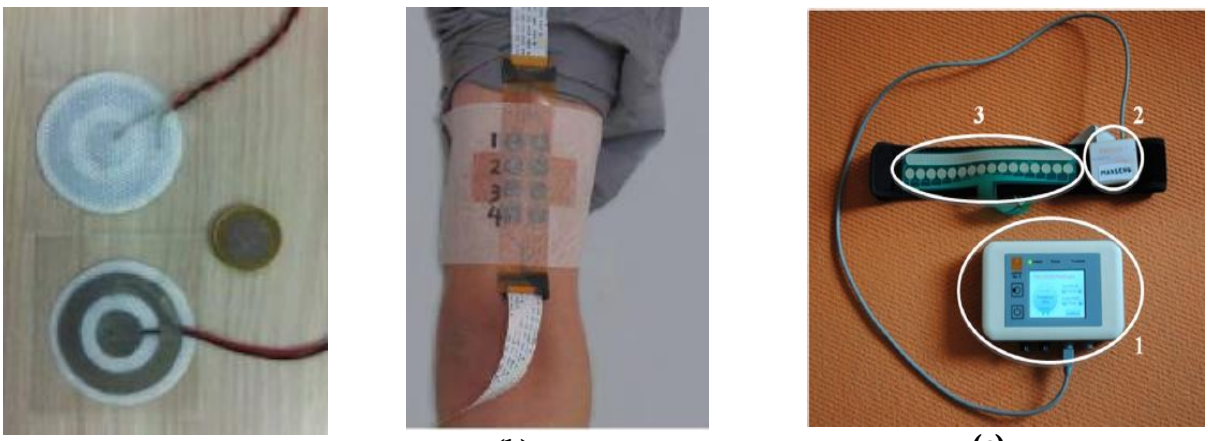

(a) **(b)** **(c)**

Figure 2.14 Examples of electrotactile feedback. source [8] and [13]

2.2.4.4 Temperature Feedback

Temperature feedback has only been used to communicate the information about the force of the grip and the position of their fingers. However, temperature provides users with extra information about their environment, and potential dangers or warnings that involve heat. Producing heat on the upper arm in correspondence to the temperature detected at the prosthetic hand was the only method of temperature feedback found within the literature [8].

A potential focus of research would be to incorporate temperature feedback with another feedback method so that they occur simultaneously since it is not a priority to occur by itself.

2.2.4.5 Audio Feedback

Wilson and Dirven [64] demonstrated the potential of deploying audio to communicate sensory feedback from a prosthesis. They examined the test subjects ability to interpret modulation of two audio channels to control a computer simulation. Their data showed that the subject could interpret two channels, but there was a 602 ms delay and the audio feedback resulted in a high cognitive load. Other studies [65] utilized triads to communicate the movement of a robotic hand. The sound of cello corresponded to the force on the thumb and a piano sound represented the force on index finger. The subjects were also able to use the audio feedback to help improve their movements and control when grasping objects.

Each of these audio feedback experiments was given their high cognitive load required; further investigation is required to determine their effectiveness whilst background noise is occurring.

2.2.4.6 Augmented Reality

Markovic et al. [66] used Google glasses to communicate the aperture angle, contact time, grasping force and EMG strength for sensory feedback of a prosthetic hand to its user. Subjects used visual feedback to improve their task performance when moving objects that required various strengths without breaking them. The subjects noted, however, that they typically only glanced at the information and did not use EMG strength signals. Clemente et al. [67] also examined the use of augmented reality for sensory feedback for prosthetic devices. They communicated information through an ellipse, with the axis lengths corresponding to grasping force and angle of grasp closure.

Moreover, [68] suggests that although performance repeatability can be increased with augmented feedback, it increases the cognitive load required from the user.

2.3 Distributed Electrotactile Simulation Interfaces

Distributed stimulation interfaces comprise a matrix of stimulation units that are placed on the skin surface. Due to many stimulation channels with independently controllable parameters, such an interface can deliver rich stimulation patterns that are modulated in space and time, thereby providing a high-bandwidth communication channel to the user. Matrix interfaces have been presented and tested in the past for sensory substitution [59]. For example, stimulation sheets placed on the abdomen or arrays positioned around the waist have been used to restore lost hearing or vision through tactile sensations [69]. In these systems, sensor data captured using a microphone or a camera were translated into stimulation patterns.

Table 2.1 Summary of available sensory feedback systems

		ADVANTAGES	LIMITATIONS
INVASIVE FEEDBACK	**TSR Stimulation**	• Promising for shoulder disarticulation and transhumeral amputation • Somatotopically matched through PHM in reinnervated skin	• Post-operation recovery time
	PNS Stimulation	• Somatotopically matched • Possibility to perceive different textures	• Rough sensibility • Can cause nerve damage depending on how invasive the electrodes are • Potentially short lifetime of implant
	CNS Stimulation	• Somatotopically matched	• Potentially short lifetime of implant
NONINVASIVE FEEDBACK	**Mechanotactile**	• Modality matched • Close to 'real' touch	• Bulky • Power consuming on the forearm
	Vibrotactile	• Cheap • Small-sized • Low power • Two-point discrimination: ~40 mm on the forearm	• Can be annoying with continuous vibration for daily use
	Electrotactile	• Two-point discrimination: ~9 mm on the forearm [28]	• Can produce an unpleasant feeling • Can interfere with EMG sensors in control of myoelectric prosthesis

Using such an interface, subjects could recognize the shape of simple objects and detect obstacles, and this demonstrates the ability of the human skin and tactile sense to convey complex information to the subject.

Table 2.2 Comparison between main sensory substitution feedback methods

Stimulation techniques	Features	Energy Consumption	System Response	Weight	Usage	Prosthetics
MTS **Mechanotactile stimulation**	Accuracy range, resolution, bandwidth	High	Slow	Large Bulky	High	[2][8][18][42]
VTS **Vibrotactile stimulation**	Vibration frequency amplitude, duration, stimulation position	Low	Fast, No interference with electrical signals	Large	High	[2][8][58]
ETS **Electrotactile stimulation**	Voltage, current amplitude, frequency, waveform, pulse width	Low	Very fast No mechanical parts	Small compact	Low	[2][8][58]

However, the application of these technologies in prosthetics faces specific challenges. First, the area of the skin available for the stimulation is smaller. Ideally, a prosthesis should be a self-contained system and the matrix of electrodes needs to be embedded in the socket. The stimulation is therefore delivered to the residual limb, which can be rather short in some amputees, decreasing the skin area available for stimulation. Next, there might be a discrepancy between the number of sensing and stimulation units, where the former is likely to have a higher resolution than the latter. The tactile sensing elements (taxels) can be rather small whereas the electrodes need to be larger to produce comfortable sensations. Therefore, mapping has to be developed from the higher density sensor data onto a lower density electrode interface. More generally, the schemes for translating the properties of recorded tactile information into stimulation profiles need to be devised. The challenge is to find a way to communicate spatial location (distribution) and intensity of the tactile stimuli using electrotactile stimulation so that these properties can be easily perceived and interpreted by the user. To this aim, the psychometric parameters of high-density stimulation interfaces need to be investigated.

Furthermore, different amounts of preprocessing can be applied to the data before feeding them back. One can feedback raw tactile stimuli (pressure distributions) or high-level features determined by processing the sensor data, as it will be explained in chapter 5. Finally, the electrical stimulation produces strong artifacts in the myoelectric signals that are recorded for prosthesis control. There are methods to address this drawback using signal processing or hardware solutions (e.g., blanking) [70].

Although there has been success in incorporating one feedback channel with electrotactile communication for one grasp, prosthetic devices often control more than one grasp.Therefore, more than one feedback channel is beneficial when closing the loop in feedback control with the user. Choi et al. demonstrated that subjects could distin- guish two channels of electrotactile feedback on their biceps. However, they did not connect the system to any sensors but instead showed that users could distinguish between the two channels. They also demonstrated that better recognition was achieved when using intermittent stimulation on both channels (switching between the two), rather than both channels being on at the same time, resulted in better recognition. Strbac et al. [66] demonstrated a different electrode design that enabled users to distinguish up to 16 stimulation locations, with up to five different frequencies at once, to provide multiple levels of feedback. Test results from a small number of able-bodied and amputee subjects demonstrated that six electrodes with four different frequency signals could be identified with more than 90% accuracy by the subjects after minimal training. The highest number of channels recognised was from one able-bodied subject identifying all 16 pads after two hours of reinforced learning. Six amputees also recognised eight different stimulation patterns that corresponded to different movements, with an average accuracy of 86%.They also noticed that there was a large difference between individual user's performances, indicating that this approach could work well for some but not others. Although this study only used simulated signal patterns instead of feedback from sensors, it demonstrated the potential of using a multichannel electrotactile feedback as a potential interface for prosthetic hands.

Hartmann et al. also demonstrated that the recognition of simple movement pat- terns using electrotactile arrays could be learnt by able bodied subjects through training. This opens future possibilities to be explored that could provide the prosthetic user with richer sensory feedback. Surface electrodes are predominantly used for myoelectric control of prosthetic devices. One problem that arises is the interaction of the electrotactile stimulation with the myoelectric surface electrodes.

Moreover,some initial work in addressing these challenges has been conducted by our group [71]. In a recent study, we have demonstrated that able-bodied subjects could recognize shape (lines, letters, geometries), retrace the trajectory, and guess the direction of movement of the tactile stimulus applied to an e-skin (64 tactile elements) when this stimulus was transmitted to the subject using a matrix electrode with 32 pads. However, the skin was not mounted on an actual prosthesis and the tests were conducted on able-bodied subjects and the users could detect movement directions easily, but had trouble determining individual positions.Nevertheless, the technology is becoming mature enough to enable this application. Recently, we have presented electrode interfaces with pads organized into a matrix (32 pads) [71]or array (16 pads) [13]. These interfaces are flexible and easy to apply to the forearm, and they are convenient for embedding into the prosthetic socket. Importantly, the production process is flexible and different shapes and sizes of both electrodes and pads can be designed, hence, arbitrary physical properties as well as resolution of stimulation points.

In summary, with the availability of the technology for high-density tactile sensing and electrotactile stimulation, the important goal of providing comprehensive feedback from the prosthesis to the user comes within reach. Significant research efforts had been done however still required to address the challenges. The ultimate goal is a prosthetic system covered with a dense network of tactile sensors to restore the feeling of touch over the whole surface of the prosthesis (whole hand and maybe even a forearm/socket). Such a prosthesis would provide a whole new experience to an amputee, improving utility and facilitating the feeling of embodiment to the level that is far beyond the conventional systems based on discrete sensing and stimulation.

2.4 Conclusion

This chapter gives a broad nature review on the recent advancements in myoelectric prosthesis. Additionally, it presents an introduction to the different stimulation techniques used in sensory feedback, with a special focus on the non-invasive sensory feedback interfaces. A brief comparison reporting the potentials and limitations among the invasive and non-invasive techniques was included. Moreover, an intercomparison between sensory substitution techquines has been presented. Finally, the chapter introduced our approach of using non-

invasive electrotactile distributed stimulation interfaces for restoring the sense of touch in prosthetics.

To conclude, there are different methods deployed for sensory feedback restoration, with different degrees of invasiveness. Each of these methods has shown to be successful in providing extra information to the prosthetic user, often through improving the control or the use. However, several limitations impair the effectiveness of this sensory feedback and affect the sense of embodiment such as the limited number of translated tactile information, the speed in communicating the sensation, additionally the time delay between visual and tactile feedback.

Accordingly, we will address these challenges and their impact on prostheses users in chapter 3 and chapter 4.

Chapter 3 Compensatory Tracking Delay Tractability in Close-Loop Dynamic Task based on Visual and Electrotactile Feedback

3.1 Introduction

Designing an artificial arm and hand replacement with physiological speeds-of response and strength which could be effortlessly controlled is the ultimate goal for upper limb prosthetics research. However, the current prosthetic systems (i.e. components and interfaces) are still a long way from realizing this goal. There has been an impressive development of prosthesis technology during the last decades, yet the rejection rates of hand prostheses are still relatively high (~ 35%) and the users still think of it to be a tool rather than a limb replacement[1]. Miscellaneous limiting factors impair the prostheses' utility such as severe weight, bulky size, high latency, high power, the lack of efficient control of the different degrees of freedom and sensory information. However, the real problem is, as has been alluded to before, the issue of how to interface a multifunctional arm or hand to an amputee in a meaningful way. Accordingly, it is for this reason that upper-limb prosthetics are often dominated by consideration of control. [8][11][2]

Childress et al [42] have presented several desirable attributes of prosthesis control as reported below:

1) Low mental loading or subconscious control.

2) Direct access and instantaneous response (speed of response). All functions, if possible, should be directly accessible to the user, and these functions should respond immediately to input commands.

3) User friendly or simple to learn to use. Any device should be intuitive and natural. An amputee should be able to learn to use the prosthesis quickly and easily.

4) Independence in multifunctional control.

5) Simultaneous, coordinated control of multiple functions (parallel control).

6) No sacrifice of human functional ability.

Any hand movement depends on both efferent motor control and afferent sensory feedback. The former element in planning a movement is visual feedback and previous experience. Afterward, the movement is achieved by motor commands that are important for position and force control. Refining and correcting the movements rely on the proprioceptive and exteroceptive feedback [72] [73]. Ergo, an ideal prosthesis should re-establish both feedforward and feedback pathways, to react effective execution of the movement[74]. Myoelectric prosthetic hands are usually controlled by recording the electrical activity of user's muscles to estimate motion intention and translate it into commands for the prosthesis. Therefore, they can be used in the restoration of lost motor functions after hand amputation. Nevertheless, this restoration is only partial with the absence of comprehensive feedback [74] [8].

Different sources of additional sensory information, such as artificial somatosensory feedback, besides visual information, sounds from the prosthesis or the contralateral arm could benefit the performance of the movement. A common method to transmit feedback information is sensory substitution [74] [75]. In this approach, a prosthesis is equipped with sensors measuring system state (e.g., grasping force) and this information is transmitted to the user by delivering tactile stimulation on the skin of the residual limb through vibration motors or electrical stimulation. Electrotactile feedback information can be transmitted by modulating the quality and intensity of the elicited sensations i.e. by changing the stimulation parameters (pulse width, amplitude, and frequency coding) and/or location of the stimulation (spatial coding) [76] [8].

Evaluating the psychophysical performance of electrical stimulation is regularly done by measuring the detection threshold, pain threshold and just noticeable difference as well as quality, intensity, comfort and location of the evoked sensation [77]. Such studies investigated electrotactile sensory feedback in an open-loop system. Despite that, this information is relevant to give a clear understanding of the qualities of electrical stimulation [78]. The perception and recognition of artificial sensory feedback are still not sufficient for the future implementation on myoelectric prostheses [78]. For these motives, the users need to be included in the "loop" thus became a part of the system [78].

Numerous studies have tested a closed-loop configuration focusing on functional tasks such as grasping different objects and placing them to another location without breaking or dropping them during the execution of the experiment[79] [80]. Even though, the outcomes are inconsistent reporting no improvement or improvement depending on diverse conditions[81]. The great extent of investigations conducted has established that there is no consensus on how the artificial sensory feedback should be delivered, resulting in a large variety of methods to assess the performance.

The possibility to predict human performance for engineering purposes has been evaluated in the past [82] [83]. Consistent and predictable performance in diverse tasks (e.g. driving, using tools or machines) has been seen, which allowed defining a model to distinguish the important variables of human behavior [82]. Consequently, closed-loop systems are relevant to accurately evaluate the performance of the user when providing sensory feedback [22] and can offer objective and standardize outcomes [84] [83].

Compensatory tracking task is the most elementary manual-control task and a standard evaluation to analyses the execution of the human operator in visual and electrotactile control systems [73]. These systems are designed to minimize the error between the controlled object and the target. Commonly, controlled systems with a proportional response (i.e. position control) are used, to simply concentrate on the effect of sensory feedback [73]. Nevertheless, controlled systems of diverse dynamics could allow investigating how its properties, command and feedback interfaces affect human behavior during closed-loop control.

It has been shown that the human controller has an adaptive nature depending on the system to be controlled [83]. The transfer function of the human changes with the control process (e.g. position control, velocity control or acceleration control). However, the closed-loop for the whole control system keeps invariant. Hence, the human operator actuates in such a way that the closed-loop system is stable [83]. Moreover, the studies conducted, using different controlled systems, performed the compensatory tracking task using visual feedback. It is relevant to assess if a similar adaptation of the human control strategy will be seen when using electrotactile sensory feedback.

The study presented in this chapter aims to prove the usability of electrotactile feedback in enabling closed-loop control in prosthetics. It evaluates the subject tolerance for different time delays while performing a dynamic control task. In addition, it compares the performance

quality of human manual control through a closed-loop compensatory tracking system while using two feedback schemes (i.e. visual and electrotactile feedback). More specifically, this task reflects more accurately the tractable and responsive ability of electrotactile feedback in prosthesis control. It addresses the adaptive behavior of the subjects "human operator or controller" to system latency when electrotactile and/or visual sensory feedback are provided, as well as if there is any significant difference in the performance between the two types.

3.2 Methods

3.2.1 Modeling Human Operator in the Closed – Control System (CLS)

Modeling the human operator using the control theory methods has been widely investigated. Nowadays, it shows an elevated potential in providing information about human execution; additionally, it helps in predicting the performance of human-machine systems. The aim is to obtain approximate transfer functions of the human operator using linear differential equations [85]. , no physical system is linear; a linear analysis could provide a profound understanding about the human execution [83]. Knowing the input and system dynamics the approximate human response could be predicted knowing the input and the dynamics of the system [86]. Similarly, the prosthetic user will be considered a human operator who controls a dynamic system. Based on this parallelism, the principles of control theory could be applied to prosthesis control.

Dosen et al [84], have constructed a Closed-Loop System toolbox (CLS) to configure and test the closed-loop human control system in standardized settings (Figure 3.1). The aforementioned toolbox has developed in Simulink MATLAB. Using this platform, we modeled and implemented the dynamic close-loop compensatory tracking system.

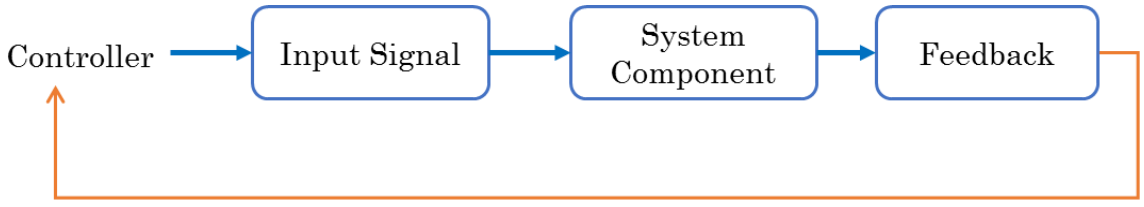

Figure 3.1 The general structure of the closed loop system.

3.2.2 Compensatory Tracking Closed – Loop System

The tracking task is considered as the most elementary manual-control task that allows measuring the frequency response of humans. The human operator needs to minimize the error e(t) between the reference trajectory r(t) and the generated trajectory y(t). The user drives a controller u(t), usually a joystick, to compensate the error [83] [86]. Different classes could be used to manifest the tracking task [87], yet the most frequently used task is the compensatory mode. In the compensatory mode exists a fixed target on the center of the screen and a controlled object that moves proportionally with the tracking error. The latter is compensated using a joystick to place the controlled object back to the fixed target. Figure 3.2 illustrates the tracking task and the error.

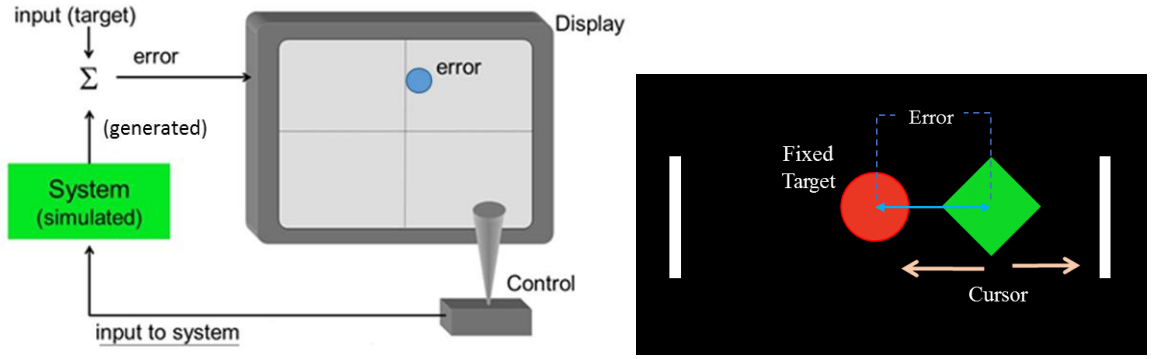

Figure 3.2 Illustration of manual – control task (compensatory tracking task). Left: the controller uses the joystick to compensate the error which the difference between the target and the controlled trajectory, Right: The black box represents the PC screen, two graphical indicators, the red is fixed and the green is the controlled, the error is the distance between the two indicators.

Figure 3.3 depicts a conventional illustration of one-dimensional compensatory tracking system. The human operator is represented as Y_H and the controlled process or plant as Y_P.

The main elements of the compensatory closed-loop system are the human operator, the controlled process and the frequency response. Hereby and below, a brief description is presented.

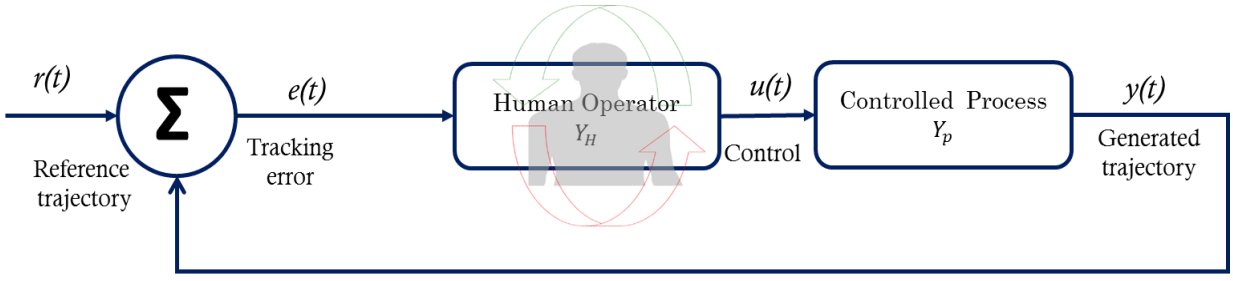

Figure 3.3 Block diagram of the one-dimensional compensatory tracking system

a) Human operator

To obtain a linear model of the human operator, three properties need to be taken into account. The time delay (τ) which indicates the human reaction time (i.e. neural synaptic delays, nerve conduction, and central processing), the gain ($K = Y_H Y_p$) is a scaling factor that determines the speed of response of the control loop (i.e. higher gain, faster response). The gain value affects the bandwidth of the control system also [83]. The lag ($\frac{1}{T_1 jw+1}$) or integrator ($\frac{1}{jw}$) indicates low pass characteristics in the human operator (i.e. low frequency components of error are considered while high frequency components are removed). The model for the human for a position control can be written as:

$$Y_H = \frac{Ke^{(-\tau jw)}}{T_1 j\omega + 1} \quad \textbf{(3.1)}$$

The transfer function and the human frequency response can be studied for different dynamic systems. The transfer function of human operators changes with the dynamic system, due to their adaptive performance. Nevertheless, the transfer function for the closed-loop systems is similar. Hence, the human operator ensures the stability of the closed-loop system [83] [86].

b) Controlled Process

Zero-order or position control is a system with no integrators, in which the relation between the input of the control signal *u(t)* is proportional to the output *y(t)* of Y_p . It is a simple gain whose value is the scaling factor between the movement of the controller and the displacement of the controlled object in the compensatory tracking task [83]. The mouse control of a computer is usually a position control, the cursor on the screen moves proportionally to the displacement of the mouse and no movement is transmitted when the mouse displacement stops. The scaling factor, which determines the relationship between the movements of the mouse respect to the cursor on the screen, is adjusted through the gain value. High values of the gain will be translated in large displacement of the cursor and vice-versa [83].

c) Frequency response

The Bode plot is a representation of the performance of a dynamic system in the frequency domain [83]. Figure 3.4- a, illustrates the human frequency response of compensatory tracking system with zero-order or position-controlled process. The amplitude response seems to be altered for lower frequencies and approaches to a slope of -20 dB at higher frequencies. This is characteristics of integration. The phase response follows the pattern of a time delay, the phase lag increases with the frequency. Therefore, the Bode diagram depicts that the human operator is a combination of a gain, an integrator and a time delay.

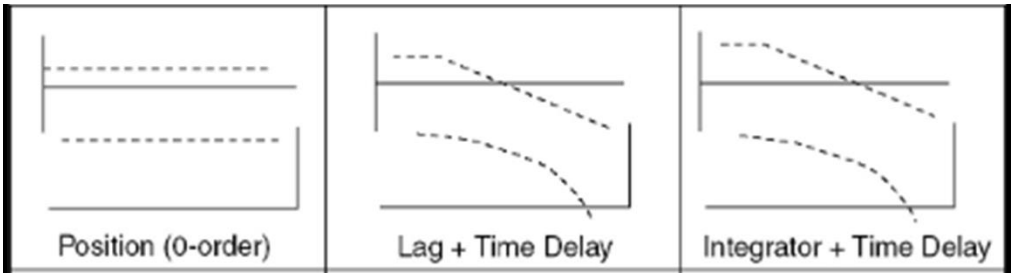

Figure 3.4 Illustration of the frequency response. Top: the amplitude ratio, Bottom: the phase shift. The position control or zero-order control is represented for (a) Controlled process, (b) Human operator and (c) the close-loop system

3.2.3 Participants

Thirteen healthy subjects (11 males and 2 females, mean age: 28.5 ±2.97 years) from Aalborg University were recruited for the final study (see Table 3.1) after conducting multiple pilot tests to optimize the testing protocol and outcome of the study. All the participants were right-handed. A specific inclusion and exclusion criteria reported below were applied. Prior to the experiments, each participant signed informed consent. In addition, a case report was prepared and filled up about each subject. The North Denmark Region Committee on Health Research Ethics (N-20160021) has approved the testing protocol. (See appendix A for the consent and the case report)

Inclusion Criteria:

- Subjects age between 18 - 50 years.
- No reported physical and/ or mental diseases(s) or major surgery that might limit participation in or completion of the study.

Exclusion criteria:

- Poor skin condition that prevents the use of self-adhesive electrodes.
- Patients with heart diseases or have a pacemaker.
- Patients with a cancerous tumor in the area of electrotactile stimulation.
- Patients with exposed orthopedic metal work in the area of electrical stimulation.
- Pregnancy.

Table 3.1 Basic Participants Characteristics

Number	13
Sex (m/f)	11/2
Age (SD)	28.5 (3)
Familiarity with Electrotactile stimulation (yes/no)	4/9

3.2.4 Study Design

A crucial aspect of the close-loop control in prosthetics is the timing of the feedback. The latency is expressed as the variation between the output stimuli in correspondence to sensory input. It should be as short as possible for an effective volitional use of the transmitted information. In addition, shorter latencies are useful to develop a sense of embodiment of the prosthesis (body ownership) of the prosthesis. Therefore, it is reasonable to avoid increasing this value significantly and ignoring its effect on the subject's performance. In order to simulate this latency which is inevitable in different closed-loop prosthetic systems. Moreover, to understand the temporal delays ranges that the user supports without the impairment of the delivery of artificial sensory feedback. An in-set latency was added to the control process, it is implemented by a time block and expressed in the block diagram as Δt.

In this study, the subjects perform a real-time compensatory tracking of a pseudorandom multi sine trajectory with a joystick after introducing different temporal delays (i.e. in-set latency that expressed as Δt) to the control process. As feedback, the tracking error e(t) i.e. the difference between the reference r(t) and the generated trajectory y(t), conveyed to the subject via either tactile feedback (by electrotactile stimulation) or visual feedback. The tracking performance was

analyzed in the time and frequency domain. The time analysis yielded information about the gross tracking quality while the frequency analysis assessed how well each individual frequency component of the reference multi sine signal was tracked (i.e. how strong the signal containing the respective frequency component was amplified/attenuated by the subject). The participants were asked to take part in two interchangeable experimental sessions performed either in two consecutive days (day 1, day 2) or on the same day (morning, afternoon). Figure 3.5 illustrates the close-loop compensatory tracking system with in-set latency introduced to the controlled process.

Table 3.2 Study Design Overview

Session 1	Session 2
Day 1	Day 2
Morning	Afternoon
60 min	45 min
Electrotactile Feedback	Visual Feedback

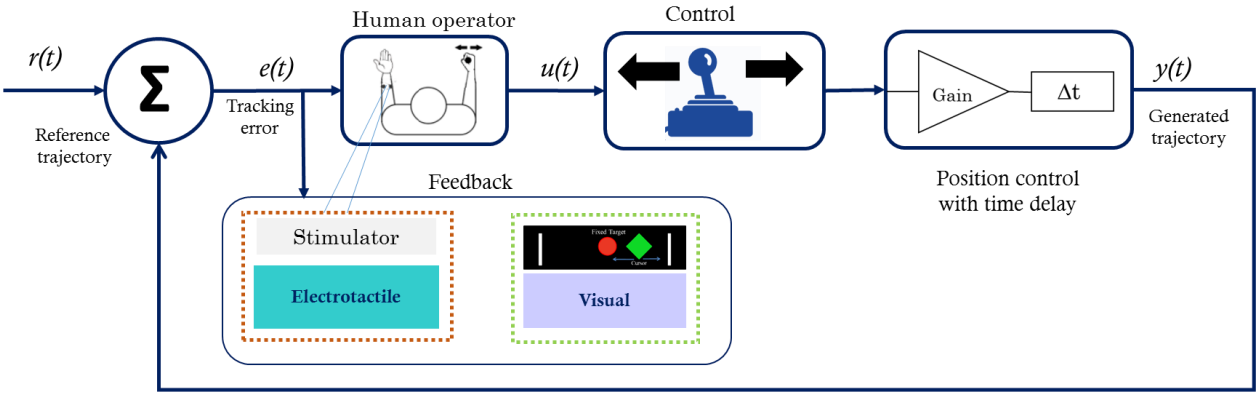

Figure 3.5 Compensatory tracking experimental setup with in-set latency in a closed loop system with either electrotactile feedback or visual feedback. The reference trajectory is r(t), y(t) is the generated trajectory, e(t) is the tracking error and u(t) is the control signal. The error was transmitted either using visual feedback or electrical feedback. The stimulator provided electrotactile stimulation through the electrodes placed in the forearm, while the monitor display provided the visual feedback. The joystick acts as controller and it transmits the commands to compensate the tracking error.

3.2.5 Experimental Setup

The testing setup includes a multichannel electrical stimulator (TremUNA, UNA systems) connected to two surface electrodes to convey electrical stimulation, joystick (APEM HF22X10U), a standard desktop computer equipped with a 24" monitor and the Matlab Simulink software as shown in Figure 3.6- a. It has been implemented in a close-loop compensatory tracking system. The subject has to follow a predefined reference trajectory by using the joystick as a controller. Both the reference signal and the generated trajectory were invisible for the participant during the experiment. On one hand, the two DOF joystick (APEM HF22X10U) has been connected to a PC with USB. It allows the movements along two axes, yet only one axis has been chosen (i.e. horizontal axis, either to the right or to the left) in order to perform the compensatory tracking task of the error (i.e. the difference between the reference trajectory and the output of the system) which in turn was provided either by visual feedback on the monitor or electrotactile feedback.

On the other hand, a fully programmable multichannel electrotactile stimulator (TremUNA, UNA systems) has been used to deliver electrical stimulation to the subjects. The stimulator is battery powered with eight channels; it generates current-controlled biphasic compensated pluses that range from 0-5mA. Two channels were selected to deliver the electrotactile feedback via two self-adhesive concentric electrodes (Spes Medica, 50mm x 50

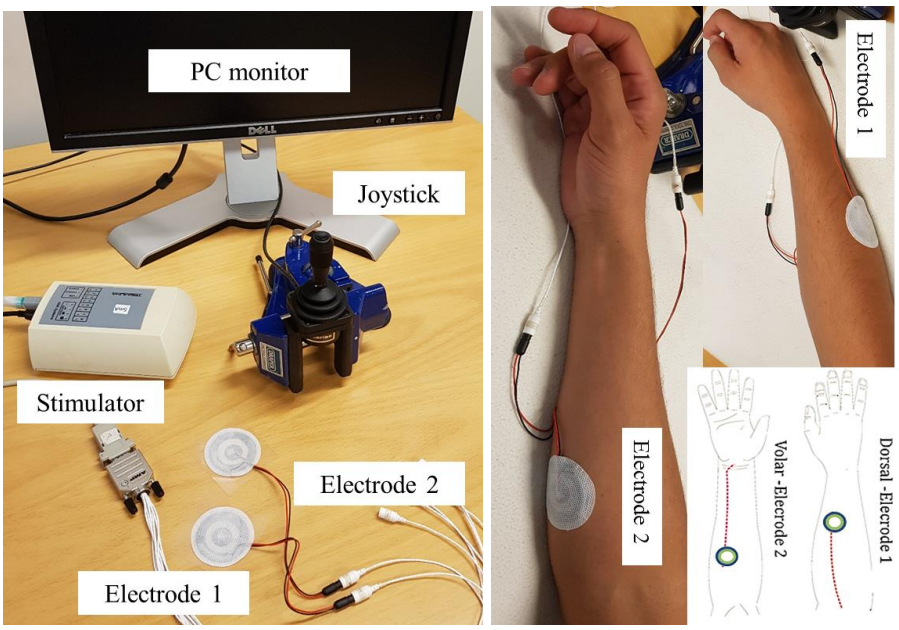

(a) **(b)**

Figure 3.6 Experimental setup elements and electrode mounting for electrotactile stimulation

mm) mounted on the forearm of the dominant hand. Electrode 1 used to map the positive tracking errors, it was mounted on the dorsal side of the forearm halfway between the wrist and the elbow; while Electrode 2 maps the negative tracking errors, it was mounted on the volar side of the forearm at one-third of the length of the forearm from the elbow as shown in Figure 3.6-b. The mounting position has been selected after several pilot studies that aimed to deliver intuitive feedback to the user while having clear sensation on both sides of the arm. The pulse width and the intensity for each channel can be adjusted independently, whereas the pulse rate was fixed (70 Hz) as it will be explained in the testing procedure. A Simulink model developed in Simulink MATLAB (2017b) using a toolbox for closed-loop human manual control [84]was employed to implement the prosthetic control within a close-loop compensatory tracking task with both the visual and electrotactile feedback as this study also focuses on the feasibility of artificial sensory feedback. It generates the reference signal or the forcing function. This function should appear random to prevent the operator from predicting the future behavior of the target unless the real-world control task consists of highly predictable signals. It has been shown that the sum of 5 or more sine waves is unpredictable to human operators [88]. The operator used the joystick as a simple interface to translate his/her control commands to the system while receiving feedback (visual or electrotactile) about his/her tracking error. Additionally, the visual interface used a custom block from the Simulink model. Two graphical markers, a red static circular target and a green dynamic rhombus represent whose x coordinate is proportional to the tracking error. The latter is the dynamic to be controlled in order to compensate the tracking error after introduction random delays. Moreover, the stimulation parameters have been regulated in real time through the same toolbox whether a graphical interface was developed to determine the thresholds of stimulation such as sensation, discomfort, and pain thresholds, pulse width, pulse rate, etc. The two electrodes electrode 1 and electrode 2 maps the positive and the negative tracking errors respectively. The electric stimulation conveyed proportionally to the tracking error while being frequency modulated. Figure 3.8 represents the experimental setup arrangement.

3.3 Experimental Procedure

The subject was seated comfortably on a chair in front of table with computer screen in a quiet environment. Starting by explaining the experimental task, the subject was asked to track a predefined target trajectory with a control signal that reflected the movement of the joystick in a proportional way. A pseudorandom multi-sine target trajectory was presented for 60 sec in

each trail; it was obtained by the summation of nine sine waves with linearly spaced frequencies of unit amplitude and frequency bandwidth (0.01-1 Hz) and random phases as shown in Figure 3.7. The frequencies of the sine waves were selected by logarithmically dividing the range between 0.2 and 4 rad/s. The trajectory was constructed by repeating the same 30-s segment two times. The basic 30-s segment was generated a new in each trial and it was long enough for the subjects not to notice the repetition and therefore experience the trajectory as essentially random. Its amplitude was normalized to the range [-0.9, 0.9]. The feedback transmitted to the subject provides the momentary tracking error and the subject's task is to compensate (nullify) this error by moving the joystick in the required direction.

Following the testing protocol, presented in Figure 3.10, the experiment has been divided mainly into two testing sessions as explained below.

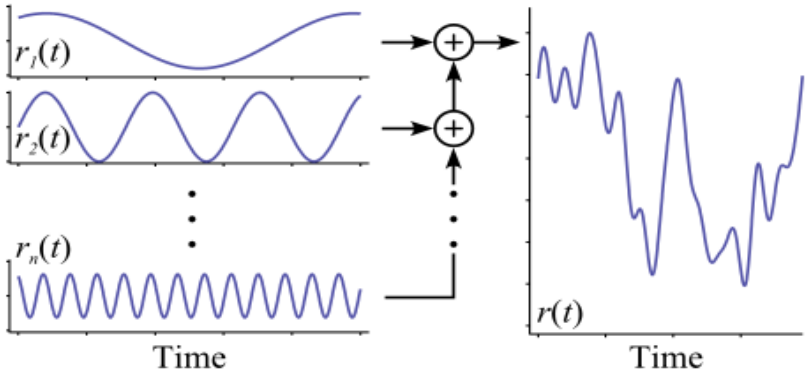

Figure 3.7 Summed-sine forcing function. We used nine sine waves, each with a different phase

Session 1: Compensation with visual feedback

The compensation with visual feedback session consists of two phases: (a) training phase 1 and (b) testing phase 1. It lasts for 45 minutes.

Training phase 1:

First, the procedure has been explained verbally to the subject. Then, the subject was familiarized with the tracking task by providing visual feedback on the PC screen. Two trails at 0 sec delay, each one lasts for 60 secs and separated by 1 min pause, been used for training the subject. A green marker deviated from the red vertical line proportionally to the normalized tracking error. If the tracking error reached extreme values of 1 and -1, the marker would hit the limits of the tracking area. The participant was instructed to move the joystick in order to cancel the disturbance (tracking error) and maintain the green marker, as near as possible, at the reference line. To this aim, the subject was supposed to move the joystick in the opposite

direction to the movement of the marker proportionally to the magnitude of the deviation (so called position-controlled system).

Testing phase 1:

Afterward, the testing phase 1 starts, five different time delays (i.e. 0, 0.2, 0.4, 0.8, 1.2 sec) were added to the control system system and introduced to the subject in pseudorandom order through fifteen trails, while the subject tracking the error solely using visual feedback. The order of the dynamic system was randomized between the

Subjects yet ensuring an equal distribution of the different introduced delays. Each delay was presented 3 times throughout the testing phase. The different time delays have been chosen after several pilot tests that investigate the minimum time delay where the subjects tracking performance deteriorates. Throughout the course of the experiment, the subject seated facing the monitor and the joystick, while the arm of the dominant hand laid on the table for a comfortable position.

Session 2: Compensation with electrotactile feedback

The compensation with electrotactile feedback session consists of three phases: (a) Threshold recording, (b) Training phase 2, and (c) Testing phase 2 as explained in the following. It lasts for around 1 hour.

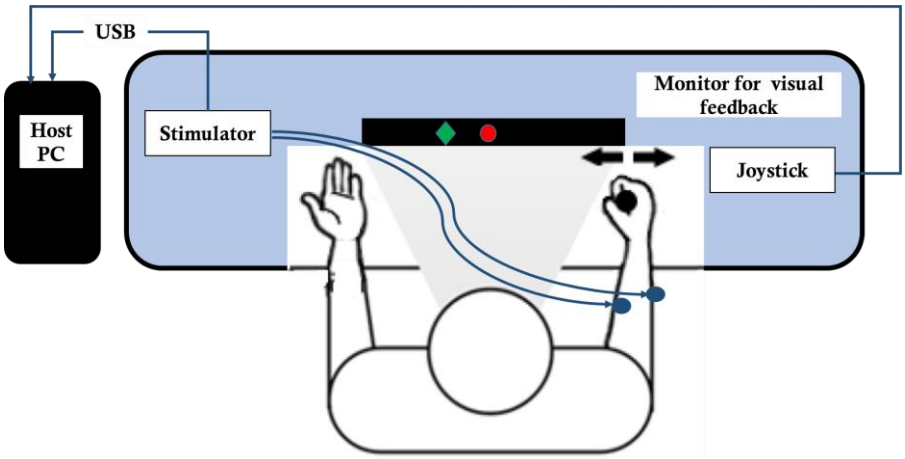

Figure 3.8 Block diagram of the experimental setup. Depending on the testing scenario, the subjects were provided either by visual feedback displayed on the monitor in front of them or by electrotactile feedback delivered via two electrodes mounted on the dominant hand in which the subject is controlling the joystick. The visual feedback consisted of a green rhombus displaying the tracking error. It moved on the horizontal axis in a defined range. The red circle is placed at the zero point to clearly indicate the area where the green rhombus should optimally be (i.e. where the tracking error is smaller than 5%). The electrotactile feedback consisted of two electrodes placed on the dorsal and volar sides of the forearm to track both positive and negative tracking error respectively.

Threshold Recording and Adjustment

Before mounting the electrodes, the skin of the forearm was cleaned by alcohol wasps in order to remove grease that may change the conductivity. As long as, we aim to apply electrotactile sensory feedback on the amputee, the position of the electrodes had to be chosen carefully. Regarding the previous, we had to take into consideration the easiness of differential identification between the dorsal and volar sides. Afterward, using the developed graphical interface in MATLAB, the sensation threshold (ST), discomfort (DT) and the pain thresholds (PT) were recorded following the method of limits. The ST represents the first detectable current intensity. The DT represents the current amplitude starts to irritate/ annoy the subject, while the PT is the minimum current intensity where the subjects perceives pain. The pulse width was incremented in steps of 50 us while the frequency and amplitude were set to 70 Hz and 35 mA, respectively. A pulse width (PW) parameter modulation has been applied, where the PW starts at 50 μs stimulation and last for 2 seconds then followed by 1 second break. A 10 μs step increase has been applied until the ST was reached, afterward the pulse width increases in a step of 50 μsec until the DT was detected. The last step has been used also to determine the PT. For each electrode, the thresholds recoding has repeated three times and the computed average was used to electro-stimulate the subject.

Training Phase 2

In the training phase 2, the electrotactile feedback reflecting the tracking error was conducted via the two electrodes simultaneously with the visual feedback aiming to teach the subject to properly interpret the elicited tactile sensation. The two electrodes communicated the sign (electrode) and magnitude (stimulation frequency) of the normalized tracking error. The activation of the electrode positioned on the ventral side of the forearm indicated a negative tracking error, while the electrode on the dorsal side signaled positive tracking error. The magnitude of the error was linearly mapped by modulating the frequency of the stimulation. The frequency increased if the controlled object was remote from the fixed target position and decreased if the controlled object was closer to the fixed target position. Consequently, no sensation was perceived when the controlled object was on the target, denoting good tracking performance. The pulse width was set to 80% of the pain threshold, while the frequency was changed in the range between 7 and 63 Hz. The subject performed four training trails at 0sec time delay, which in turn distributed into two hybrid trails (i.e. receiving both visual and electrotactile stimulation) and two electrotactile trails (i.e. no visual feedback) as showing in

Figure 3.9. The hybrid tracking with simultaneous electrotactile and visual feedback, allows the subjects to learn how to relate the movement of the marker to the pattern of electrical stimulation delivered through two electrodes, as explained above. The training trials were separated from each other with a 1-minute pause.

Testing phase 2

After the training phase, the subject starts the close-loop tracking using only electrotactile feedback (i.e.no visual display); the same number of trails and delays were tested (15 trails with randomized order, where each delay presented three times). The strategy for successful tracking was similar to that applied during the visual feedback. In case the participant felt the stimulation on the dorsal side (electrode 1 activated) or on the ventral side (electrode 2 activated), he/she needs to move the joystick to the opposite direction and the magnitude of the joystick movement was proportional to the intensity (i.e. pulse width modulation).

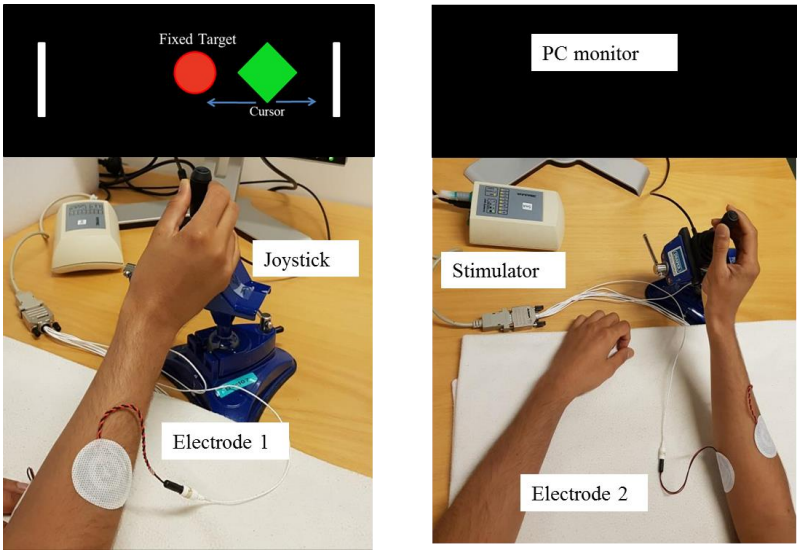

Figure 3.9 Subject performing the compensatory tracking with electrotactile feedback: a) during the training phase with hybrid feedback (i.e. while receiving both visual and electrotactile at the same time), b) during the testing phase only with electrotactile feedback (no visual feedback at all).

3.4 Data Analysis

With the main aim of proving the usability of electrotactile feedback in enabling closed-loop control in prosthetics. It evaluates the subject tolerance for different introduced time delays while performing a dynamic control task. In addition, it compares the performance quality of human manual control through a closed-loop compensatory tracking system while using two feedback schemes (i.e. visual and electrotactile feedback). More specifically, this study reflects

more accurately the tractable and responsive ability of subjects while receiving different feedback types (electrotactile feedback vs. visual feedback) in prosthesis control.

Several methods could be used to quantify the quality of the compensatory tracking system. The data analysis of the collected data from the experimental sessions was implemented in MATLAB (R2017b). The analyzed signals are the reference trajectory *r(t)*, the output trajectory *y(t)*, the error $e(t) = r(t) - y(t)$, which is the difference between the previously mentioned signals and the control signal *u(t)* from the joystick.

Two outcome measures were evaluated; the correlation coefficient CORR (peak of cross-correlation function) and the root mean square error (RMSE). The CORR was established computing the cross-correlation coefficient, which evaluates the similarity between the reference *r(t)* and the output trajectory *y(t).* It has been calculated for each subject and for each applied trail, then the average of the three repetition for each time delay (i.e. $t_1 = 0$ *sec,* $t_2 = 0.2$ *sec,* $t_3 = 0.4$ *sec,* $t_4 = 0.8$ *sec and* $t_5 = 1.2$ *sec).* Similarly, following the same procedure explained previously, the

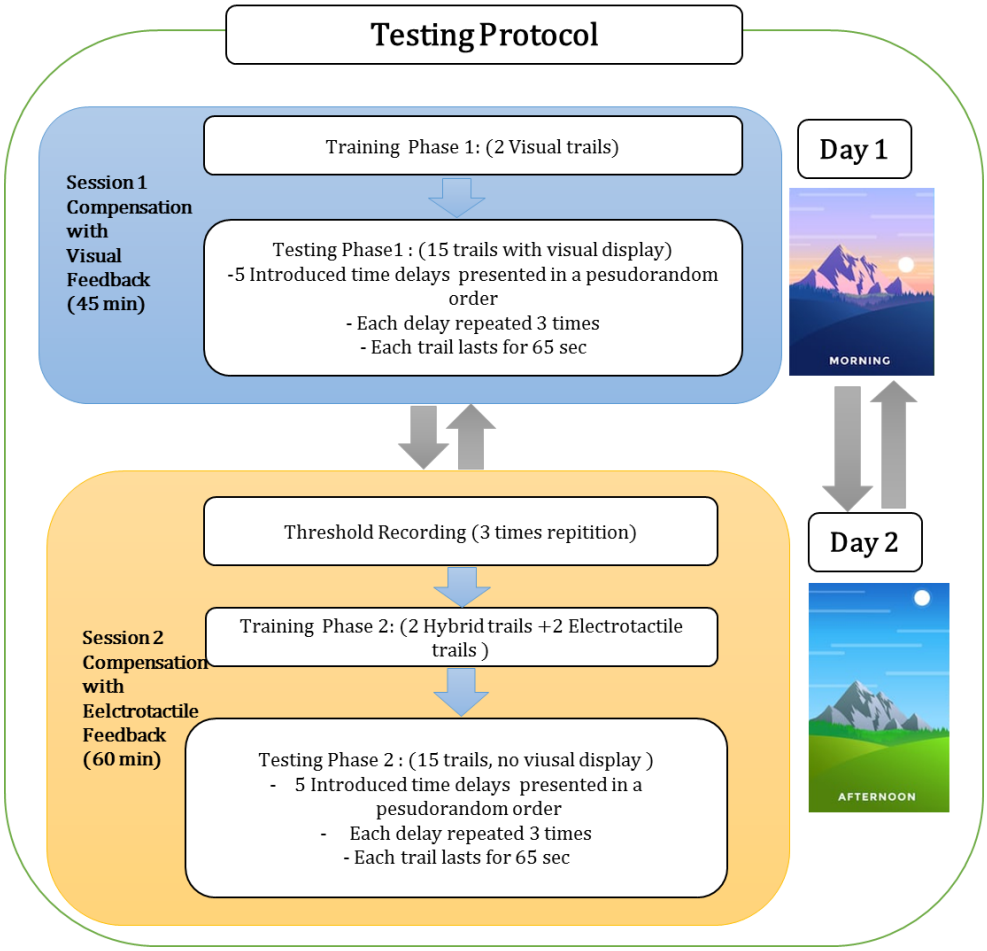

Figure 3.10 Testing protocol summary

RMSE were calculated. The RMSE used to evaluate the average amplitude difference. Hence, the CORR and the RMSE indices, determines how efficiently the subject reproduces the reference trajectory. Moreover, it shows how much the subjects supports and adapts to the delays introduced to the controlled process in the dynamic closed-loop system. Consequently, the higher the correlation and the lower RMSE values the better the performance in the close loop compensatory tracking system.

3.5 Results Summary

Figure. 3.11 depicts two representative tracking trails from the tested conditions. It shows that best tracking occurs with visual feedback, while with electrotactile feedback the tracking fitting with reference signal deteriorates especially with long time delays.

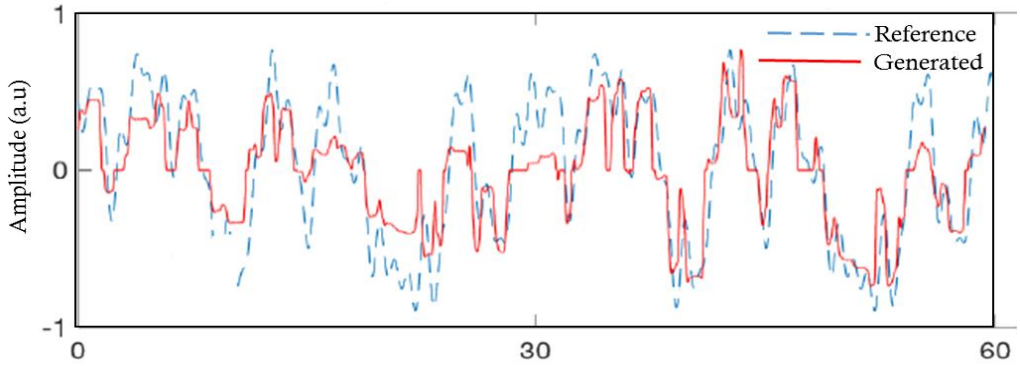

(a)

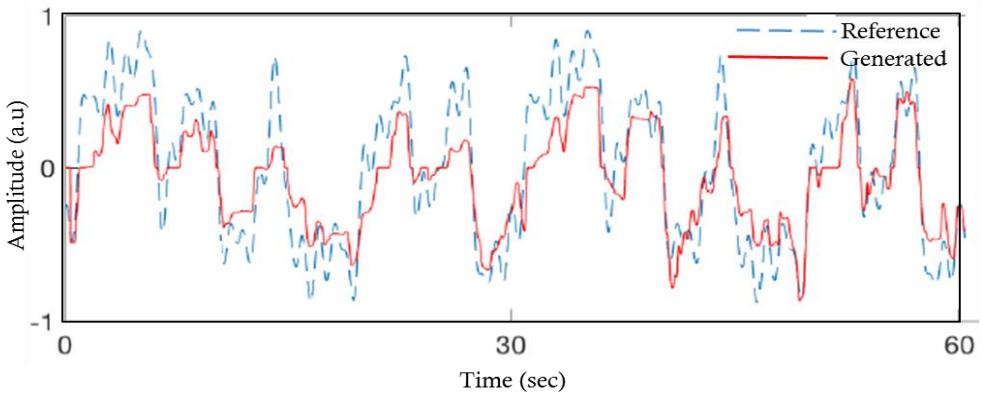

(b)

Figure 3.11 Two exemplary representative performance at time delay t= 0sec of one subject. The blue dashed line and the solid red line represents the reference trajectory and the generated trajectory respectively. a) Top: Compensatory tracking with visual feedback (CORR=91.45, RMSE = 0.2), b) Compensatory tracking with electrotactile feedback (CORR= 91, RMSE=0.24)

Figure 3.12 and Figure 3.13 depicts the overall average results (CORR and RMSE) of the tracking trails from the tested conditions during the two compensation sessions of time inserted time delays in the dynamic close loop with electrotactile and visual feedback. It shows that best tracking occurs with visual feedback, while with electrotactile feedback the tracking fitting with reference signal deteriorate especially with long time delays.

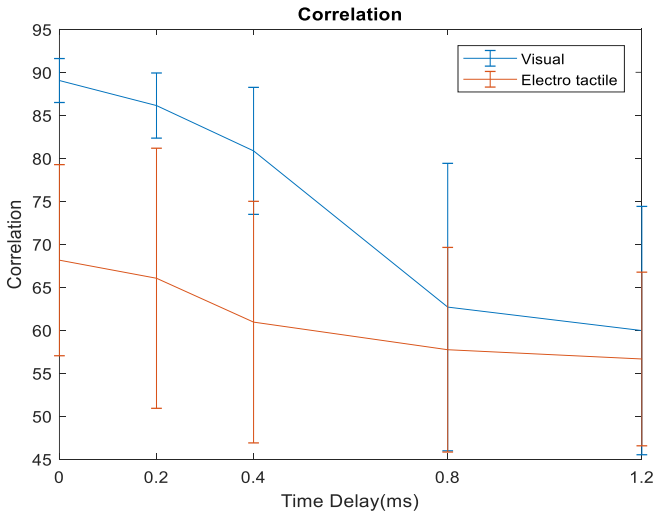

Figure 3.12 The overall average correlation across the subjects for different in-set latency time delays (t1 =0 sec, t2 =0.2 sec, t3 =0.4 sec, t4 = 0.8 sec and t5 =1.2 sec). The red line represents the compensation using electrotactile feedback and the blue line represents the compensation using visual feedback.

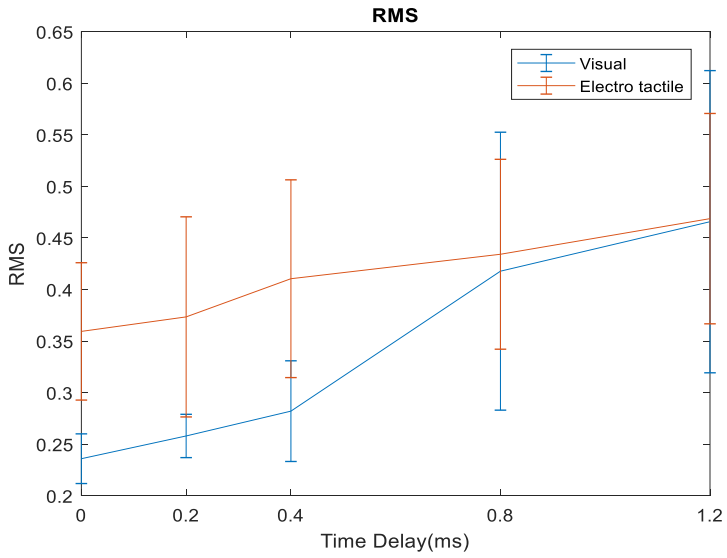

Figure 3.13 The overall average RMSE across the subjects for different introduced time delays (t1 =0 sec, t2 =0.2 sec, t3 =0.4 sec, t4 = 0.8 sec and t5 =1.2 sec). The red line represents the compensation using electrotactile feedback and the blue line represents the compensation using visual feedback.

3.6 Discussion

The experimental results show that tracking using visual feedback enables better control with no delay (0 sec), while tracking using electrotactile feedback is less susceptible to delays. Moreover, the outcomes have shown that electrotactile feedback performance is less prone to changes with longer delays. However, visual feedback drops faster than electrotactile with increased time delays. This is a good indication for the effectiveness of electrotactile feedback in enabling close- loop control in prosthetics since some delays are inevitable. In another flip, the constant performance of electrotactile feedback could assist the user in performing dynamic and continuous tasks in real-time (such as holding a cup of coffee over the time needed to drink it), which may raise the embodiment rate and acceptance of the protheses.

3.7 Conclusion

Latter day hand prostheses lack sensory feedback that impairs closed-loop control and embodiment. Several techniques have been proposed to reconstruct sensory feedback for prosthetics in order to correct and enhance multifunctional control performance, as vision alone does not offer enough information. Providing sensory feedback through sensory substitution by electrotactile stimulation has been widely investigated. However, the assessment of tractable time delay and responsive ability of subjects while receiving electrotactile feedback in a closed-loop dynamic task has rarely tested. The study presented in this chapter explains the concept of closed-loop control; it aims to assess the performance of the human operator in a position control system while receiving two different feedback schemes. A close-loop compensatory tracking system that simulates the prosthesis control is to be presented and implemented using the developed CLS toolbox in Simulink MATLAB. The reported results demonstrate that tracking using visual feedback enables better control with no delay, while tracking using electrotactile feedback is less susceptible to delays. This in turn, is a good indication for the usability of electrotactile feedback in prosthetic control, since some level of delay is inevitable.

Chapter 4 Multichannel Electrotactile Stimulation System for Restoration of Sensory Information

4.1 Introduction

Restoring sensory feedback is a long-standing challenge in prosthetic research [89], [42]. Modern myoelectric prostheses respond to electrical muscle activity and thereby restore lost motor functions, but the amputee users still do not "feel" their artificial limbs. Apart from a single recent example [7], commercial prostheses do not provide somatosensory feedback to the user. Therefore, the replacement is only partial. Such an issue is critical since sensory feedback is necessary for the motor control in able-bodied subjects, especially during dexterous activities such as manipulation and grasping [90].

The topic of sensory feedback in prosthetics has being investigated intensively in recent years [91], [43], [17], [9], [8]. Several sophisticated systems rely on direct neural stimulation to elicit tactile sensations [40], [92], [93], [94]. These approaches usually deliver feedback somatotopically, by activating the same sensory structures that were in charge of the feedback before amputation (e.g., a contact on prosthesis finger feels as touch on phantom finger). Preliminary results are promising [92], but more extensive studies on humans are needed to understand how to effectively and safely stimulate afferent pathways of the human nervous system to provide clinically usable sensory feedback. Moreover, these approaches are invasive and require a surgical procedure, which may affect their acceptance by prosthesis users.

Non-invasive sensory feedback systems could-be proven as an interesting alternative to invasive solutions. The implicit assumption is that it might not be necessary for an artificial system to exactly restore the biological information transmission, provided that an intuitive communication between the prosthetic device and the human brain is established (sensory substitution). The study described afterward in this chapter focuses on non-invasive systems for

sensory restoration. With respect to previous studies, it focuses on increasing the information transfer by associating the stimulation not to a simple physical variable (such as force) but to complex sensations (such as the location of touch).

Traditionally, the non-invasive sensory feedback systems rely on a few discrete sensing and stimulation units [43] [8]. In a commonly used approach, a sensor is used to measure a global prosthesis variable (e.g. overall grasping force), and this information is then transmitted to the prosthesis user through a single stimulation unit, which can be a vibration motor or an electrode placed on the residual limb [8] [95]. The intensity and/or frequency of stimulation is modulated according to the measured variable. For example, the higher the grasping force, the higher is the stimulation intensity delivered to the user, which leads to a stronger tactile sensation [96]. The user needs to learn to associate the elicited sensation to the measured variable. The latter could be a challenging task to learn, and typically, only few levels of grasping force/hand aperture can be reliably communicated [97] [98] [99] [100].

The contemporary methods for feedback restoration are therefore characterized by a limited information transfer. To mitigate this drawback, feedback interfaces comprising several stimulation units have been proposed. In principle, multichannel stimulation could allow to better exploit the inherent potential of the human skin as the feedback stimulation can be distributed over a large skin area (spatial coding). For example, an array of vibration motors has been previously used to communicate hand aperture [101] and grasping force [102] feedback. Advanced interfaces for electrotactile stimulation integrating multiple electrode pads have also been recently tested [103]. In [58], an electrode array integrating 16 pads placed circumferentially around the forearm was employed to deliver force feedback from Michelangelo Hand prosthesis. A matrix electrode with 4 x 8 pads has been used to transmit tactile data recorded by an e-skin to the subject forearm [104]. The tactile data recorded by four neighboring taxels were fused and delivered through a spatially-congruent electrode pad. The spatial coding and artificial skin were used in another experiment [105] where the stimulation was delivered through a 4 x 2 arrangement of conventional self-adhesive concentric electrodes. Preliminary experiments on the ability to localize touch delivered to the artificial skin by identifying the elicited electrotactile sensation have been performed in two subjects. These studies have shown the potential of multichannel electrical stimulation, however, they also pointed out that spatial localization is a challenging task, especially considering the low density of tactile receptors on the human forearm (stimulation target in hand prosthetics).

This chapter presents the study of assessing the reliability of information transmission while using non-invasive interfaces with many stimulation points. We used a novel, compact electrotactile interface in the form of a dense 6x4-electrode matrix printed on a flexible substrate (11 x 5 cm2). An electrode matrix is particularly suited for transmitting tactile information from an artificial skin covering the prosthetic device, as demonstrated in our previous study [104]. However, a compact interface where the pads are closely situated can be challenging specifically when the subject's task is localizing the tactile stimulus. Good spatial localization is salient for transmitting more accurate tactile information to the prosthesis user (e.g., contact location) or for conveying other prosthesis variables using spatial coding (e.g., aperture [101]). Wherefore, this study investigates the improvement of the quality of localization by exploiting parameter modulation flexibility provided by the electrotactile interface. The electrotactile stimulation allows independent modulation of intensity and frequency, while these parameters are intrinsically coupled in commonly used vibration motors [106]. We have therefore developed and tested a dual-parameter modulation scheme (intensity and frequency) for assisting the subject in correctly identifying an active pad within the matrix. Furthermore, for the first time, the performance of a matrix electrotactile interface is compared to that of the human skin computer-controlled over analogous contact areas.

In this vein, Section 4.2 describes the materials and the methods used for testing the subjects. Then, Section 4.3 addresses the experimental procedure. The collected data analysis and the results are presented in Sections 4.4 and 4.5 respectively. Finally, the discussion is provided in Section 4.6, followed by section 4.7 which we presents the use and integration of virtual reality with the developed sensory feedback system. At last, a conclusion is presented in this respect.

4.2 Materials and Methods

4.2.1 Simulation Setup

A fully programmable computer- controlled stimulator prototype (IntFES- ver2 MAXSENS) developed by Tecnalia Research and Innovation, Serbia was used to generate electrotactile stimulation profiles which in turn will be delivered to the subject's forearm through a flexible matrix of electrodes. The stimulator is battery-powered; it generates symmetric and current-controlled pulses with pulse intensity in the range of 0-5mA with 0.1mA step, frequency from 1 to 400 Hz with 1Hz step, and pulse width from 50 to 1000μs with 10 μs step. Current

controlled stimulation has been selected to minimize the influence of capacitive discharge at the skin-electrode interface. Moreover, it ensures a reliable activation of the cutaneous nerves and guarantees that the nerve stimulation thereby the elicited tactile stimulation is not altered

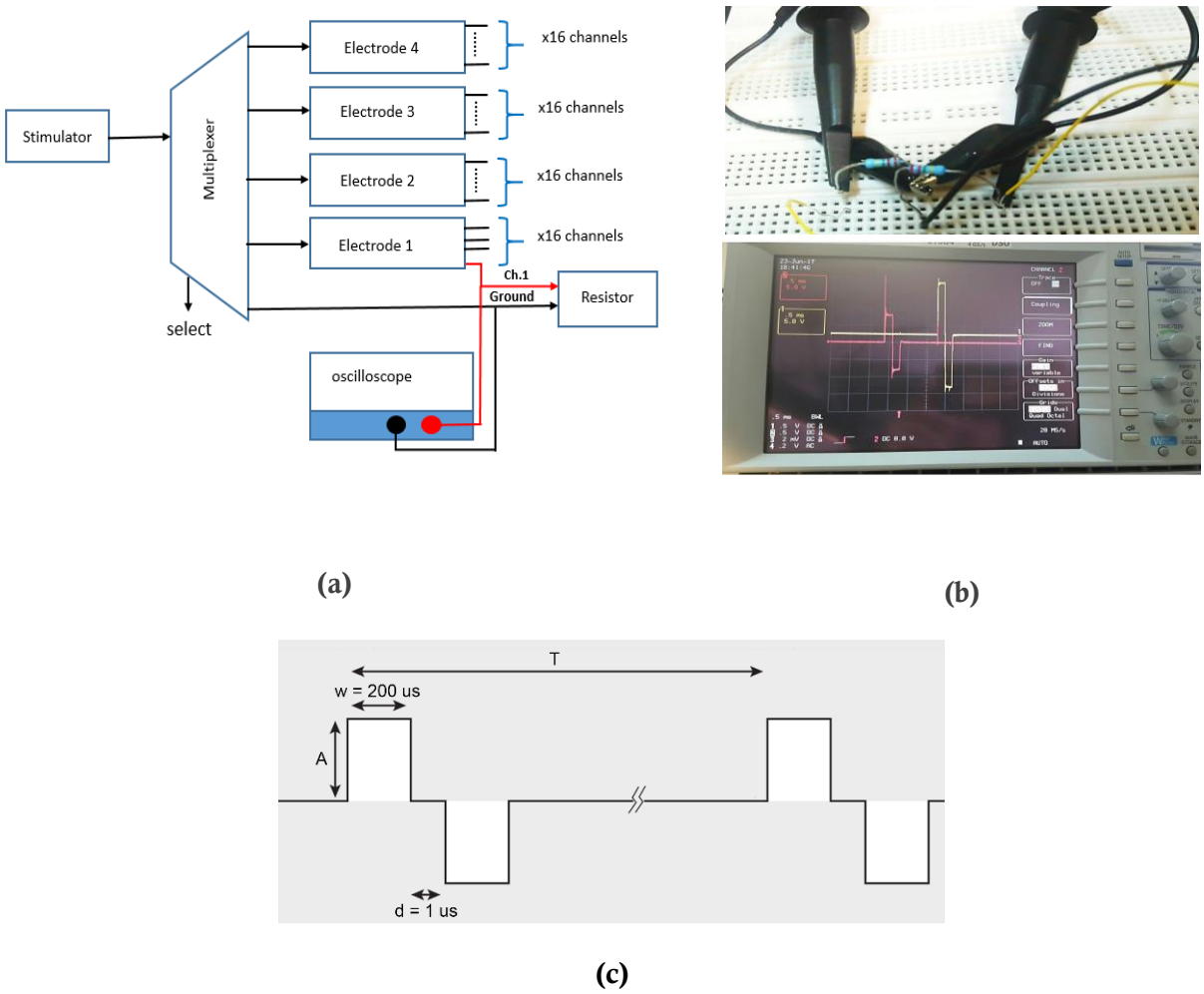

Figure 4.1 Testing setup of the stimulator and generated waveform. a) Block diagram of the testing setup, b) Real photo of the issued signals from the stimulator, c) Typical stimulation waveform. Notation: A – pulse amplitude; w – pulse width; d – inter-pulse delay; T – inter-pulse interval (pulse rate = frequency = 1/T).

throughout the experiment due to changes in skin moisture and hydrogel adhesion. It produces charge-balanced biphasic continuous electrostimulation pulses in any combination of electrodes simultaneously or individually in each electrode. Biphasic signals are commonly used for delivering tactile stimulation as it gives sensations that are more comfortable and leads to less skin reddening compared to monophasic signals [12][8]. The stimulator functionality has been confirmed by testing by an oscilloscope. Figure 4.1-a, b and c & Figure 4.2 show the testing setup of the simulator, the issued waveform, and its characteristics.

An analog multiplexer connects the stimulator to the electrode matrix. It distributes the pluses in time and space over the electrode matrix, thus forming a multichannel stimulation interface. Two custom designed flexible matrix electrodes developed by Tecnalia Research and Innovation were connected to the stimulator. Each matrix electrode consists of 16 oval units (pads) with a longitudinal radius of 5 mm and transversal radius of 3 mm. The units are arranged in a 6 x 2 grid, with 4 lateral pads (two at each side). The center-to-center distance between two adjacent pads is 20 mm and 14 mm in the longitudinal and the transversal direction respectively. Each pad is made of Ag/AgCl conductive layer and conductive hydrogel circular elements of 5-mm radius (AG730, Axelgaard, DK) are added on top of each pad to improve the electrical contact between the pad and the skin. An insulation coating is distributed on top of the electrode, excluding the pad areas. The conductive pads on the electrode matrix acted as cathodes whereas a single self-adhesive electrode (ValuTrode Foam [107]) placed on the dorsal side of the forearm operates as the common anode. The ValuTrode bottom electrode is made of glycerin, water and poly(acrylate) co-polymer. It is a well-known product on the market, recognized for its durability and multiple applications to the skin. We used the rectangular ValuTode electrode with size 5 x 9 cm2. During testing, the two flexible matrix electrodes were overlapped in their central part in order to obtain a rectangular array including 6 x 4 pads, distributed over a total area of 11 x 5 cm2. Hereafter, we will refer to this rectangular array as “the electrode matrix”. The 4 lateral pads (two at each side) were excluded in this study. The stimulation setup and electrodes dimensions are presented in Figure 4.3.

The electrode matrix was placed on the volar side of the subject forearm, while the common electrode was positioned on the dorsal side. This part of the forearm is well known in its higher tactile sensitivity and acuity. The electrotactile interface has been designed so that the spacing between the pads is higher than the spatial discrimination threshold on the forearm [108] while the number of pads is still sufficient for a flexible mapping of prospective feedback variables. For example, for an intuitive spatial mapping between contact on the prosthesis and

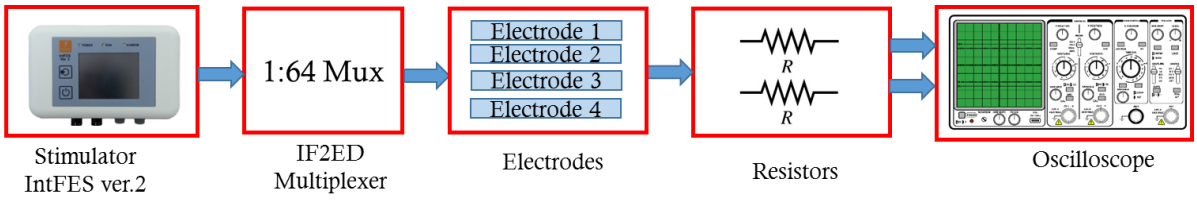

Figure 4.2 Testing chain of the stimulator

forearm stimulation, the four columns of the matrix could be associated to the four fingers (4 x 5) and the thumb could be represented on the remaining row (4 x 1).

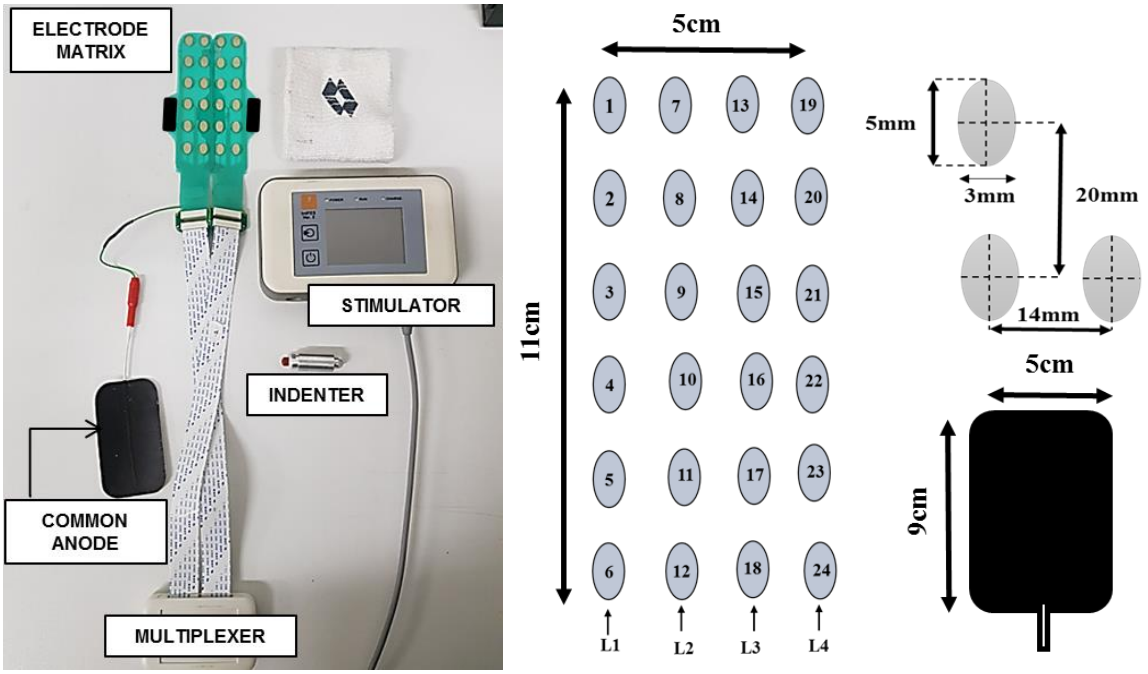

Figure 4.3 Experimental Stimulation setup: a) The indenter is used for mechanical stimulation, while all other elements are used for electrotactile stimulation experiments, b) illustration of the electrode matrix with dimensions.

4.2.2 Participants

The study was conducted in Cosmic research lab, DITEN department at University of Genoa, Italy. Eight healthy subjects participated in the final study (Table 4.1) after conducting multiple pilot tests to optimize the outcome of the study. A specific inclusion and exclusion criteria reported below were formed. Prior to the experiments, each participant signed an informed consent. The testing protocol has been approved by the Regione Liguria Ethical Committee (approval ID 172REG2016). (See Appendix B for the consent form and the protocol)

Inclusion Criteria:

- Subjects age between 18 - 65 years.
- No reported physical and/ or mental diseases(s) or major surgery that might limit participation in or completion of the study.

Exclusion criteria:

- Poor skin condition that prevents the use of self-adhesive electrodes.
- Patients with heart diseases or have pacemaker.
- Patients with a cancerous tumor in the area of electrotactile stimulation.
- Patients with exposed orthopedic metal work in the area of electrical stimulation.
- Pregnancy.

Table 4.1 Basic Participants Characteristics

Number	8
-Sex (m/f)	6/2
Age (SD)	35(±8)
Familiarity with Electrotactile stimulation (yes/no)	2/6

4.2.3 Study Design

The participants were asked to take part in two experimental sessions performed in two consecutive days. It is summarized in Table 4.2. (Refer to Appendix B for further information)

Table 4.2 Study Design Overview

Session 1	Session 2	Session 3
Day 1	Day 2	Day 2
60 -90 min	60 -90 min	30 min
Electrotactile stimulation	Electrotactile stimulation	Mechanical stimulation
Interleaved stimulation (10, 400, 10, 400 Hz)	Conventional stimulation (50 Hz)	Rubber Indenter (radius ~ 4mm)

4.2.4 Subject Preparation and Electrode Mounting

At the beginning of each session, (*phase zero*). The participant was comfortably seated on a chair in front of a table in a quite environment to avoid distraction. He/she ws asked to remove hand accessories such as rings, hand watch, etc. The skin was cleaned by an alcohol pad then moistened with a water-soaked cotton to assure better attachment of the electrodes and improve the electrical connectivity. With the forearm of the non-dominant hand (always left as all the participants were right-handed) placed on the table surface and the volar side oriented upwards, the electrode matrix was mounted on the skin of the volar side of the pre-moistened forearm of the subject at one third of the forearm length. In order to have repeatability and comparable results for different participants and for same participant over different sessions, a specific procedure has been taken for electrode matrix mounting. First, we measured the length of the forearm from the elbow to the wrist by a measuring tape. Second, the columns of the matrix were aligned with the four fingers, taking a reference point along the longitudinal direction the intersection of two specific muscles. Minutely, the intersection between the two superficial flexors, the palmaris longus and the flexor carpi ulnaris muscles has been taken as the reference position for pad number 22 as shown in Figure 4.4. The specified position was identified while asking the subject to contract the muscles of the forearm. Afterward, an adhesive bandage to prevent electrode displacement and enhance contact had wrapped the matrix.

The experimental procedure was explained to the subject and the subject received the stimulation for 5min at a self-selected comfortable intensity to familiarize him/her with electrotactile stimulation. Whenever a prickly sensation, spread or muscle contraction was reported, the electrode matrix position was adjusted by moving it few millimeters. The electrode matrix location remained fixed during the three phases for all main experimental sessions,

because the electrode location affects the perceptual thresholds and the qualitative aspects of the electrotactile percepts.

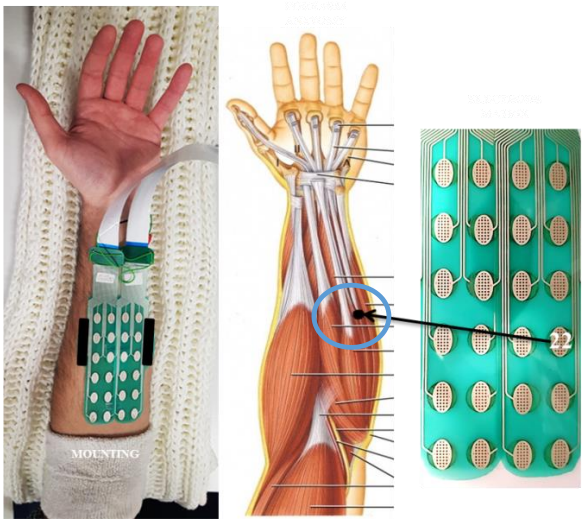

Figure 4.4 Electrode mounting. The reference position for electrode matrix is indicated by a black dot, it corresponds to the intersection between two superficial flexors, i.e. the palmaris longus and the flexor carpi ulnaris muscles. Reference pad for that position is number 22.

4.3 Experimental Procedure

The experimental procedure was implemented over two main sessions that were performed in two consecutive days. Then, session 3 was used to test mechanical stimulation too. The electric stimulation was tested using two coding schemes:

1) A conventional approach with uniform frequency (50 Hz) for all pads.

2) A dual-parameter modulation of intensity and frequency interleaved across the electrode matrix columns. This approach has been followed in order to prove that additional cues (i.e. parameter modulation) would improve the subjects' identification rate of the stimulated pad.

In the latter scheme, the pads within the columns 1-4 were activated at the frequencies of 10, 400, 10 and 400 Hz, respectively. In addition, the stimulation at 10 Hz was delivered at a lower intensity compared to 400 Hz. Therefore, the frequency and intensity were interleaved across columns of the matrix. The Interleaved stimulation or session one has been tested on Day 1, while the conventional stimulation and the mechanical stimulation respectively were tested in session two on Day 2. In the second session and after detaching the electrode matrix, we could easily see the position of the pads marked on the skin. The experimenter draws the

marked positions of the pads with a skin-friendly marker before starting the mechanical stimulation. Then, a rubber indenter (radius 4mm, contact area of approximately 8-10mm, diameter ~same size of the pad) was used to mechanically stimulate the skin of the participant. Each experimental session lasted ~1-1.5 hours and this short duration hinder fatigue and distraction of the participant.

To foster attention and concentration, a silent environment was chosen to avoid any distractions for the participant. Moreover, to maintain alertness and minimize adaptation1, the subjects were always given sufficient rest during the experiments [63], [109]. Break between the trials was around 3-4 minutes. In the second session, a break has been introduced between conventional electrical and mechanical stimulation was at least 5 minutes. After that period, the participant was asked if she/he needed a longer break. In case of an affirmative response, we added 5 more minutes of rest.

4.3.1 Testing Protocol

The aim of the experimental study is assessing the subject's ability in localizing the electrotactile stimulation delivered by the electrode matrix. Moreover, comparing the electrotactile stimulation identification rate of the subject to mechanical stimulation localization rate. Each stimulation modality (interleaved, uniform and mechanical) was testing following the same testing protocol, which in turn has been divided into three phases: Intensity adjustment, training, and testing. It is summarized in Figure 4.7.

1) **Intensity adjustment:** (*Phase 1*) subsequently to the warming up phase where the subject was prepared and the electrodes mounted, the subject was asked to define a clearly perceived stimulation intensity for each activated pad while avoiding discomfort and pain. For this purpose, the stimulation intensity has been increased gradually (steps of 0.1 mA) and the participant was asked to report when a clear sensation (mean ± standard deviation across all pads and all subjects: 1.41 ± 0.38 mA) was achieved. Then, the pad was activated/deactivated few times and the subject was asked to confirm that the sensation is indeed clear. If not, the intensity was increased for one step and the test was repeated. Due to the large number of stimulation pads (24), this procedure had to be performed only once per pad. This was nevertheless sufficient since the aim was not to reliably detect sensation threshold but to elicit sensation that can be clearly felt. The pads were activated in

a systematic way, column by column. Inside each column, adjacent pads were not activated sequentially: instead, a specific order was chosen to minimize the decrease of intensity over time, due to a prolonged stimulus (same order for all columns, referring to column 1 in Figure 4.5 a: 1-3-6-4-2-5). Whenever numb feelings reported, strongly affecting the possibility of localizing the stimulus as the sensation spread over to the whole forearm, the electrode array position then was slightly adjusted.

In the case of interleaved stimulation, the experimenter additionally needed to adjust the intensities for the 10 Hz and 400 Hz stimulation. To set the low stimulation intensity for 10 Hz, the subject was asked to look for "low but clear" sensation (mean ± standard deviation across all pads belonging to columns 1, 3 and all subjects: 1.47 ± 0.55 mA). These values (level 1) were commonly associated with 1-2 steps above the sensation threshold. To set the higher stimulation intensity for 400 Hz, the subject was asked to look for "high but not painful" sensation (mean ± standard deviation across all pads belonging to columns 2, 4 and all subjects: 1.15 ± 0.26 mA), typically stopping 2-3 steps above level 1. After setting the intensity values for the two frequencies, the experimenter let the participant experience the sensations by moving the active pad across different columns, and small adjustments were allowed.

The intensity of the mechanical stimulation was preliminarily tuned for the stimulation to be clearly perceived by the participant. In any case, preliminary studies showed that there was no relevant difference in localization for different intensities of mechanical stimulation.

2) **Training: (*Phase 2*)** after the intensity adjustment, which assisted in obtaining clear and localized sensation, moreover avoiding uncomfortable stimulation, a training phase were applied. The training phase aims from one hand to familiarize the participant with the electrotactile stimulation and on the other hand, builds a mental map between the elicited sensation and the position of the stimulated pad in the electrode matrix. To this purpose, a sketch of the matrix electrode including the real-size 24 numbered active pads were placed on the table adjoining the forearm, preserving spatial correspondence with the matrix electrode. The training phase consists of two stages.

In the first stage, the participant was trained by experiencing sequential stimulation over each column from the top (wrist) to the bottom (elbow), while the experimenter orally reported the pad number. A total of 24 stimulations were presented to the participant, whilst he/she knew in advance which column and pad would be stimulated. In addition, it was expected that the participant associate the felt sensation with pad location which stimulated.

In the second training stage, reinforced learning was performed. The participant previously knew only the column to be stimulated, but the pads were selected and stimulated randomly. He/she was asked to guess the activated pad and then the experimenter provided verbal feedback about the correctness of the guess. This phase lasted approximately 15 minutes.

3) **Testing:** (*Phase 3*) during this phase, the participant's task was to provide an estimate of the position of the stimulated pad, and no feedback was provided about the correctness of the guess. The single pads were activated in a pseudorandom order so that each pad was presented two times (48 stimulations). The participant was asked to identify the activated pad, by indicating its number or identifying its position over the sketch. In few cases, the subject could not decide on the location, and this was registered as a "missed sensation".

In the training and testing phase during electrical stimulation, the participant was allowed to freely direct the look from the forearm to the sketch and back (Figure 4.5 a). Our approach was motivated by the fact that in the clinical application of this interface, e.g., during training of electrotactile feedback and even during prosthesis use, the subject will be able to look into his/her residual limb/prosthesis. In any case, there was no visual information related to the stimulation, and the electrode matrix was fully covered with white medical bandage. Nevertheless, this type of visual contact can assist the spatial acuity through the visual enhancement of touch [110].

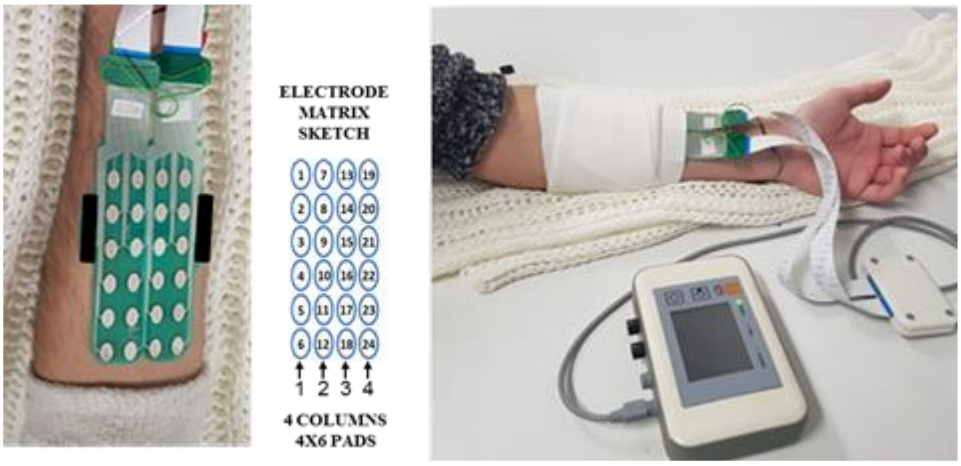

(a)

(b)

Figure 4.5 Testing phases: a) Phase 0, Phase 1: subject preparation and intensity adjustment, The spatial correspondence between the matrix electrode and the geometrical arrangement of the pads in the sketch is preserved, Right: Relaxation arm position b) Left : phase 2: Training , Right: Electrostimulation tests: a sketch of the matrix electrode (4 columns, 6 rows) is placed on the table next to the forearm.

During mechanical stimulation, a screen was placed between the participant's forearm and the sketch of the matrix electrode to prevent the participant having visual cues to identify the stimulation location (Figure 4.6). In all modalities, the duration of the stimulus delivered to the subject was 2 s. In both conventional and interleaved stimulation modalities, the pulse width and inter-pulse delay were set to w = 200 μs and d = 1 μs (Figure 4.1), respectively. The delay between a positive and negative pulse is fixed by construction of the stimulator, and therefore it cannot be adjusted. Considering that it is not possible to exhaustively test the parameter space, the pulse width was set heuristically, based on previous experience [111]. The chosen pulse width

allows for good control of tactile sensations in most of the subjects when using amplitude modulation, i.e., a reasonable range between detection and pain thresholds.

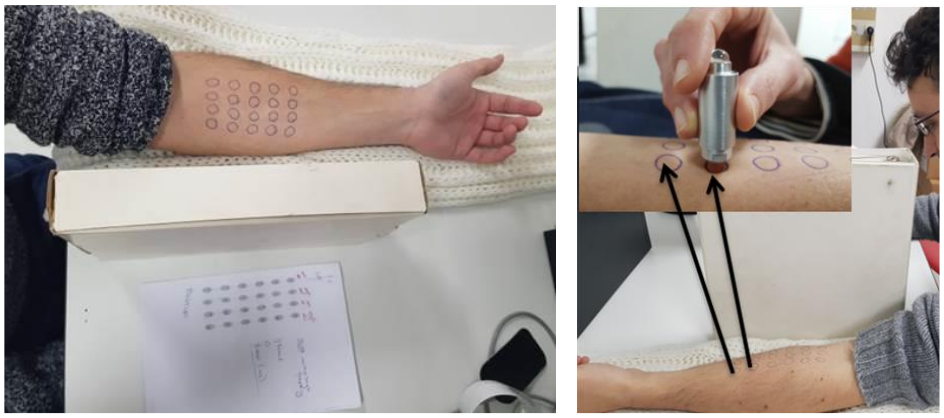

(a) **(b)**

Figure 4.6 Experiments with mechanical stimulation. A screen is placed between the participant's forearm and the sketch of the matrix electrode. (b) Top view. (b) Side view.

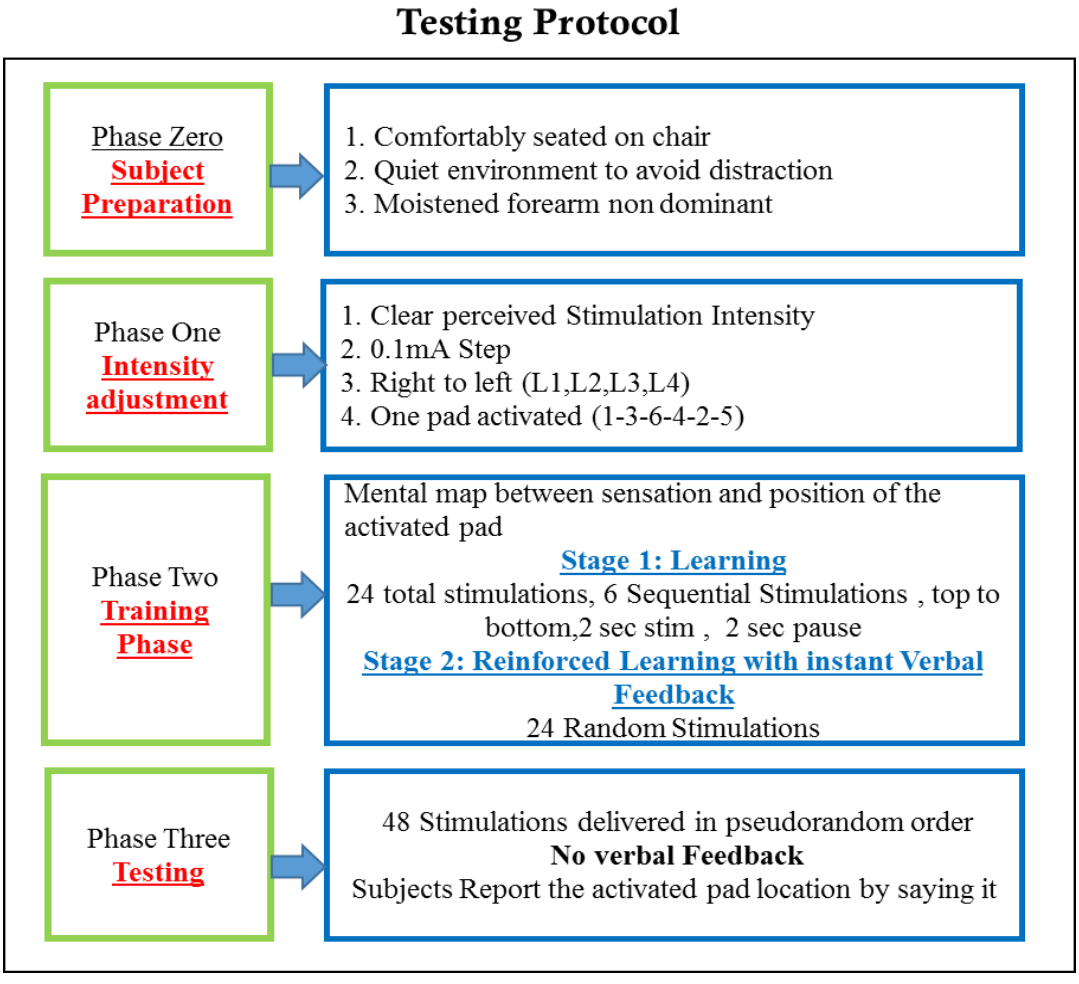

Figure 4.7 Testing Protocol

4.4 Data Analysis

The main outcome measure was the success rate (SR) in locating the stimulus or the Correct Identification Rate (CIR) which is defined as the ratio of the correctly identified trails to the total applied trails. It represents the identification of the exact pad at which the stimulation was delivered.

$$\boldsymbol{SR} = \frac{\text{Number of correctly identified trails}}{\text{Number of total trials}} \times 100\% \quad \textbf{(4.1)}$$

However, our intended application is in prosthetics, where small errors can be often tolerated. Therefore, the SR was computed also for pointing to the first neighbor around the correct pad (one-position error) and to the pad within the same column as the correct pad (correct column). The latter (correct column) is of interest when mapping prosthesis variables to the electrode pads, since mistaking the column could represent a much larger error (see Sect 4.6).

The SRs were computed per subject for each specific stimulation modality (mechanical, uniform frequency, and interleaved stimulation). The SRs of all subjects were then averaged to obtain the overall mean SR and its standard deviation. The results were reported as mean ± standard deviation in the text and figures. The data were tested for normality using KolmogorovSmirnov test. In all cases, the tests indicated normal distributions, and therefore one-way repeated measure ANOVA was used to assess statistically significant differences at the level of the group followed by Tukey's honestly significant difference test for post hoc pairwise comparison. One-way ANOVA tests were used to compare the success rates in recognizing the specific pad or column across stimulation modalities. The threshold for the statistical significance was adopted at $p < 0.05$, and the statistical analysis was conducted in Matlab R2017b (MathWorks, US).

4.5 Results

Figure 4.8 shows the performance for individual subjects across stimulation modalities. The bars represent the SR in (i) correctly identifying the right pad (light blue), (ii) wrongly identifying the pad but pointing to the right column (orange), (iii) wrongly identifying the pad and the column (grey). The variability across subjects is noticeable for mechanical stimulation.

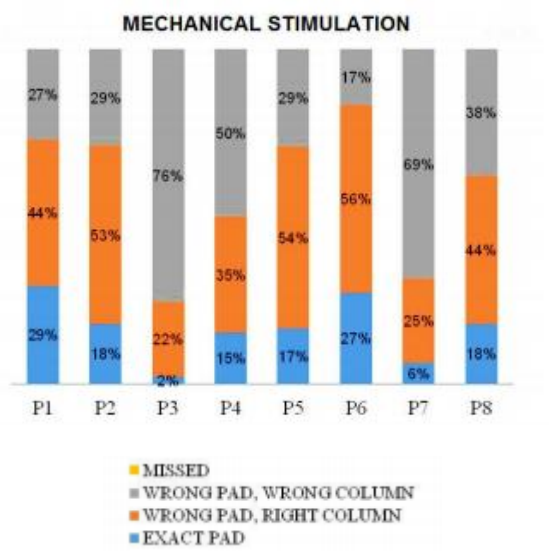

(a)

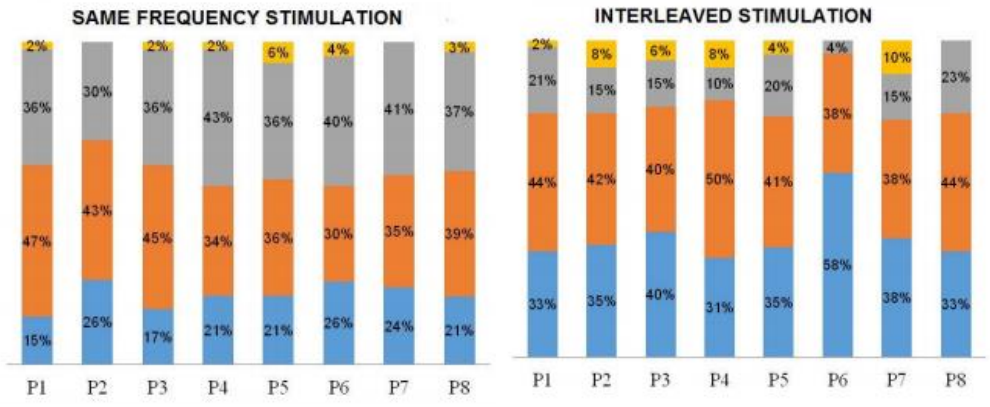

(b) **(c)**

Figure 4.8 The results for individual subjects (P1-P8). Reported percentages are associated to identifying the right pad (light blue), missing the pad but addressing the right column (orange), missing the pad and the column (grey), no answer (yellow).

The summary results, i.e. overall SRs, are shown in Figure 4.9. In general, pad recognition was not an easy task for the subjects (Figure 4.8-a). The overall SR for the mechanical stimulation was 17±9%. The electrotactile stimulation using the same frequency for

all pads (50 Hz) was characterized with a similar SR (21±4%). Therefore, the samefrequency electrotactile stimulation provided comparable quality of spatial localization to that of the mechanical stimulation. However, with both modalities, the performance was still substantially better than pure chance, where the subject would simply randomly select one of the pads (1/24 ~ 4%). Importantly, the SR for the electrotactile stimulation that used the interleaved frequencies and intensities was significantly better (38±9%) compared to both mechanical ($p < 0.001$) and the same-frequency electrical stimulation ($p < 0.001$). The performance almost doubled with the interleaved stimulation scheme. Therefore, the dual parameter modulation substantially improved the subjects' ability to correctly localize the elicited tactile sensation.

The summary performance in localizing the stimulus up to an error margin around the active pad is reported in Figures 4.8 b-d. Figure 4.8-b gives percent of trials in which the subject pointed to a correct pad or its immediate neighbor within the same column (one-position, within-column error tolerance). Figure 4.9-c is a percent of trials in which the subject pointed to a correct pad or any other pad that belonged to the same column (within-column error tolerance). Again, the SRs in the case of one-position error (Figure 4.9-b) for interleaved stimulation (70±11%) was significantly higher than for the same-frequency electrical (42±6%, $p < 0.01$) and mechanical stimulation (45±20%, $p< 0.01$). If a small localization error can be tolerated, the interleaved stimulation can therefore lead to a very good performance (e.g. SR up to 96% for subject P6). More generally, with the interleaved stimulation, the subjects could reliably detect the right column (Figure 4.9-c). The success rate for this modality was significantly better (80±7%) than for the same-frequency (60±5%, $p < 0.01$) and the mechanical stimulation (59±21%, $p < 0.01$). Finally, Figure 4.7-d reports for all modalities the percent of trials in which the subjects pointed to a correct pad or its immediate neighbor, regardless of the column. This figure further emphasizes the equivalence of mechanical stimulation (SRs: 63±21%) and same-frequency electrostimulation (SRs: 64±9%). The interleaved coding leads to a higher average SR (~79±8%), though this time there was no statistically significant difference with the other two modalities.

The overall success rates for the recognition of individual pads of the matrix electrode in each of the stimulation modalities are show in Figure 4.10 -b (mechanical), c (uniform frequency), and d (interleaved stimulation). The figure once again demonstrates that the interleaved modality is the technique which allows for the best recognition of single pads. With mechanical and same-frequency stimulation, there is a trend that the pads on the borders of the

electrode area are more successfully recognized compared to the inner pads. In the case of interleaved stimulation, the SR increases for most of the pads and some inner pads reach comparably high SRs.

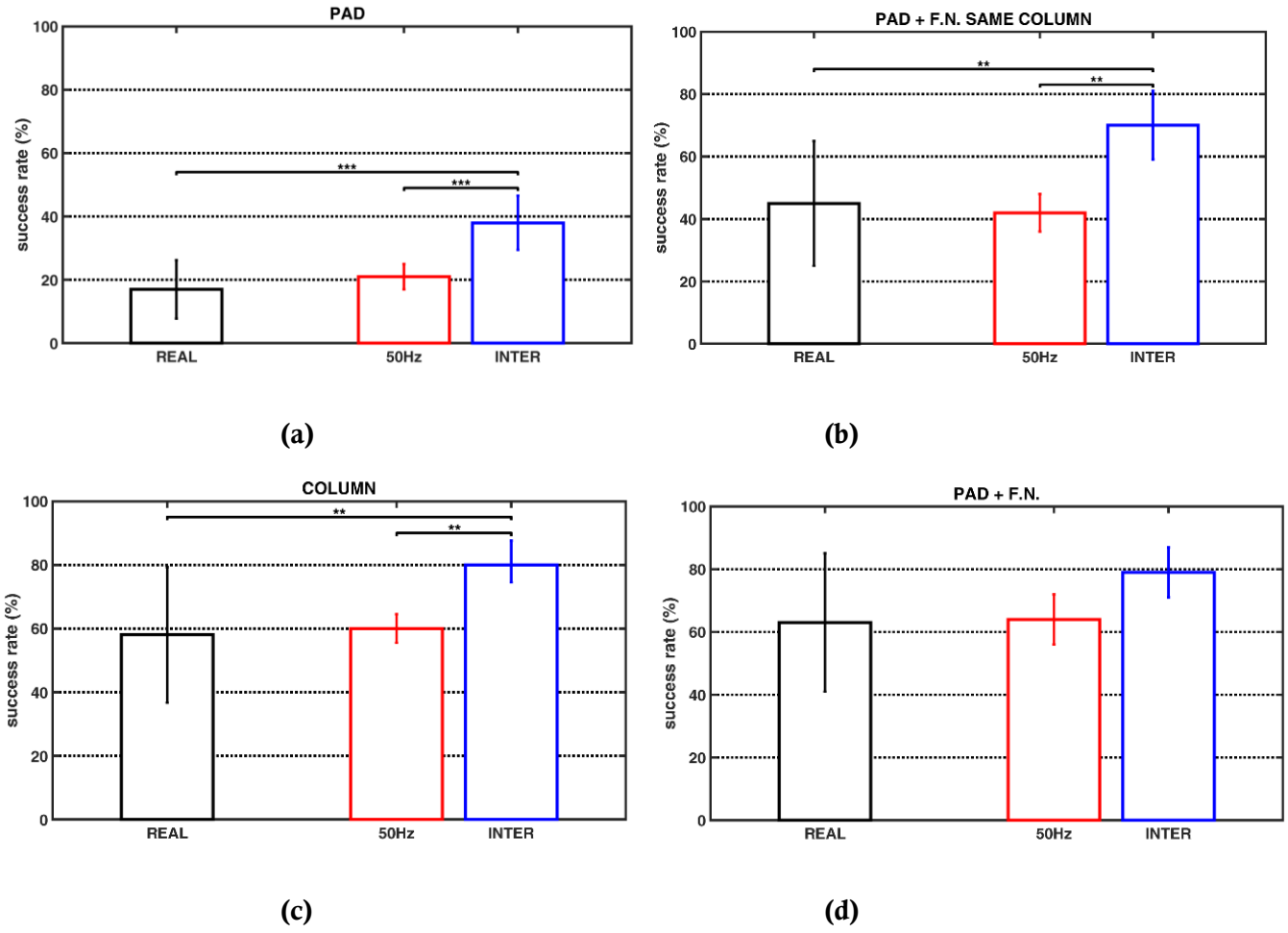

Figure 4.9 The summary results for all subjects (Sample size n = tested subjects = 8) Bars and stars indicated statistical significance (, p<0.05 , **, p<0.01, ***, p<0.001). The bars show the success rates (mean ± standard deviation) : a) in identifying the right pad ,b) pointing to the right pad or first neighbors (F.N.) within the same column , c) pointing to the right pad or any pad belonging to the same column , d) and pointing to the right pad or any of its first neighbors, regardless of the column*

4.6 Discussion

We have investigated if the modulation of additional parameters (frequency and intensity) can improve the spatial localization of the electrotactile stimuli. In addition, the electrotactile localization was compared to that of mechanical stimulation, since the latter is commonly used to evaluate the spatial acuity of the skin. In addition, the electrotactile localization was compared to that of mechanical stimulation. This was done to compare a

method for sensory substitution (electrical stimulation) with the stimulation as it is typically experienced in daily life, i.e., someone/something touching the skin. It would be also interesting in the future to compare the electrical stimulation with vibrations, which is an alternative method

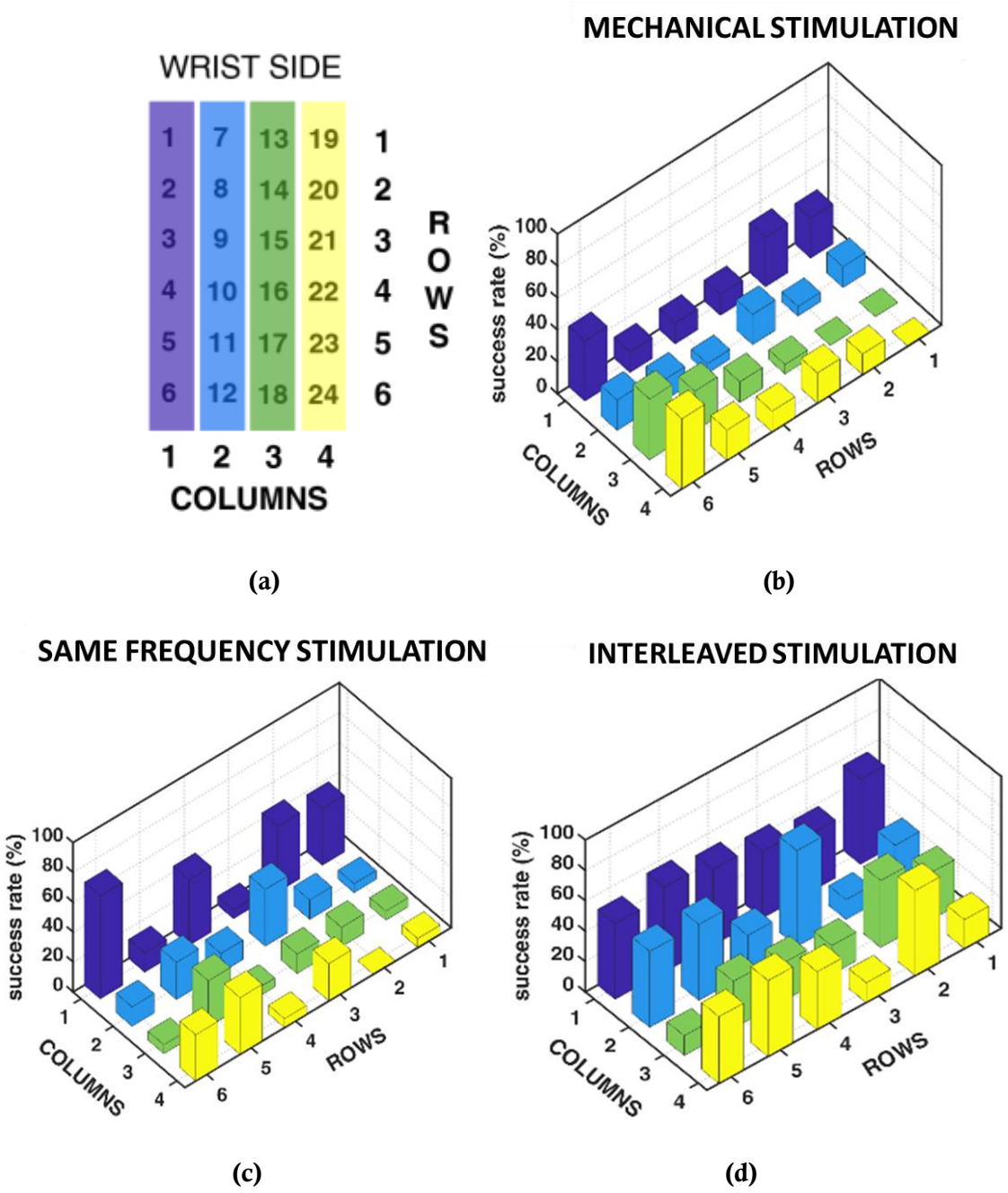

Figure 4.10 Success rates for the identification of each pad. The scheme reported in (a) illustrates the orientation of the matrix electrode with respect to the forearm.

for sensory substitution.

The first important conclusion of the study is that the electrotactile stimulation delivered conventionally, using the same frequency for all the pads, resulted in a similar performance as

the mechanical stimulation. The electrotactile stimulation is non-specific and activates a combination of mechanotactile receptors. In addition, the electrical current spreads in the tissue, especially in this configuration where the common electrode is positioned outside of the integrated matrix. The fact that the electrical and mechanical stimulation performed similarly is an encouraging outcome for the application of multichannel interfaces with significant number of pads to the feedback restoration in prosthetics.

The second important conclusion is related to the fact that the electrical stimulation has an intrinsic potential, namely, the flexibility in parameter modulation, which can be used to increase the reliability of information transmission to the subject. The present experiment has demonstrated how dual-parameter modulation can be used to substantially improve the performance in spatial localization of the elicited tactile sensation. The subjects were more successful in identifying the stimulation location using the interleaved stimulation modality compared to other modalities both when locating the correct pad (Figure 4.9-a), or when accepting (small or large) errors within the right column (Figure 4.9-b and 9c). This means that an electrotactile interface can be used to equip a prosthesis user with an artificial tactile sense that can overcome some limitations of the direct mechanical stimulation (e.g., low-density of receptors and thereby poor spatial localization over the forearm). This is a unique advantage of electrical stimulation because the parameters can be independently modulated. In vibration motors, for example, the parameters are often mechanically coupled [63], [112] and in modality matched stimulation there is often only one parameter to modulate (e.g., the pushing force). Since the aim of the present study was to improve localization, we decided to exploit both frequency and intensity (dual-parameter modulation) to make the distinction between the columns as clear as possible. However, in the present study, it cannot be determined how much each of the parameters individually (frequency versus intensity) affected the localization. This question could be investigated in the future by systematically testing combinations of intensity and frequency using factorial experimental design [113] to assess the main effect as well as the interaction between the stimulation parameters. The "wining" modulation scheme was determined through extensive pilot tests. For example, one approach that has been tested was to associate different stimulation frequencies to each column, e.g., 5, 10, 20, 50 Hz for columns 1, 2, 3, 4. Different combinations of frequencies have been evaluated but the approach was not effective. Therefore, using only frequency modulation did not improve the localization. Finally, the interleaved frequencies with substantial gap were selected (10 vs 400 Hz), and the modulation of frequency had to be complemented with the interleaved intensity, in order to further increase

the contrast between the columns. The frequency of 400 Hz was chosen as this was the maximum of the stimulator, but it is likely that the results would be similar with other high frequencies as well (e.g., 10 vs 100 Hz), as the elicited sensations are similar. The fact that different frequencies were used in the two conditions (same-frequency versus interleaved) might have in itself affected the localization, although for vibro-simulation this effect seems not to be substantial [105], [73]. This could have been addressed by testing two same-frequency conditions (with 10 Hz and with 400 Hz). However, this was not feasible due to time constraints and therefore we have opted for a single (in-between) frequency from a range that is conventionally used [63]. In particular, in a past publication [114] we have actually shown that higher frequencies than 25 Hz and above up to 100 Hz are preferred for sensory feedback. The lack of randomization is a limitation of the present study that was caused by technical constraints. However, it is unlikely that this has affected the results because we assume that the adopted order was in fact less favorable for the novel modality (dual-parameter modulation). The interleaved stimulation was tested in the first session and the same-frequency and mechanical stimulation were assessed in the second session, and yet the best results were obtained with the interleaved stimulation. Therefore, dual-parameter modulation resulted in the best performance although the participants were not yet acquainted with electrotactile stimulation.

Nevertheless, the potential impact of familiarization and training remains an assumption that was not tested explicitly in the present study. The enhanced capability of distinguishing the single pad inside the column when using dual-parameter modulation might enable high-resolution contact localization. For example, the proposed high- resolution interface can be used to transmit high-resolution information on contact position or contact mechanics (e.g. force distribution) which might be required for advanced tasks such as dexterous manipulation. For that, the multichannel interface is to be combined with the multichannel sensing systems including several sensors on fingers and palm, such as e-skins developed in robotics but now increasingly considered for prosthetic applications [115]. However, a drawback of this method is that the spatial localization is improved at the expense of utilizing the two additional stimulation parameters (intensity and frequency). Therefore, they cannot be used anymore to convey feedback information through parameter modulation, as proposed in other approaches (e.g. increasing frequency/intensity to indicate higher grasping force and/or aperture [116] [111] [71]). However, the "intensity variables" can still be represented through a spatial code e.g. force magnitude could be transmitted through the location of the stimulation, as for example in [13]. These preliminary experiments have to be enriched with further exploration focused on tuning

the stimulation parameters to reliably convey desired feedback information while maintaining the spatial acuity. A large body of literature investigating how stimulation parameters affect spatial performance (see e.g. [103] [58] [105]) can be used as a guideline for this exploration.

Final translation into prosthetics implies the integration of the stimulation interface into the socket (in the same way EMG electrodes are currently integrated). One possibility would be to produce the electrodes using conductive silicone so that they are an integral part of the silicone liner. In recent studies, transcutaneous electrical nerve stimulation has been used to provide somatotopic sensory feedback non-invasively (e.g. [117] [118] [119]). With this approach, referred sensations occur in the phantom hand, which is good for prosthesis embodiment and can facilitate contact localization. The present study relies on electrotactile stimulation that normally does not elicit somatotopic feedback (if there is no phantom representation on the residual limb [120]).

Nevertheless, we still do not know how training affects the feedback integration into motor control. It might be that with a long-term training even non-somatotopic feedback becomes integrated and processed subconsciously, as suggested in [8]. The role of training is certainly crucial for the feedback interface with that many channels to be usable in the real application, especially when combined with prosthesis control. Importantly, there are encouraging results in literature showing that even a relatively short training can be powerful. In [111], a subject has reached a success rate > 90% in localizing 16 pads of an array electrode after only 2 hours of training. We believe that such training can substantially decrease the initial cognitive effort, though this needs to be tested in future studies.

Overall, the usability and acceptance of the proposed matrix interface is still to be investigated. The next step in this research will be to investigate how well the subjects could perceive several electrotactile stimuli that are delivered simultaneously or sequentially along the columns (two or more active pads). If the subject could identify the active pads in each column, even when they are activated at the same time, this would allow transmitting several levels of different prosthesis variables concurrently. How many channels of feedback information the patient could interpret and exploit simultaneously depends likely on many factors, such as subjective aptitude and motivation, sensory information encoding, and training and experience. Determining the effective bandwidth of this compact multichannel feedback interface is indeed an important point for future research.

4.7 On the use of virtual prosthesis in the sensory feedback interface system

The impressive developments in computer science and information technology, engineering and rehabilitation methods are gradually adding more capabilities to modern prostheses, moving towards the goal of replicating natural hand function. Upper limb myoelectric prostheses shows sophisticated mechanical designs. However, as we stated trough this chapter, the major problems in upper limb prosthetics are providing tactile feedback to explore the surrounding and reliable independent command sources for intuitively and efficiently controlling multiple degrees of freedom simultaneously. The idea of integrating Virtual reality (VR) and augmented reality (AR) in prosthetics and rehabilitation have been proposed as a method to quickly develop and evaluate control strategies, prototype devices, and train subject.

Several groups have investigated the usage and the simulation of prosthetic control in VR. Hauschild *et al* [121] built a VR model of a simulated prosthetic arm in order to virtually train patients with that prosthesis. The VR environment is custom-built in that case, a magnetic tracking system is used and the sEMG control is very basic, consisting only of open/close commands. Similarly Lambrecht *et al* [122] show the usage of a VR environment for testing different control strategies. Moreover, VR has being used to reduce phantom limb pain, for example, Snow el al [123]developed a VR system coupled to haptic feedback provided by a robotic arm. In addition, Ortiz-Catalan *et al* [41]use augmented reality (AR) to achieve the same results on reduction of phantom limb pain. In addition, the need for realistic grasping and manipulation of virtual objects has always been an objective for VR. [25] summarizes prevalent reaching and grasping techniques being used. As the focus of these applications are speed and ease of use, various nonphysical tricks (space warping, nonphysical forces) are leveraged to achieve desired visual effects. Physical consistency is often compromised for enhanced visual experience. [124] presents a VR system that captures and analyses human demonstration for motion intentions to explore multi-fingertip haptic interface for programming dual arm multi-finger robots.

A significant feature of virtual reality as a tool is the ability to superimpose computer, by generating virtual objects onto the physical world in real time, thus allowing the user to interact with the real/virtual world. Driven by its high potent, we believe that developing an interactive,

intuitive, and natural prosthesis -that could deliver the functionality of grasp also provide tactile sensation – will be strengthen by the immersion of VR.

As far as, sensory feedback requires as reported by Peerdeman el al [125]: 1) Continuous and proportional feedback on grasping force, 2) Position feedback to the user, 3) Easy and intuitive interpretation of stimulation used for feedback, and 4) Unobtrusive, real-time adjustable feedback. Moreover, considering our main objective about restoring the sense of touch in upper limb prosthetics and in a follow up development of the proposed high- resolution interface that would be used to transmit real-time, high-resolution information on contact position or contact mechanics (e.g. force distribution) which might be required for advanced tasks such as dexterous manipulation.

The reported work in this section brings the idea of combining the optimum of the VR technology and research about dexterous hand manipulation to the aforementioned developed multichannel electrotactile stimulation interface. Particularly, we developed a fully programmable virtual reality (VR) based multichannel electro-tactile feedback stimulation system that communicates the state (e.g. contact interaction, grasping force, object manipulation) of the simulated multi-DOF prosthesis to the user. The sensory data collected from the simulated touch sensors were coded in an intuitive manner that could be easily identified by the able-bodied subjects and amputees.

4.7.1 System description

The system setup includes a multichannel electrotactile stimulation system (Int-FES ver2 , Tecnalia Research & Innovation, San Sebastian, ES) and Laptop PC (Intel coreTM i7-4710HQ CPU at 2.5GHz, 8 GB RAM) running MATLAB (R2017b, by MathWorks). As well, a MATLAB application with GUI for controlling the virtual prosthesis movements, object manipulation and grasping, and mapping the collected sensor data from the simulated prosthesis into electrotactile stimulation feedback profiles. Figure 4.7 illustrates the block diagram of the system.

In order to present a sense of realism about the hand-object interaction to the user, MuJoCo HAPTIX virtual reality hand simulator was used [126]. This software is an open source simulator that was developed to meet the needs of the DARPA Hand Proprioception & Touch Interfaces (HAPTIX) program. It has a full feature GUI that enables the control and the visualization of the virtual prosthesis. Moreover, it can be controlled programmatically over a

TCP/IP socket connection through MATLAB or C++. The VR prosthesis simulator shows that humans can indeed perform manipulation tasks with virtual objects, which in turn clears the way to collecting rich and physically consistent dataset of hand-object interactions. Moreover, It allows the recording of every aspect of the interaction happens – including joint kinematics and dynamics, contact interactions, simulated sensor readings etc.

The simulator provides the model of the Modular Prosthetic limb (MPL) [127], consists of 22 DOF (19 in the fingers and 3 in the wrist) and 13 actuated DOF. Finger flexion and extension are coupled using differential arrangement and actuated using a single actuator. Ring and little finger's adduction-abduction are coupled and actuated using a signal actuator. Index finger MCP adduction abduction, all thumb joints and all wrist joints have independent actuation. In accordance with the sensing capabilities of the real hand, the state of the system is exposed to the users via MuJoCo's simulated sensors. Sensory capabilities include - joint position and velocity sensors on all 22 joints, actuator position, velocity and force sensors on all 13 actuators, touch sensors and inertial measurement units on all 5 finger tips. See Figure 4.9.

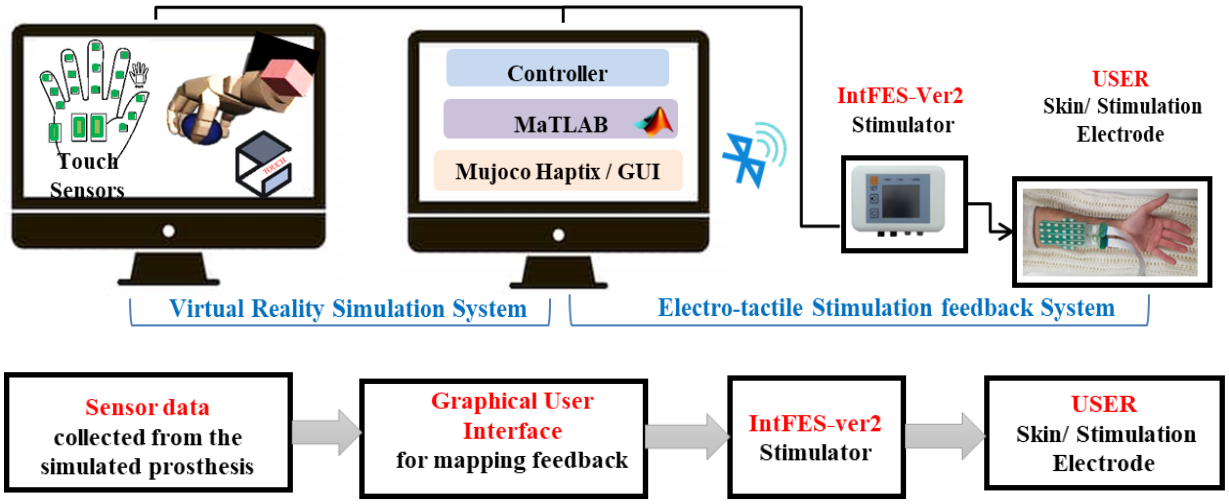

Figure 4.11 Block Diagram of the virtual reality simulation system and the electrotactile stimulation feedback system. The Virtual prosthesis simulated on the Laptop PC is controlled through a graphical interface developed in MAT LAB. The tactile Feedback resulting from different object manipulations with the virtual prosthesis is presented to the user in the form of electrotactile stimulation provided by the IntFES-ver2 stimulator.

A graphical user interfaces GUI was developed in MATLAB, to control the virtual hand movements (e.g. forward, backward, Upward, downward) remotely in the virtual space, and it could simulate several hand gestures such as open/ close the hand, flexion/extension , etc.. Additionally, it implements six grasp types (i.e. spherical grasp, cylindrical grasp, pinch grasp) to manipulate objects (e.g. sphere, cylinder, etc.) in the VR as shown in Figure 4.10. On the other

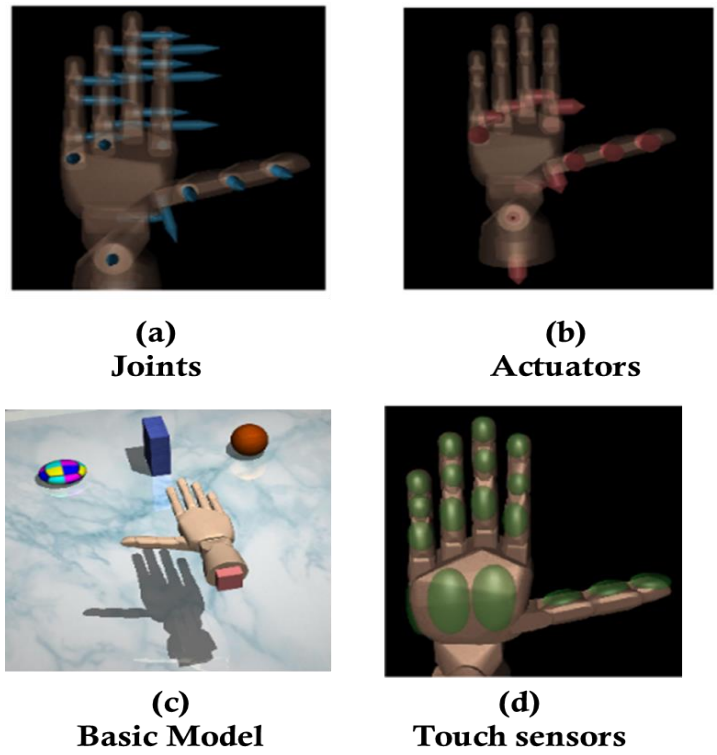

Figure 4.12 MLP Sensor configuration of the virtual prosthesis

hand, the tactile sensory data collected from the simulated prosthesis upon hand-object interaction were mapped into stimulation parameters and transmitted via Bluetooth to the developed multichannel electro-tactile stimulation system. The latter is a fully-programmable and integrated electrotactile interface comprising a stimulation unit and a custom designed flexible electrode array that is made of 24 pads to deliver tactile feedback to the subject [128][129]. The electrode matrix was chosen to cover the volar side of the forearm, and accordingly the inter-pad distance meets the two-point discrimination threshold for electrical stimulation. While one single self-adhesive electrode acts as a common anode, the Ag/AgCl conductive pads were used as cathodes and they were covered with hydrogel pads (AG730, Axelgaard, DK) to improve electrode-skin contact.

4.7.2 Mapping Protocol and stimulation patterns

After combining the developed distributed multichannel interface with the multichannel sensing system that including several sensors on fingers and palm simulated in VR virtual prosthesis. The simulated touch sensors state had been acquired and translated into different stimulation patterns as shown in Figure 4.11. The touch sensors on the distal, middle and

proximal phalanges of the pinky, ring, middle, index and the thumb were mapped in 1:1 ratio, while the side, pinky and thumb palm touch sensors were mapped in 1:3 ratio.

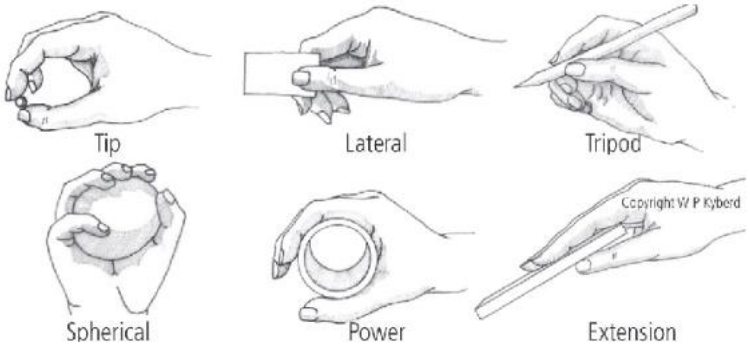

Figure 4.13 Implemented Grasp classification to retrieve tactile sensory information and mapped to the user through the stimulation interface

The presented dual parameter modulation might be used to convey feedback information, as proposed in other approaches (e.g. increasing frequency/intensity to indicate higher grasping force and/or aperture). This work still in infancy stage, further exploration is needed on tuning the stimulation parameters to reliably convey desired feedback information while maintaining the spatial acuity. Currently, we are investigating the feasibility of the proposed system by testing it on able-bodied subjects and later on amputees (e.g. identification of objects or touch modalities), and expand the capacity of the sensory feedback system to encode more intuitive stimulation patterns to transmit tactile signals and different touch modalities of sensory information acquired from different grasps.

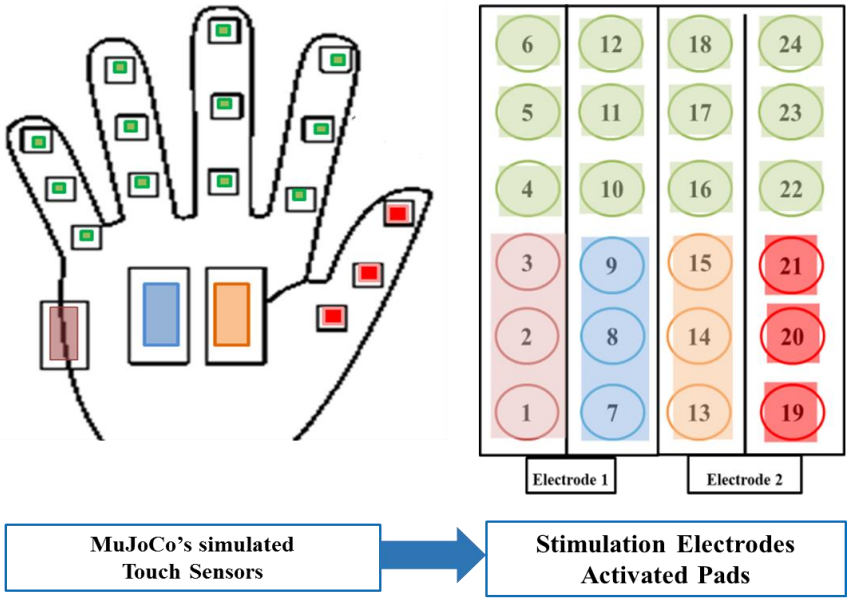

Figure 4.14 Stimulation Map from tactile simulated sensors to stimulation active pads . The color tactile feedback map from the simulated touch sensors prosthesis (18 touch sensors) into the flexible stimulation electrode (24 pads).

4.8 Conclusion

The study presented in this chapter assessed the subject ability to localize electrical stimuli delivered through a compact matrix electrode with many pads. The results demonstrated that conventionally applied electrotactile stimulation (single frequency) can reach similar performance in tactile acuity as mechanical stimulation. With a novel dual-parameter modulation scheme, the electrotactile interface provided higher discriminability than the mechanical stimulation. This is an important outcome for the provision of sensory feedback in prosthetics, as it implies that an electrotactile matrix interface can be used to transmit reliable high fidelity feedback from the prosthesis, by exploiting the flexibility in spatial and parameter modulation characteristic of electrotactile stimulation.

Moreover, this chapter presented our idea of immersing VR virtual reality with the sensory feedback interface in order to enable a real –time tactile feedback to prosthetic users.

Chapter 5 Artificial Tactile Sensing and E-Skins In Prosthetics

5.1 Introduction

Upper limb prosthesis has made a substantial progress in reproducing some of original hand functions e.g. grasping force, aperture. These achievements are still in tentative stage and need to be elaborated more to meet user's needs[14][8]. The sense of touch relies on a dense network of mechanoreceptors to deliver spatially distributed information. Providing comparable high-resolution tactile information of the human sense touch requires adequate artificial sensing systems, which integrates high-density network of sensing units. With this aim, prosthesis is furnished with tactile sensors, from which the data are acquired, suitably coded and communicated to the user by activating spared tactile sensory structures using either invasive (e.g. direct nerve or brain stimulation)[130] [131]or non-invasive interfaces (e.g. electrotactile and mechanical stimulation[9][75].

In the recent decades, the increasing demand for restoring sensory feedback inspires the exploration of sensing transduction mechanisms [132] [35] and their applications in various systems, such as upper limb prostheses [133] [34], virtual reality systems [126] [134], remote operation [135] [136] touch screens [134], and robotic hands [137] [138]. However, enabling tactile sensation in upper limb prostheses is still not as mature as that in other fields, yet the achievements could be adopted into this field. Given that grasping, is one of the major functions of hands, most studies of prosthesis tactile sensing focus on grasp force or pressure in order to prevent slip and achieve a stable grasp. The measured characteristics of touch, however, can be not only force and pressure, but also stiffness, texture, or shape. E-skin is an artificial skin that aims to imitate the human skin. It is a hybrid stack wise arrangement of tactile sensing elements, interface electronics and embedded electronic system and communication interface.

In this scope, this chapter presents the e-skin system concept and it is potent ability to reconstruct tactile sensations in prosthetics. The human sense of touch has been introduced

along with the physiology of the human skin in section 5.2 and 5.3. Then, in section 5.4, presents a brief review about the evolution of the tactile sensing and artificial skins. Finally, section 5.5, the e-skin system was explained regarding our pivotal target as a group in restoring the sense of touch in prosthetics. It provided a survey about the main compartments of the e-skin (i.e. tactile sensing, interface electronic and the embedded electronic system) starting from the state of art and how to get inspired of what have been implemented on the robotic field, to pave the way of achieving an e-skin compatible to upper limb prosthetics.

5.2 Sense of Touch

The sense of touch in humans comprises three main sub-modalities, i.e. cutaneous, kinesthetic, and haptic characterized based on the sensory input location.

1) The cutaneous sense receives sensory inputs from the receptors embedded in the skin. In fact, the cutaneous system involves physical contact with the stimuli and provides awareness of the stimulation of the outer surface of body by means of receptors in the skin and associated somatosensory area of central nervous system (CNS).

2) The kinesthetic system, receiving sensory inputs from the receptors within muscles, tendons, and joints [139], provides information about the static and dynamic body postures on the basis of 1) afferent information originating from the muscles, joints, and skin; and 2) efferene copy, which is the correlate of muscle efference available to the higher brain.

3) The haptic sense perceives heat, cooling, and various stimuli that produce pain by using significant information about objects and events both from cutaneous and kinesthetic systems [140][139].

The human sense of touch deals with the spatiotemporal perception of external stimuli through a large number of receptors (e.g. mechanoreceptors for pressure/vibration, thermoreceptors for temperature, and nociceptors for pain/damage [141] that are distributed all over the body with variable density. The response to mechanical stimulus is mediated by mechanoreceptors that are embedded in the skin at different depths. Their number, per square centimeter area, is estimated to be 241 in the fingertips and 58 in the palm of adult humans.

5.3 Physiology of the Human Skin

The human skin is a flexible waterproof barrier, which separates the human being from the outside environment. It relies on sensory receptors that provide information about the contact and the surrounding environment. Moreover, it is capable of sensing touch that includes mechanical stimulation, heat, and pain. There are two major types of skin in humans, hairy skin and glabrous skin. The receptors found in the glabrous skin will be elaborated in this section since this skin type covers the parts of the body mainly used for tactile exploration (fingertips, palms of the hands, soles of the feet, and the lips) [142]. Compared to hairy skin, it has a thicker epidermis and a more rigid appearance. As the name suggests, it furthermore lacks hair follicles. The glabrous skin of the human hand contains 17.000 tactile units, i.e. primary afferent neurons with sensory endings in the dermis specialized for sensing deformations of the skin that occur when the hand interacts with objects [143]. Their function is to provide information about physical properties of the object and the contact between hand and object, i.e. sensations related to pressure, vibration, shape, texture, stiffness etc [45]. The mechanoreceptors are sensory units distributed in human skin to detect mechanical stimulation, a sequence of voltage pulses is generated and transmitted through neurons to the brain where the information is processed. Mechanoreceptors in the glabrous skin of human hands include four types: Merkel cells, Meissner corpuscles, Ruffini endings, and Pacinian corpuscles. They are responsible for the detection of different stimulations. Generally, according to their adaptation rate, four types of mechanoreceptors are categorized into two classes: fast adapting units (FA) and slow adapting units (SA). Then, based on their receptive fields, each class is divided into two groups: II and I. SA-I and FA-I receptors have small receptive field with a sharp border, while SA II and FA II receptors have large receptive field with diffuse border [24], as shown in Figure 5.1 These four types of mechanoreceptors have different functional properties about the receptive speed, the receptive field, and the perceptive function, which are summarized in the table presented in Figure 5.1. In terms of the receptive speed, Meissner corpuscles and Pacinian corpuscles are mainly responsible for rapid or dynamic stimulation, while Merkel cells and Ruffini endings respond to sustained stimulation. Meissner corpuscles are sensitive to light touch, while Pacinian corpuscles tend to detect deep pressure touch and high frequency vibration. Merkel cells are sensitive to low frequency vibration, while Ruffini endings usually respond to stretching of the skin. In terms of the location and the receptive field, Meissner corpuscles and Merkel cells concentrate in the outer layer of the skin on fingertips and have small receptive fields. On the

contrary, Pacinian corpuscles and Ruffini endings are distributed more uniformly in deep layer of the skin on fingers and the palm. In terms of the function of perception, Merkel cells and Pacinian corpuscles might be related to the sensation of stiffness. Merkel cells and Ruffini endings could detect slip and shape due to their response to steady pressure and skin stretch. Besides, Meissner corpuscles and Pacinian corpuscles contribute to the perception of texture, such as surface roughness, because they are sensitive to rapid vibration, which is too small to activate the other two types of mechanoreceptors [142]. Additionally, the spatial resolution is the smallest distance for one to distinguish two-point touch and varies across the body. It is as close as 0.5 mm on fingertips while 7 mm on the palm..

The human skin can be an ideal model of artificial tactile sensors given its good performance of tactile sensing. In general, artificial sensors are expected to demonstrate small resolution, high sensitivity, low hysteresis, fast and linear response, wide dynamic range and high reliability. A spatial resolution of 5-40 mm could be satisfactory. Typically, 20-60 Hz would be fine for sampling rate in common tasks, while for special task, such as texture recognition, a higher sampling rate about 1-2.5 kHz is necessary[141]. A force sensitivity range of 0.3-10 N is

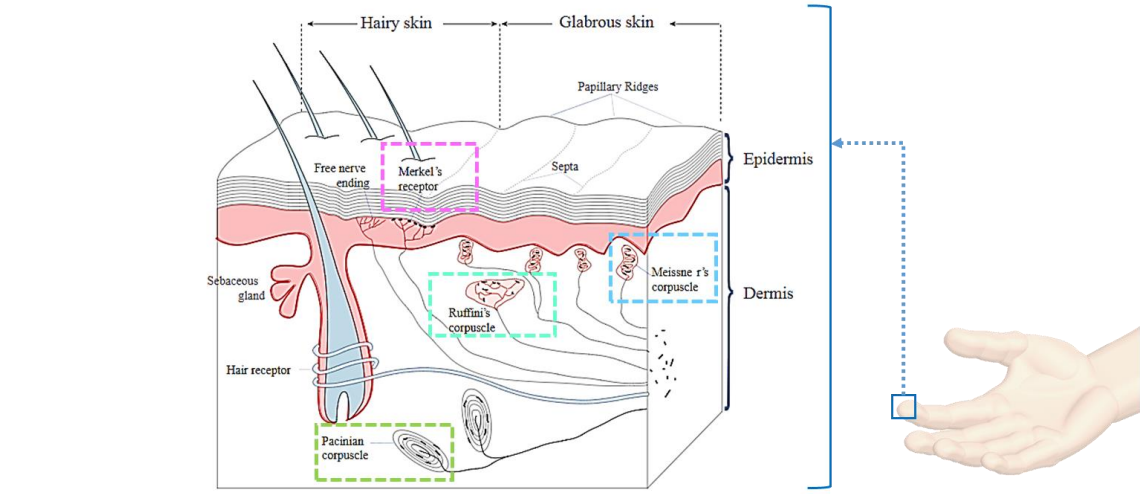

	Meissner corpuscles	Pacinian corpuscles	Merkel cells	Ruffini endings
Classification	FA I	FA II	SA I	SA II
Adaptation rate	Fast	Fast	Slow	Slow
Receptive field	Small and sharp	Large and diffuse	Small and sharp	Large and diffuse
Density (units/cm^2)	140	20	70	10
Spatial resolution (mm)	3-4	10+	0.5	7+
Stimuli frequency (Hz)	5-50	40-500+	0.4-40	<7
Sensory function	High frequency vibration detection. Temporal changes in skin deformation.	High frequency vibration detection; Temporal changes in skin deformation. Tool use.	Low frequency vibration detection (static force); Pattern/form detection; Texture perception; Tactile flow perception.	Low frequency vibration detection (static force); Finger position; Stable grasp; Tangential force/ skin stretch.

Figure 5.1 Schematic illustration of the distribution and classification of the mechanoreceptors in the human skin.

required. For human-like skin or sensors, robust, flexible, stretchable and soft materials are desired to be embedded on various 3D structures. Additionally, low cost, low power consumption and scalability are also important for manufacture and implementation.

5.4 Artificial Skins: Concept and Evolution

Being inspired by the human skin, several efforts have been made to develop an artificial skin that combines a wide variety of tactile sensors to mimic the native sensory system of the human body, which brings many potential applications in robotics, artificial intelligence, prosthetics, and health monitoring technologies. The pursuit of artificial skin has inspires innovations in materials/structures and mechanisms/approaches to match the e-skin to the remarkable skin's characteristics, including mechanical durability and stretchability, biodegradability, and the ability to measure a diversity of complex sensations over large areas. Moreover, new materials and fabrication strategies are being developed to make mechanically compliant and multifunctional skin-like electronics, and improve human-machine interfaces that enable transmission of the skin's signals to the body.

An artificial skin with sensory capabilities is commonly referred in literature as sensitive skin, smart skin, or e-skin.Such skins requires a high macroscale integration of various sensors on a thin flexible substrate. Usually, the e-skin is structured as a networked system of "patches" implemented as hybrid stack-wise arrangements incorporating tactile sensing (i.e. mechanical into electrical transduction, signal conditioning and acquisition) and touch interpretation.

In 1974, Clippinger demonstrated a prosthetic hand capable of discrete sensor feedback [144]. Nearly a decade later, Hewlett-Packard (HP) marketed a personal computer (HP-150) that was equipped with a touchscreen, allowing users to activate functions by simply touching the display. It was the first mass-marketed electronic device capitalizing on the intuitive nature of human touch. In 1985, General Electric (GE) built the first sensitive skin for a robotic arm using discrete infrared sensors placed on a flexible sheet at a resolution of 5 cm. The fabricated sensitive skin was proximally aware of its surroundings, allowing the robot's arm to avert potential obstacles and effectively maneuver within its physical environment. Despite the robotic arm's lack of fingers and low resolution, it was capable of demonstrating that electronics integrated into a membrane could allow for natural human machine interaction. In the 1990s, scientists began using flexible electronic materials to create large area, low-cost and printable sensor sheets. Jiang et al. proposed one of the first flexible sensor sheets for tactile shear force

sensing by creating silicon (Si) microelectromechanical (MEM) islands by etching thin Si wafers and integrating them on flexible polyimide foils. Around the same time, flexible arrays fabricated from organic semiconductors began to emerge that rivaled the performance of amorphous Si [145].Just before the turn of the millennium, the first Sensitive Skin Workshop was held in Washington DC under the aegis of the National Science Foundation and the Defense Advanced Research Projects Agency, bringing together approximately sixty researchers from different sectors of academia, industry, and government. It was discovered that there was significant industrial interest in e-skins for various applications, ranging from robotics to health care.

Significant progress in the development and advancement of e-skin has been achieved in recent years, and particular emphasis has been placed on mimicking the mechanically compliant yet highly sensitive properties of human skin. Suo and coworkers have developed stretchable electrodes[20],and Rogers and coworkers have transformed a typically brittle material, Si, into flexible, high-performance electronics by using ultrathin (100 nm) films connected by stretchable interconnects [146].Someya and coworkers have fabricated flexible pentacene-based organic field-effect transistors (OFETs) for large-area integrated pressure-sensitive sheets with active matrix readout [29], while Bauer and coworkers have investigated novel pressure sensing methods using foam dielectrics [147]and ferroelectrets [148] integrated with FETs. Bao's group has investigated the use of microstructured elastomeric dielectrics for highly sensitive capacitive pressure sensors [149] and has developed a composite conductive elastomer exhibiting repeatable self-healing and mechanical force sensing capabilities[150]. Other groups have developed stretchable optoelectronics, including light-emitting diodes (LEDs) [151] and organic photovoltaics (OPVs) [152] for integration with e-skin.

J. Kim et al.[21] fabricated a stretchable artificial skin based on ultrathin single crystalline silicon nanoribbons that integrate pressure, temperature and humidity sensor arrays for skin prosthesis. It has being integrated also with electro-resistive heaters which could be warmed to facilitate the native skin perception. A fully printed fingerprint three axis tactile force and temperature sensor was developed by, and used to measure tactile and slip force. He et al. developed a flexible self-powered and self/clean T-ZNO/PVDF/fabric multifunctional e-skin [153]. T. Li et al. designed a CNT-based flexible skin-inspired sensory array for fingertips using silk-screen printing technique. The skin relies on three sensing materials and it can measure pressure, temperature, and humidity. Recently, Núñez et al. developed a transparent tactile e-skin along with single layer graphene and coplanar interdigitated capacitive electrodes[154].

They also demonstrate the feasibility of large-scale and low-cost fabrication of a flexible and transparent e-skin for pressure sensing on a prosthetic hand [154].Finally, Osborn et al.[155] created a multilayered electronic dermis (e-dermis) that mimics the behavior of mechanoreceptors and nociceptors to deliver neuromorphic tactile and pain information to an amputee. A time line summary of the evolution of tactile e-skin is shown in Figure. 5.2.

Along the aforementioned, our research group is being addressing this topic since roughly 10 years in a holistic way, managing the seamless design and implementation of the mechanical and electronic systems of the e-skin. In addition, we are working on the development of multichannel stimulations interfaces to communicate and translate the captured information into feedback signals through non-invasive electrotactile stimulation to the user's especially upper limb amputees and stroke patients. More specifically, our focus is the development of:

1) Distributed sensing system or sensing arrays (i.e. skin patches) based on piezoelectric polymers as sensing materials.

2) Electronic Interface.

3) Tactile data processing algorithms.

4) Dedicated digital embedded electronic systems.

5) Distributed non – invasive stimulation system based on electrotactile feedback.

Figure 5.3 depicts our proposed approach and application scenario. It is summarized by embedding artificial distributed sensing and stimulation in prosthetic systems to provide high-fidelity, high-bandwidth tactile feedback to the prosthesis user. Besides, an embedded electronic system for sensor signal acquisition and processing

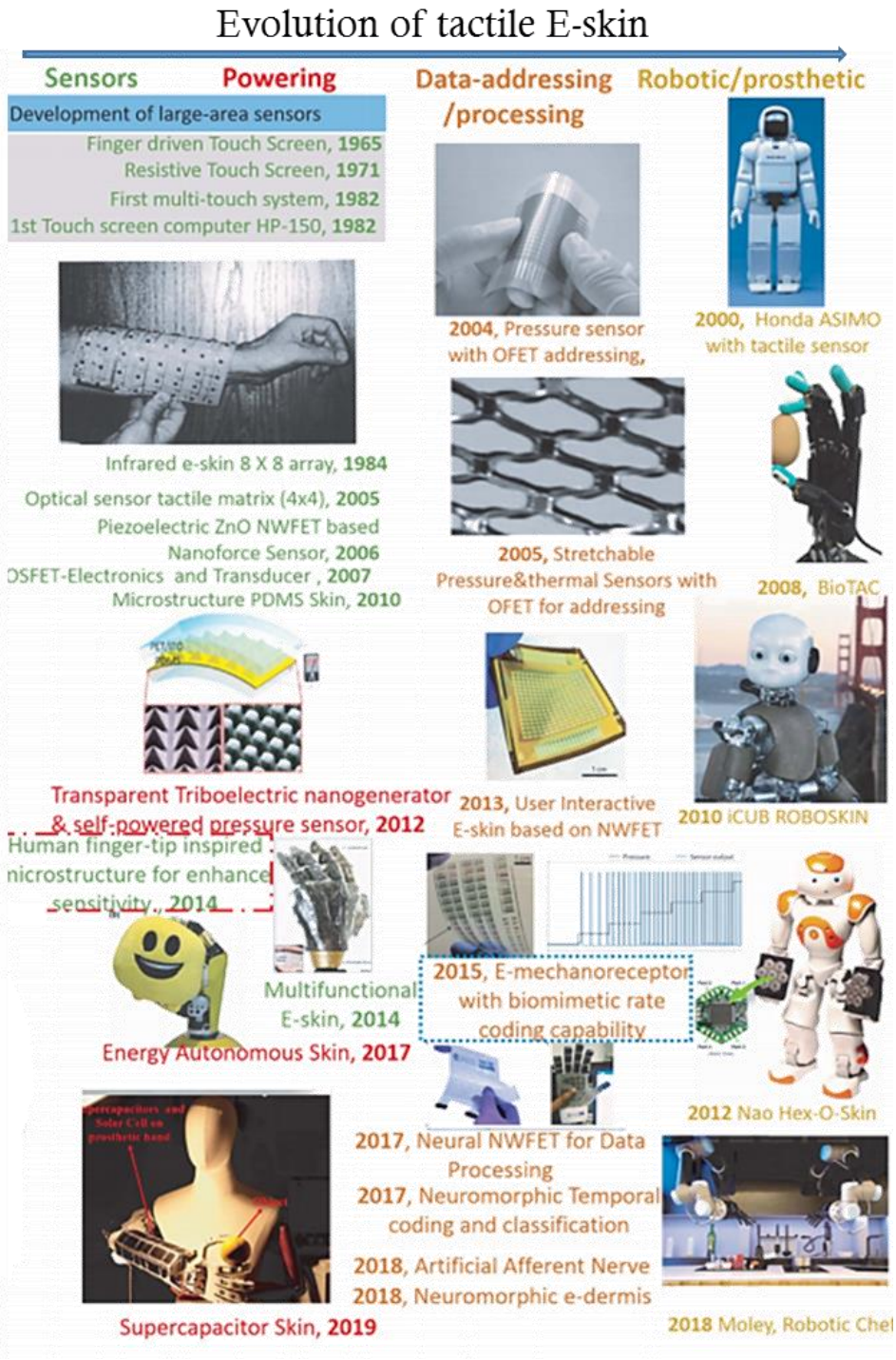

Figure 5.2 The time life for evolution of tactile e-skin

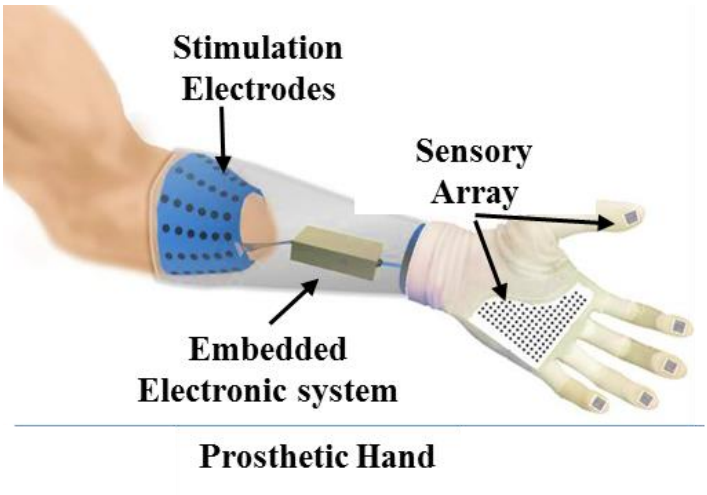

Figure 5.3 Application scenario for restoring the sense of touch in prosthetics

5.5 E-Skin System

Despite the significant progress in the development of sensing materials and sensing technologies, obtaining a functional e-skin system is still hindered by several limitations in microfabrication and cost issues and only few has been employed successfully in autonomous robots. Additionally, the translation of these technologies to human- machine interfaces is still not a straight forward. Today, the majority of research focuses on developing sensors, which measure specific object properties. Emulating the biological sense of touch for hand prostheses mainly depends on the development of i) an articulated tactile sensing system that includes tactile sensors and/or sensors that measure pain, temperature, and proprioception[133][156], ii) an adaptive sensory signal encoding algorithms, and iii) signal transmission and transduction methods to convey the sensory information to the nervous system.

Usually, e-skin is structured as a networked system of "patches" implemented as hybrid stack-wise arrangements incorporating tactile sensing (i.e. mechanical into electrical transduction, signal conditioning and acquisition) and touch interpretation. The scale of the e – skin ranges from small patch such as skin for fingertips to large area for robotics or prosthetics. Nevertheless, generally an e-skin is composed of a protective layer, a sensor layer, a signal-processing layer, and a substrate [35].The polymer based protective layer (such as PDMS) protects the sensor array, and transfers the tactile information (and other interactions) to the sensor array when the skin is touched/approached; the sensor array converts the tactile information into electrical signals, which are further acquired and processed by the signal

processing layer and then transmitted to the bottom structural material layer (i.e. the substrate). In addition to the flexibility (to conform to various curved surfaces/shapes) and stretchability (to support joint movement), the overall structure should be able to simultaneously sense different physical stimuli (including strain, twist, temperature, and humidity) with high sensitivity, and to differentiate them with good temporal and spatial resolutions. For instance, to emulate the human skin in terms of touch/pressure sensitivity, an e-skin should be able to recognize both mediums (10-100 KPa) and low pressures (less than 10 KPa). [133][12].

Figure 5.3 shows an example of this general structure of the e-skin (adapted from [157]). Briefly, the electronic skin system should comprises three main compartments which are the sensing arrays that would reproduce the sense of touch , interface electronic to convert analog to digital tactile signals and tactile data and processing and decoding system. In the following, the e-skin system elements is explained while mainly focusing on our application scenario and its requirements [158].

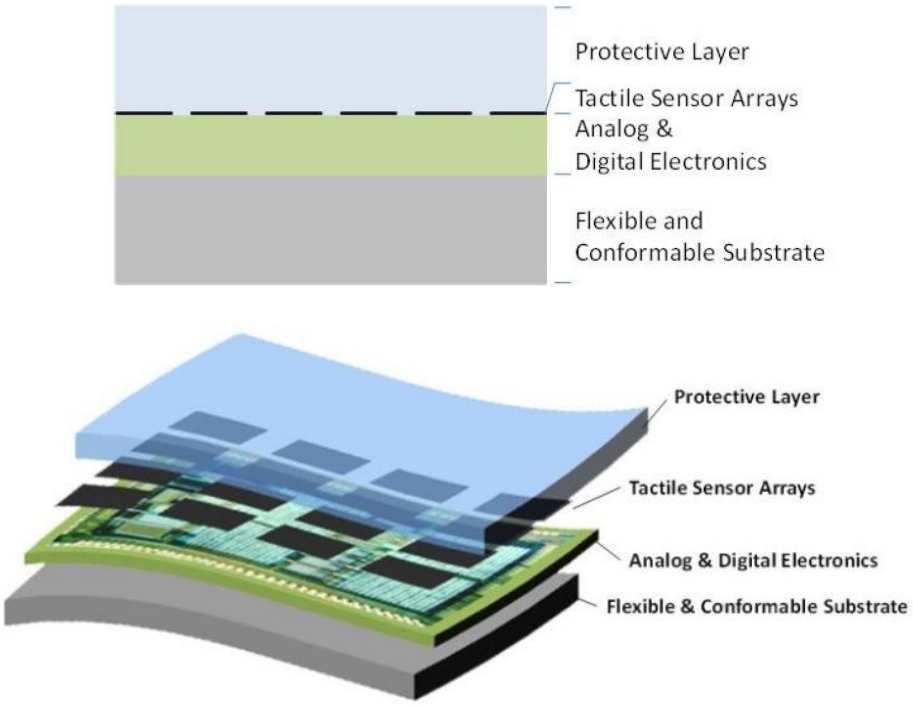

Figure 5.4 Illustration of the E-skin general structure

5.5.1 Tactile Sensing Systems

Enabling tactile sensation in upper limb prostheses is still not as mature as that in other fields (such as robotics, touch screens, etc.), yet the achievements could be adopted into this field. Given that grasping is one of the major functions of hands, most studies of prosthesis tactile

sensing focus on grasp force or pressure in order to prevent slip and achieve a stable grasp. The measured characteristics of touch, however, can be not only force and pressure, but also stiffness, texture, or shape. Thus, different transduction techniques are desired to be synthesized to realize a human like tactile sensing system [132]. This section presents available tactile sensing techniques which have potential to be applied in hand prostheses, namely, resistive sensors (such as strain gauges piezoresistors), capacitive sensors, piezoelectric sensors, optical sensors. In addition, it will present a survey of the current state of art of distributed sensing and highlight limitations in view of new solutions for advanced prosthetic systems. Finally, the design requirements for tactile sensing system in prosthetics is depicted.

5.5.1.1 Tactile Sensing Systems

a) Resistive sensors

Strain Gauges: A strain gauge is a device adhered on the surface of an object to measure the strain caused by external pressure. The resistance of the foil changes with the stress applied on it. Strain gauges are more suitable to measure dynamic strains rather than static ones because of high temperature and humidity sensitivities. They also exhibit nonlinear response. Generally, the smaller a strain gauge is, the higher accuracy can be achieved, because the measured strain is the average strain over the gauge length. Besides, sensors of smaller size are flexible and robust to be applied over dexterous surfaces, such as prostheses, robots and medical devices[159]. Da Silva et al. proposed a finger-mounted tactile sensor based on the strain gauge which presented a linear response, a wide force sensitivity of 0-100 N with a resolution of 0.3 N, and a low hysteresis of 1.7% [160] [18].

Piezoresistors: Piezoresistive tactile sensors also belongs to resistive sensors. Its resistance varies with the deformation caused by the applied force on it, so the force can be obtained by the measurement in a piezoresistor's resistance. Due to the easy measurement of resistance, piezoresistive tactile sensors have friendly electronic interface. They exhibit good sensitivity and are less susceptible to interference[135].Another advantage is the easiness to be implemented in microelectromechanical systems (MEMSs) or integrated to printed circuit boards [161].Despite the mentioned advantages, piezoresistors suffer from hysteresis, temperature sensitivity, fragility, rigidity and high cost. Jorgovanovic et al.[162] presented the static and dynamic characterization of piezoresistive sensors used for detecting the positions of prosthetic finger joints. The feasibility of wireless communication between sensors and a receiving device, to reduce wires, was also discussed. Kane et al. [163]proposed a piezoresistive stress sensor array

with high spatial resolution comparable to human dermis (≈300 μm). It exhibited high potential for dexterous manipulation applications. Various applications with piezoresistive tactile sensors can also be found in stress and force measurement [163], stiffness of soft tissues detection [164]fingertip sensing [165] etc.

b) Capacitive Sensors

A capacitive sensor is among the most sensitive sensors for detecting small force changes. It generally consists of two parallel conductive layers which are separated by dielectric materials. When force is applied on the capacitors, the capacitance between the layers varies with the reduced distance between layers and the deformation of the middle dielectric material as well. Capacitive sensors exhibit high sensitivity, robust performance, a large dynamic range lower. Capacitive tactile sensor array integrated into a prosthetic hand thumb finger [166], temperature sensitivity and low power consumption [167]. It can be used for both dynamic and static force measurement. Additionally, their sensitivity to noise leads to relatively complex electronics for noise filtration. Capacitive sensors are considered as effective sensing elements and have been applied to multi-axis force measurement for gripping and objects manipulation, texture recognition [167] and touch screen application [168], etc.

A capacitive sensor for shear sensing was proposed with a size of 4 N [135]. It showed a high repeatability and approximately linear output within ±2 N; however, its dimension (3.5 mm×1.6 mm ×1.6 mm) was a point to be considered in practical applications. Another capacitive tactile sensor was presented for gripping force measurement with a sensor range of 0-3000 mN [166].

c) Piezoelectric Sensors

Piezoelectric effect is the ability of certain materials to generate an electrical charge in response to external mechanical stress. A piezoelectric tactile sensor is a device based on piezoelectric effect to measure changes, such as force, by converting them to an electrical voltage. Measurement in voltage mode is the simplest way to obtain the applied force. Piezoelectric sensing is one of the few sensing techniques that do not require power supply, which is considered as an outstanding advantage. Besides, it also exhibits high sensitivity, reliability and fast dynamic response. A wide response range of 0 to 1 kHz enables it to be a good choice for vibrations measurement [169]. However, due to the decrease of the output voltage, piezoelectric sensors are unsuitable for measuring static force and show low spatial resolution and poor temperature stability [169].

Various piezoelectric materials can be used for constructing piezoelectric tactile sensors. One of the most widely used one is polyvinylidene fluoride (PVDF). PVDF is a semicrystalline polymer consisting of long chain molecules with repeated unit CF-CH. Its strong piezoelectricity is attributed to the high electronegativity of fluoride atoms comparing with carbon atoms which leads to a large dipole moment [170].

PVDF has many advantages mechanical flexibility, dimensional stability, high piezoelectric coefficients, low weight, formability into very thin sheets (5 μm) and relatively low price. Another promising piezoelectric material is zinc oxide (ZnO) nanotransducer because of its high flexibility and bio-compatibility[32].Also, its ability to generate electrical power when subjected to mechanical vibration leads to various potential applications, including wearable and self-power medical devices [171]. ZnO is proposed to be a good candidate material for pressure and temperature sensor to be applied to prosthetic limbs. During the past years, piezoelectric sensors have been used in prosthetic hands for the detection of slip [32], texture [172]and stiffness [173].

d) Optical Sensors

An optical fiber force sensor generally consists of a light source, a transduction medium, and an optical detector, which is often a vision sensor or a photodiode. The light generated by the light source, usually light emitting diodes (LEDs), passes through the transduction medium which includes optical fibers and a modulator, and finally reaches the detector [174]. Then the detector circuit converts the light signal into electrical signal to be further processed by following electronic devices. The intensity or the spectrum of the modulated light changes according to the variation of the applied force, which is the working principle of optical sensors. This major advantage enables optical sensors to be used in minimally invasive surgeries (MISs) where magnetic resonant imaging (MRI) are widely used to provide high quality images of living organs [174]. In addition, optical sensors have simple and compact structure, and high spatial resolution [175]. Most optical fibers are fragile and not as flexible as electric wires due to their rigidity. Also, their complexity and relatively large size is another problem to be considered for dexterous hand applications.

Table 5.1 Characteristics of different tactile sensors used for e-skin fabrication

Tactile sensors	Working principle	Advantages	Disadvantages
Piezoresistive	Its resistance varies with the deformation caused by applied force.	Simple electronics High sensitivity; Ease of integrating in MEMS Compatible with VLSI Resistant to interference Low cost	Hysteresis Temperature Sensitivity Fragile and Rigid Lack of reproducibility High power consumption
Capacitive	Its capacitance varies with the deformation caused by applied force.	Sensitivity of small force change Reliability Large dynamic range suitable for both dynamic and static force measurement; Low temperature sensitivity; Low power consumption.	Limited spatial resolution; Noise sensitivity; Complex electronics Cross-talk between elements Hysteresis
Piezoelectric	An electric voltage will be produced when a force applied to it.	No need for power supply High reliability Fast dynamic response High sensitivity High accuracy	Low spatial resolution High temperature sensitivity Inability to sense static value.
Optical	The intensity or the spectrum of light varies with the applied force.	Immune to electromagnetic fields; High spatial resolution Wide sensing range Good reliability	Fragile and rigid; Large size; Inability to transparency and highly reflective surface.

5.5.1.2 Tactile Sensing systems on commercial robotic hands

Wide varieties of commercial sensor systems have been developed for robotic hands. The most relevant for tactile sensing are BioTac, Weiss, TekscanTM, Peratech, and DigiTacts. Although these technologies are very advanced, they also present limitations. Among main issues:

1) Narrow applicability (e.g., BioTac only available for fingertips)

2) High power consumption (Weiss 250 mW)

3) Large sensor array size and/or thickness (Peratech: large size, e.g. 15 × 36 cm2, Weiss: large thickness, i.e. 2cm for fingertips),

4) Low framerate (Weiss 400 f/s, TekscanTM 200 f/s, DigiTacts 100 f/s),

5) Low resolution (DigiTacts, 22 taxels), 6) difficult system integration (TekscanTM complex wiring), and high price (e.g. BioTac).

These drawbacks limit system applicability in situations that require compact, robust, flexible and power efficient solutions, as for prosthetic applications.

5.5.1.3 Tactile Sensory systems on prosthetic hands

Sensors for prosthetic hands transduce various modalities of tactile stimuli aiming at recreating naturalistic perception. It is expected that artificial tactile sensors demonstrate small spatial resolution (≤1mm for fingertips, 5mm for hand palm, 20-30mm (e.g. limbs, torso, etc.), high sensitivity varying from 0.01 to 10N, which extend along the tactile frequency range (<1Hz-1 kHz), low hysteresis, fast and linear response (less than 1 ms), wide dynamic range and high reliability. Furthermore, it needs to exhibit high electro-mechanical bandwidth to detect fast events (e.g. incipient slip), large force/pressure (e.g. 1-1000 gram) for daily activities, adequate size and pitch (eg.1cm2/1.5-2mm for fingertips), and customizable shape of e-skin patches and sensor number. Additionally, low cost, low power consumption and scalability are major factors for the prosthetic application. Today's tactile sensing systems encounter many challenges that limits their integration in prosthetic systems, such as designs issues, spatial distribution, low signal to noise ratio (SNR), cross talk, wireless communication, and the lack of signal processing and machine learning methods to encode the acquired data from tactile sensors [12][157] . The main design requirements are summarized in the Table 5.2.

Table 5.2 Design requirements for tactile sensing system in prosthetics

Design criteria		Character guideline
Detectable force range (Dynamic range)		0.01N-10N
Spatial resolution Tactile Sensing element (taxel) pitch (for arrays only)		≤1mm for small sensing areas (e.g. fingertips) ≥ 5mm ÷ 20-30mm for large sensing arrays (e.g. limbs, torso, etc.)
Sensor frequency bandwidth (sensor response time)		0.1 Hz -1kHz , About 1kHz (1ms)
Mechanical sensing detection capability		Normal and shear forces; vibrations
Sensor System characteristics	Mechanical	Flexible, stretchable, conformable and soft, robust and durable.
	Electrical	Low power, minimal wiring and cross talk, electrically and magnetically minimal sensitivity.
Sensor response		Monotonic, not necessarily linear, low hysteresis, stable and repeatable
Temporal variation		Both dynamic and static

Prosthetic hands, if at all sensorized, typically possess two kinds of sensors: position sensors, for providing hand with proprioceptive information, and force/tactile sensors, for estimating mechanical interactions with the environment. However, the measured characteristics cannot be limited to force or position only; ideally, they should also include stiffness, texture, shape, etc.. Osborn et al. have used them in the development of a closed-loop upper limb prosthetic system that measures contact force to detect object slippage and reduce grip strength to prevent breaking of the objects [29]. Other tactile sensors use piezoelectricity, and they are usually employed to measure dynamic forces/pressures. Southampton hand used two different types of sensors on the fingertips in order to restore tactile information: piezoelectric sensors based on PZT for slippage detection and FSR sensors for measuring force [34]. For applications that requires high sensitivity and resolution, capacitive sensors are considered the best candidates, as they can be used for both static and dynamic force measurement. A capacitive based tactile sensor has been utilized for measuring the gripping force in the range of 0-3000 mN and it has been tested on the prosthetic hand. Finally, looking on the commercial prosthetics hands, only the Senor Hand from Otto Bock is provided with a slippage detecting system (i.e. SUVA sensor system) while the recent models such as i-Limb, the Bebionic are not yet provided with force or tactile feedback [34] [158] [134].

5.5.2 Embedded Electronic System

The electronic system embedded into the limb prosthesis takes as input data from the sensor array and processes them to extract meaningful information to be conveyed to the user through electrostimulation. It includes the interface and acquisition system and the tactile data processing and decoding system. The functional block diagram of the prosthetic embedded electronic system is given in Figure 5.5. The analog front-end (AFE) circuit converts sensor signals into voltage e.g. charge amplifier/charge integrator circuits or capacitance to voltage converter [176]. Data acquisition handles three basic tasks: analog to digital conversion (ADC), down sampling, and noise filtering. The ADC sampling rate is beyond the Nyquist rate (oversampling). The down sampling process aims to bring back the data rate to the Nyquist rate. After that, a low pass filter is used for suppressing undesired high frequency noise components. After data acquisition, data fusion is applied.

a) Interface and electronic data acquisition system

Interface electronics includes blocks for signal conditioning and data acquisition. Signal Conditioning implements a set of circuit level functions such as low noise amplification, input/output impedance adaptation, setting the reference DC values (e.g. signal ground), low pass or band pass filtering (e.g. antialiasing low pass filter). The output of the signal conditioning circuit is input to analog to digital (A/D) converter. Usually a dedicated signal conditioning channel is needed for each sensor element in the array with a single A/D converter. Signal conditioning channels (one for each sensor element of the array) are time multiplexed via an analog multiplexer at the input of the A/D converter.

Data acquisition involves addressing the signal conditioning channel and digitization (i.e. analog to digital conversion) of the analog input. The tactile sensing control can query and read tactile data from any sensor in the system. The ability to query individual tactile sensors is helpful e.g. for diagnostics and calibration. Issues like wiring complexity also influence the interface electronics, in particular for large skin area arrays. The addressing can be serial and fixed to decrease complexity at the expenses of an increase of array scanning rate. An alternative

arrangement for signal conditioning and data acquisition is to translate the sensed signal

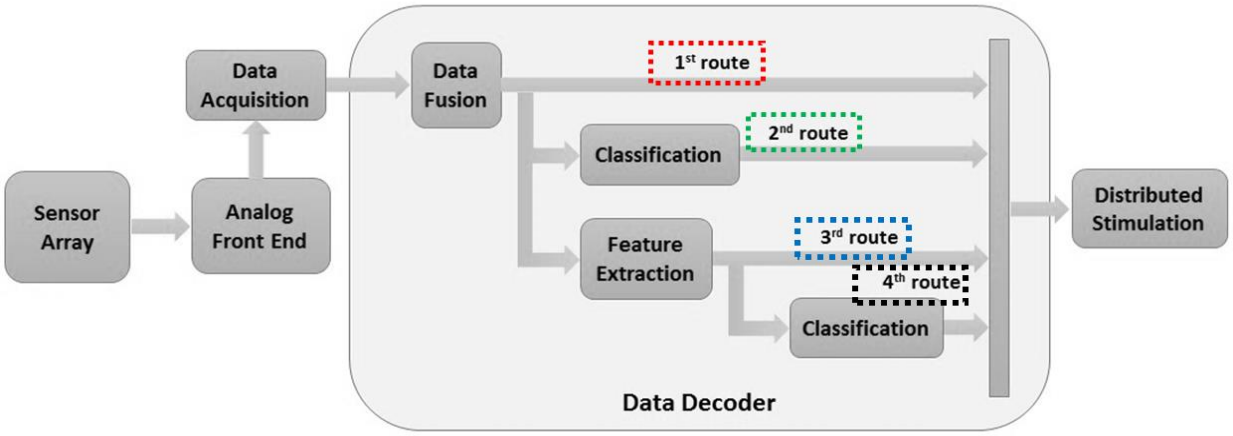

Figure 5.5 Functional block diagram for the embedded electronic system. 1st route: Raw Tactile Data, 2nd route: Classification, 3rd route: Extracting general contact Features, 4th route: Classification based on feature extraction

into a frequency value, which is subsequently digitized and acquired via a digital counter. The advantage of this approach is the robustness of the sensor output signal with respect to noise and disturbances. Wiring is minimized as the sensor output is a single signal/wire. On the other hand, the acquisition time can be very long as it depends on the oscillating frequency and on the sensing resolution

b) Tactile Data Decoding and decoding system

Research efforts have mainly focused on providing force feedback rather than the spatial tactile sensation (e.g. surface texture and shape) [18]. While force feedback is important for the control of grasping, restoring other tactile sensations associated to distribute sensing is also relevant for promoting embodiment. Robotics research demonstrated that it is possible to extract high level features from tactile data such as the classification of touch modalities (e.g. Rolling, poking, sliding) or discrimination of the attributes (e.g. texture, roughness, shape) of contact objects, [177]. A similar approach could be applied in prosthetics. However, high-level features relevant in this context still need to be clearly identified. As shown in Figure 5.5, four possible routes could be pursued regarding the type of information to be communicated to the subject. i.e. i) "raw" tactile data; ii) touch modalities; iii) general contact features (e.g. 3D force distribution); or iv) general contact classification based on feature extraction.

In a recent study, (***first route***) "raw" tactile data were transmitted from the e-skin to the subject: a sensor fusion process was applied to map more sensing elements to less stimulation channels. Gastaldo et al. (***second route***) developed a Machine Learning pattern-recognition system based on tensor signals. Other approaches are possible, as significant work on the classification of touch modalities using tactile sensors has been reported in literature [178]). ***Third route*** is employing different methods (including modeling skin mechanics) for feature extraction from sensor data (e.g. contact force/pressure distribution, touch location, contact area, etc.) and conveying such information directly to the stimulator. In the ***fourth route***, the signal is processed to first emphasize relevant features in tactile data, to be subsequently used for more general touch classification. To give an example, [177] worked over different touch attributes, such as pressure intensity, contact area, discrimination threshold, and temporal information (i.e. touch duration, frequency of repetition) to classify the touch modalities, such as tapping, pushing, scratching. Second stage classification may also include more general information, e.g. Binary classification of object incipient sliding or the classification of the contact object material/texture starting from friction information contained into the force distribution.

Importantly, the system must operate in real time. For example, in, data were acquired from an array of 64 sensors in blocks of 50 samples corresponding to time window of 50ms. The system used PVDF piezoelectric tactile sensors and the sampling rate was 2 kHz. Therefore, 100 data array (i.e. sensor dimension) were acquired during each time window. These data needed

to be processed and the results sent to the stimulator within 50ms, which was the refresh rate of the stimulator. Increasing the number of sensors may dramatically increase the amount of data to be processed and thus compromise real time operation.

c) Hardware implementations of tactile data decoding

Real time response can be achieved by implementing tactile data decoding algorithms in hardware. Until now, the implementation of tactile data decoding algorithms has been mostly limited to software-based solutions. No hardware implementations for the feature extraction or/and classification are present in the literature. Main challenge is the high amount of data to be processed, which increases hardware complexity and power consumption. [179] presented an architecture based on FPGAs that implements a direct interface to the sensor without ADC. An ARM Cortex M4 STM32F303 has been used to implement recognition algorithms for gestures that are applied with static contact on the sensor surface [180]. A multimodal bio-inspired tactile sensing module using three microcontroller units for texture classification is introduced in [181]. Such systems implement good functional solutions for tactile data decoding, but they are not appropriate for the prosthetic application. High processing time, algorithm complexity, high power consumption and size restrict the current implementations to networked PCB systems which are not convenient for mobile (battery powered) and compact implementation within a prosthesis. Ibrahim et al. [182] presented recently a real-time FPGA implementation of tensorial support vector machine for classification of touch modalities. Although this solution achieves real time operation, it still requires a high amount of power consumption arriving to unacceptable values (order of Watt) for a large number of touch modalities. If we target an ASIC implementation of this system [182]: the power consumption may be decreased 14 times compared to the FPGA implementation [183]. The amount of power varies from 43mW when dealing with only 2 input touch modalities classification to more than 244mW when the system deals with 8 touch modalities [183]. Extending the lifetime of the prosthetic device could be achieved by pursuing two fundamental approaches: 1) reducing system power consumption (mostly computational part), or 2) increasing energy storage capacity by exploiting energy harvesters. To reduce the power consumption, the overall power system consumption may be considerably reduced by employing smart and adaptive systems [184]. On the other hand, power supply availability is a limiting factor in wearable devices whose form factor constrains battery size. Wearable harvesters that collect energy from the environment are a promising technology to achieve the long-life goal for truly wearable devices. Although harvesting energy for powering

wearable devices is challenging due to strict constraints in terms of size and weight, such systems have recently demonstrated the possibility to harvest an amount of power up to 16 mW [184].

5.6 Conclusion

Given the importance of tactile sensing in daily life interactions and exploration of the environment, researches are still striving to understand the sense of touch and aims to develop smart tactile sensing systems that could mimic its characteristics and functions. Tactile sensors range from simple sensors to sense contact location to complex systems to measure surface properties, stiffness, texture, and temperature. E-skin is an artificial skin based on tactile sensing systems that aims to replicate the human skin. It could be fabricated using several transduction techniques, materials and structural designs, depending on the targeted application. E-skin should be flexible and stretchable; additionally, it must have multifunctional sensing capabilities that cover large areas at low cost.

It has been included in numerous applications especially in robotics, however their implementation into prosthetics still in its infancy stage due to the technical difficulties and complicated nature of the human tactile sensation. Future potential lie on the fabrication and the development of flexible, stretchable and robust large-area multifunctional intelligent e-skins that have tremendous sensing and processing capabilities to enable tactile sensations in active prosthetics.

This chapter presents the e-skin system concept while focusing on our application scenario. First, the human sense of touch has been introduced along with the physiology of the human skin. Secondly, a brief review about the evolution of the tactile sensing and artificial skins have been presented. Thirdly, the e-skin system were explained concerning our main target as a group in restoring the sense of touch in prosthetics. It provided a survey about the main compartments of the e-skin (i.e. tactile sensing, interface electronic and the embedded electronic system) starting from the state of art and how to get inspired of what have been implemented on the robotic field, to pave the way of achieving an electronic skin compatible to prosthetics application requirements.

Keeping the same background, the next chapter will present the novel piezoelectric based screen-printed e-skin that is intended to cover the fingertips and the palm of the of the Ottobock

Michelangelo prosthetic hand and our assistive glove for stroke patients and the contribution of this thesis in characterizing and validating it.

Chapter 6 Screen – Printed E-Skin Based on Piezoelectric Polymer Sensors

6.1 Introduction

Electronic skin is a touch sensitive system that provides quantitative information about contact properties (e.g. contact force [185] or contact shape [186]) or given properties of the contact object (e.g. surface texture [187] or object shape [188]) or contact event (e.g. discrimination between touch modalities [189]) through processing tactile sensor outputs. The e-skin is as an assembled electronic system that incorporate functional and structural materials coupled to suitable electronic interface to read sensor signals. Artificial skin systems are implemented in a wide range of applications such as robotics [132] , prosthetics [133], and teleoperation systems [190].

As the functional properties of the e-skin mostly depend on the sensor type, it is worth focusing on the sensor itself. Based on the sensing mechanism employed, various tactile sensors have been developed like piezoelectric, piezo-resistive, capacitive, optical, electromagnetic, ultrasonic, etc. [178]. The development of tactile sensors based on piezoelectric polymers has been extensively investigated in recent years due to their outstanding advantages. They exhibit high sensitivity, fast dynamic response and large workable range from <1Hz to 1 KHz, covering the whole frequency bandwidth of human skin mechanoreceptors [169]. Drawbacks of these materials are their poor temperature stability and their inability to measure static forces [191].

Different piezoelectric materials such as quartz single crystals, ceramics and piezoelectric polymers have been used to fabricate piezoelectric tactile sensors. Polymer materials, especially polyvinylidene fluoride (PVDF) and its (TrFE) Trifluoroethylene copolymers with their ultra-sensitivity, high deformability, mechanical flexibility and piezo, pyro and ferroelectric stability have been proven being good candidates for flexible tactile sensors, which can meet the cutting edge requirements of dynamic tactile sensing and can be easily integrated into artificial e-skin [169].

Regtien et al. [192] stated the advantage of P(VDF-TrFE) as tactile sensors and Seminara et al. [169] concluded that PVDF films can be integrated in multimodal sensitive layers, mimicking the behavior of the human skin. Khan et al. [190] demonstrated all screen-printed tactile P(VDF-TrFE) sensor arrays for robotic applications, Hsu et al. proved the strain sensitivity of PVDF-arrays on flexible substrates [193] and Tien et al. exploited the multimodality with P(VDF-TrFE) gated OFETs for simultaneous detection of pressure and temperature [194]. In general, the cross-sensitivity between the temperature and pressure-sensing channel in ferroelectrics (therefore also in PVDF) can become an issue in certain applications and therefore a separation of the piezo- and pyroelectric effect may be advantageous [195].

PVDF is a semi-crystalline polymer synthesized by the polymerization of H2C = CF2 monomer. Its copolymer, Poly(vinylidene fluoride trifluoroethylene) or P(VDF-TrFE), is a ferroelectric material that does not need to undergo the mechanical stretching of the molecular chains along one of the transversal axes leading to easier fabrication. Different fabrication technologies have been reported to realize P(VDF-TrFE) based sensors such as spin coating, electrospinning, sol-gel, chemical vapor deposition, micro-machined mold transfer, inkjet printing [196]. The frequently used techniques such as spin coater and inkjet have limitations of process speed and overlay registration accuracy in multilayered structures. Despite the high lateral resolution, patterning of large areas (>2 mm) through ink-jet printing requires repeated deposition of droplets, which often results in a non-uniform layer thickness and edges. In addition, patterning of P(VDF-TrFE) after spin coating requires photolithography, which leads to more complexity of the manufacturing process. The cost-effectiveness and faster fabrication of sensors over large areas make screen-printing a very attractive technique [197].

Hoda et al. recently developed all screen-printed tactile sensing arrays (in the following: sensing patches) based on P(VDF-TrFE) piezoelectric polymers for prosthetic applications [198], where arrays of piezoelectric polymer sensors provided of their metal contacts have been screen-printed on a transparent plastic foil. The same fabrication process has been used to design and fabricate ad-hoc sensing patches to be mounted over two different platforms, i.e. an assistive sensorized glove and the Michelangelo prosthetic Hand by Ottobock [31].

The focus of this study is the validation of the developed technology, i.e. ascertaining that -printed sensors are working as expected. It is noteworthy at this stage to remarkably come to the reader's mind that characterizing sensor behavior directly would be a quite complex, lengthy, risky and hardly reproducible process. Indeed, a cylindrical indenter would be needed for

compression tests [169]. Nonetheless, direct contact of the indenter with the sensor would have various shortcomings: (1) the contact would hardly be uniformly distributed as both the indenter and sensor surfaces have natural roughness; (2) the contact surface could then not be precisely determined; (3) the direct indenter contact leads to sensor damage. Wherefore, an indirect procedure has been used. It requires the integration of a protective layer on top of the sensing patch, giving rise to what we call the skin patch. As sensors are embedded into the skin mechanical structure, a model is needed to relate the incoming force to sensor charge response, accounting for stress transmission through the cover layer. Reference for that is a validated model of analogous skin structure based on a rigid substrate, PVDF piezoelectric polymer sensors and the same (elastic) protective layer [199].

In particular, the study presented in this chapter reports the experimental setup and procedures, which allow a fast characterization of piezoelectric sensors embedded into an elastic layer and working in thickness mode (i.e. a pure compression mode). For that, direct compression tests have been replaced by indentation tests over the skin surface, performed continuously over the whole frequency range of interest for tactile applications (<1 Hz – 1 kHz). This in turn, validates the skin fabrication technology. Finally, a protocol for quick e-skin validation is provided. This chapter presents the analyzed results related to P(VDF-TrFE) electromechanical characterization and sensor validation by comparing the d33 piezoelectric coefficient with values found in the literature. It is organized as follows: Section 6.2 presents the materials and methods, briefly illustrating the e-skin design and technology, the reference skin model and the experimental setup. The results related to the validation of screen printed sensor arrays are reported in section III. Finally, discussion and conclusive remarks are given in section IV and V.

6.2 Materials and Methods

6.2.1 Electronic Skin Design and Technology

6.2.1.1 Screen – Printed Piezoelectric Polymer Sensor Arrays

Fully screen-printed flexible sensor arrays based on P(VDF-TrFE) piezoelectric polymer sensors have been fabricated by JOANNEUM RESEARCH (in the following, JNR). They patented a low-temperature sol-gel based synthesis for P(VDF-TrFE) inks. Main steps of the overall manufacturing process used by JNR to print ferroelectric sensor arrays based on P(VDF-

TrFE) repeated units is illustrated in Figure 5.1. The fabrication of these sensor arrays is done by screen-printing at a Thieme LAB 1000. A transparent and flexible (175 μm thick) DIN A4 plastic foil (Melinex® ST 725) is used as a substrate, to ensure high flexibility and good adhesion of the functional materials applied during the screen printing process (Figure 6.1-a). First, the circular bottom electrodes of the P(VDF-TrFE) are screen-printed (Figure 6.1-b). In the second step, the ferroelectric polymer PVDF-TrFE is screen-printed onto the bottom electrodes, followed by a short curing step at 110 ° C. The curing step supports the formation of the crystalline piezo- and pyroelectric β -phase and accelerates evaporation of the solvent. Figure 6.1-c also includes the third step of screen printing top electrodes. Either PEDOT: PSS or silver or carbon have been used as top electrodes [200]: it is worth noting that the carbon layer (Figure 6.1-d) is alternative to the usage of PEDOT:PSS or silver (Figure 6.1c). Conductive silver ink has been always used for electrical interconnections (Figure 6.1e).

A final UV-curable lacquer layer is deposited on top for overall sensor protection. A poling procedure is then needed to align in the thickness direction randomly oriented dipoles contained in P(VDF-TrFE) crystallites. This has been achieved by hysteresis poling of each sensor with an alternating electric field at a frequency between 2 and 10 Hz and a magnitude of 100 MV/m, corresponding to twice the coercive field strength. Final geometries of sensor array patches (called below as sensing patches) have been obtained through cutting with a Trotec Speedy 300 laser. The full deposition process has been thoroughly illustrated in, to which the reader is referred for further details.

Figure 6.2 depicts (a) the cross-sectional view of a single sensor unit and (b) the structure of a sensing patch built on a sensor array (c) a reprinted microscope photo (d) a photo for a real sample.

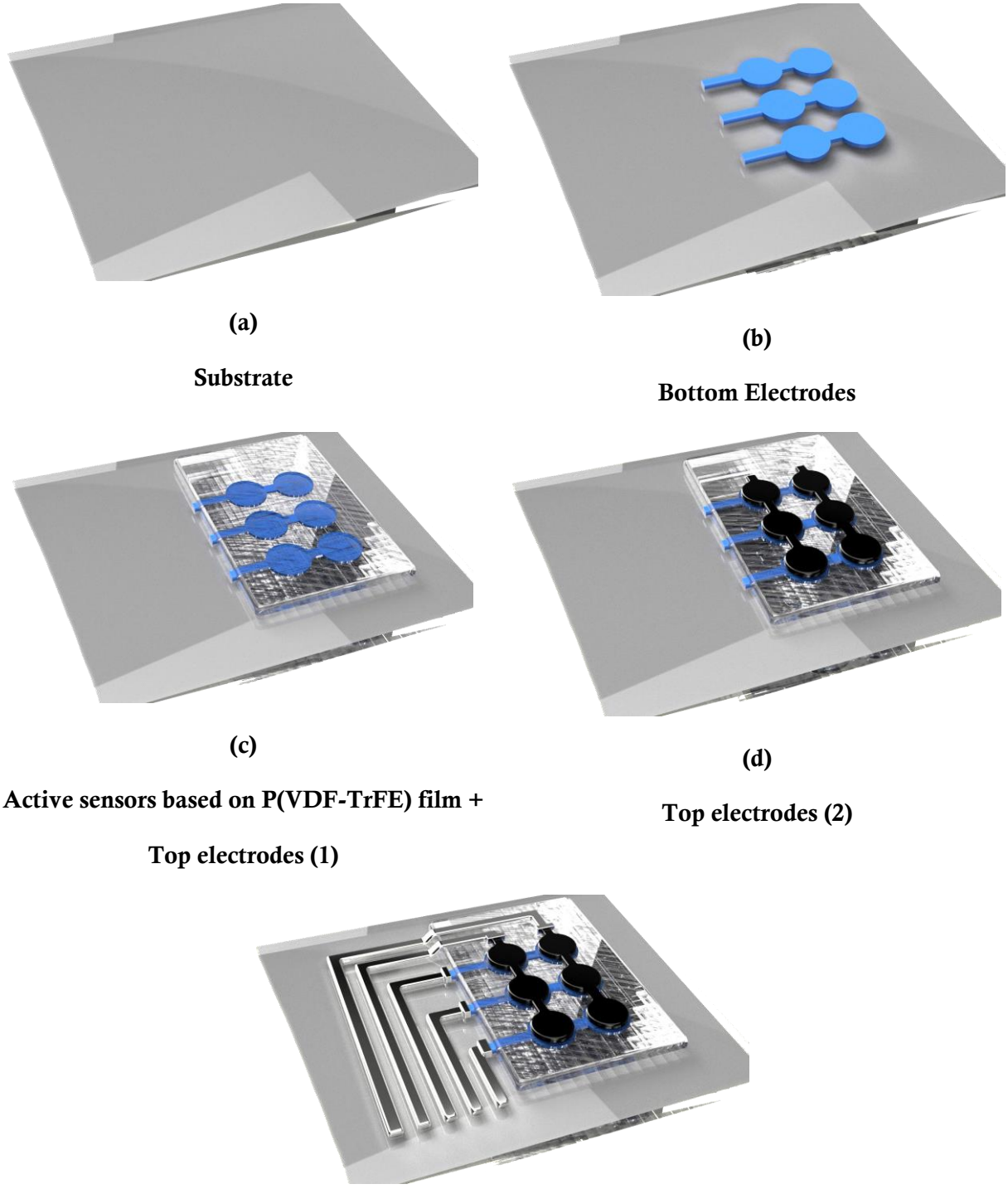

Figure 6.1 Illustration of fabrication process flow of printed ferroelectric sensor arrays based on P(VDF-TrFE) repeated units (reprinted with permission from JNR).

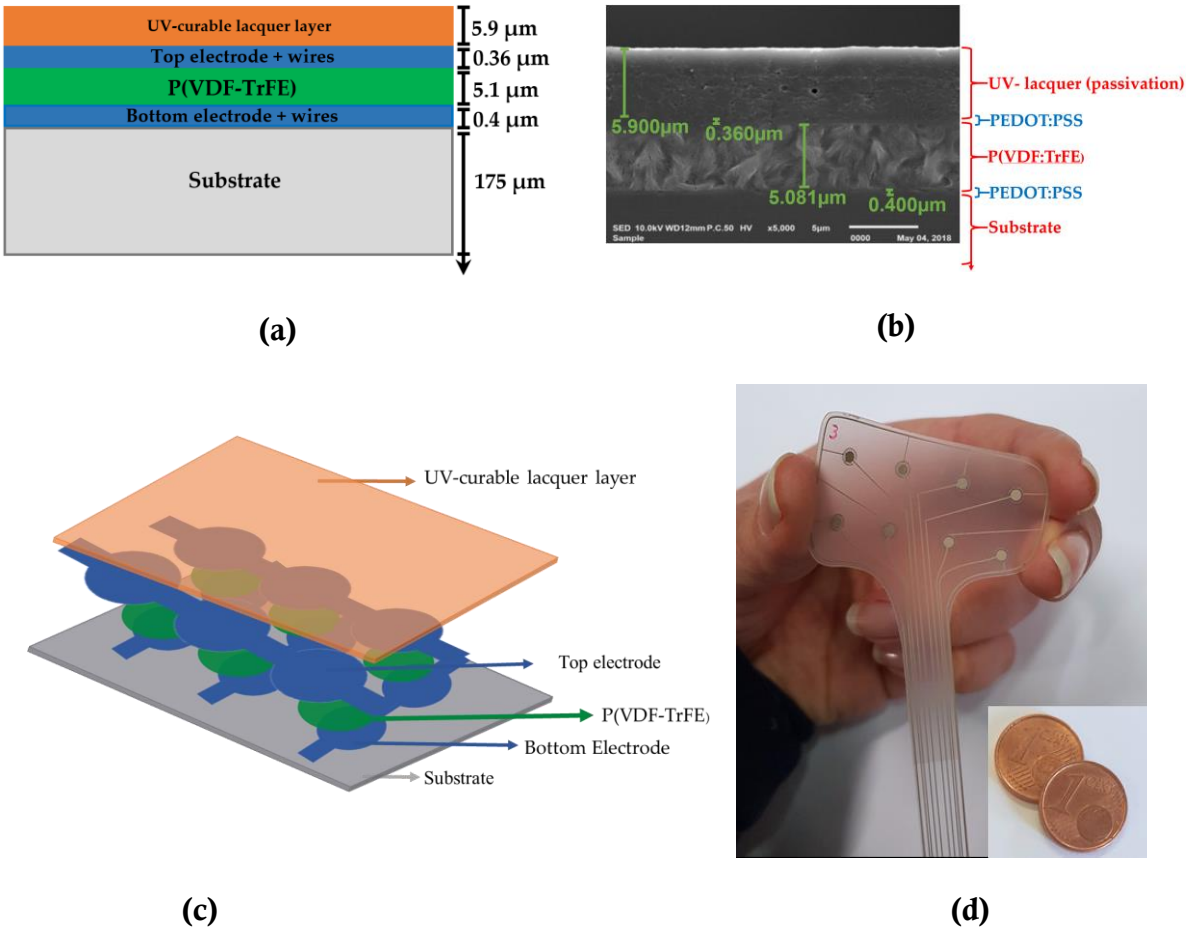

Figure 6.2 (a) Cross sectional view of a single sensor unit: sketch with indicative thicknesses of various layers, (b) Reprinted microscopic photo of the sensing element Sketch of the sensing patch, (c) Sketch of the sensing patch, & (d) Picture of a real sample

6.2.1.2 Design of the sensing patches

Two complete sets of sensing patches have been designed. The former is intended for a textile glove with sensorized fingertips and palm, while the latter includes skin patches for the fingers and palm of the prosthetic Michelangelo Hand designed by Ottobock [5].

Sensor densities of the fingertips and the palm have been oriented by psychophysical measurements of the spatial acuity of the human skin [201]. The point localization threshold is ~1–2 mm on the fingertip and around 1cm for the palm. To define the point-localization threshold, a stimulus is presented to the skin, followed in time by a second stimulus that may or may not be applied to the same site. Observers are required to say whether the two stimuli occur at the same or different locations. Obviously, these values are only reference values, as the spatial acuity of the artificial skin is strongly dependent on the thickness and the material of the

protective layer, as demonstrated in [199]. In particular, we refer to the proportionality coefficient γ plotted in Figure 4 of [199]which gives a measure of the skin spatial acuity through the sensor receptive field, i.e. the spatial concentration of the mechanical stress information around a single sensor. The γ coefficient depends on the thickness of the elastic cover layer and vanishes at a distance between the point force and the sensor axis that marks the transition to the region where the force does no longer affect the specified sensor.

Five different patch geometries have been systematically characterized and their correspondent results are presented in the current article. Their layouts are illustrated in Figure 6.3.

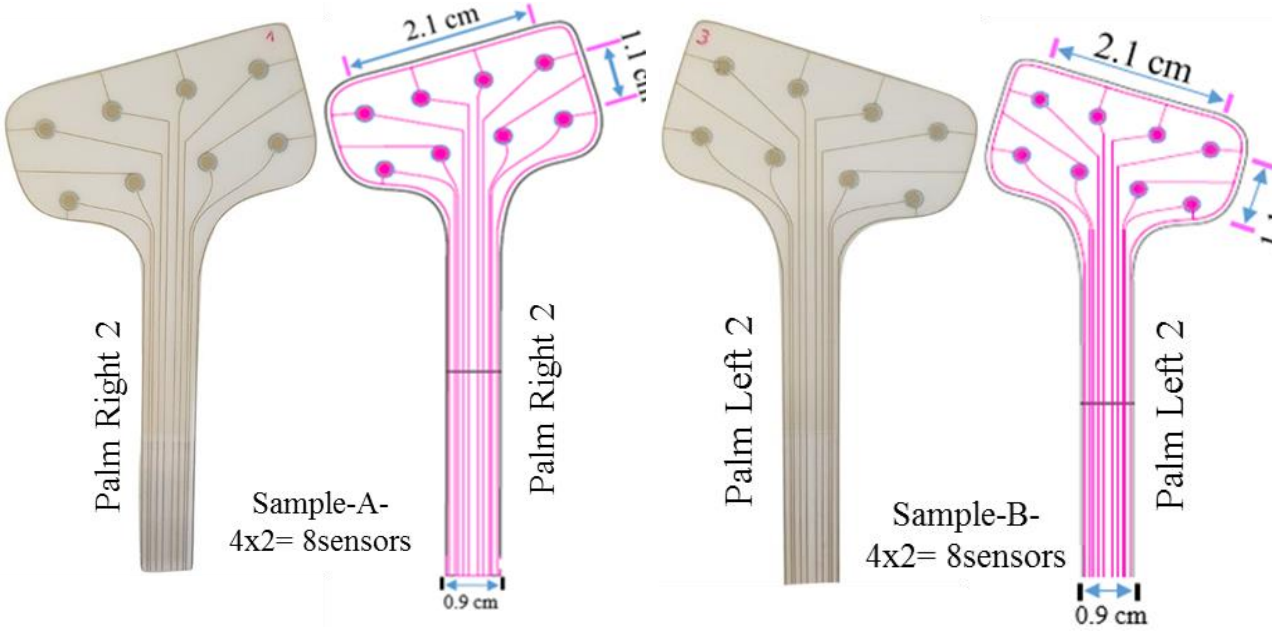

(a) **(b)**

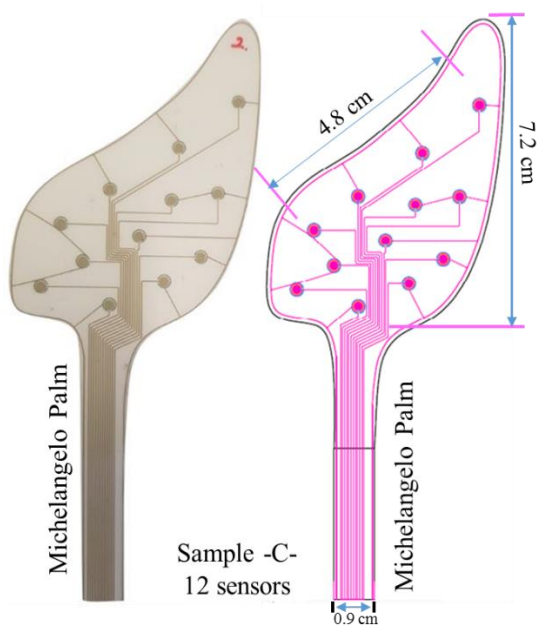

(c)

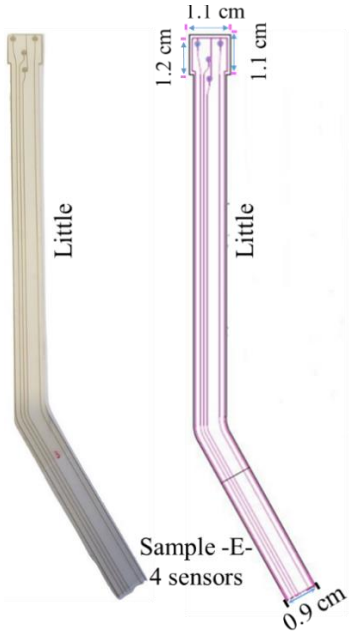

(d)

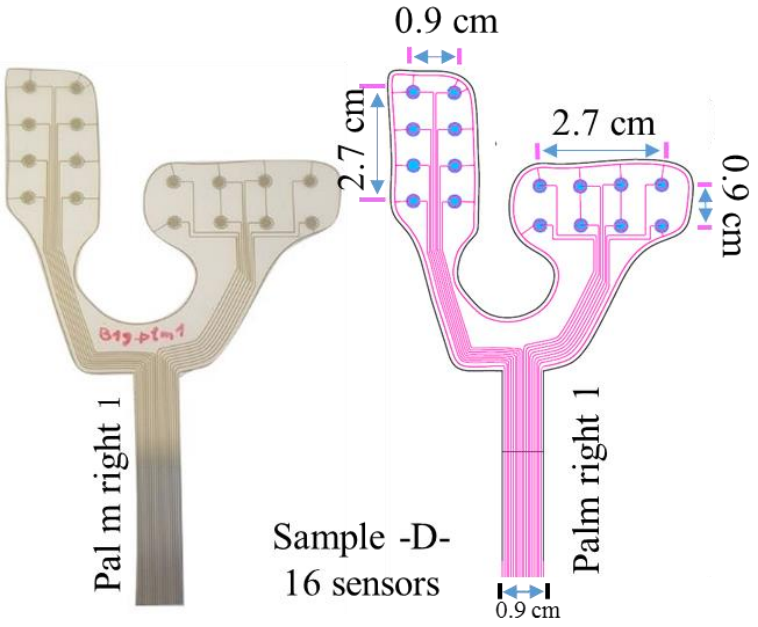

(e)

Figure 6.3 Design of Different Sensing Patches. (a) Sample A-Palm right 2 - 4x2 array = 8 taxels, Taxel diameter = 2mm, center-to-center pitch = 1 cm, total sensing area = 2.1 x 1.1 cm2. (b) Sample B- Palm left 2 – 4x2 array = 8 taxels, Taxel diameter = 2mm, pitch = 1.1 cm, total sensing area = 2.1 x 1.1 cm2. (c) Sample C-Michelangelo palm -12 taxels, taxel diameter = 2mm. (d) Sample E- Michelangelo little -4 taxels, taxel diameter = 1mm, total sensing area: square side =1.1 cm (e) Sample D- Palm right 1 – two 4x2 arrays -16 taxels, Taxel diameter = 2mm, center-to-center pitch =0.9cm, total sensing area = 0.9 x 2.7 cm2.

6.2.2 Experimental setup

Twelve skin patches of five categories (A, B, C, D, E designs as shown in Figure 5.3) were tested using the mechanical chain shown in Figure 4 and described in [199]. Each sensing patch was integrated on a rigid substrate and covered by an elastic protective layer, thus building a skin patch (see the bottom part of Figure 5.4). In particular, the same elastomer material has been used for stress transmission as in [199]. Building a skin structure that mimics as close as possible the conditions imposed by the latter model has two implications. On one hand, we would like to enable sensors to work in pure compressive mode. This would need to ensure that the coupling does not lead to the development of significant values of the normal stresses T1 and T2 in the sensor. Operationally, in order to be able to keep the sensing patch intact for use after the validation stage, we have simply laid it over the rigid substrate with no further constraint. This implies that the boundary conditions at the contact sensing patch – rigid substrate would be a simple roller. On the other hand, the upper protective layer is kept in contact with the substrate, constraining the lateral boundary of its bottom surface with double-sided adhesive tape (Model 3M300L, 3M). This scheme allows one to assume a roller type boundary condition at the elastomer at the bottom with constrained boundaries. The applied coupling scenario is illustrated in Figure 6.5.

Tests were performed using a mechanical input (force) and electrical output (charge). A rigid plate was fixed on the moving head of an electromechanical shaker (Brüel&Kjaer, Minishaker Type 4810). A rigid spherical indenter (R = 4mm) and a piezoelectric force transducer (Model 208C01, PCB Piezotronics) were coupled on the upper head of the rigid frame. The skin patch assembled on the rigid circular plate was then mounted on a fixed support and faced down side.

A preload was first applied to guarantee indenter-PDMS contact during the whole mechanical stimulation. It has been controlled by a laser (Waycon LAS TM10), allowing us to fix the displacement of the rigid plate at a certain value for certain preload, through displacement-force calibration curves.

A swept sine signal was then provided to an electromechanical shaker by a graphical user interface (GUI) developed with NI LabVIEW on a host PC and NI DAQ data acquisition board. This signal was amplified using a Power Amplifier (Type 2706). All these elements have been accurately aligned before any test. Forces in the frequency range of (0.5-1kHz) have been applied

through the spherical indenter shown in Figure 4 and coupled to the electromechanical shaker. The force transducer (stimulus) and the charge developed by the sensor (response) were conditioned by PCB Sensor Signal Conditioner (482C54) and processed in frequency to give the

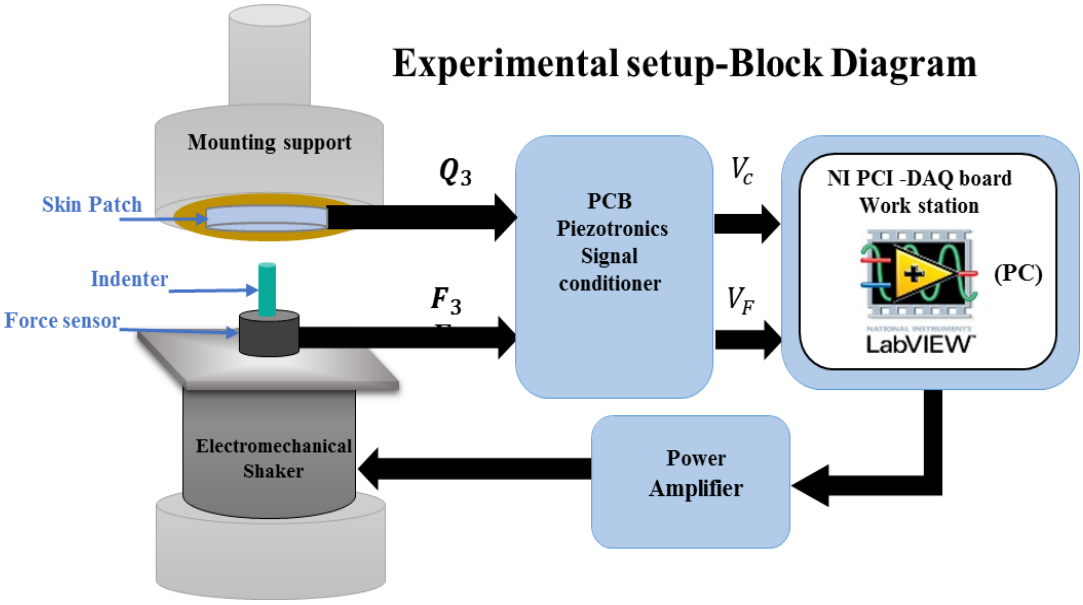

(a)

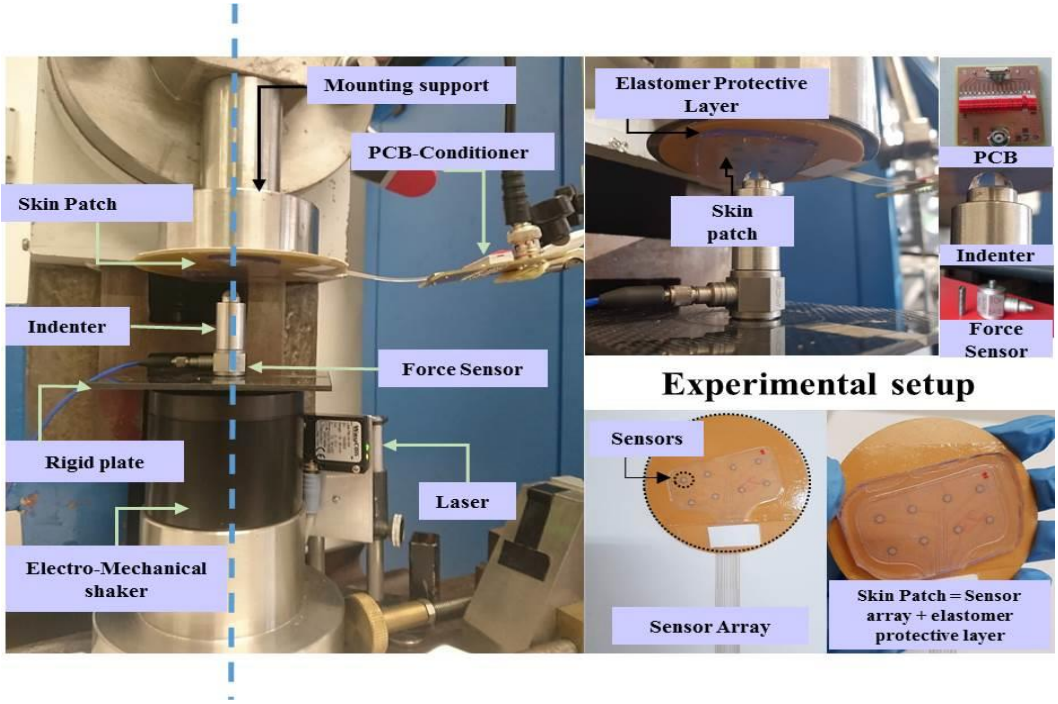

(b)

Figure 6.4 Experimental setup. Top: Block Diagram, Bottom: Pictures of the setup. The blue dotted line shows the alignment of the testing elements.

system response function (FRF) at each frequency step. We recall that FRF corresponds to the ratio between the Fourier transform of the output charge and that of the input force.

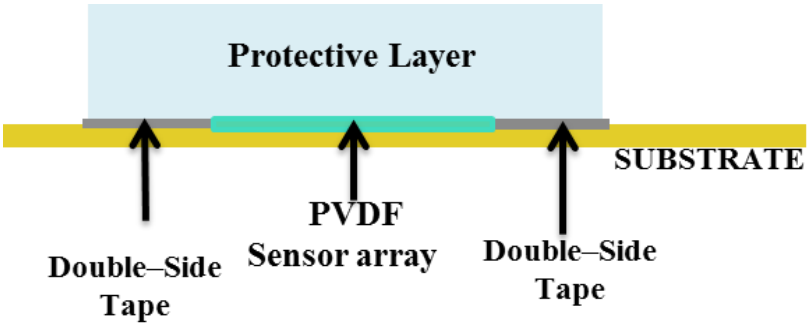

Figure 6.5 The applied coupling scenario

6.2.3 Reference skin structure and model

As mentioned in the introduction, in order to validate the sensor behavior without damaging the sensors themselves, sensing patches need be integrated into a rigid substrate and covered by an elastomer. Hence the indenter force is applied to the surface of the protective layer and transmitted to the sensors, working in thickness mode. In order to derive the stress acting on the sensor, our previous model has been used [199] and is briefly summarized below (Figure. 6.6).

The ultimate use of the model is to estimate the electrical sensor output from a measure of a basic mechanical action at the skin surface. In other words, using the constitutive relationship of the sensors working in thickness-mode (purely compressive), one might write:

$$Q_3 = \pi r_T^2 d_{33} \bar{T}_3 \qquad \textbf{(6.1)}$$

where Q_3 is the total sensor charge measured by the charge amplifier [202], r_T is the sensor radius, d33 is the P(VDF-TrFE) piezoelectric coefficient and T_3 is the normal stress component and T_3 averaged over a single extended sensor.

In order to relate $\bar{T}_3$ to the acting force F_3, we have employed the model of [199].It is worth noting that PVDF and P(VDF-TrFE) have the same constitutive equations, therefore their purely compressive behavior is identical (though the associated values of d_{33} are different), and the model can be adequately applied.

Application of the model leads to the following relationship between the charge and the imposed force F_3:

$$Q_3 = -d_{33}\frac{3}{2}\left(\frac{r_T}{h}\right)^2 \sigma\left(\frac{a}{h},\frac{r_T}{h}\right) F_3 \qquad \textbf{(6.2)}$$

Where h is the elastomer thickness, a is the contact radius and σ is an output function of the theory, expressed as a double integral to be solved numerically, for each chosen value of $\frac{r_T}{h}$ and $\frac{a}{h}$

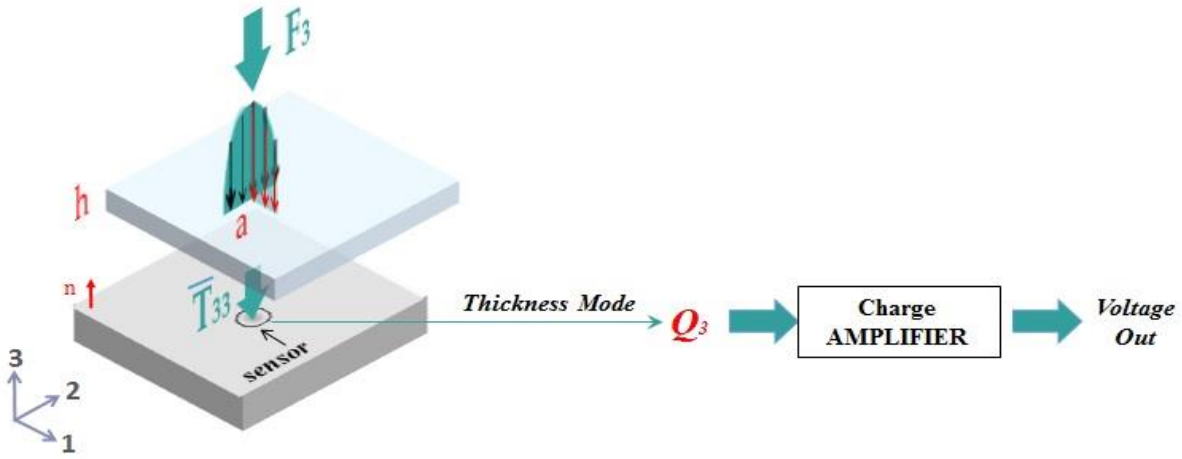

Figure 6.6 Sketch of the general working mechanism of the (PVDF-TrFE) sensor. The Hertzian input force (with contact radius a) is transmitted to the sensor (with radius rT) through the elastomer layer of thickness h. With the presupposition that the sensor works solely in compressive mode, it directly converts the received normal stress T3 into electrical displacement D3, through a characterizing piezoelectric coefficient, namely the d33 (1). A charge amplifier is used to convert the total sensor charge into voltage.

The radius "a "of the imprint is related to the applied load "F_3" by the equation [203]:

$$a^3 = \frac{3F_3R}{4E}(1-\nu^2), \qquad \textbf{(6.3)}$$

Where R is the indenter radius, and E and ν are the Young modulus and the Poisson ratio of the elastic protective layer, respectively. Note that the given preload affects the contact radius a (5.3) while the amplitude of the dynamic swept sine force determines the PVDF charge. On the contrary, the dynamic component does not affect the computation of the contact radius, as the dynamic signal amplitude is negligible with respect to the preload.

For a given skin geometry, associated with a specific, (2) allows one to estimate the effective piezoelectric coefficient d_{33} of each P(VDF-TrFE) sensor, once the charge Q_3 and the (normal) applied force F_3 centered on that specific sensor have been measured. Comparison with the expected value of d_{33} [191] [200] helps validating sensor functioning.

The effect of the finite thickness of the elastomer layer has been expressed by the value of sigma for the given skin geometry presented in this paper and calculated numerically through FEM simulations as discussed in [199]. In particular, we considered an elastic, virtually incompressible, medium (Poisson ratio sufficiently close to 0.5) consisting of a layer of finite thickness h = 2.5mm, length l = 40mm and width b = 20mm. Length and width of the layer have been chosen arbitrarily, with the sole requirement of the distance between the elastomer side and the sensor center being much larger than the sensor radius, such to justify the assumption ion that the lateral boundaries do not affect the stress field acting on the sensor significantly.

The free surface is presumed to be subjected to an external Hertzian pressure distribution, the contact radius a being dependent from *R, F_3, E* and ν, as for (3). The indenter radius R is 4mm in all the present study, the employed value for the elastomer modulus E is the result of the experimental characterization of the elastic layer reported in [199] and corresponds to 16 [MPa] (slope of the linear portion of the stress-strain curve), while ν is assumed to equal 0.5. As said above, the contact radius is mainly a function of the given preload, as the dynamic signal amplitude is negligible with respect to the preload itself. As discussed in the previous section, a roller type boundary condition was assumed at the lower boundary, while the perimeter is constrained.

The proportionality coefficient sigma which allows to estimate the d33 value of each sensor (2), based on the measured ratio between Q3 and F3, is reported in Figure 6.7 below. The value of the contact radius a changes with the following preload values: PL = 0.6, 1, 2, 3N. It is worth pointing out that the present results are consistent with those found in Figure 10 of [199]. As well, note that values of σ obtained for palm sensors differ slightly from the fingertip ones as depends on the ratio $\frac{r_T}{h}$ (recall (6.2)).

In addition, we have verified the consistency of the experimental setup for the sensing patch with the pure compressive mode assumption. Then, we have performed a series of simulations aiming to evaluate the stress tensor in the sensing patch as a function of the preload,

subject to a roller type boundary condition at the bottom and free lateral boundaries. These simulations show that the normal stresses T_1 and T_2 keep at least an order of magnitude smaller than T3 within the sensing patch. Recalling the form of the complete constitutive relationship [169]

$$D_3 = d_{31}T_1 + d_{32}T_2 + d_{33}T_3 \tag{6.4}$$

and noting that d_{31} and d_{31} are smaller than d33 [169], we end-up concluding that the assumption of pure compressive mode was sufficiently adequate for the experimental setting.

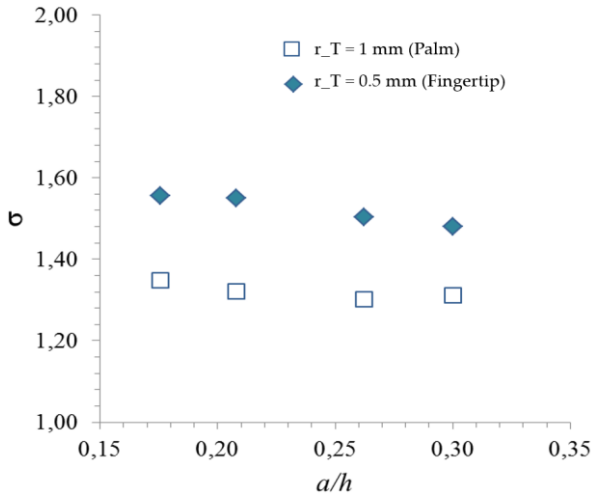

Figure 6.7 Results for the numerical COMSOL simulations for the finite case. The proportionality coefficient σ between average normal stress on the sensor and overall (Hertzian) contact force F3 (2) is plotted versus the imprint radius a (contact size) scaled by the elastomer thickness h. Note that the applied force is centered on the sensor. The two curves are associated to two different sensor sizes: = 1mm (sensors on the palm), = 0.5mm (sensors on the fingertip)

6.3 Results

6.3.1 Morphology of the Sensing Patches: Issues

All sensing patches have been visually inspected using first a photo scanner (EPSON perfection V800 photo) and then an optical microscope (Nikon eclipse LV100 and Wild M32).

Some fabrication defaults have been detected and presented in Figure 6.8. They are listed below:

1) ***Faults in the top sensor electrode*:** The choice of silver ink for the top electrode has been the result of a compromise between resolution, conductivity and top-electrode performance. Using silver, the printing resolution was very good and the conductivity was very high at 100° temperature treatment. However, at a careful examination, small defects were detected, due to solvents in the ink (Figure 6.8b).

2) ***Interrupted tracks:*** During high-voltage hysteresis poling, sensor lines burned due to current exceeding a threshold value when short circuits between top and bottom electrode occurred, caused by their too short distance. (Figure 6.8c).

3) ***Short circuits:*** They occurred between sensor lines or due to misalignment between top and bottom electrodes The high required resolution led to too short distances between lines and top/bottom electrodes, causing short-circuits due to shrinkage of the whole DIN A3 deposition substrate during high temperature treatment. Figure 5.9 shows the heat map of the substrate prone to shrinkage. We observed that certain sensor arrays (such as M-Palm) lie on the blue sweet spot, corresponding to less shrinkage. This guarantees a larger number of working sensors. Other samples (such as palm right 2) are on the red zones, associated to high shrinkage. This causes higher number of short circuits, which in turn leads to less working sensors than expected. (Figure 6.8d).

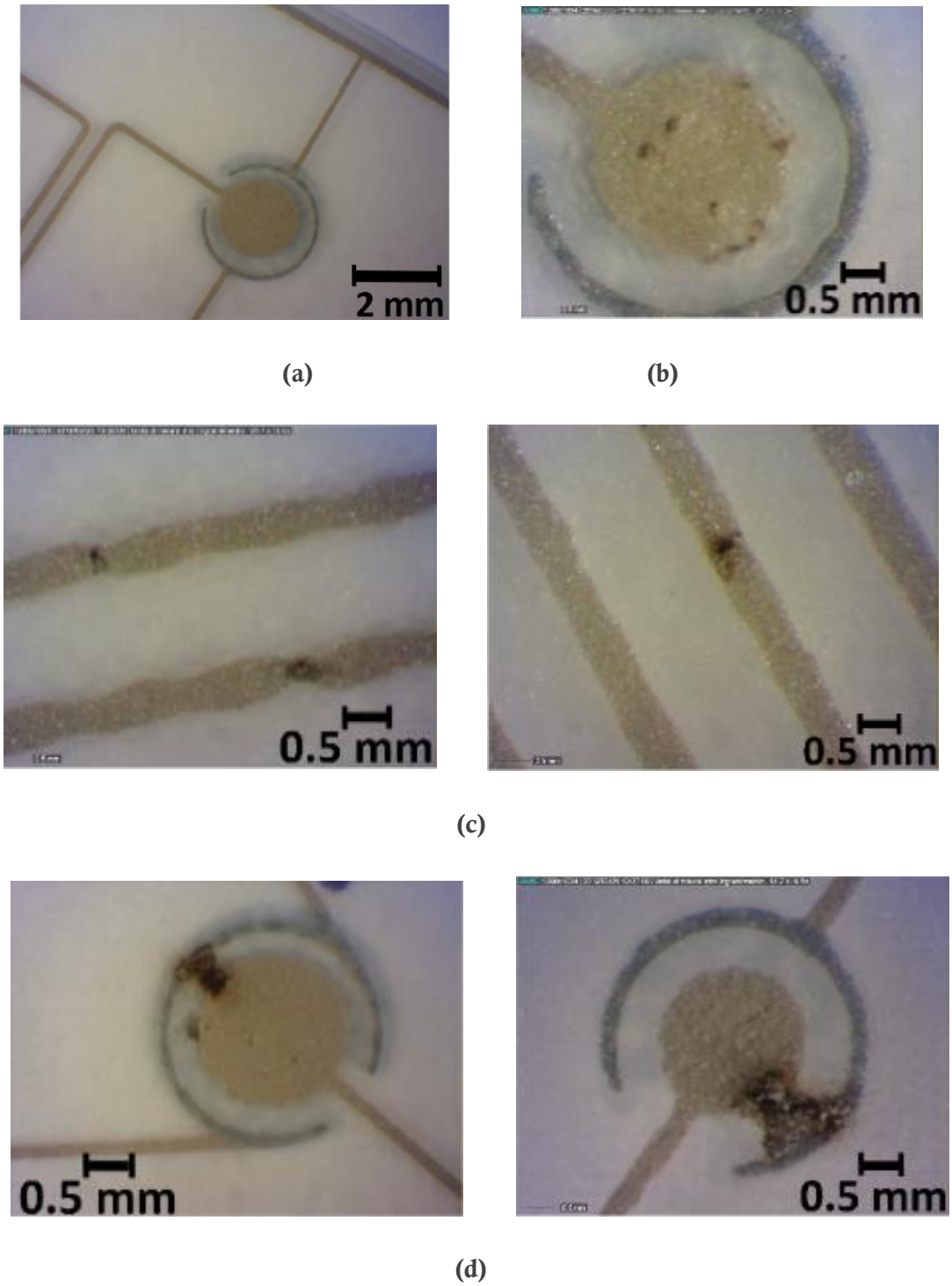

Figure 6.8 (a) Normal sensor, (b) Fault in the sensor top electrode (pole), (c) Cut in the sensor tracks, due to short circuits during the poling procedure, (d) Shortcuts between sensor tracks.

In summary, the required high resolution (i.e. small sensor size, short distance between top and bottom electrodes, short distance between sensor tracks) is challenging, for example such fine structures cannot be distributed over such a large area (DIN A3) if the substrate is not dimensionally stable during all process

steps (including sensor polarization). How these fabrication defaults affected sensor behavior is illustrated in Sect. 3.2.3.

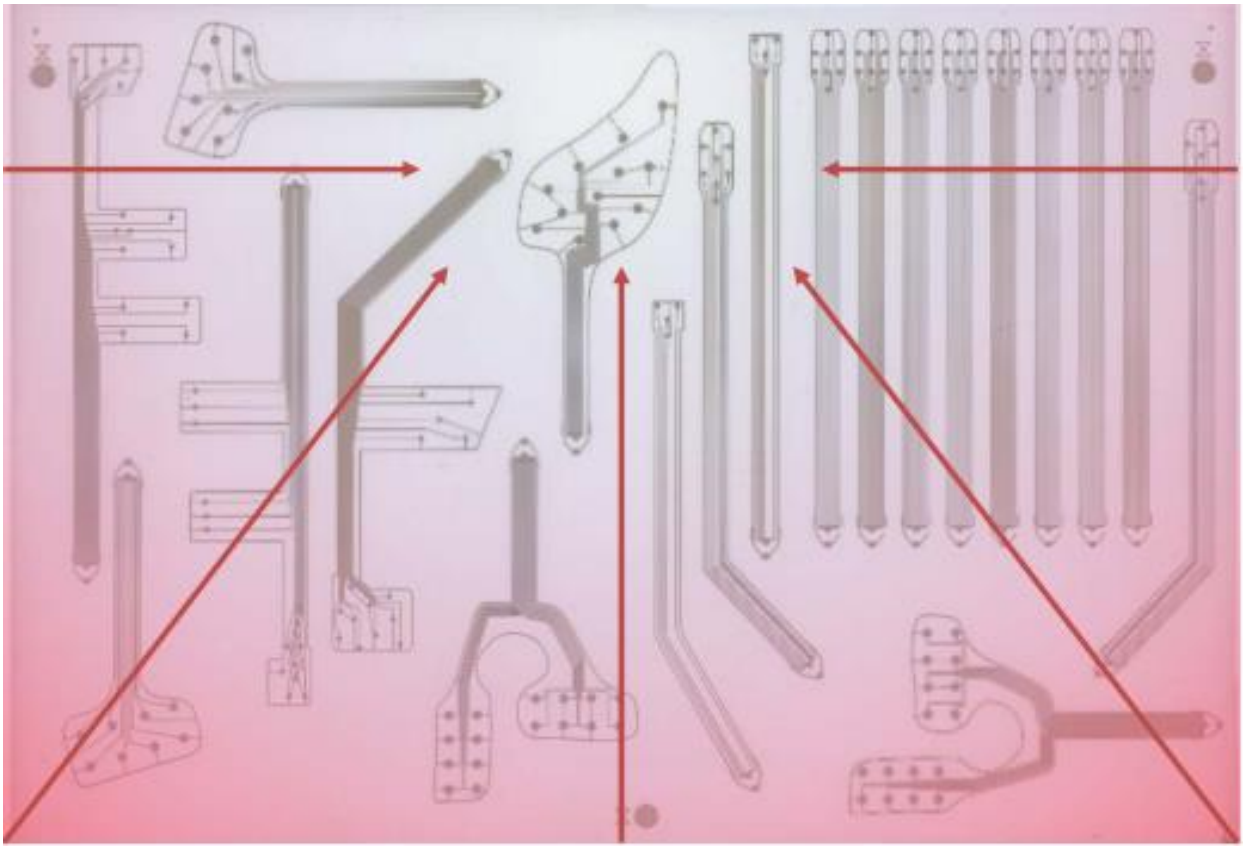

Figure 6.9 The heat map of the deposition substrate (DIN A3) prone to shrinkage

6.3.2 Experimental tests

A series of experiments were conducted to extract the sensor behavior, i.e. ultimately their d_{33} values, from indentation tests on the skin surface, by using the model illustrated in Sect. 2.3. Before running each test, a preload has been applied to guarantee indenter-skin contact during the entire mechanical stimulation. As specified in Section 6.3.2. , this preload is responsible for determining the contact radius *a* (3), as for all tests the amplitude of the dynamic oscillation is maintained low enough (F_dyn = 0.09 N) not to affect significantly the contact area.

Different P(VDF-TrFE) sensing patches have been tested as described in Section 6.2.2. We applied a swept sine signal from 0.5Hz up to 1000Hz by an electromechanical shaker at each sensor epicenter on the e-skin outer surface, causing e-skin indentation aligned with each sensor center. We recorded the sensor frequency-response function one-shot over the whole frequency range. The numerical model described in Section 6.2.3 has been integrated into the LabVIEW

software, directly giving the frequency behavior of the d33 piezoelectric modulus (both real and imaginary parts) of each solicited sensor, calculated from the sensor frequency response function as for (2). Sigma values have been extracted from Figure 6.7, each time in accordance with the specific preload and sensor radius.

6.3.2.1 Frequency range selection

In a preliminary stage, we investigated the minimal value of the applied preload that ensured a stable behavior of d_{33}. Multiple tests at preloads less than 1N have been run over the whole frequency range (0.5Hz-1000Hz), especially at preload 0.6N. Main observation is that this low value for the preload does not ensure a stable contact during oscillations of the indenter over the skin patch, due to the dynamic amplitude of the indenter oscillation being not enough smaller than the preload itself. This causes noisy behavior for the d33. For that reason, in the rest of the study results at this preload are not reported.

Then, tests have been at preloads 1, 2, 3 N. It turned out that resonances do exist and their characteristic frequencies depend on the preload. In particular, preliminary resonance at 50 Hz has been easily eliminated by adequately grounding the whole machine. In the 300 - 750 Hz range, a systematic preload-dependent resonance peak is responsible for sign flipping of the real part of the d33 coefficient. At low preloads (i.e. PL = 1N) the resonance falls in the 300-500Hz range, while at higher preloads (i.e. PL= 2,3N) the resonance shifts to the 500 -750Hz frequency range. Around 950 Hz, a mechanical resonance appears due to high vibrations from the shaker system while stopping. As reported in [199], resonances may derive from a variety of causes (e.g. movable contacts, contact surface asperities, motor-induced vibrations), which cannot be reliably controlled.

The model can only be applied with dynamic contacts with forcing frequencies that fall outside the range of any significant resonance [199]. Therefore, a non-resonant 50-250 Hz frequency range has been identified, where the frequency response function is systematically quite flat. In particular, the imaginary part of the d_{33} piezoelectric coefficient, which accounts for any viscoelastic component of the response, is systematically roughly an order of magnitude smaller than the real (elastic) part. The aforementioned statements are clarified in the representative example reported in Figure 6.10, where both real and imaginary parts of d_{33} are expressed as a function of frequency and the non-resonant range is highlighted.

Based on these results, hereafter the imaginary part of the d_{33} coefficient will be ignored and Re will be removed from the notation. In other words, the system is treated as purely elastic. Moreover, each run has been performed stimulating the skin over the whole frequency range, yet the corresponding d33 response is averaged over the non-resonant range only.

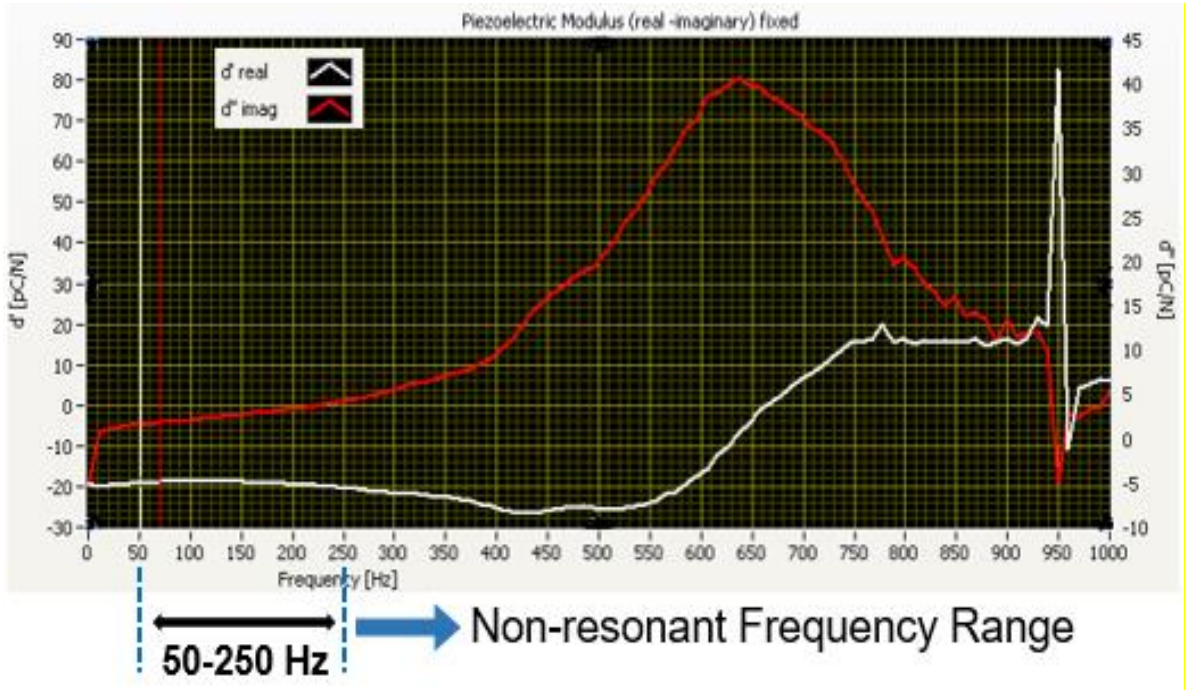

Figure 6.10 Example of the frequency behavior of both the real and imaginary part of the d33 piezoelectric coefficient. The scale for the Im (d33) (= d'') is on the right y-axis.

6.3.2.2 Systematic sensor validation

Each sensing patch has been tested, by stimulating the e-skin surface with the same indenter (R = 4mm) aligned with the epicenter of each selected sensor. As mentioned in Sect. 3.2.1, each run has been performed at small force amplitude (F_dyn = 0.09 N) and the corresponding d_{33} response has been averaged over the non-resonant range to get a single value of that coefficient for each sensor.

Two sets of data have been obtained. The former data set (96 sensors, 10 different samples, 4 categories of patches) focuses on Palm sensors (i.e. sensors with diameter = 2mm, belonging to arrays designed to cover the palm), all tested at different preloads. While the second data set (8 sensors, 2 samples, Michelangelo little) focuses on finger sensors (i.e. sensors with diameter = 1mm, belonging to arrays designed to cover the fingertips) as shown in Figure 6.11.

6.3.3 Data Analysis

6.3.3.1 First Analysis: Palm sensors

We selected four palm patch designs that vary in their positions and sensor number. These designs have been assigned to four categories as reported in the Table below.

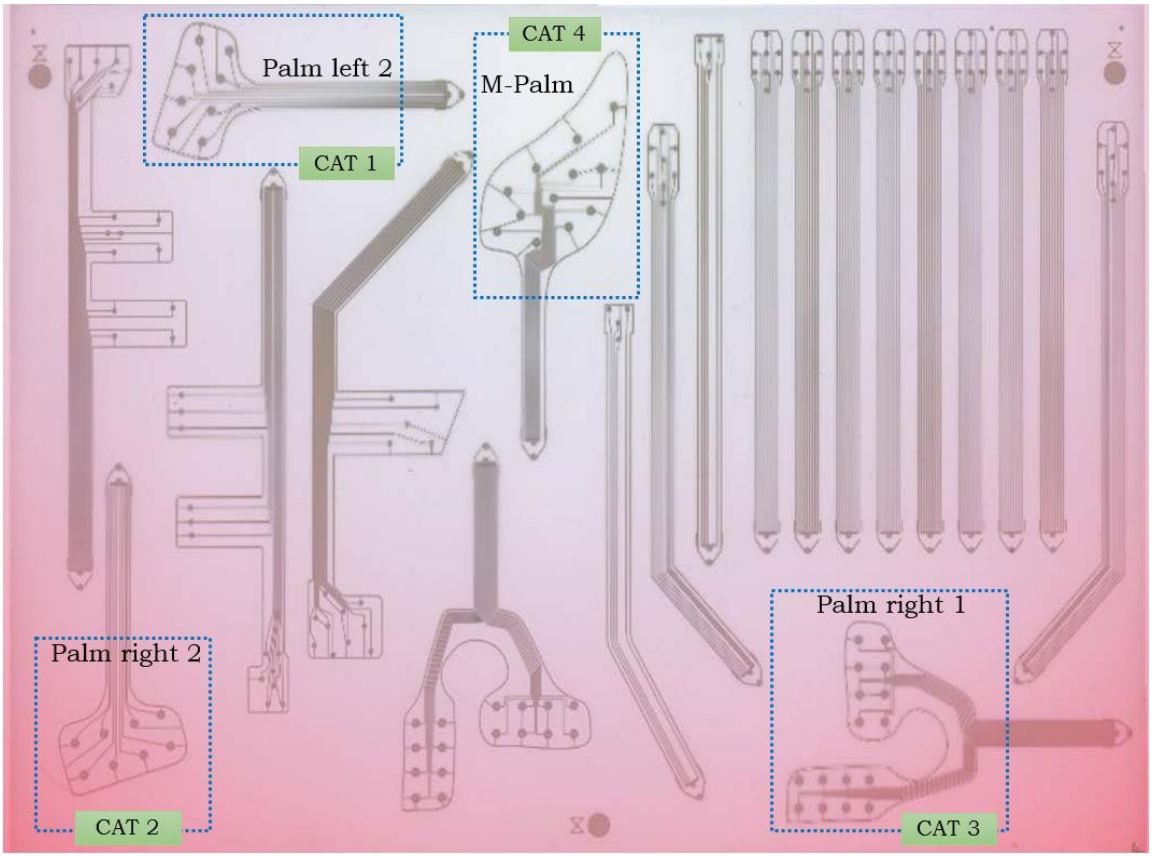

(a)

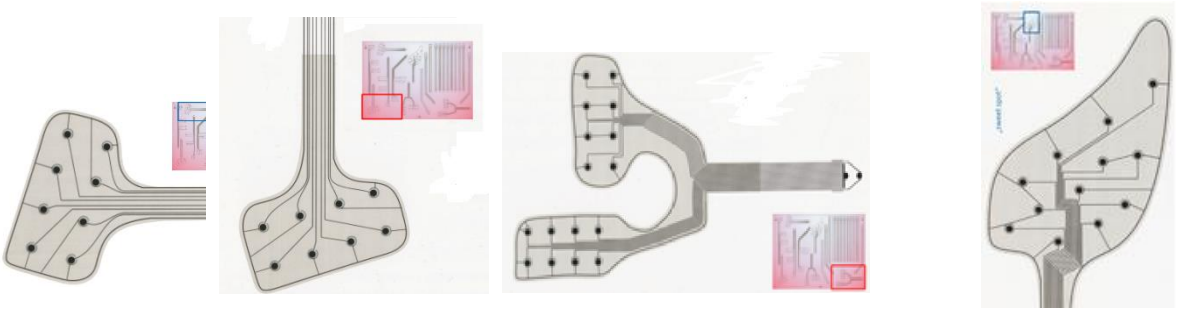

CAT 1 **CAT 2** **CAT 3** **CAT 4**

(b)

Figure 6.11 Compared categories (CAT1, CAT2, CAT3, and CAT 4) and heat map on the A3 fabrication substrate.

Table 6.1 Palm patches categories (Data set 1, palm sensors)

Category	Category name	Number of Tested patches	Number of sensors/patches
Category 1	Palm left 2	3	8
Category 2	Palm right 2	4	8
Category 3	Palm right 1	1	16
Category 4	Michelangelo palm	2	12

Figure 6.11 illustrates how these categories are distributed over the A3 substrate used for patch fabrication. A comparative study has been performed to examine whether the shape and position over the A3 fabrication substrate affected the sensor behaviour at different preloads.

67 sensors out of the whole set (96 sensors) have been selected, eliminating sensors that did not work due to fabrication failures (see Section 6.3.1) and few sensors which gave physically non-acceptable values for d_{33}. Note that the number of not-working sensors was quite high for this first fabrication batch. Figure 6.12 shows the cloud distribution of the averaged d_{33} values for the palm sensors. In addition, the table 6.2 summarizes the RMS (mean average of d_{33}) values, the standard deviation (STD) and standard mean error (SE).

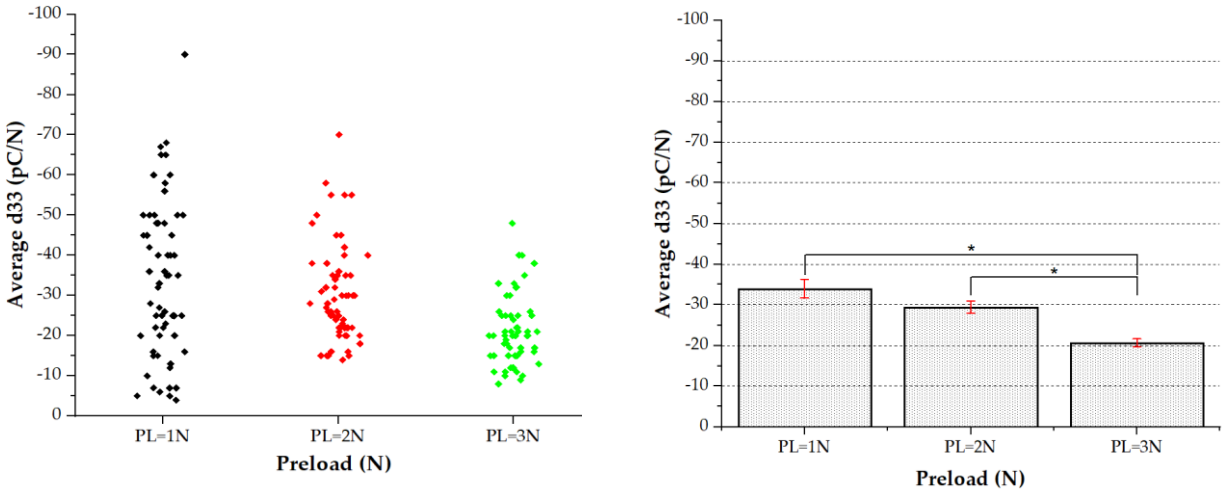

(a) **(b)**

Figure 6.12 (a) Cloud distribution of working palm sensors .(b) Statistical study: one way balanced anova, average d33 vs. preload

Table 6.2 Statistical Study variables (Data set 1, palm sensors)

Preload (N)	**Number of Working sensors N**	**Root mean square RMS**	**Standard deviation STD**	**Standard Error of Mean SE**
PL=1 N	67	-34.31148	19.50004	2.49672
PL=2 N	67	-30.21311	12.30056	1.57493
PL=3N	67	-21.04918	8.46646	1.08402

All categories have been analyzed, in order to check whether any dependence of the patch behavior on the specific category existed. This was needed to understand if a specific patch position affected sensor behavior, e.g. due to not uniform polarization or other unwanted effects related to the shrinkage of the substrate during the fabrication process.

The results presented in Figure 6.13 show that indeed sensor response to preload does significantly depend on the category, which is associated to a specific position on the substrate. Moreover, the Table 6.3 repots the RMS (mean average of d_{33}) values, the standard deviation (STD) and standard mean error (SE).

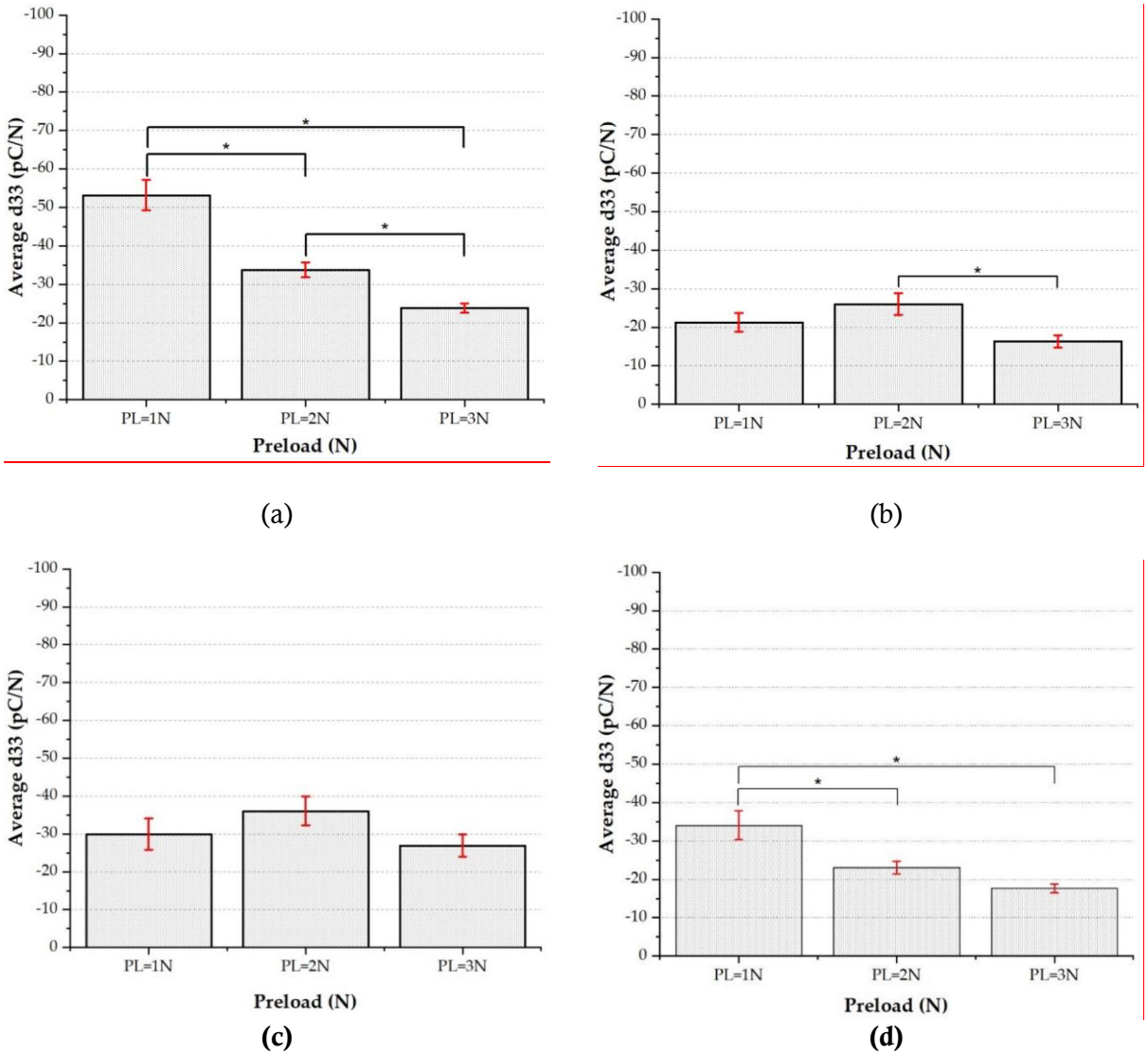

Figure 6.13 Average d33 vs Preload () for four different categories: (a) Category 1 (palm left 2). (b) Category 2 (palm right 2). (c) Category 3 (palm right 1). (d) Category 4 (Michelangelo palm). One-way anova has been applied for statistical analysis

Table 6.3 Statistical Study variables: a) CAT 1 (palm left 2), b) Category 2 (palm right 2), c) Category 3 (palm right 1), and d) Category 4 (Michelangelo palm)

CAT1 Preload (N)	Number of Working sensors N	Root mean square RMS	Standard deviation STD	Standard Error of Mean SE
PL=1 N	18	-53.22222	16.9239	3.989
PL=2 N	18	-33.77778	8.11357	1.91239
PL=3N	18	-23.83333	5.22719	1.23206

CAT2 Preload (N)	Number of Working sensors N	Root mean square RMS	Standard deviation STD	Standard Error of Mean SE
PL=1 N	23	-21.26087	11.50185	2.3983
PL=2 N	23	-26.04348	13.57966	2.83155
PL=3N	23	-16.34783	7.61941	1.58876

CAT3 Preload (N)	Number of Working sensors N	Root mean square RMS	Standard deviation STD	Standard Error of Mean SE
PL=1 N	13	-29.92308	14.91901	4.13779
PL=2 N	13	-36.07692	13.85317	3.84218
PL=3N	13	-26.92308	10.45197	2.89885

CAT4 Preload (N)	Number of Working sensors N	Root mean square RMS	Standard deviation STD	Standard Error of Mean SE
PL=1 N	13	-34.07692	13.5429	3.75613
PL=2 N	13	-23.07692	5.86603	1.62694
PL=3N	13	-17.61538	4.13397	1.14656

In particular, note that results for categories 2 (Figure 6.13- b) and 3 (Figure 6.13-c) show a dependence of d_{33} on the preload which turns out not to be statistically significant. It is worth pointing out that categories 2 and 3 are those located in the red zone of the heat map, where strong substrate shrinkage occurred. In order to check the effectiveness of the sensor fabrication technology, we have then decided to discard results referring to categories 2 and 3.

On the other hand, it is reassuring to note that, as shown in Figure 6.14, patches belonging to the same category (including those in the red zone) are statistically equivalent among themselves, a result which does suggest the reproducibility of the fabrication process for each patch.

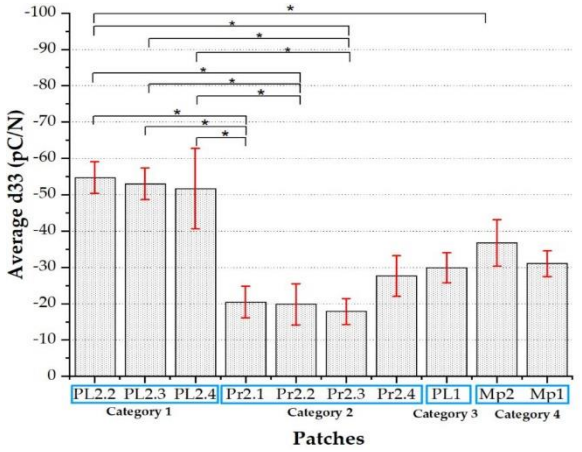

(a)

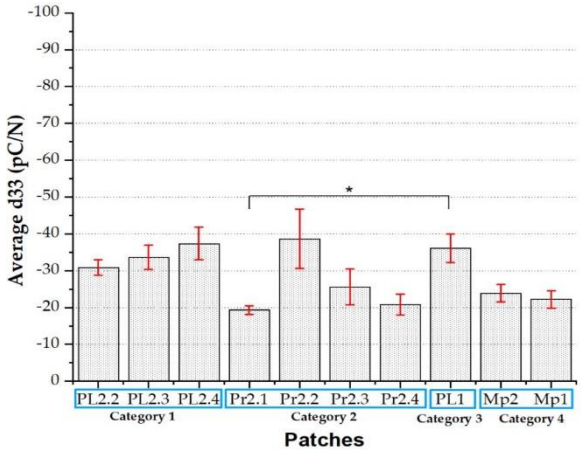

(b)

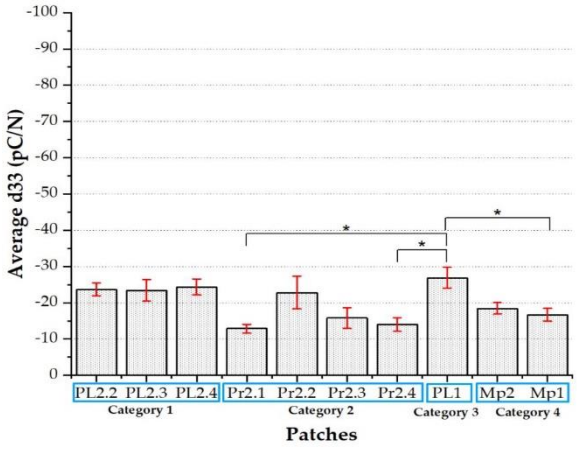

(c)

Figure 6.14 Average d33 vs patches at PL=1N, 2N, and 3N arranged respectively as (a), (b) and (c). The four categories and all corresponding patches can be distinguished on the x-axis.

Table 6.4 Statistical Study variables for all patches tested at three different preloads

All CATs (Preload =1N)	Number of Working sensors	Root mean square RMS	Standard deviation STD	Standard Error of Mean SE
PL2.2	7	-54.71429	11.52843	4.35734
PL2.3	5	-53	9.74679	4.3589
PL2.4	6	-51.66667	27.06043	11.04737
Pr2.1	7	-20.42857	11.41428	4.31419
Pr2.2	6	-19.83333	13.87684	5.6652
Pr2.3	5	-17.8	8.04363	3.59722
Pr2.4	5	-27.6	12.54193	5.60892
PL1	13	-29.92308	14.91901	4.13779
Mp2	7	-36.71429	16.92842	6.39834
Mp1	6	-31	8.67179	3.54024

All CATs (Preload =2N)	Number of Working sensors	Root mean square RMS	Standard deviation STD	Standard Error of Mean SE
PL2.2	7	-30.85714	5.45981	2.06361
PL2.3	5	-33.6	7.36885	3.29545
PL2.4	6	-37.33333	10.8382	4.42468
Pr2.1	7	-19.28571	3.03942	1.14879
Pr2.2	6	-38.66667	19.81582	8.08977
Pr2.3	5	-25.6	10.83051	4.84355
Pr2.4	5	-20.8	6.22093	2.78209
PL1	13	-36.07692	13.85317	3.84218
Mp2	7	-23.85714	6.33584	2.39472
Mp1	6	-22.16667	5.70672	2.32976

All CATs (Preload =3N)	Number of Working sensors	Root mean square RMS	Standard deviation STD	Standard Error of Mean SE
PL2.2	7	-23.71429	4.75094	1.79569
PL2.3	5	-23.4	6.65582	2.97658
PL2.4	6	-24.33333	5.46504	2.23109
Pr2.1	7	-12.85714	3.13202	1.18379
Pr2.2	6	-22.83333	11.08903	4.52708
Pr2.3	5	-15.8	6.41872	2.87054
Pr2.4	5	-14	4.24264	1.89737
PL1	13	-26.92308	10.45197	2.89885
Mp2	7	-18.42857	4.15761	1.57143
Mp1	6	-16.66667	4.27395	1.74483

Results for all sensors belonging to the two categories located in the sweet spot associated to low shrinkage (i.e. categories 1 and 4) are plotted in the Figures 6.15 and 6.16. They show d_{33} values mostly compatible with the state of the art [191].

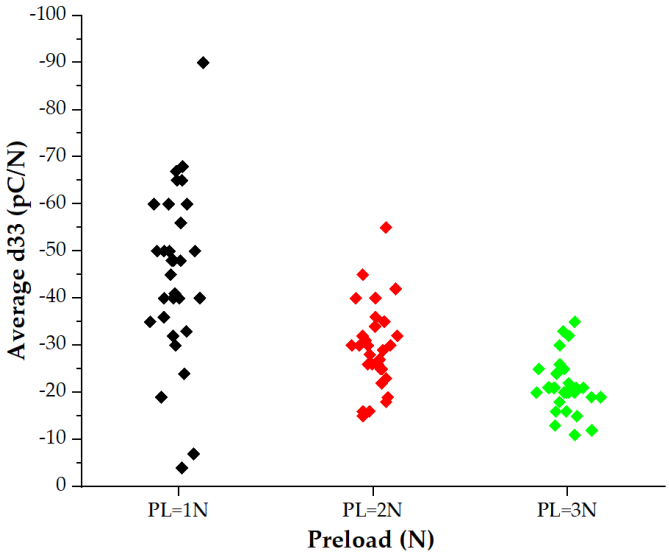

Figure 6.15 Average d33 vs preload. Sensors belonging to categories 1 and 4, only. To avoid dot superposition, values associated with the same preload are plotted such that dots do not lie on the same vertical line

It turns out that as the preload increases the average d_{33} decreases and values for different sensors exhibit a lower dispersion.

In Figures 6.16, a best-fit line is used to compute the average of the d_{33} values associated with all sensors. Data related to the highest preload (= 3 N) are well fitted using a d_{33} value equal to approximately -22 [pC/N], while data corresponding to the lower preload (= 1 N) yield a d_{33} value of approximately -46 [pC/N].

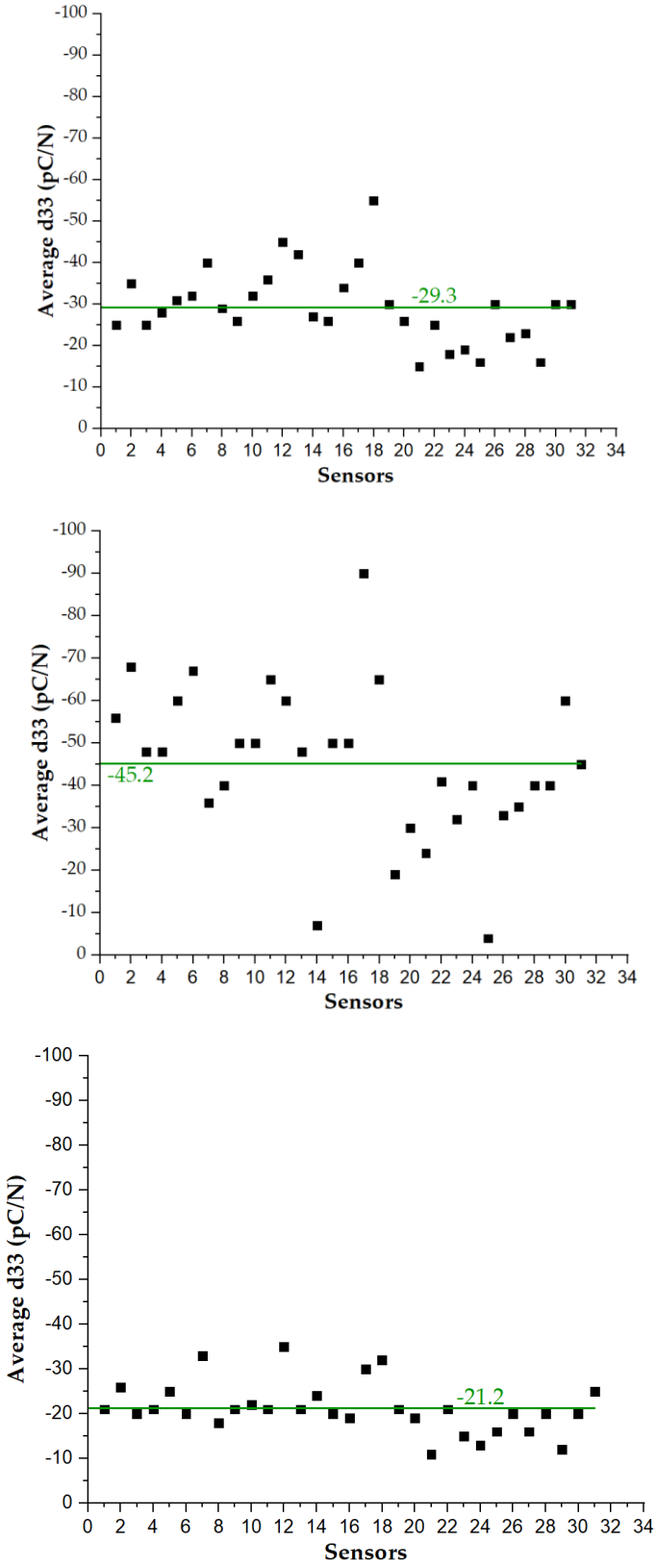

Figure 6.16 Average d33 for each sensor at PL=1N (top), 2N (middle), 3N (bottom)

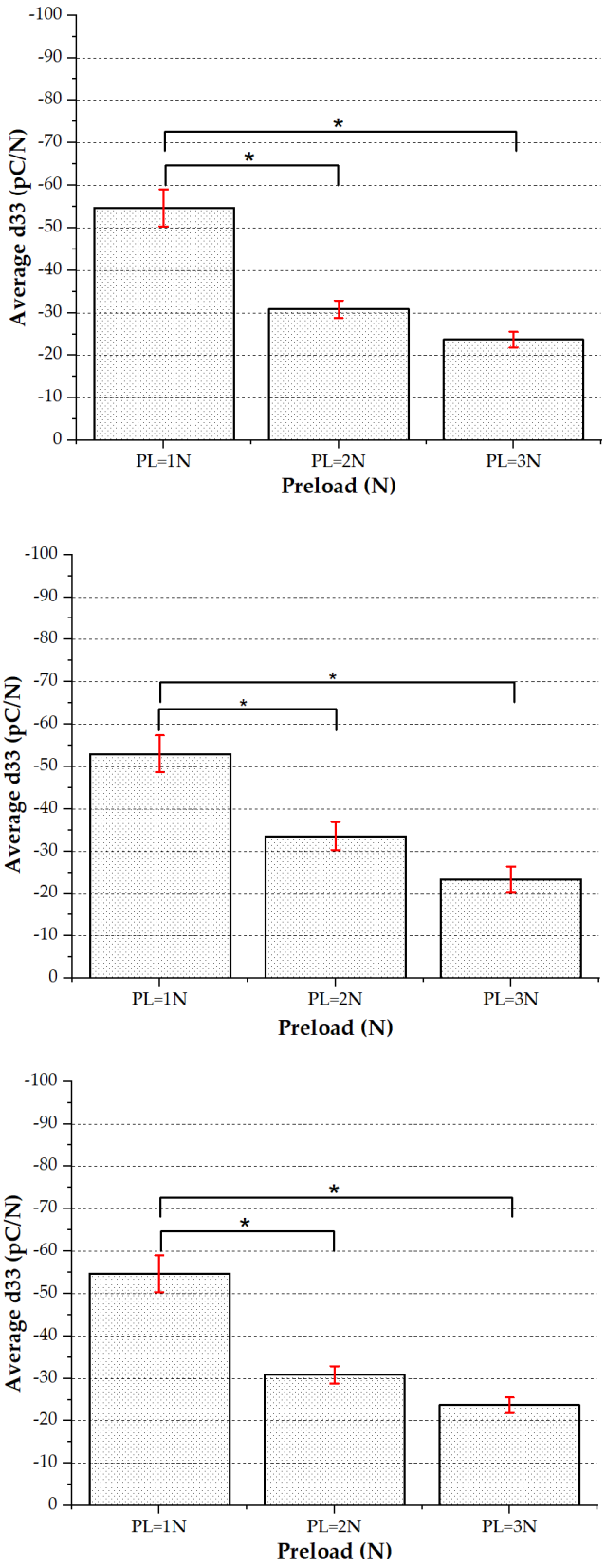

Figure 6.17 Average d33 vs preload for the three analyzed patches belonging to category 1: Palm left 2.2. (top), Palm left 2.3 (middle), Palm left 2.4 (bottom).

Table 6.5 Statistical Study variables

Preload (N)	Number of Working sensors N	Root mean square RMS	Standard deviation STD	Standard Error of Mean SE
PL=1 N	7	-54.71429	11.52843	4.35734
PL=2 N	7	-30.85714	5.45981	2.06361
PL=3N	7	-23.71429	4.75094	1.79569

Preload (N)	Number of Working sensors N	Root mean square RMS	Standard deviation STD	Standard Error of Mean SE
PL=1 N	5	-53	9.74679	4.3589
PL=2 N	5	-33.6	7.36885	3.29545
PL=3N	5	-23.4	6.65582	2.97658

Preload (N)	Number of Working sensors N	Root mean square RMS	Standard deviation STD	Standard Error of Mean SE
PL=1 N	6	-51.66667	27.06043	11.04737
PL=2 N	6	-37.33333	10.8382	4.42468
PL=3N	6	-24.33333	5.46504	2.23109

6.3.3.2 Second analysis: finger sensors

A second data set were analyzed which focuses on finger sensors. Two samples of Michelangelo little finger were tested using the experimental setup and methodology reported above. Each sample has four taxels with a 1mm diameter each. Figure. 18 shows the analyzed results after applying unbalance on-Way ANOVA. The results indicate a statistically significant difference of d_{33} between different applied preloads. Moreover, there is a systematic decrease of d_{33} with increased preload.

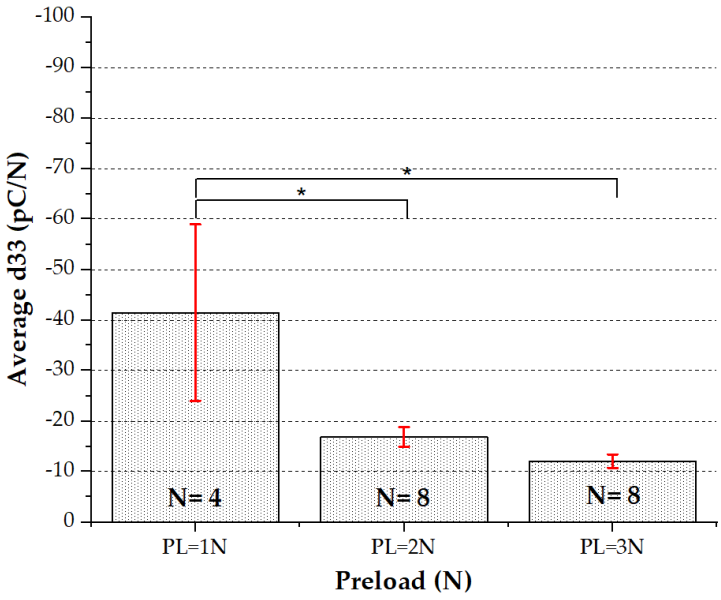

Figure 6.18 Average d33 vs preload for the two samples of Michelangelo little: ML.1 and ML.2. Statistical study: unbalanced one-Way ANOVA.

Table 6.6 Statistical Study variables

Preload (N)	Number of Working sensors N	Root mean square RMS	Standard deviation STD	Standard Error of Mean SE
PL=1 N	4	-41.5	34.93327	17.46663
PL=2 N	8	-16.875	5.54044	1.95884
PL=3N	8	-12.0625	3.82135	1.35105

6.4 Discussion

For all categories, the patches are statistically equivalent among themselves when belonging to the same category, which proves the reproducibility of the whole deposition process. Excluding categories located in the red zone (i.e. CAT 2 and CAT 3) of the heat map which associated to high shrinkage, the single sensors belonging to the other two categories (CAT 1 and CAT 4) show a piezoelectric behavior (i.e. d_{33} values) which are quite compatible with the current state of art.

Moreover, all analyzed patches belonging to categories 1 and 4 have quite systematic decreasing behavior for d_{33} vs PL. This has been checked using one-way Anova for statistical analysis. Systematically, sensor average d_{33} behavior at PL = 1N is statistically different from that at PL = 3N, both for the two categories (Figures 6.13-a, 6.13- d) and for single patches from category 1 (Figure 16). This would be compatible with a non-linearity of d_{33} with respect to the

preload and with some non-linearity in the stress-strain curve observed for this elastomer layer around 2MPa.

The dispersed behavior of d_{33} (i.e. sensor response) does depend both on the fabrication process (including deposition and assembly) and on the alignment of the indenter with the sensor center. For later testing, a laser-like positioning system could be used in the future to align the indenter precisely, thus avoiding errors due to wrong positioning. As for the fabrication process, these errors are the results of different factors including different point-to-point values for the sensor radius and/or for the local layer thickness and inhomogeneity in PVDF film polarization. These factors combined are considered intrinsic in the whole fabrication process and could not be decoupled in the present tests.

Consequently, coming to this end, a quick time saving protocol for future sensing patches validation could be extracted. It could be summarized as the following. As a first step, the sensing patch will be coupled on the rigid substrate by an adhesive tape only on the borders. Second, after mounting the sensing patch on the mechanical chain, choose a reference sensor and centralize it, taking into account the collinear alignment of the indenter tip with the sensor kernel. In addition, a laser positioning system to lessen the dispersion of sensor behavior. Third, accordingly apply the lowest preload (1N), then run the indentation test and when it is done release the indenter. Afterward, a three-minute pause will be taken to allow the protective layer to relax. Then, the preload will be increased gradually (e.g. 3N) and another indentation test will be applied as explained previously. Further on, another sensor will be selected and the procedure will be repeated all over (i.e. centering, application of preload, indentation test, indenter release and time break) until all the complete set of sensory belonging to sensory array covered. Finally, the sensors behavior need to be studied and analyzed. It is important to note that, except for the initial coupling procedure and the sensor centering, the rest of the procedure could be automatized. Additionally, the sensor data could be organized and displayed into graphs instantly with each test run. With automation, the testing duration will decrease drastically for example it would take less than an hour to test a patch with 8 sensors.

In Section 6.2.2, we described how we coupled the sensing patch to the substrate and to the protective layer, to be able to test sensor behavior without damaging the sensors themselves. Applying double-sided adhesive tape all over the sensors in the validation stage is not feasible unless the cover layer is the final layer, because sensors would be damaged during tape removal

(Figure. 6.18). It would be also better to avoid the adhesive tape between the substrate and the sensors themselves, as damages may occur during tape removal.

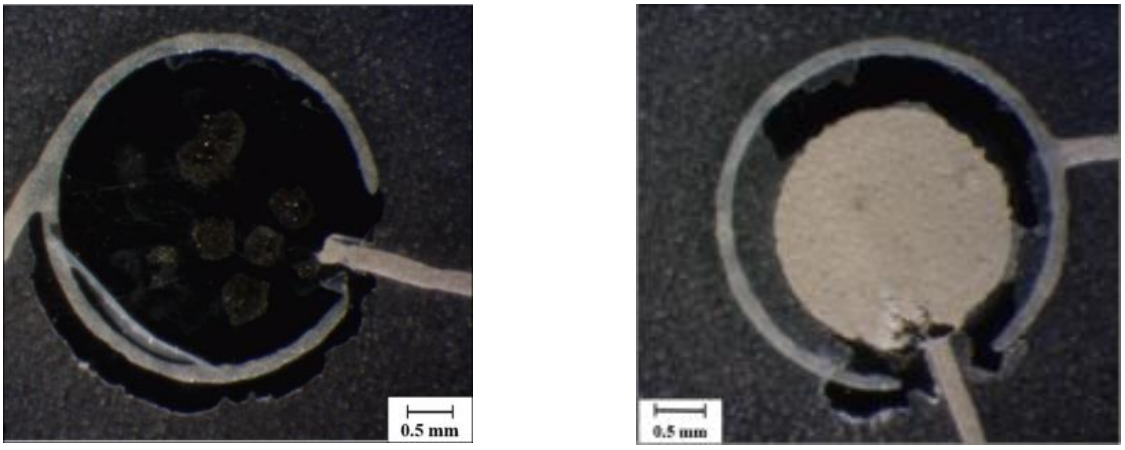

Figure 6.19 Sensor electrodes have been severely damaged after coupling with adhesive tape all over the skin patch.

Therefore, the choice of the coupling procedure is somehow obliged in the validation stage. Operationally, as described in Section 6.2.2, we placed double-sided adhesive tape around the sensor

Therefore, the choice of the coupling procedure is somehow obliged in the validation stage. Operationally, as described in Section 6.2.2, we placed double-sided adhesive tape around the sensor array (Table 6.7-a), to rigidly couple to the substrate the protective layer on its boundaries, thus keeping in place the sensing patch itself. We also proved through simulations that this configuration leads to negligible normal stresses other than $T_{33,}$ thus confirming that sensors work in thickness mode, as required by the model.

However, this coupling procedure can only be used in a validation stage, as discussed in the following. In real applications shear contact forces on the skin surface will be possible, which requires using a real rigid coupling between the sensing patch and both the cover layer and the substrate (Table 6.7 -b), to avoid any sliding due to shear forces. This is achieved in practice by using an adhesive layer below and all-over the sensing patch itself. Care would only be needed during tape integration as not-uniform stress transmission and sensor bending can be naturally induced by the inclusion of air bubbles into the coupling adhesive layer. An underestimation of the d_{33} value is expected due to the addition of deformable adhesive layers between the sensor and both the substrate and the cover, which are not accounted for into the model. This leads not to be perfectly compliant with the model, as normal stresses other than T_{33} may contribute to the measured charge: preliminary simulations confirmed this prediction and hint at a contribution

of normal T_{11} and T_{22} stresses which is not negligible with respect to the normal T_{33} component. New models and more extensive simulations will be thus needed to describe the real application system.

Table 6.7 Illustration of Different coupling methods

Solution1: Validation stage Double-sided adhesive tape around sensor array	**(a)** 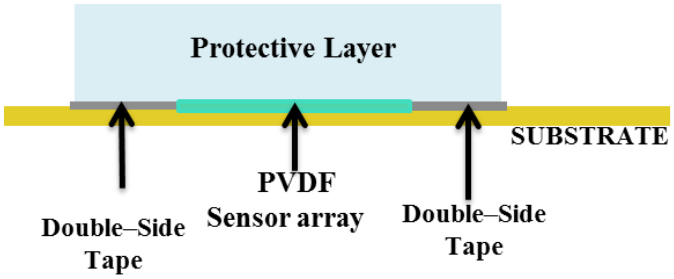
Solution 2: Real applications All over double-sided adhesive tape below and above the sensor array	**(b)** 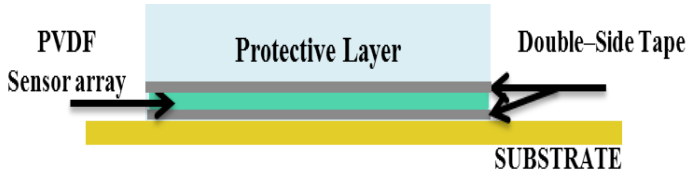

6.5 Conclusion

Before integrating the sensing arrays into the glove and the prosthetic hand, we needed to define a set of tools for the validation of the new skin technology. Throughout this study, a non-invasive method to validate PVDF sensor deposition techniques has been established and demonstrated. This methodology is independent of the specific deposition technique therefore; the validation procedure could be extended to cover wider applications such as robotic, medical applications, etc. Explicitly, this paper reports the validation of the fabrication technology of flexible screen-printed sensor arrays based on P(VDF-TrFE) piezoelectric polymers.

Extensive preliminary tests with an electromechanical setup have been performed on four different patch categories belonging to the first fabrication batch. In particular, eleven sensing patches have been characterized, 84 sensors in total. P(VDF-TrFE) sensors worked in thickness-mode and a protective layer has been integrated on top of the sensing patch for stress transmission and sensor protection. Dynamic skin indentation with normal force centered on each sensor has been performed, with three different preloads (1, 2, 3N). An average value of the d_{33} coefficient over a non-resonant frequency range has been extracted for each sensor,

without damaging the sensor itself. Obtaining expected (modeled) behavior of the electrical response of each sensor to measured mechanical (normal) force at the skin surface proves that the combination of both fabrication and assembly processes was successful.

Throughout the study course, several issues were observed such as the substrate shrinkage problem that occurred during the fabrication process. The proposed validation and characterization assisted in the optimization of the manufacturing process in order to minimize the arise errors (e.g. defaults in tracks, shortcut between connection lines, sensor shape deformation). Therefore, maximizing the number of working sensors.

Moreover, it demonstrated that for every reported sensing category (i.e. CAT1, CAT 2, CAT 3, and CAT 4), the sensing patches are statistically equivalent among themselves, which proves the reproducibility and it is considered as one of the main requirements when fabricating large quantities. More specifically, after excluding the sensing categories that fall in the red zone of the heat map i.e. that have been prone to high substrate shrinkage, the remnant sensors show a quite compatible state of art d_{33} values.

In addition, all the analyzed sensing patches that lie in categories 1 and 4 have a systematic declining behavior for d_{33} () versus preload (N). This in turn, would show a compatibility with the non-linearity of d_{33} with respect to the preload and with the few non-linearities in the stress-strain curve observed for the PDMS protective layer around 2MPa [199]. Obtaining expected (modeled) behavior of the electrical response of each sensor to measured mechanical (normal) force at the skin surface proves that the combination of both fabrication and assembly processes was successful.

In another flip, the current paper paves the way to define a practical, repeatable and reproducible simple characterization protocol for the e-skin patches. It assures the necessity of using a laser-like positioning system to flawlessly align the indenter with the sensor kernel, therefore eliminating the errors arise from misalignment, which impair the characterization and optimize the systematic analysis.

Despite all mentioned above, a critical limitation of the developed model is the disability to predict the behavior of the artificial skin in real applications. Since, real case scenarios require another sensor integration procedure that is summarized by using adhesive layers on both sensing array profiles (i.e. below and above the sensing array) to avoid sliding.

Into the bargain, the implementation of the presented screen-printed artificial skin (e-skin) in rehabilitation platforms especially in assistive glove or hand prosthesis would likely lead to film degradation and consequent P(VDF-TrFE) aging and fatigue. Estimating the piezoelectric d_{33} coefficient from the overall system response function is a practical tool to measure the reliability of the e-skin degradation rate, whenever embedded sensors are not accessible anymore for a direct characterization. Sheathing the sensing arrays with thin adhesive layers to firmly couple it to the protective layer and the substratum, would also participate in lessening the deterioration of the sensing arrays and the sliding effect of it. Therefore, the value of d_{33} extracted by the model would be underestimated, as long as the deformable adhesive layer is not included into the model. However, measuring how the film degrades over time implies differentially comparing the current value of d_{33} to an initial value, with no influence of the wrong estimation of that absolute initial value.

In the rearmost, we are looking for developing a new simulation model to extract the behavior of the sensors when integrated in real time applications such as hand prosthesis and assistive glove.

Chapter 7 Outlook and Future work

Conclusively, the following chapter epitomizes the carried work in this thesis. Besides, it sheds light on the impact of the achieved results. Then, further developments and commentary are provided in relevance to the main objective of restoring the sense of touch in prosthetics.

With the significant breakthroughs in advanced prosthetics in recent decades, more sophisticated models of body-powered myoelectric prostheses have made it through. A recent example is a prosthesis that emulates the hand motion with 22 degrees of freedom. However, the myoelectric prostheses they still show limited sensory. Closing the loop control in prosthetics control through the restoration of sensory feedback has been reported by users as a future goal, as it lessens the cognitive load needed to perform a task which improves the utility and easiness of use of the prosthetic system. Moreover, it enables sensation to the prosthetic limb that makes it more natural to the users. The implementation of sensory feedback for both for proprioception, grasping, and manipulating with the prosthesis is a critical challenge.

Peerdeman et al. developed a survey, which examined the requirements for feedback and arranaged the feedback restoration priorities for the users in hierarchical order of importance as follows:

1) Continuous and proportional feedback on grasping force should be provided

2) Position feedback should be provided to user

3) Interpretation of stimulation used for feedback should be easy and intuitive

4) Feedback should be unobtrusive to user and others

5) Feedback should be adjustable

In this scope, the presented thesis proposed a distributed sensing and stimulation system for restoration of sense of touch in prosthetics. To this aim, the prosthesis will integrate distributed sensing system (e-skin) to acquire tactile sensation, an embedded electronic system

for sensor acquisition and processing, and a multichannel stimulation interface to provide high-bandwidth tactile feedback to the user.

Sensory Substitution methods vary in their levels of invasiveness and could be used to restore sensory feedback. However, the most common non-invasive method to close the loop is to activate tactile sensation through stimulating the skin of the residual limb either by using direct mechanical (e.g. vibrators) or electrical stimulation. Electrotactile stimulation can elicit various sensations by modulating stimulation parameters (e.g. pulse width, intensity, and frequency) and/or spatial modulation (e.g. change the active channel). Electrotactile feedback shows potential for a quick and easily controllable method of feedback that users can identify multiple sites of feedback at once. However, currently this sensation is often referred to as a tingling feeling and occasional feeling of touch. Most of the closed-loop prosthetic systems feedback provides feedback through one stimulation unit through amplitude modulation. Using a single unit to communicate more than one sensation may be difficult for the user to understand or result in a high cognitive load for the user. Multichannel stimulation interfaces are promising as they could accommodate the prosthetic system flexibility and translate multiple information to the user (e.g. wrist rotation, grasping force, aperture) at the same time, thus emulates the naturalness of touch

7.1 At the Stimulation System

Attempting to mimic the naturalness of sensation and decrease the cognitive load by relying solely on visual feedback, this thesis presented a novel non-invasive compact multichannel interface for electrotactile feedback, comprising 24 pads electrode matrix, with fully programmable stimulation unit, that investigates the ability of able-bodied human subjects to localize the electrotactile stimulus delivered through the electrode matrix. Moreover, it designed a novel dual parameter -modulation (interleaved frequency and intensity) and compared it to conventional stimulation (same frequency for all pads). In addition and for the first time the electrotactile stimulation was compared to mechanical stimulation. The experimental results demonstrated that the proposed interleaved coding substantially improved the spatial localization compared to same-frequency stimulation. Furthermore, it showed that same-frequency stimulation was equivalent to mechanical stimulation, whereas the performance with dual-parameter modulation was significantly better. These outcomes are highly encouraging for the application of a multichannel interface for the restoration of feedback in

prosthetics. The high-resolution augmented interfaces might be used to explore novel scenarios for effective communication with the prosthesis user enabled by maximizing information transmission.

As a step forward, to implement long-term use of prosthesis, and providing higher naturalness and physiological feedback there is a need further testing of the developed distributed electrota tile feedback interface in real-time context (i.e. in every day environment with normal background and distractions). Moreover, as the electrotactile feedback suffers from the variation of perception from subject to subject, also with location of electrode, an examination of repeated application, and recalibration techniques of electrodes location is required. Besides, most studies focus on force feedback currently, while studies of tactile feedback can be extended to various tactile features, such as texture, shape and stiffness.

Another consideration is regarding the timing of the sensory feedback. Delay from the sensory input should be in the order of milliseconds. A too prolonged stimulus could be made the feedback less effective and cause adaptation. Most of the examinations studies of the effectiveness of sensory feedback are carried out in isolation of the control system. Consequently, closed-loop systems are relevant to accurately evaluate the performance and the adaptive behavior of the users while providing sensory feedback and it could offer an objective and standardize measure of it. In this regard, this thesis described and developed a close-loop compensatory tracking system to evaluate the usability and effectiveness of electrotactile sensory feedback in real-time position control. It examined the subject's adaptive performance and tolerance to random latencies while performing the dynamic control task and simultaneously receiving feedback (either visual or electrotactile) for communicating the momentary tracking error. In contras to open loop tracking [15], which assesses only the quality of perception, closed-loop tracking requires the subject needs to perceive, interpret and react to feedback with an appropriate control action. Thus, this task reflects more accurately the conditions of sensory substitution in online prosthesis control. Moreover, it reported the minimum time delay needed for an abrupt impairment of users' performance. The experimental results have shown that electrotactile feedback performance is less prone to changes with longer delays. However, visual feedback drops faster than electrotactile with increased time delays. This is a good indication for the effectiveness of electrotactile feedback in enabling close- loop control in prosthetics, since some delays are inevitable. In another flip, the constant performance of electrotactile feedback could assist the user in performing dynamic and continuous tasks over time (such as holding a

cup of coffee over the time needed to drink it), which raises the embodiment rate. For future developments, further refinement study could be suggested to evaluate the speed of communicating sensations. Additionally, more objective investigation of sensory adaptation phenomena (such as stimulus frequency, waveform, intensities etc...). Rubber illusion tests could be performed to better understand the electrotactile feedback effect on the embodiment rate. Scientific efforts is required to be undertaken on the particular waveform characteristics to improve the induced sensation to the subject to achieve a more natural feeling of pressure, as has been demonstrated in direct nerve stimulation techniques. Additional care and analysis is also required to ensure that minimal interference occurs with the EMG interface used for myoelectric control, so it does not significantly impact the control of the prosthetic device.

Further testing on hybrid tactile feedback systems that combine several stimulation methods together is required to be explored in order to determine a preson's ability to recognize feedback types simultaneously and the cognitive load.

7.2 At the sensing System

A fully equipped prosthetic device would include tactile sensors and embedded electronics for closed-loop prosthesis control. As previously discussed, providing high resolution tactile information that imitate the human sense of touch requires an articulated artificial sensing system that integrates high-density sensing arrays (e-skin) to a measure the variable touch attributes. E-skin in the form of tactile sensing arrays (skin patches) can be integrated onto the upper limb prosthetic device to record information about touch, given back to the amputee as a sensory feedback. This thesis realized a novel, flexible, screen- printed e-skin based on P(VDF-TrFE) piezoelectric polymers, that would cover the fingertips and the palm of the prosthetic hand (particularly the Michelangelo hand by Ottobock) assistive sensorized glove for stroke patients. Moreover, it developed a new validation methodology to examine the sensors behaviour while being solicited. Such methodology is not limited to prosthetics applications; it could be extended to cover wider applications such as robotic and medical application. The characterization results showed compatibility between the expected (modeled) behavior of the electrical response of each sensor to measured mechanical (normal) force at the skin surface, which in turn proved the combination of both fabrication and assembly processes was successful. This paves the way to define to define a practical, simplified and reproducible characterization protocol for e-skin patches. A critical limitation of the developed system is still not capable to

predict the behavior of the artificial skin in real-time applications. To overcome such limitation, we will be working on developing a new simulation model to extract the sensors behavior when integrated in real time application scenarios like hand prosthetics or assistive gloves. Particularly, the newly fabricated skin patches will be coupled to the Michelangelo prosthetic hand and then tested in close-loop interaction.

Wider scenarios could be explored and investigated on how to give back sensor data captured by the e-skin to the prosthesis user and how to help the human brain to successfully interpret the elicited artificial tactile information. One of the dilemmas in prosthetics is which kind of information - whether raw or processed data- about a touched object should be sent back to the user. In one hand, the sensor signals could be directly communicated to the user, who needs to meaningfully interpret this information. On the other hand, inspired by robotics, sensor data can be locally processed at the body periphery (prosthesis socket with embedded electronics) and high-level tactile information (e.g., texture properties, grasp stability) can be extracted and delivered to the user. Machine Learning algorithms have been exploited to classify and interpret input touch modalities as they represent a powerful technology for tackling clustering, classification and regression problems in complex domains. In addition, we believe that these algorithms would be an assist in optimizing the information transfer to the user, and it may decrease the cognitive load to adapt to different sensation.

A demanding focus, for the immediate future should therefore be placed on implementing a simple feedback strategy that can be practically used at home every day so that prosthetic users can begin to take advantage of the benefits that sensory feedback could provide them.

References

[1] B. T. Nghiem *et al.*, "Providing a Sense of Touch to Prosthetic Hands," *Plast. Reconstr. Surg.*, 2015.

[2] C. Antfolk, M. D'alonzo, B. Rosén, G. Lundborg, F. Sebelius, and C. Cipriani, "Sensory feedback in upper limb prosthetics," *Expert Rev. Med. Devices*, vol. 10, no. 1, pp. 45–54, 2013.

[3] E. Biddiss and T. Chau, "Upper limb prosthesis use and abandonment: A survey of the last 25 years," *Prosthetics and Orthotics International*. 2007.

[4] "bebionic hand | Ottobock US." [Online]. Available: https://www.ottobockus.com/prosthetics/upper-limb-prosthetics/solution-overview/bebionic-hand/. [Accessed: 21-Nov-2019].

[5] "Michelangelo prosthetic hand | Ottobock US." .

[6] "Our products | Touch Bionics." [Online]. Available: https://touchbionics.com/products. [Accessed: 21-Nov-2019].

[7] "VINCENTevolution 3." [Online]. Available: https://vincentsystems.de/en/prosthetics/vincent-evolution-3/. [Accessed: 21-Nov-2019].

[8] B. Stephens-Fripp, G. Alici, and R. Mutlu, "A review of non-invasive sensory feedback methods for transradial prosthetic hands," *IEEE Access*, vol. 6, pp. 6878–6899, 2018.

[9] P. Svensson, U. Wijk, A. Björkman, and C. Antfolk, "A review of invasive and non-invasive sensory feedback in upper limb prostheses," *Expert Rev. Med. Devices*, vol. 14, no. 6, pp. 439–447, 2017.

[10] N. V. Iqbal, K. Subramaniam, and P. Shaniba Asmi, "A Review on Upper-Limb Myoelectric Prosthetic Control," *IETE J. Res.*, vol. 64, no. 6, pp. 740–752, 2018.

[11] M. Asghari Oskoei and H. Hu, "Myoelectric control systems-A survey," *Biomedical Signal Processing and Control*. 2007.

[12] H. Fares *et al.*, "Distributed sensing and stimulation systems for sense of touch restoration in prosthetics," in *Proceedings - 2017 1st New Generation of CAS, NGCAS 2017*, 2017.

[13] M. Štrbac *et al.*, "Integrated and flexible multichannel interface for electrotactile stimulation," *J. Neural Eng.*, vol. 13, no. 4, 2016.

[14] D. Farina and S. Amsüss, "Reflections on the present and future of upper limb prostheses," *Expert Rev. Med. Devices*, 2016.

[15] D. S. Childress, "CLOSED-LOOP CONTROL IN PROSTHETIC SYSTEMS: HISTORICAL PERSPECTIVE*," 1980.

[16] M. S. Peerdeman B, Boere D, Witteveen H, Huis in `t Veld R, Hermens H, Stramigioli S, Rietman H, Veltink P, "Myoelectric forearm prostheses: state of the art from a user-centered perspective.," *J. Rehabil. Res. Dev.*, 2011.

[17] S. J.S., E. K.R., C. J.P., and H. J.S., "Applications of sensory feedback in motorized upper extremity prosthesis: A review," *Expert Rev. Med. Devices*, 2014.

[18] K. Li, Y. Fang, Y. Zhou, and H. Liu, "Non-Invasive Stimulation-Based Tactile Sensation for Upper-Extremity Prosthesis: A Review," *IEEE Sens. J.*, vol. 17, no. 9, pp. 2625–2635, 2017.

[19] C. Antfolk, V. Kopta, J. Farserotu, J. D. Decotignie, and C. Enz, "The WiseSkin artificial skin for tactile prosthetics: A power budget investigation," in *International Symposium on Medical Information and Communication Technology, ISMICT*, 2014.

[20] J. Farserotu *et al.*, "Tactile prosthetics in WiseSkin," in *Proceedings -Design, Automation and Test in Europe, DATE*, 2015.

[21] J. Kim *et al.*, "Stretchable silicon nanoribbon electronics for skin prosthesis," *Nat. Commun.*, 2014.

[22] C. Behrend, W. Reizner, J. A. Marchessault, and W. C. Hammert, "Update on advances in upper extremity prosthetics," *Journal of Hand Surgery*. 2011.

[23] R. F. Weir and D. Ph, "Design of Artificial Arms and Hands for Prosthetic Applications," *Stand. Handb. Biomed. Eng. Des.*, 2004.

[24] I. Saunders and S. Vijayakumar, "The role of feed-forward and feedback processes for closed-loop prosthesis control," *J. Neuroeng. Rehabil.*, 2011.

[25] F. Relvas, D. Mendes, A. Ferreira, and J. Jorge, "Separating degrees of freedom for object manipulation in VR," in *2016 23 Encontro Portugues de Computacao Grafica e Interacao, EPCGI 2016*, 2017.

[26] R. M. Enoka and J. Duchateau, "Physiology of muscle activation and force generation," in *Surface Electromyography: Physiology, Engineering and Applications*, 2016.

[27] A. D. Roche, H. Rehbaum, D. Farina, and O. C. Aszmann, "Prosthetic Myoelectric Control Strategies: A Clinical Perspective," *Curr. Surg. Reports*, 2014.

[28] A. D. Roche, B. Lakey, I. Mendez, I. Vujaklija, D. Farina, and O. C. Aszmann, "Clinical Perspectives in Upper Limb Prostheses: An Update," *Curr. Surg. Reports*, 2019.

[29] J. L. Betthauser *et al.*, "Limb Position Tolerant Pattern Recognition for Myoelectric Prosthesis Control with Adaptive Sparse Representations from Extreme Learning," *IEEE Trans. Biomed. Eng.*, vol. 65, no. 4, pp. 770–778, Apr. 2018.

[30] "SensorHand Speed | Myo Terminal Devices | Myo Hands and Components | Upper Limb Prosthetics | Prosthetics | Ottobock US B2B Site." [Online]. Available: https://shop.ottobock.us/Prosthetics/Upper-Limb-Prosthetics/Myo-Hands-and-Components/Myo-Terminal-Devices/SensorHand-Speed/p/8E38~58-L7~91~24. [Accessed: 21-Nov-2019].

[31] "Michelangelo prosthetic hand | Ottobock US." [Online]. Available: https://www.ottobockus.com/prosthetics/upper-limb-prosthetics/solution-overview/michelangelo-prosthetic-hand/. [Accessed: 21-Nov-2019].

[32] D. P. J. Cotton, P. H. Chappell, A. Cranny, N. M. White, and S. P. Beeby, "A novel thick-film piezoelectric slip sensor for a prosthetic hand," *IEEE Sens. J.*, 2007.

[33] A. Saudabayev and H. A. Varol, "Sensors for robotic hands: A survey of state of the art," *IEEE Access*. 2015.

[34] A. L. Ciancio *et al.*, "Control of prosthetic hands via the peripheral nervous system," *Front. Neurosci.*, vol. 10, no. APR, Apr. 2016.

[35] L. Zou, C. Ge, Z. J. Wang, E. Cretu, and X. Li, "Novel tactile sensor technology and smart tactile sensing systems: A review," *Sensors (Switzerland)*. 2017.

[36] "DLR - Institute of Robotics and Mechatronics - DLR/HIT Hand." [Online]. Available: https://www.dlr.de/rm/en/desktopdefault.aspx/tabid-9467/16255_read-8918/. [Accessed: 21-Nov-2019].

[37] P. J. Kyberd, C. Light, P. H. Chappell, J. M. Nightingale, D. Whatley, and M. Evans, "The design of anthropomorphic prosthetic hands: A study of the Southampton Hand," *Robotica*, 2001.

[38] "The LUKE/DEKA advanced prosthetic arm." [Online]. Available:

https://www.research.va.gov/research_in_action/The-LUKE-DEKA-advanced-prosthetic-arm.cfm. [Accessed: 21-Nov-2019].

[39] M. C. Carrozza, P. Dario, F. Vecchi, S. Roccella, M. Zecca, and F. Sebastiani, "The CyberHand: On the design of a cybernetic prosthetic hand intended to be interfaced to the peripheral nervous system," in *IEEE International Conference on Intelligent Robots and Systems*, 2003, vol. 3, pp. 2642–2647.

[40] D. W. Tan, M. A. Schiefer, M. W. Keith, J. R. Anderson, J. Tyler, and D. J. Tyler, "A neural interface provides long-term stable natural touch perception," *Sci. Transl. Med.*, 2014.

[41] M. Ortiz-Catalan, N. Sander, M. B. Kristoffersen, B. Håkansson, and R. Brånemark, "Treatment of phantom limb pain (PLP) based on augmented reality and gaming controlled by myoelectric pattern recognition: A case study of a chronic PLP patient," *Front. Neurosci.*, 2014.

[42] D. S. Childress, "Closed-loop control in prosthetic systems: Historical perspective," *Ann. Biomed. Eng.*, 1980.

[43] C. Antfolk, M. D'alonzo, B. Rosén, G. Lundborg, F. Sebelius, and C. Cipriani, "Sensory feedback in upper limb prosthetics," *Expert Rev. Med. Devices*, vol. 10, no. 1, pp. 45–54, 2013.

[44] M. Gasson, B. Hutt, I. Goodhew, P. Kyberd, and K. Warwick, "Invasive neural prosthesis for neural signal detection and nerve stimulation," *Int. J. Adapt. Control Signal Process.*, 2005.

[45] R. S. Johansson and J. R. Flanagan, "Coding and use of tactile signals from the fingertips in object manipulation tasks," *Nature Reviews Neuroscience*. 2009.

[46] M. Botvinick and J. Cohen, "Rubber hands 'feel' touch that eyes see [8]," *Nature*. 1998.

[47] S. Shimada, K. Fukuda, and K. Hiraki, "Rubber hand illusion under delayed visual feedback," *PLoS One*, 2009.

[48] R. S. Johansson and I. Birznieks, "First spikes in ensembles of human tactile afferents code complex spatial fingertip events," *Nat. Neurosci.*, 2004.

[49] T. A. Kuiken, G. A. Dumanian, R. D. Lipschutz, L. A. Miller, and K. A. Stubblefield, "The use of targeted muscle reinnervation for improved myoelectric prosthesis control in a bilateral shoulder disarticulation amputee," *Prosthet. Orthot. Int.*, 2004.

[50] J. S. Hebert *et al.*, "Novel targeted sensory reinnervation technique to restore functional hand sensation after transhumeral amputation," *IEEE Trans. Neural Syst. Rehabil. Eng.*, 2014.

[51] K. Horch, S. Meek, T. G. Taylor, and D. T. Hutchinson, "Object discrimination with an artificial hand using electrical stimulation of peripheral tactile and proprioceptive pathways with intrafascicular electrodes," *IEEE Trans. Neural Syst. Rehabil. Eng.*, 2011.

[52] M. Ortiz-Catalan, B. Ha˚kansson, and R. Bra˚nemark, "An osseointegrated human-machine gateway for long-term sensory feedback and motor control of artificial limbs," *Sci. Transl. Med.*, 2014.

[53] R. R. Riso, "Strategies for providing upper extremity amputees with tactile and hand position feedback - Moving closer to the bionic arm," *Technology and Health Care*. 1999.

[54] A. Anani and L. Korner, "Discrimination of phantom hand sensations elicited by afferent electrical nerve stimulation in below-elbow amputees," *Med. Prog. Technol.*, 1979.

[55] E. L. Graczyk, M. A. Schiefer, H. P. Saal, B. P. Delhaye, S. J. Bensmaia, and D. J. Tyler, "The neural basis of perceived intensity in natural and artificial touch," *Sci. Transl. Med.*, 2016.

[56] S. J. Bensmaia and L. E. Miller, "Restoring sensorimotor function through intracortical interfaces: Progress and looming challenges," *Nature Reviews Neuroscience*. 2014.

[57] S. Casini, M. Morvidoni, M. Bianchi, M. Catalano, G. Grioli, and A. Bicchi, "Design and realization of the CUFF - Clenching upper-limb force feedback wearable device for distributed mechano-tactile stimulation of normal and tangential skin forces," in *IEEE International Conference on Intelligent Robots and*

Systems, 2015.

[58] K. A. Kaczmarek, J. G. Webster, P. Bach-y-Rita, and W. J. Tompkins, "Electrotactile and Vibrotactile Displays for Sensory Substitution Systems," *IEEE Trans. Biomed. Eng.*, 1991.

[59] P. Bach-y-Rita and S. W. Kercel, "Sensory substitution and the human-machine interface," *Trends in Cognitive Sciences*. 2003.

[60] J. L. Pons *et al.*, "The MANUS-HAND Dextrous Robotics Upper Limb Prosthesis: Mechanical and Manipulation Aspects," *Auton. Robots*, 2004.

[61] A. Kargov *et al.*, "Applications of a Fluidic Artificial Hand in the Field of Rehabilitation," in *Rehabilitation Robotics*, 2007.

[62] "SmartHand | The BioRobotics Institute." [Online]. Available: http://sssa.bioroboticsinstitute.it/projects/SmartHand. [Accessed: 22-Nov-2019].

[63] K. A. Kaczmarek, "Electrotactile adaptation on the abdomen: Preliminary results," *IEEE Trans. Rehabil. Eng.*, 2000.

[64] S. Wilson and S. Dirven, "Audio sensory substitution for human-in-the-loop force feedback of upper limb prosthetics," in *M2VIP 2016 - Proceedings of 23rd International Conference on Mechatronics and Machine Vision in Practice*, 2017.

[65] J. Gonzalez, H. Suzuki, N. Natsumi, M. Sekine, and W. Yu, "Auditory display as a prosthetic hand sensory feedback for reaching and grasping tasks," in *Proceedings of the Annual International Conference of the IEEE Engineering in Medicine and Biology Society, EMBS*, 2012.

[66] M. Markovic, H. Karnal, B. Graimann, D. Farina, and S. Dosen, "GLIMPSE: Google Glass interface for sensory feedback in myoelectric hand prostheses," *J. Neural Eng.*, 2017.

[67] F. Clemente, S. Dosen, L. Lonini, M. Markovic, D. Farina, and C. Cipriani, "Humans Can Integrate Augmented Reality Feedback in Their Sensorimotor Control of a Robotic Hand," *IEEE Trans. Human-Machine Syst.*, 2017.

[68] C. Cipriani, J. L. Segil, F. Clemente, R. F. Richard, and B. Edin, "Humans can integrate feedback of discrete events in their sensorimotor control of a robotic hand," *Exp. Brain Res.*, 2014.

[69] F. A. Saunders, "Information transmission across the skin: High-resolution tactile sensory aids for the deaf and the blind," *Int. J. Neurosci.*, 1983.

[70] C. Hartmann, S. Došen, S. Amsuess, and D. Farina, "Closed-loop control of myoelectric prostheses with electrotactile feedback: Influence of stimulation artifact and blanking," *IEEE Trans. Neural Syst. Rehabil. Eng.*, 2015.

[71] M. Franceschi, L. Seminara, S. Dosen, M. Strbac, M. Valle, and D. Farina, "A System for Electrotactile Feedback Using Electronic Skin and Flexible Matrix Electrodes: Experimental Evaluation," *IEEE Trans. Haptics*, 2017.

[72] E. R. Kandel, J. H. Schwartz, and T. M. Jessell, *Principles of Neural Science, fourth addition*. 2000.

[73] L. P. Paredes, S. Dosen, F. Rattay, B. Graimann, and D. Farina, "The impact of the stimulation frequency on closed-loop control with electrotactile feedback," *J. Neuroeng. Rehabil.*, 2015.

[74] J. S. Schofield, K. R. Evans, J. P. Carey, and J. S. Hebert, "Applications of sensory feedback in motorized upper extremity prosthesis: A review," *Expert Rev. Med. Devices*, vol. 11, no. 5, pp. 499–511, 2014.

[75] B. Stephens-Fripp, G. Alici, and R. Mutlu, "A review of non-invasive sensory feedback methods for transradial prosthetic hands," *IEEE Access*. 2018.

[76] P. Svensson, U. Wijk, A. Björkman, and C. Antfolk, "A review of invasive and non-invasive sensory feedback in upper limb prostheses," *Expert Review of Medical Devices*. 2017.

[77] H. Kajimoto, N. Kawakami, and S. Tachi, "Psychophysical evaluation of receptor selectivity in electro-tactile display," *13th Int. Sympo. Meas. Control Robot.*, 2003.

[78] S. Dosen, "Closed Loop Control of Dynamic Systems using Electrotactile Feedback Neurophysiological Biomarkers of Peripheral Muscle Fatigue View project EXTEND-Bidirectional Hyper-Connected Neural System View project," 2013.

[79] N. Fallahian, H. Saeedi, H. Mokhtarinia, and F. Tabatabai Ghomshe, "Sensory feedback add-on for upper-limb prostheses," *Prosthet. Orthot. Int.*, 2017.

[80] A. Ajoudani *et al.*, "Exploring teleimpedance and tactile feedback for intuitive control of the pisa/IIT soft hand," *IEEE Trans. Haptics*, 2014.

[81] D. S. *et al.*, "Building an internal model of a myoelectric prosthesis via closed-loop control for consistent and routine grasping," *Exp. Brain Res.*, 2015.

[82] "Control Theory for Humans | Quantitative Approaches To Modeling Performance | Taylor & Francis Group." [Online]. Available: https://www.taylorfrancis.com/books/9781315144948. [Accessed: 22-Nov-2019].

[83] R. J. Jagacinski and J. M. Flach, *Control Theory for Humans*. CRC Press, 2018.

[84] S. Dosen, M. Markovic, C. Hartmann, and D. Farina, "Sensory feedback in prosthetics: A standardized test bench for closed-loop control," *IEEE Trans. Neural Syst. Rehabil. Eng.*, 2015.

[85] T. T. Ivancevic, B. Jovanovic, and S. Markovic, "Fuzzy Control Strategies in Human Operator and Sport Modeling," *Fuzzy Inf. Eng.*, 2010.

[86] U. Menon, T. B. Sheridan, and W. R. Ferrel, "Man-Machine Systems: Information, Control and Decision Models of Human Performance," *Oper. Res. Q.*, 1976.

[87] S. S. Hacisalihzade, *Biomedical applications of control engineering*. Springer, 2013.

[88] D. McRuer, "Human dynamics in man-machine systems," *Automatica*, vol. 16, no. 3, pp. 237–253, 1980.

[89] M. Rakić, "Paper 11: The 'Belgrade Hand Prosthesis,'" *Proc. Inst. Mech. Eng. Conf. Proc.*, vol. 183, no. 10, pp. 60–67, Sep. 1968.

[90] R. S. Johansson and K. J. Cole, "Sensory-motor coordination during grasping and manipulative actions," *Curr. Opin. Neurobiol.*, 1992.

[91] D. J. Tyler, "Restoring the human touch: Prosthetics imbued with haptics give their wearers fine motor control and a sense of connection," *IEEE Spectr.*, 2016.

[92] S. Raspopovic *et al.*, "Restoring natural sensory feedback in real-time bidirectional hand prostheses (with supplemental material)," *Sci. Transl. Med.*, 2014.

[93] M. Schiefer, D. Tan, S. M. Sidek, and D. J. Tyler, "Sensory feedback by peripheral nerve stimulation improves task performance in individuals with upper limb loss using a myoelectric prosthesis," *J. Neural Eng.*, 2015.

[94] E. L. Graczyk, L. Resnik, M. A. Schiefer, M. S. Schmitt, and D. J. Tyler, "Home use of a neural-connected sensory prosthesis provides the functional and psychosocial experience of having a hand again," *Sci. Rep.*, 2018.

[95] M. A. Schiefer, E. L. Graczyk, S. M. Sidik, D. W. Tan, and D. J. Tyler, "Artificial tactile and proprioceptive feedback improves performance and confidence on object identification tasks," *PLoS One*, 2018.

[96] F. Clemente *et al.*, "Intraneural sensory feedback restores grip force control and motor coordination while using a prosthetic hand," *J. Neural Eng.*, 2019.

[97] F. M. Petrini *et al.*, "Six-Month Assessment of a Hand Prosthesis with Intraneural Tactile Feedback," *Ann.*

Neurol., 2019.

[98] G. Valle *et al.*, "Biomimetic Intraneural Sensory Feedback Enhances Sensation Naturalness, Tactile Sensitivity, and Manual Dexterity in a Bidirectional Prosthesis," *Neuron*, 2018.

[99] S. Wendelken *et al.*, "Restoration of motor control and proprioceptive and cutaneous sensation in humans with prior upper-limb amputation via multiple Utah Slanted Electrode Arrays (USEAs) implanted in residual peripheral arm nerves," *J. Neuroeng. Rehabil.*, 2017.

[100] G. A. Tabot *et al.*, "Restoring the sense of touch with a prosthetic hand through a brain interface," *Proc. Natl. Acad. Sci. U. S. A.*, 2013.

[101] S. N. Flesher *et al.*, "Intracortical microstimulation of human somatosensory cortex," *Sci. Transl. Med.*, 2016.

[102] J. A. Cronin *et al.*, "Task-Specific Somatosensory Feedback via Cortical Stimulation in Humans," *IEEE Trans. Haptics*, 2016.

[103] A. Y. J. Szeto and F. A. Saunders, "Electrocutaneous Stimulation for Sensory Communication in Rehabilitation Engineering," *IEEE Trans. Biomed. Eng.*, 1982.

[104] R. W. Cholewiak, J. C. Brill, and A. Schwab, "Vibrotactile localization on the abdomen: Effects of place and space," *Percept. Psychophys.*, 2004.

[105] R. W. Cholewiak and A. A. Collins, "Vibrotactile localization on the arm: Effects of place, space, and age," *Percept. Psychophys.*, 2003.

[106] K. O. Sofia and L. Jones, "Mechanical and psychophysical studies of surface wave propagation during vibrotactile stimulation," *IEEE Trans. Haptics*, 2013.

[107] A. B. Anani and L. M. Körner, "Afferent electrical nerve stimulation: Human tracking performance relevant to prosthesis sensory feedback," *Med. Biol. Eng. Comput.*, 1979.

[108] M. Markovic *et al.*, "The clinical relevance of advanced artificial feedback in the control of a multi-functional myoelectric prosthesis," *J. Neuroeng. Rehabil.*, vol. 15, no. 1, 2018.

[109] B. Geng, K. Yoshida, L. Petrini, and W. Jensen, "Evaluation of sensation evoked by electrocutaneous stimulation on forearm in nondisabled subjects," *J. Rehabil. Res. Dev.*, 2012.

[110] S. Dosen, A. Ninu, T. Yakimovich, H. Dietl, and D. Farina, "A Novel Method to Generate Amplitude-Frequency Modulated Vibrotactile Stimulation," *IEEE Trans. Haptics*, 2016.

[111] S. Dosen *et al.*, "Multichannel electrotactile feedback with spatial and mixed coding for closed-loop control of grasping force in hand prostheses," *IEEE Trans. Neural Syst. Rehabil. Eng.*, 2017.

[112] S. G. Meek, S. C. Jacobsen, and P. P. Goulding, "Extended physiologic taction: Design and evaluation of a proportional force feedback system," *J. Rehabil. Res. Dev.*, 1989.

[113] L. A. Jones, D. Held, and I. Hunter, "Surface waves and spatial localization in vibrotactile displays," in *2010 IEEE Haptics Symposium, HAPTICS 2010*, 2010.

[114] G. Chai, X. Sui, S. Li, L. He, and N. Lan, "Characterization of evoked tactile sensation in forearm amputees with transcutaneous electrical nerve stimulation," *J. Neural Eng.*, 2015.

[115] C. Hartmann *et al.*, "Towards prosthetic systems providing comprehensive tactile feedback for utility and embodiment," in *IEEE 2014 Biomedical Circuits and Systems Conference, BioCAS 2014 - Proceedings*, 2014.

[116] C. Pylatiuk, A. Kargov, and S. Schulz, "Design and evaluation of a low-cost force feedback system for myoelectric prosthetic hands," in *Journal of Prosthetics and Orthotics*, 2006.

[117] E. D'Anna *et al.*, "A somatotopic bidirectional hand prosthesis with transcutaneous electrical nerve stimulation based sensory feedback," *Sci. Rep.*, 2017.

[118] M. Li *et al.*, "Discrimination and recognition of phantom finger sensation through transcutaneous electrical nerve stimulation," *Front. Neurosci.*, 2018.

[119] C. Antfolk *et al.*, "Artificial redirection of sensation from prosthetic fingers to the phantom hand map on transradial amputees: Vibrotactile versus mechanotactile sensory feedback," *IEEE Trans. Neural Syst. Rehabil. Eng.*, 2013.

[120] G. Chai, D. Zhang, and X. Zhu, "Developing non-somatotopic phantom finger sensation to comparable levels of somatotopic sensation through user training with electrotactile stimulation," *IEEE Trans. Neural Syst. Rehabil. Eng.*, 2017.

[121] M. Hauschild, R. Davoodi, and G. E. Loeb, "A virtual reality environment for designing and fitting neural prosthetic limbs," *IEEE Trans. Neural Syst. Rehabil. Eng.*, 2007.

[122] J. M. Lambrecht, C. L. Pulliam, and R. F. Kirsch, "Virtual reality environment for simulating tasks with a myoelectric prosthesis: An assessment and training tool," *J. Prosthetics Orthot.*, 2011.

[123] P. W. Snow, I. Sedki, M. Sinisi, R. Comley, and R. C. V. Loureiro, "Robotic therapy for phantom limb pain in upper limb amputees," in *IEEE International Conference on Rehabilitation Robotics*, 2017.

[124] H. Kawasaki, T. Mouri, and S. Ueki, "Virtual Robot Teaching for Humanoid Both-Hands Robots Using Multi-Fingered Haptic Interface," in *The Thousand Faces of Virtual Reality*, 2014.

[125] B. Peerdeman, "Myoelectric forearm prostheses:State of the art from a user-centered perspective," *Journal of Rehabilitation Research and Development*. 2011.

[126] V. Kumar and E. Todorov, "MuJoCo HAPTIX: A virtual reality system for hand manipulation," in *IEEE-RAS International Conference on Humanoid Robots*, 2015.

[127] "(No Title)." [Online]. Available: https://www.jhuapl.edu/Home/PageNotFound?aspxerrorpath=/Rejected-By-UrlScan. [Accessed: 21-Nov-2019].

[128] H. Fares, L. Seminara, H. Chible, S. Dosen, and M. Valle, "Multi-Channel Electrotactile Stimulation System for Touch Substitution: A Case Study," in *PRIME 2018 - 14th Conference on Ph.D. Research in Microelectronics and Electronics*, 2018.

[129] L. Seminara *et al.*, "Dual-parameter modulation improves stimulus localization in multichannel electrotactile stimulation," *IEEE Trans. Haptics*, 2019.

[130] S. Micera, "Staying in Touch: Toward the Restoration of Sensory Feedback in Hand Prostheses Using Peripheral Neural Stimulation," *IEEE Pulse*, 2016.

[131] D. J. Tyler, "Neural interfaces for somatosensory feedback," *Curr. Opin. Neurol.*, 2015.

[132] R. S. Dahiya, G. Metta, M. Valle, and G. Sandini, "Tactile sensing-from humans to humanoids," *IEEE Trans. Robot.*, 2010.

[133] A. Chortos, J. Liu, and Z. Bao, "Pursuing prosthetic electronic skin," *Nature Materials*. 2016.

[134] C. Chi, X. Sun, N. Xue, T. Li, and C. Liu, "Recent progress in technologies for tactile sensors," *Sensors (Switzerland)*. 2018.

[135] M. I. Tiwana, S. J. Redmond, and N. H. Lovell, "A review of tactile sensing technologies with applications in biomedical engineering," *Sensors and Actuators, A: Physical*. 2012.

[136] C. Lucarotti, C. M. Oddo, N. Vitiello, and M. C. Carrozza, "Synthetic and bio-artificial tactile sensing: A review," *Sensors (Switzerland)*. 2013.

[137] D. Silvera-Tawil, D. Rye, and M. Velonaki, "Artificial skin and tactile sensing for socially interactive robots: A review," *Rob. Auton. Syst.*, 2015.

[138] P. S. Girão, P. M. P. Ramos, O. Postolache, and J. Miguel Dias Pereira, "Tactile sensors for robotic applications," *Measurement: Journal of the International Measurement Confederation*. 2013.

[139] M. S. A. Graziano and M. M. Botvinick, "How the brain represents the body: insights from neurophysiology and psychology," *Common mechanisms in perception and action (Attention and performance XIX)*. 2002.

[140] R. L. Klatzky and S. J. Lederman, "Touch," in *Handbook of Psychology*, Hoboken, NJ, USA: John Wiley & Sons, Inc., 2003.

[141] R. S. Johansson and G. Westling, "Roles of glabrous skin receptors and sensorimotor memory in automatic control of precision grip when lifting rougher or more slippery objects," *Exp. Brain Res.*, vol. 56, no. 3, pp. 550–564, Oct. 1984.

[142] I. Darian-Smith, "The Sense of Touch: Performance and Peripheral Neural Processes," in *Comprehensive Physiology*, 2011.

[143] A. B. Vallbo' and R. S. ~ohansson~, "Properties of cutaneous mechanoreceptors in the human hand-related to touch sensation," 1984.

[144] F. W. Clippinger and M. D. Roger Avery Bert R Titus, "A SENSORY FEEDBACK SYSTEM FOR AN UPPER-LIMB AMPUTATION PROSTHESIS."

[145] B. Crone *et al.*, "Large-scale complementary integrated circuits based on organic transistors," *Nature*, vol. 403, no. 6769, pp. 521–523, Feb. 2000.

[146] D.-H. Kim *et al.*, "Materials and noncoplanar mesh designs for integrated circuits with linear elastic responses to extreme mechanical deformations," *Proc. Natl. Acad. Sci.*, vol. 105, no. 48, pp. 18675–18680, Dec. 2008.

[147] C. Metzger *et al.*, "Flexible-foam-based capacitive sensor arrays for object detection at low cost," *Appl. Phys. Lett.*, 2008.

[148] I. Graz *et al.*, "Flexible ferroelectret field-effect transistor for large-area sensor skins and microphones," *Appl. Phys. Lett.*, 2006.

[149] S. C. B. Mannsfeld *et al.*, "Highly sensitive flexible pressure sensors with microstructured rubber dielectric layers," *Nat. Mater.*, 2010.

[150] B. C. K. Tee, C. Wang, R. Allen, and Z. Bao, "An electrically and mechanically self-healing composite with pressure- and flexion-sensitive properties for electronic skin applications," *Nat. Nanotechnol.*, 2012.

[151] Z. Yu, X. Niu, Z. Liu, and Q. Pei, "Intrinsically stretchable polymer light-emitting devices using carbon nanotube-polymer composite electrodes," *Adv. Mater.*, 2011.

[152] D. J. Lipomi, B. C. K. Tee, M. Vosgueritchian, and Z. Bao, "Stretchable organic solar cells," *Adv. Mater.*, 2011.

[153] H. He *et al.*, "A flexible self-powered T-ZnO/PVDF/fabric electronic-skin with multi-functions of tactile-perception, atmosphere-detection and self-clean," *Nano Energy*, 2017.

[154] C. G. Núñez, W. T. Navaraj, E. O. Polat, and R. Dahiya, "Energy-Autonomous, Flexible, and Transparent Tactile Skin," *Adv. Funct. Mater.*, 2017.

[155] L. E. Osborn *et al.*, "Prosthesis with neuromorphic multilayered e-dermis perceives touch and pain," *Sci. Robot.*, 2018.

[156] A. Chortos and Z. Bao, "Skin-inspired electronic devices," *Materials Today*. 2014.

[157] A. Ibrahim, L. Pinna, L. Seminara, and M. Valle, "Achievements and open issues toward embedding tactile sensing and interpretation into electronic skin systems," in *Material-Integrated Intelligent Systems: Technology and Applications*, 2016.

[158] M. T. Almansoori, X. Li, and L. Zheng, "A Brief Review on E-skin and its Multifunctional Sensing Applications," *Curr. Smart Mater.*, 2019.

[159] J. Engel, J. Chen, and C. Liu, "Development of polyimide flexible tactile sensor skin," *J. Micromechanics Microengineering*, 2003.

[160] J. G. Da Silva, A. A. De Carvalho, and D. D. Da Silva, "A strain gauge tactile sensor for finger-mounted applications," *IEEE Trans. Instrum. Meas.*, 2002.

[161] S. Stassi, V. Cauda, G. Canavese, and C. F. Pirri, "Flexible tactile sensing based on piezoresistive composites: A review," *Sensors (Switzerland)*. 2014.

[162] N. Jorgovanovic, S. Dosen, D. J. Djozic, G. Krajoski, and D. Farina, "Virtual grasping: Closed-loop force control using electrotactile feedback," *Comput. Math. Methods Med.*, 2014.

[163] B. J. Kane, M. R. Cutkosky, and G. T. A. Kovacs, "Traction stress sensor array for use in high-resolution robotic tactile imaging," *J. Microelectromechanical Syst.*, 2000.

[164] M. Kalantari, M. Ramezanifard, R. Ahmadi, J. Dargahi, and J. Kövecses, "A piezoresistive tactile sensor for tissue characterization during catheter-based cardiac surgery," *Int. J. Med. Robot. Comput. Assist. Surg.*, 2011.

[165] R. Koiva, M. Zenker, C. Schurmann, R. Haschke, and H. J. Ritter, "A highly sensitive 3D-shaped tactile sensor," in *2013 IEEE/ASME International Conference on Advanced Intelligent Mechatronics: Mechatronics for Human Wellbeing, AIM 2013*, 2013.

[166] Y. Wang, K. Xi, G. Liang, M. Mei, and Z. Chen, "A flexible capacitive tactile sensor array for prosthetic hand real-time contact force measurement," in *2014 IEEE International Conference on Information and Automation, ICIA 2014*, 2014.

[167] H. B. Muhammad *et al.*, "A capacitive tactile sensor array for surface texture discrimination," in *Microelectronic Engineering*, 2011.

[168] H. K. Kim, S. Lee, and K. S. Yun, "Capacitive tactile sensor array for touch screen application," in *Sensors and Actuators, A: Physical*, 2011.

[169] L. Seminara, M. Capurro, P. Cirillo, G. Cannata, and M. Valle, "Electromechanical characterization of piezoelectric PVDF polymer films for tactile sensors in robotics applications," *Sensors Actuators, A Phys.*, 2011.

[170] J. Dargahi, "Piezoelectric tactile sensor with three sensing elements for robotic, endoscopic and prosthetic applications," *Sensors Actuators, A Phys.*, 2000.

[171] I. Dakua and N. Afzulpurkar, "Piezoelectric energy generation and harvesting at the nano-scale: Materials and devices," *Nanomaterials and Nanotechnology*. 2013.

[172] S. Takamuku, G. Gómez, K. Hosoda, and R. Pfeifer, "Haptic discrimination of material properties by a robotic hand," in *2007 IEEE 6th International Conference on Development and Learning, ICDL*, 2007.

[173] S. Omata and Y. Terunuma, "New tactile sensor like the human hand and its applications," *Sensors Actuators A. Phys.*, 1992.

[174] H. Maekawa, K. Tanie, and K. Komoritya, "Finger-shaped tactile sensor using an optical waveguide," in *Proceedings of the IEEE International Conference on Systems, Man and Cybernetics*, 1993.

[175] A. Ataollahi, P. Polygerinos, P. Puangmali, L. D. Seneviratne, and K. Althoefer, "Tactile sensor array using prismatic-tip optical fibers for dexterous robotic hands," in *IEEE/RSJ 2010 International Conference on Intelligent Robots and Systems, IROS 2010 - Conference Proceedings*, 2010.

[176] L. Pinna, A. Ibrahim, and M. Valle, "Interface Electronics for Tactile Sensors Based on Piezoelectric Polymers," *IEEE Sens. J.*, 2017.

[177] D. Silvera-Tawil, D. Rye, and M. Velonaki, "Interpretation of Social Touch on an Artificial Arm Covered with an EIT-based Sensitive Skin," *Int. J. Soc. Robot.*, 2014.

[178] Z. Kappassov, J. A. Corrales, and V. Perdereau, "Tactile sensing in dexterous robot hands - Review," *Rob. Auton. Syst.*, 2015.

[179] O. Oballe-Peinado, J. A. Hidalgo-Lopez, J. A. Sanchez-Duran, J. Castellanos-Ramos, and F. Vidal-Verdu, "Architecture of a tactile sensor suite for artificial hands based on FPGAs," in *Proceedings of the IEEE RAS and EMBS International Conference on Biomedical Robotics and Biomechatronics*, 2012.

[180] A. Cirillo, P. Cirillo, G. De Maria, C. Natale, and S. Pirozzi, "A Distributed Tactile Sensor for Intuitive Human-Robot Interfacing," *J. Sensors*, 2017.

[181] T. E. Alves De Oliveira, A. M. Cretu, and E. M. Petriu, "Multimodal Bio-Inspired Tactile Sensing Module," *IEEE Sens. J.*, 2017.

[182] A. Ibrahim, P. Gastaldo, H. Chible, and M. Valle, "Real-time digital signal processing based on FPGAs for electronic skin implementation," *Sensors (Switzerland)*, 2017.

[183] L. Seminara *et al.*, "Electronic skin and electrocutaneous stimulation to restore the sense of touch in hand prosthetics," in *Proceedings - IEEE International Symposium on Circuits and Systems*, 2017.

[184] M. Magno *et al.*, "InfiniTime: Multi-sensor wearable bracelet with human body harvesting," *Sustain. Comput. Informatics Syst.*, 2016.

[185] L. Seminara, M. Capurro, and M. Valle, "Tactile data processing method for the reconstruction of contact force distributions," *Mechatronics*, 2015.

[186] W. Wasko, A. Albini, P. Maiolino, F. Mastrogiovanni, and G. Cannata, "Contact modelling and tactile data processing for robot skins," *Sensors (Switzerland)*, 2019.

[187] J. A. Fishel and G. E. Loeb, "Bayesian exploration for intelligent identification of textures," *Front. Neurorobot.*, 2012.

[188] N. Jamali, C. Ciliberto, L. Rosasco, and L. Natale, "Active perception: Building objects' models using tactile exploration," in *IEEE-RAS International Conference on Humanoid Robots*, 2016.

[189] P. Gastaldo, L. Pinna, L. Seminara, M. Valle, and R. Zunino, "A tensor-based approach to touch modality classification by using machine learning," *Rob. Auton. Syst.*, 2015.

[190] S. Khan, S. Ali, and A. Bermak, "Recent Developments in Printing Flexible and Wearable Sensing Electronics for Healthcare Applications," *Sensors*, vol. 19, no. 5, p. 1230, Mar. 2019.

[191] B. Stadlober, M. Zirkl, and M. Irimia-Vladu, "Route towards sustainable smart sensors: Ferroelectric polyvinylidene fluoride-based materials and their integration in flexible electronics," *Chem. Soc. Rev.*, vol. 48, no. 6, pp. 1787–1825, 2019.

[192] P. P. L. Regtien, "Sensors for applications in robotics," *Sensors and Actuators*, 1986.

[193] Y. J. Hsu, Z. Jia, and I. Kymissis, "A locally amplified strain sensor based on a piezoelectric polymer and organic field-effect transistors," *IEEE Trans. Electron Devices*, 2011.

[194] N. T. Tien *et al.*, "A flexible bimodal sensor array for simultaneous sensing of pressure and temperature," *Adv. Mater.*, 2014.

[195] B. Ploss, B. Ploss, F. G. Shin, H. L. W. Chan, and C. L. Choy, "Pyroelectric or piezoelectric compensated ferroelectric composites," *Appl. Phys. Lett.*, 2000.

[196] X. Wang, F. Sun, G. Yin, Y. Wang, B. Liu, and M. Dong, "Tactile-sensing based on flexible PVDF nanofibers via electrospinning: A review," *Sensors (Switzerland)*. 2018.

[197] Y. Xin *et al.*, "PVDF tactile sensors for detecting contact force and slip: A review," *Ferroelectrics*, 2016.

[198] H. Fares *et al.*, "Screen Printed Tactile Sensing Arrays for Prosthetic Applications," in *Proceedings - IEEE International Symposium on Circuits and Systems*, 2018, vol. 2018-May.

[199] L. Seminara, "Modeling electronic skin response to normal distributed force," *Sensors (Switzerland)*, vol. 18, no. 2, 2018.

[200] M. Zirkl *et al.*, "An all-printed ferroelectric active matrix sensor network based on only five functional materials forming a touchless control interface," *Adv. Mater.*, vol. 23, no. 18, pp. 2069–2074, 2011.

[201] S. J. Lederman and R. L. Klatzky, "Haptic perception: A tutorial," *Attention, Perception, and Psychophysics*, vol. 71, no. 7. pp. 1439–1459, 2009.

[202] L. PINNA and M. VALLE, "Charge Amplifier Design Methodology for Pvdf-Based Tactile Sensors," *J. Circuits, Syst. Comput.*, vol. 22, no. 08, p. 1350066, 2013.

[203] L. Seminara, "Modeling electronic skin response to normal distributed force," *Sensors (Switzerland)*, 2018.

Appendix A - Case Report

Case report Participant Number:
Date:

Compensatory error Tracking- Assessment of control time delay _visual vs. Electrotactile

Participant info:

Number:

Age:

Sex:

Prior experience with Electrotactile and tracking systems:

"At the beginning of test" checklist

Participant receives information and instructions about the study and the risks

Participant reads and signs the informed consent form,

The case report is printed to be filled

The electrodes will be mounted on the dorsal and ventral side of the dominant arm

Any familiar knowledge with CLS-compensatory tracking

Visual Feedback

Electrotactile feedback

"Before test" checklist: Recording thresholds and training

The hand is clean and sterilized, no rings, hand watches, bracelets, etc..

The electrodes are mounted (dorsal 1/3 elbow, Ventral midway between wrist and elbow)
no skin injuries, scratches, wounds in the stimulated area

The stimulator is fully charged, Taking care of subject safety

Testing setup is ready and checked

Record ST (sensation threshold), DT (Discomfort threshold) and PT (Pain threshold), 3 times

Training: 3 times at zero delay

Visual

Hybrid

Electro

Comments:

“Test” checklist

Test setup is ready: **Session 1: Visual tracking**

15 trails (3times x 5 delays), pause 1 min between each two trails

The five conditions are ordered randomly by generating a random series of 1,2,3,4,5

The order is: | | | | | |

| | | | | |

| | | | | |

Test setup is ready: **Session 2: Electrotactile tracking**

15 trails (3times x 5 delays), pause 1 min between each two trails

The five conditions are ordered randomly by generating a random series of 1,2,3,4,5

The order is: | | | | | |

| | | | | |

| | | | | |

“At the beginning of the test” checklist

Participant receives information and instructions about the study and the risks

The electrodes are mounted on the hand

Convention for naming the files:

The last two digits are the repetition number.

Day 1

Start time: Finish time:

Day 2

Start time: Finish time:

(S1)

Informeret samtykke til deltagelse i et sundhedsvidenskabeligt forskningsprojekt.

Forskningsprojektets titel: Effektiv og intuitiv lukket-loop kontrol af myoelektriske proteser

Erklæring fra forsøgspersonen:

Jeg har fået skriftlig og mundtlig information og jeg ved nok om formål, metode, fordele og ulemper til at sige ja til at deltage.

Jeg ved, at det er frivilligt at deltage, og at jeg altid kan trække mit samtykke tilbage uden at miste mine nuværende eller fremtidige rettigheder til behandling.

Jeg giver samtykke til, at deltage i forskningsprojektet og har fået en kopi af dette samtykkeark samt en kopi af den skriftlige information om projektet til eget brug.

Forsøgspersonens navn:

Dato: _____ Underskrift:

Ønsker du at blive informeret om forskningsprojektets resultat samt eventuelle konsekvenser for dig?:

Ja _____ (sæt x) Nej _____ (sæt x)

Erklæring fra den, der afgiver information:

Jeg erklærer, at forsøgspersonen har modtaget mundtlig og skriftlig information om forsøget.

Efter min overbevisning er der givet tilstrækkelig information til, at der kan træffes beslutning om deltagelse i forsøget.

Navnet på den, der har afgivet information:

Dato: _____ Underskrift:

Projektidentifikation: (Fx komiteens Projekt-ID, EudraCT nr., versions nr./dato eller lign.)

Standardsamtykkeerklæring udarbejdet af Den Nationale Videnskabsetiske Komité, december 2011.

Effektiv og intuitiv lukket-loop kontrol af myoelektriske proteser

Samtykkeerklæring - Version 1

S1)

Informed Consent to Participation in a Health Scientific Research Project

Title of the research project: Effective and intuitive closed-loop control of myoelectric prostheses

Declaration by the Volunteer

I have received information about the research project both in writing and orally, and I have sufficient knowledge of the objective, method, advantages and disadvantages to confirm my participation.

I know that participation is voluntary and that I can always withdraw my consent without losing my present or future rights to treatment.

I hereby give my consent to participation in the research project and confirm that I have received a copy of this form and of all written information for my own use.

Name of the Volunteer:

Date: _____ Signature:

Would you like to be informed of the results of the research project and of the consequences for you, if any?

Yes_____ No _____ (tick the appropriate field)

Declaration by the Person giving Information

I hereby declare that the Volunteer has received information both in writing and orally about the research project.

I believe that the information given is sufficient for making a decision on participation in the research project.

Name of the person giving the information:

Date: _____ Signature:

Project identification: (e.g. project ID of the Committee, EudraCT No., version No./date etc.)

Standard declaration of consent issued by Den Nationale Videnskabsetiske Komité, December 2011.
Translation into English made by Center for Sensory-Motor Interaction, Aalborg University

Results for each tested subject following the testing protocol reported in chapter 3

The results presented represent the results collected form testing 13 subjects.

Correlation variation versus time delay in (msec) for both Visual and Electrotactile Tracking	RMS variation versus time delay in (msec) for both Visual and Electrotactile Tracking

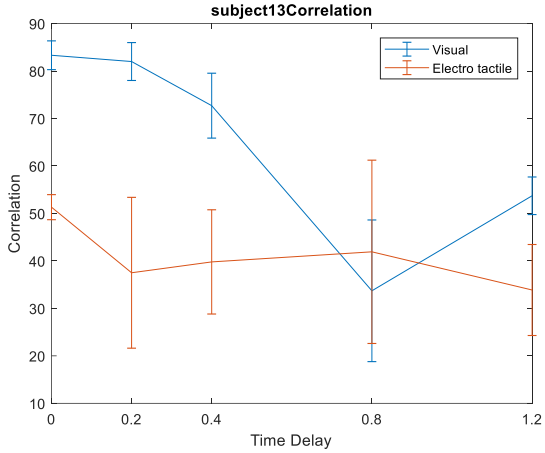
subject13Correlation
Visual
Electro tactile
Correlation
Time Delay

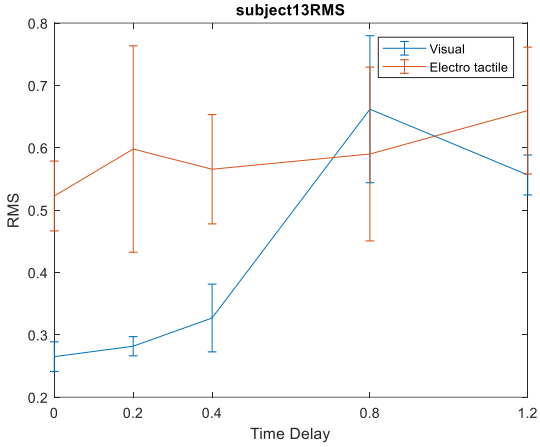
subject13RMS
Visual
Electro tactile
RMS
Time Delay

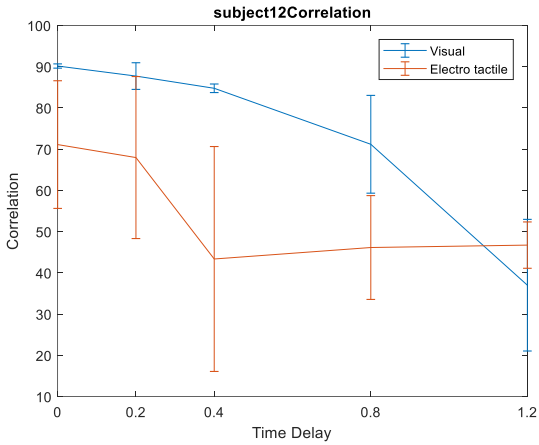
subject12Correlation
Visual
Electro tactile
Correlation
Time Delay

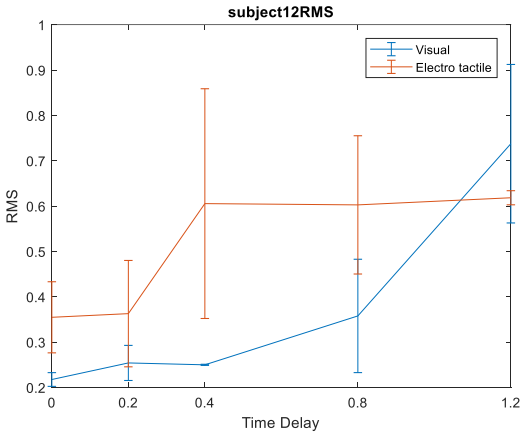
subject12RMS
Visual
Electro tactile
RMS
Time Delay

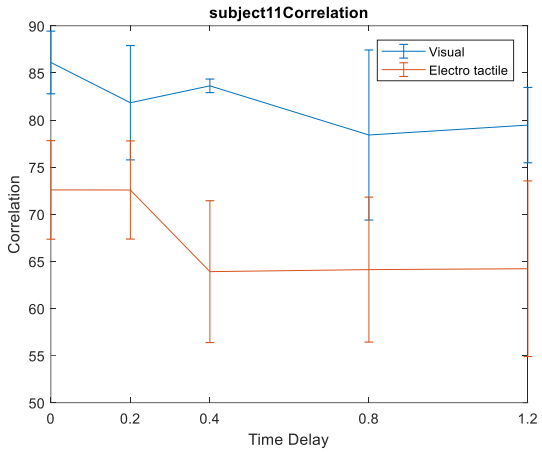
subject11Correlation
Visual
Electro tactile
Correlation
Time Delay

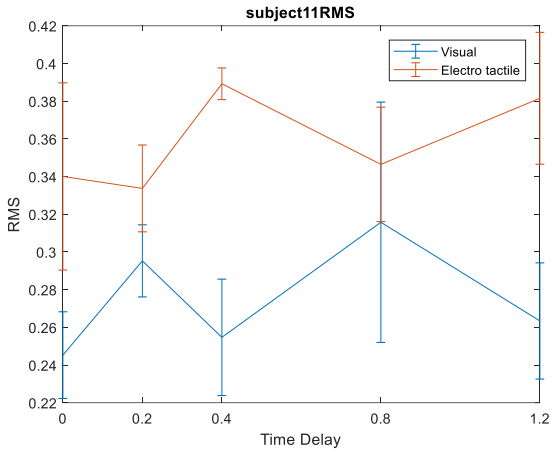
subject11RMS
Visual
Electro tactile
RMS
Time Delay

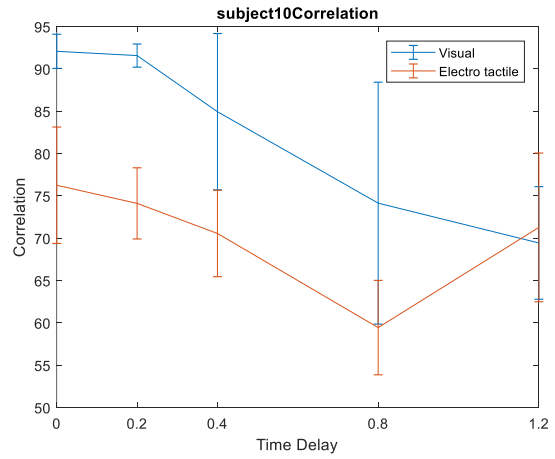
subject10Correlation
Visual
Electro tactile
Correlation
Time Delay

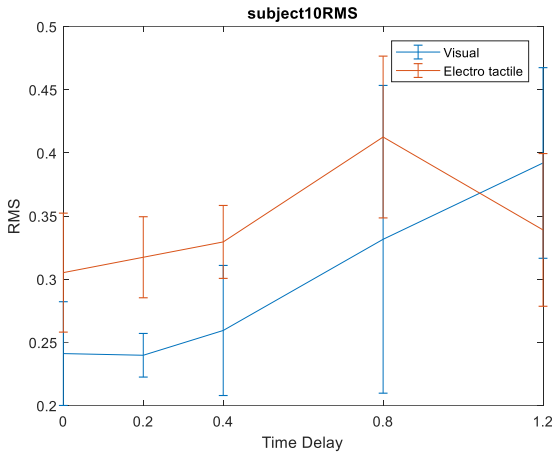
subject10RMS
Visual
Electro tactile
RMS
Time Delay

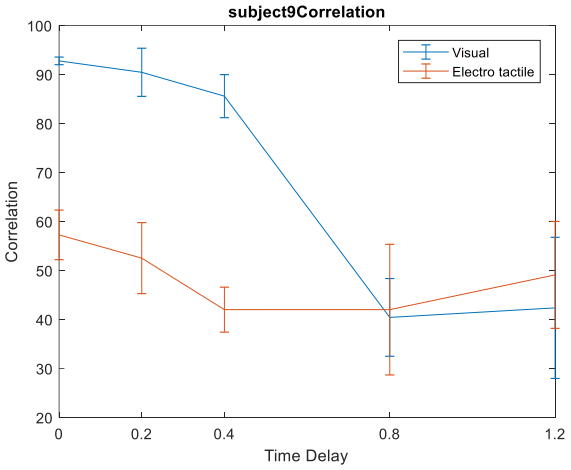
subject9Correlation
Visual
Electro tactile
Correlation
Time Delay

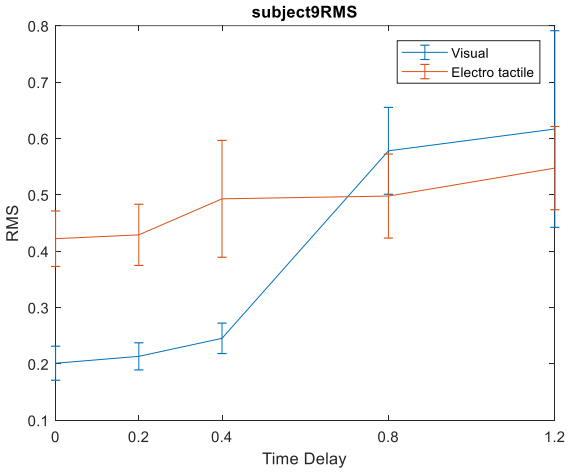
subject9RMS
Visual
Electro tactile
RMS
Time Delay

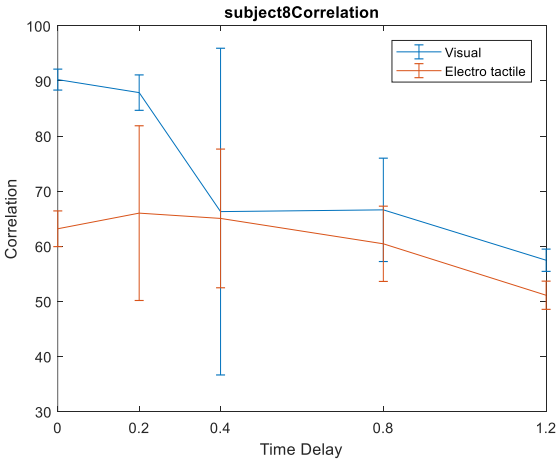
subject8Correlation
Visual
Electro tactile
Correlation
Time Delay

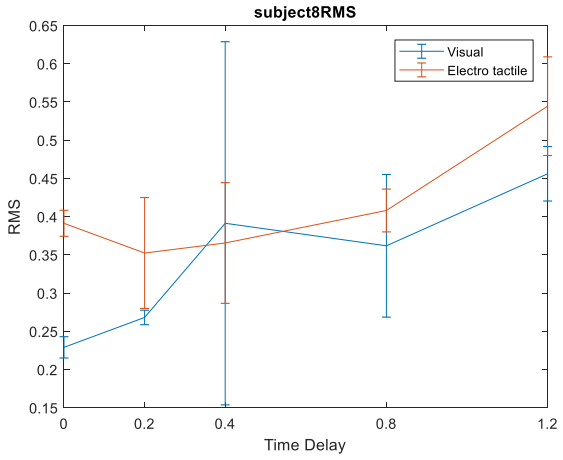
subject8RMS
Visual
Electro tactile
RMS
Time Delay

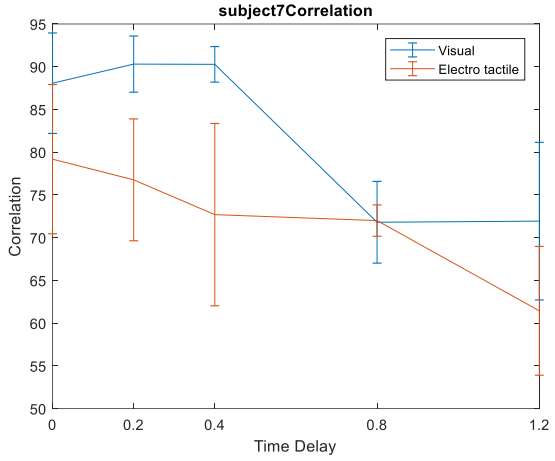
subject7Correlation
Visual
Electro tactile
Correlation
Time Delay

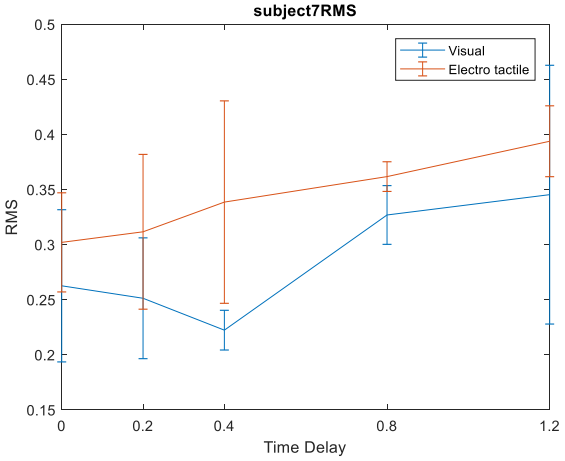
subject7RMS
Visual
Electro tactile
RMS
Time Delay

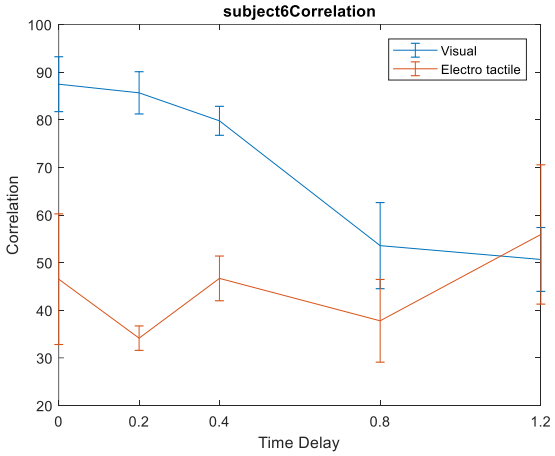
subject6Correlation
Visual
Electro tactile
Correlation
Time Delay

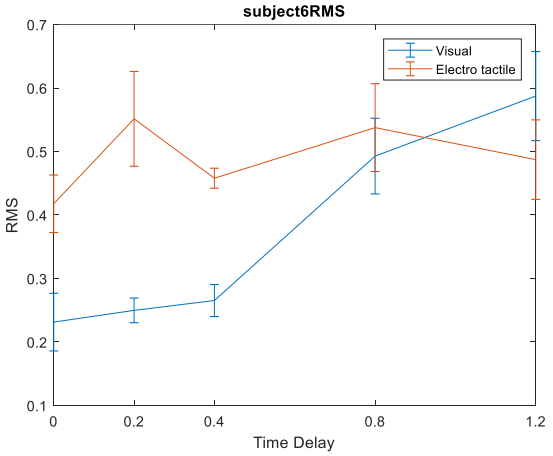
subject6RMS
Visual
Electro tactile
RMS
Time Delay

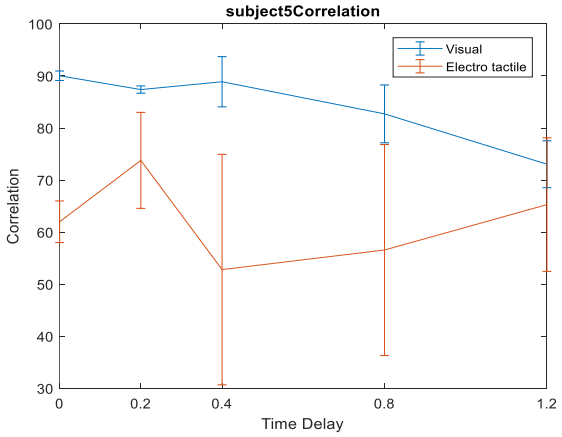
subject5Correlation
Visual
Electro tactile
Correlation
Time Delay

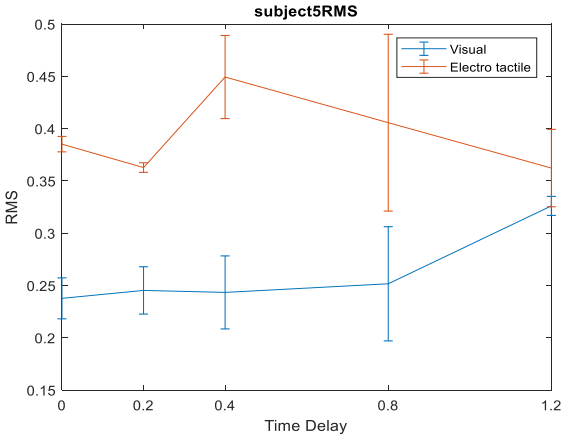
subject5RMS
Visual
Electro tactile
RMS
Time Delay

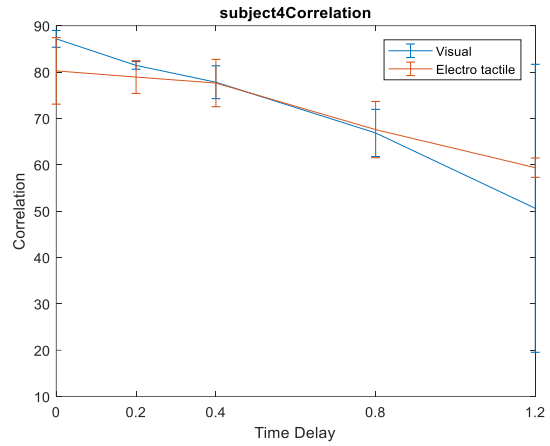
subject4Correlation
Visual
Electro tactile
Correlation
Time Delay

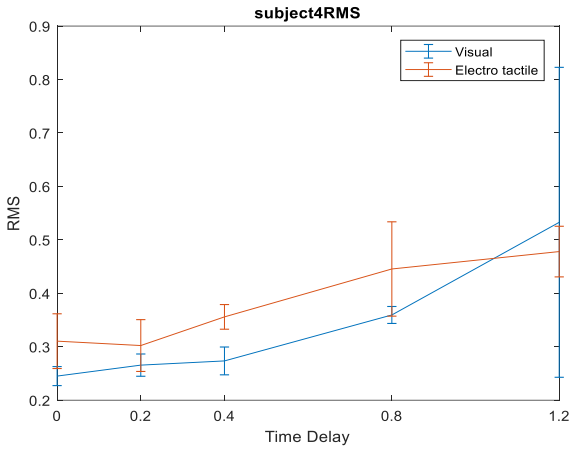
subject4RMS
Visual
Electro tactile
RMS
Time Delay

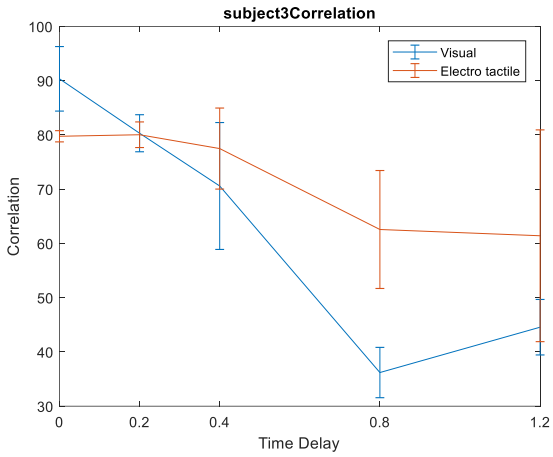
subject3Correlation
Visual
Electro tactile
Correlation
Time Delay

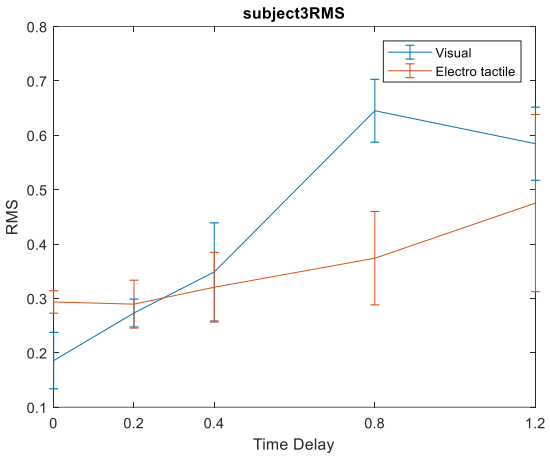
subject3RMS
Visual
Electro tactile
RMS
Time Delay

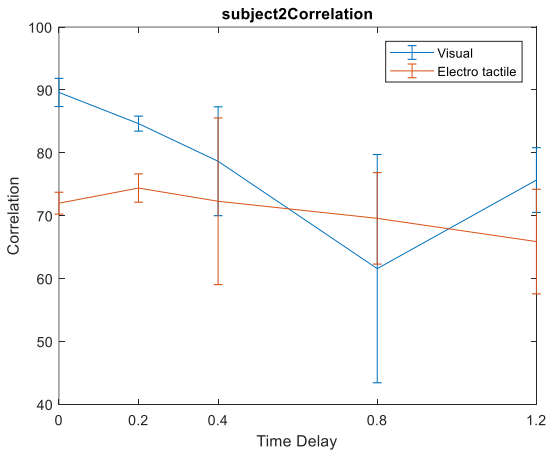
subject2Correlation
Visual
Electro tactile
Correlation
Time Delay

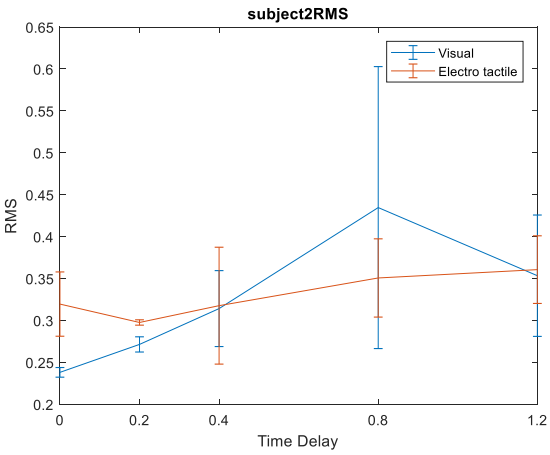
subject2RMS
Visual
Electro tactile
RMS
Time Delay

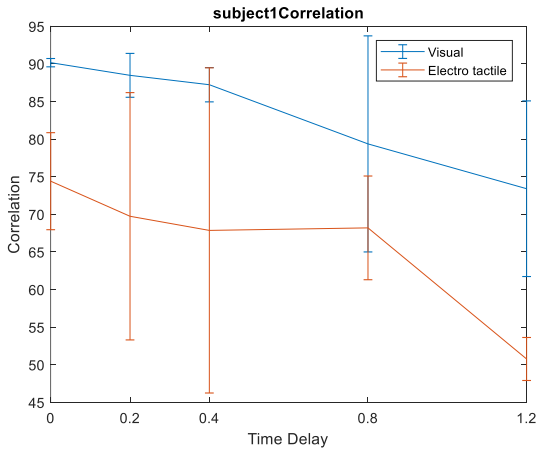
subject1Correlation
Visual
Electro tactile
Correlation
Time Delay
95
90
85
80
75
70
65
60
55
50
45
0
0.2
0.4
0.8
1.2

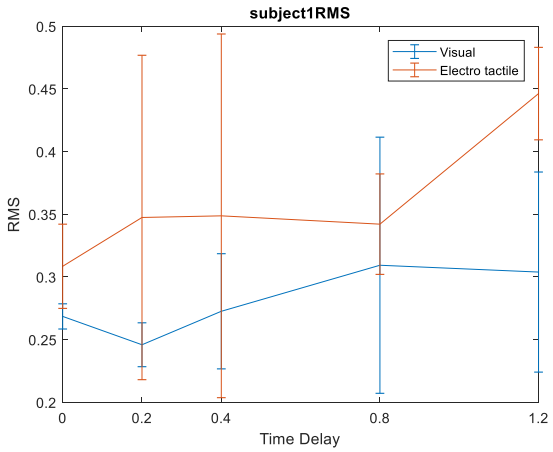
subject1RMS
Visual
Electro tactile
RMS
Time Delay
0.5
0.45
0.4
0.35
0.3
0.25
0.2
0
0.2
0.4
0.8
1.2

Correlation variation versus time delay in (m sec) for both Visual and Electrotactile Tracking

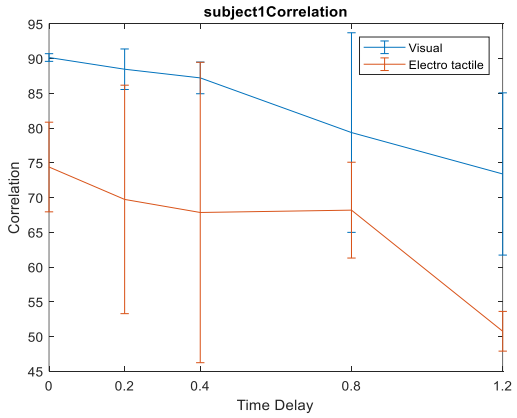

RMS variation versus time delay in ms for both Visual and Electrotactile Tracking

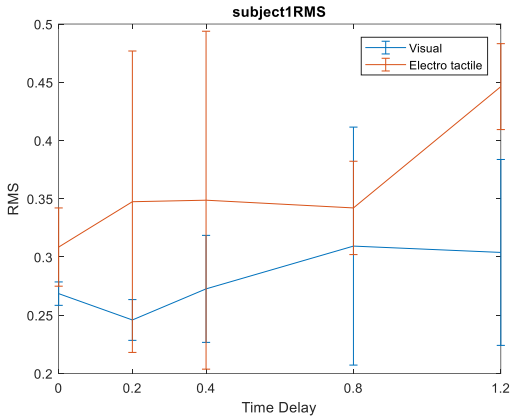

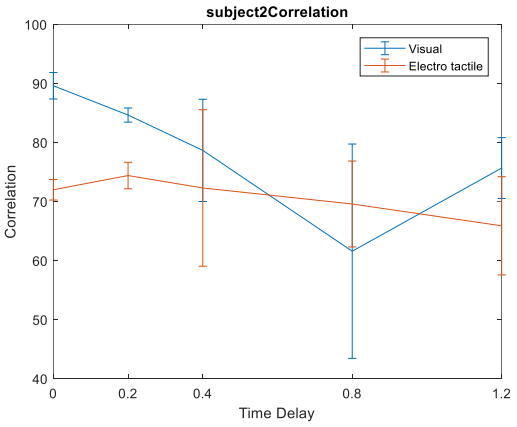

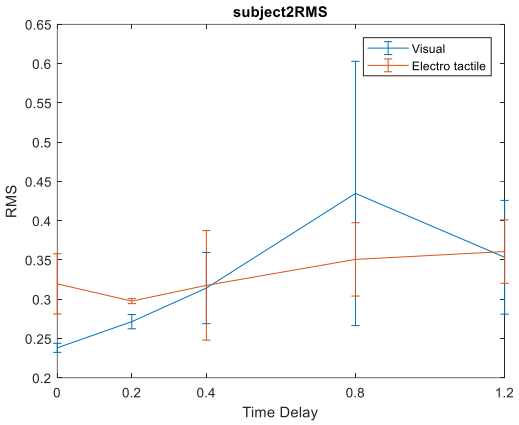

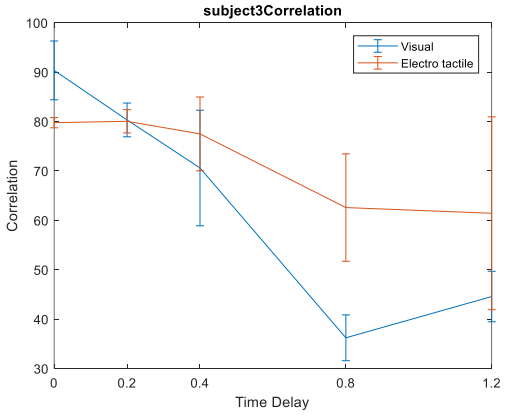

Appendix B - Information Notes To The Participant

COSMIClab
Dipartimento di Ingegneria Navale, Elettrica, Elettronica e delle Telecomunicazioni
Università degli Studi di Genova

INFORMATION NOTES TO THE PARTICIPANT

TITLE OF THE STUDY: **Dual-parameter modulation improves stimulus localization in multichannel electrotactile stimulation**

VERSIONE: 2.0

DATE: 01 December, 2017

PRINCIPAL INVESTIGATOR: Prof. Maurizio Valle

RESEARCH TEAM: Hoda Fares, Marta Franceschi, Lucia Seminara.

Dear Madam / Dear Sir,

At COSMIC lab (DITEN - Electrical, Electronic, Telecommunications and Naval Engineering Department of the University of Genoa), a scientific study is being carried out in the prosthetic field, aiming at transmitting artificial tactile information to the patient through electrostimulation.

This document is intended to inform you about the nature and purpose of the Study, your participation, your rights and responsibilities.

The protocol of the Study that will be proposed to you is in accordance with the European Union Clinical Practice Rules and the current revision of the Helsinki Declaration.

Before you decide if you want to participate, please read these pages carefully and ask for further clarifications if needed.

In the event that, after reading and understanding all the information provided here, you decide to participate to the Study, you will be required to sign and personally date the Informed Consent form attached to this document.

It is important that you know that **your participation is totally voluntary and free** and that you may decide not to participate or withdraw from the study at any time, even after the start of the experiments.

Dip. Ingegneria Navale, Elettrica, Elettronica e delle Telecomunicazioni, Via Opera Pia 11A, 16145 Genova
Tel: 010.353.2775 ▪ maurizio.valle@unige.it

COSMICLab
Dipartimento di Ingegneria Navale, Elettrica, Elettronica e delle Telecomunicazioni
Università degli Studi di Genova

I. Abstract

Myoelectric prostheses are successfully controlled using muscle electrical activity, thereby restoring lost motor functions. The association between muscle activity and prosthesis functions provides an intuitive connection between the brain and the prosthesis; however, this connection is unidirectional. **A bilateral communication between the brain and the periphery is necessary for human movement learning and execution, but the somatosensory feedback from the prosthesis to the user is still missing**. Integrating an advanced distributed sensing (artificial skin) and stimulation system into a myoelectric prosthesis would allow closing the prosthesis control loop by providing sensory feedback to the user. A prosthetic system that not only responds to the control signals provided by the user, but also transmits back to the user the information about the current state of the prosthesis fosters the prosthesis embodiment and utility. It is an important step towards improving the quality of life of people with limb amputation and key point in research on active prosthetics.

II. Current study

In this study, we only use the *stimulation* interface. The system comprises a multichannel stimulator connected to a flexible electrode array to be placed on the forearm.

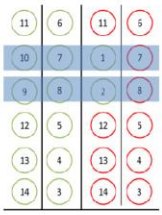

Electrotactile stimulation is conducted by delivering low-level electrical current pulses through the electrodes placed on the skin, to stimulate skin afferents and activate the tactile sense.

While testing the prosthetic system on amputees is the final goal, at present we study how this works on healthy and voluntary subjects.

Our present goals are:

1) Communicate the spatial location of a certain event by activating a single PAD (= Circle) in the stimulation array

Dip. Ingegneria Navale, Elettrica, Elettronica e delle Telecomunicazioni, Via Opera Pia 11A, 16145 Genova
Tel: 010.353.2775 ▪ maurizio.valle@unige.it

COSMIClab
Dipartimento di Ingegneria Navale, Elettrica, Elettronica e delle Telecomunicazioni
Università degli Studi di Genova

2) Communicate more information at the same time by simultaneously activating 2 PADS in the stimulation array

EXPERIMENT 1: It is made of four experimental sessions and lasts for about 1-1.5 hours.

SESSION 1 – 3: The participant will be asked to localize the electrostimulation, by indicating the pad number or its position (over a sketch of the 24-electrode array).

The experimenter will use either a single electrostimulation frequency or different combinations of electrostimulation frequencies will be assigned to the different columns in the array.

1) ***Single*** stimulation frequency all over the pads = 50HZ

2) ***Increasing*** stimulation frequencies 5Hz (column 1), 10Hz (column 2), 20Hz (column 3), 50Hz (column 4)

3) ***Interleaved*** stimulation frequencies 10Hz (column 1), 400Hz (column 2), 10Hz (column 3), 400Hz (column 4)

Step 1: PREPARATION

The subjects will seat comfortably on a chair in front of a table. The forearm of the dominant arm will be placed on the table surface, with the volar side oriented upwards. An electrode array will be positioned on the volar aspect of the subject forearm. The array will be placed at one third of the forearm length distal to the elbow. The electrode array will be then secured with medical tape to prevent movement and improve contact.

Step 2: STIMULATION INTENSITY DETERMINATION

Electrotactile STIMULATION INTENSITY will be determined for all employed stimulation pads (24), individually, at fixed frequencies (single 50 Hz frequency for all pads in session 1, increasing frequencies for increasing column number in session 2, interleaved frequencies for increasing column number in session 3). For each pad and at each frequency, the participant is asked to identify A LOW BUT CLEAR SENSATION. In order to determine this value, the current pulse amplitude, starting at zero, will be increased in steps of 0.1 mA until the subject will report to feel a LOW BUT CLEAR stimulation.

Step 3: LOCALIZATION TESTS

The participant will be asked to localize the electrostimulation, by indicating the pad number or its position (over a sketch of the 24-electrode array).

Dip. Ingegneria Navale, Elettrica, Elettronica e delle Telecomunicazioni, Via Opera Pia 11A, 16145 Genova
Tel: 010.353.2775 ▪ maurizio.valle@unige.it

COSMICLab
Dipartimento di Ingegneria Navale, Elettrica, Elettronica e delle Telecomunicazioni
Università degli Studi di Genova

SESSION 4: The flexible electrode array will be removed from the skin and **circles corresponding to the stimulation pads will be drawn over the real skin with a pen.**

Preventing the sight of the arm, the participant will be mechanically stimulated on a specific circle with a spherical soft indenter. **The participant will be asked to localize the mechanical stimulation over the real skin**, by indicating the circle number or its position over the drawn sketch of the array.

Dip. Ingegneria Navale, Elettrica, Elettronica e delle Telecomunicazioni, Via Opera Pia 11A, 16145 Genova
Tel: 010.353.2775 ▪ maurizio.valle@unige.it

COSMIClab
Dipartimento di Ingegneria Navale, Elettrica, Elettronica e delle Telecomunicazioni
Università degli Studi di Genova

ELIGIBILITY OF PARTICIPANTS

We will exclude from the following study subjects (i) in drug therapies, (ii) abusing of drugs or alcohol, or (iii) being involved in similar medical / clinical / scientific studies. In addition, patients with pacemakers or suffering from diabetes or epilepsy or being pregnant will be advised not to participate in this study.
Healthy and voluntary subjects who are allowed to participate in this study will be between the ages of 18 and 65.

RISKS

This study does not involve the use of food or drugs, nor does it generate any physical risk. To avoid fatigue and annoyance, the intensity of the electrostimulation will be decided by you, based on preliminary tests. Furthermore, you can interrupt the procedure at any time, in case of problems or worries of any kind.
There is no risk in electrostimulation generated by IntFES Ver 2 - MAXSENS, as long as the safety rules are followed. No side effects have ever been reported due to electrical stimulation, which is generally perceived as a slight pinch, judged as a rather pleasant sensation by the subjects.

BENEFITS

No particular clinical benefits are foreseen, as a result of the experimentation.

NO EXPENSES

Participation in the Study does not entail any additional expenses for you, which will be charged to COSMIClab.

PROBLEMS OR QUESTIONS

Whenever you have questions related to this study you can contact the COSMIClab Director, Prof. Maurizio Valle at the telephone number 010 353 2775 or at the email address maurizio.valle@unige.it

PRIVACY AND CONFIDENTIALITY

Any information, personal or sensitive data that concern you (name and surname, personal data or other sensitive data) and whose treatment is connected and indispensable to your participation in this Study, will be processed in ways that guarantee the absolute confidentiality and security of the same, in accordance with the rules for the protection of persons and other subjects regarding the processing of personal data (Legislative Decree 30/06/03, No. 196 and subsequent amendments and additions) and in compliance to the authorization of the Privacy Authority.

In particular, pursuant to and for the purposes of art. 13, paragraph 1, of Legislative Decree 196/03 we ask you to take into account the following explanation.

Dip. Ingegneria Navale, Elettrica, Elettronica e delle Telecomunicazioni, Via Opera Pia 11A, 16145 Genova
Tel: 010.353.2775 ▪ maurizio.valle@unige.it

COSMIClab
Dipartimento di Ingegneria Navale, Elettrica, Elettronica e delle Telecomunicazioni
Università degli Studi di Genova

The consent to the processing of your personal data is freely expressed and can be revoked at any time without causing any disadvantage or prejudice, unless the data, originally or as a result of a processing, no longer allow identifying you (anonymous data).

The consent to the processing of your personal data, although having an optional nature, is essential for the completion of this Study, as well as for the fulfillment of the related legal obligations.

In the absence of said consent, the Study cannot be carried out with your participation.

Your personal and sensitive data will be collected and processed by authorized investigators, for the exclusive purposes related to the completion of this Study and the verification of the progress of the same. Personal and sensitive data will not be made accessible and available to third parties, except for researchers belonging to the Department of Health Science and Technology - Center for Sensory-Motor Interaction - Integrative Neuroscience, Faculty of Medicine in Aalborg, Denmark, who will have direct access to your data in order to evaluate the correctness of the collected data and in such a way as to guarantee data confidentiality.

The eventual dissemination of data, also abroad, through scientific publications, presentations to the Regulatory Authorities, presentation in congresses, conferences and seminars, will take place exclusively following a statistical elaboration of the same and, therefore, in absolutely anonymous form.

The owner of the processing of personal data is COSMIClab - Dept. of Naval, Electrical, Electronic and Telecommunications Engineering - in person of the Principal Investigator Prof. Maurizio Valle. Responsible for the processing of personal data in the Department is the General Manager.

We also remind you that you can exercise at any time the rights referred to in art. 7 of Legislative Decree 196/03 below and request a complete list of people who processed your data, by writing to

Head of the Department Prof. Maurizio Valle C / O Department of Naval, Electrical, Electronic and Telecommunications Engineering - based in Genoa, Via Opera Pia 11A - 16128 (GE) or by writing to the e-mail address maurizio.valle@unige.it

Art. 7

(Right to access personal data and other rights)

1. The interested party has the right to obtain confirmation of the existence or not of personal data concerning him / her, even if not yet registered, and their communication in intelligible form.

2. The interested party has the right to obtain the indication:

a) of the origin of personal data;

b) of the purposes and methods of the processing;

c) of the logic applied in case of treatment carried out with the aid of electronic instruments;

d) of the identifying details of the holder, of the responsible and of the designated representative according to article 5, paragraph 2;

Dip. Ingegneria Navale, Elettrica, Elettronica e delle Telecomunicazioni, Via Opera Pia 11A, 16145 Genova
Tel: 010.353.2775 ▪ maurizio.valle@unige.it

COSMICLab
Dipartimento di Ingegneria Navale, Elettrica, Elettronica e delle Telecomunicazioni
Università degli Studi di Genova

e) of the subjects or categories of subjects to whom the personal data may be communicated or who may become aware of it as designated representative in the territory of the State, managers or agents.

3. The interested party has the right to obtain:

a) updates, rectification or integration of data;

b) the cancellation, transformation into anonymous form or blocking of data processed unlawfully, including data whose retention is unnecessary for the purposes for which the data were collected or subsequently processed;

c) the attestation that the operations referred to in letters a) and b) have been brought to the attention, also as regards their content, of those to whom the data have been communicated or disseminated, except in the case where this fulfillment is proven impossible or involves means manifestly disproportionate to the protected right.

4. The interested party has the right to object, in whole or in part:

a) on legitimate grounds, the processing of personal data concerning him / her, even though they are relevant to the purpose of the collection;

b) the processing of personal data concerning him for the purpose of sending advertising or direct sales material or for carrying out market research or commercial communication.

Finally, we remind you that by signing the Informed Consent form you are authorizing such access and the processing of information concerning you and that the Investigator Responsible of the Study may decide not to collect your data any more independently from your consent. You may, however, authorize the use and processing of collected personal data, in the event that you would withdraw before the conclusion of the study.

Dip. Ingegneria Navale, Elettrica, Elettronica e delle Telecomunicazioni, Via Opera Pia 11A, 16145 Genova
Tel: 010.353.2775 ▪ maurizio.valle@unige.it

COSMICLab
Dipartimento di Ingegneria Navale, Elettrica, Elettronica e delle Telecomunicazioni
Università degli Studi di Genova

INFORMED CONSENT MODULE and DATA PROCESSING CONSENT

Name*……Surname*……

Date of birth*……Gender … Mail address*……

I declare:

- to accept participating to the Study "Transmission of tactile information through electrostimulation";
- to have read and understood the information sheet version n. 2 of 01/12/2017 which was delivered to me, which confirms what was reported to me verbally;
- to have had the opportunity to ask clarifying questions and to have had satisfactory answers;
- that my consent is the expression of a free decision, not influenced by promises of economic or other benefits, or obligations towards the investigators;
- to be aware that participation in the study is voluntary and I am free to withdraw from the study at any time and without motivating my decision, having received the certainty that both the refusal to participate in the study and my eventual withdrawal will not involve any effect;

Therefore I freely agree to participate in the Study.

- In case of my withdrawal I agree to retain all the documentation relating to me collected up to that time.

Date Signature (participant)

…… ……

I also express my consent pursuant to the D.L. 196 of 30/06/2003 regarding the protection of personal data, so that the processing of my personal data is carried out for the specific purposes of the research within the limits and with the methods indicated in this document of information and consent.

I received a copy of the patient information and informed consent.

Date Signature (participant)

…… ……

Signature (experimenter)

……

Dip. Ingegneria Navale, Elettrica, Elettronica e delle Telecomunicazioni, Via Opera Pia 11A, 16145 Genova
Tel: 010.353.2775 ▪ maurizio.valle@unige.it

Appendix C - Curriculum Vitae

FARES **HODA**
PhD Student-Cosmic Lab-DITEN-University of Genoa-Italy
Via Opera Pia 11A, I 16145 ,Genova, Italy.
+39 388 724 6301
hoda.fares@edu.unige.it

Education

2016-until now: PhD Student, Cosmic Lab, Department of Electrical, Electronic and Telecommunications Engineering and Naval Architecture (DITEN) - University of Genoa-Italy. Thesis: Human-Machine Interface Based on tactile sensing for the Restoration of the Sense of Touch in Prosthetics.
2015-2016: Second Cycle in Biochemistry, Faculty of Science Section1 (FES1), Department of Biology, Lebanese University.
2011-2012: Master II Research (M2R) Degree in Renewable Energies, Ecole Supérieur d'Ingénieur de Beyrouth (ESIB), Université Saint-Joseph de Beyrouth (USJ) & Ecole Doctorale de Sciences et de Technologie (EDST) - Lebanese University. Master thesis: Comparative Study of Methods for calculating solar gains in Thermal modeling systems. Grade: Good.
2006-2011: Master I Degree in Electrical and Electronics Engineering, - Faculty of Engineering (ULFG3) – Department of Electronics and Telecommunications, Lebanese University. Section: Industrial Digital Control. Grade: Very Good
2005-2006: First Cycle in Biology, Lebanese University - Faculty of Science- Department of Biology, Section I .Grade: Very Good

Experience

2014-2016: Lecturer, IUL UNIVERSITY, FACULTY of Economics and business Administration, LEBANON.
2013-2014: Teaching Associate, Math Success Center (MSC), LEBANON.
2012-2013: Research Engineer, Ecole Doctorale de Sciences et de Technologie (EDST) - Lebanese University & Ecole Supérieur d'Ingénieur de Beyrouth (ESIB) - Saint-Joseph University.
Research Axis: Comparative study of methods for calculating solar gains in thermal modeling systems.
2011-2012: Research Engineer, YLE Testing and Automation solutions Company, LEBANON.
Research Axis: Non-contact Video –Extensometer for Stress and Strain Measurement.
2009-2010: Electronic Engineer, Electro Mechanical Enterprises (EME).
2008-2009: Electronic Engineer, Design Engineering Partners (DEP).

Publications and Presentations

2019-2020: IEEE International Conference on Electronics, Circuits and Systems, to be held in Genoa, Italy, 2019
Hoda Fares, Strahinja Dosen, Maurizio Valle, "Toward Enabling Tactile Sensation in Active Prostheses: Artificial Skin Patches for Hand Prostheses", 2019 IEEE International Conference on Electronics, Circuits and Systems, to be held in Genoa, Italy. (In press)
2019-2020: IEEE International Conference on Electronics, Circuits and Systems, to be held in Genoa, Italy, 2019
Hoda Fares, Strahinja Dosen, Maurizio Valle, "Integration of a Virtual Prostheses with a Multichannel Tactile Feedback Interface", 2019 IEEE International Conference on Electronics, Circuits and Systems, to be held in Genoa, Italy. (In press)
2019-2020: SSNR Summer school on Neurorehabilitation Symposium, Baiona, Spain, 2019
Hoda Fares, Jakob. L Dideriksen, Strahinja Dosen, Maurizio Valle, "Compensatory Tracking Delay Tractability in Closed-loop Dynamic Task-based on Visual and Electrotactile Feedback", 2019 Summer school on Neurorehabilitation Symposium, Baiona, Spain. (in press)
2019: Innovation in Rehabilitation Technologies Workshop (IRT workshop), Genoa, Italy, 2019
Lucia Seminara, Hoda Fares, Yahya Abbas, Moustafa Saleh, Mohamad Alameh, Flavio Ansovini, Maria Pacelli, Rita Paradiso, Martin Zirkl, Matija Strbac, Strahinja Dosen, Maurizio Valle, (University of Genoa, Italy; SMARTEX srl, Pisa; JOHANNEUM RESEARCH, Graz AT; Tecnalia Serbia, Belgrado RS; Aalborg University, Aalborg DK) "A new concept of haptic interface for the reconstruction of the sense of touch.",2019,IRT Workshop, Genoa, Italy.
2017-2018: IEEE Biomedical Circuits and Systems Conference (BIOCAS), Cleveland, Ohio, USA, 2018
Mohamad Alameh, Moustafa Saleh, Hoda Fares, Ali Ibrahim, Flavio Ansovini , Marta Franceschi, Lucia Seminara, Maurizio Valle, Strahinja Dosen, Dario Farina, "Live Demonstration: System Based on Electronic Skin and

Cutaneous Electrostimulation for Sensory Feedback in Prosthetics", 2018 IEEE Biomedical Circuits and Systems Conference (BIOCAS), Cleveland, Ohio, USA, 2018.

2017-2018: Conference on Ph.D. Research in Microelectronics and Electronics (PRIME), Prague, 2018

H. Fares, L. Seminara, H. Chible, S. Dosen and M. Valle, "Multi-Channel Electrotactile Stimulation System for Touch Substitution: A Case Study," 2018 14th Conference on Ph.D. Research in Microelectronics and Electronics (PRIME), Prague, 2018, pp. 213-216. doi: 10.1109/PRIME.2018.8430345.

2017-2018: IEEE International Symposium on Circuits and Systems (ISCAS), Florence, Italy, 2018

H. Fares et al., "Screen Printed Tactile Sensing Arrays for Prosthetic Applications," 2018 IEEE International Symposium on Circuits and Systems (ISCAS), Florence, Italy, 2018, pp. 1-4. doi: 10.1109/ISCAS.2018.8351892

2017-2018: IEEE International Symposium on Circuits and Systems (ISCAS), Florence, Italy, 2018.

M. Franceschi et al., "Live Demonstration: Electrotactile feedback from an electronic skin through flexible electrode matrix," 2018 IEEE International Symposium on Circuits and Systems (ISCAS), Florence, Italy, 2018, pp. 1-1. doi: 10.1109/ISCAS.2018.8351822.

2016-2017: New Generation of Circuits and Systems Conference, NGCAS 2017-Genoa-Italy

H. Fares et al., "Distributed Sensing and Stimulation Systems for Sense of Touch Restoration in Prosthetics," 2017 New Generation of CAS (NGCAS), Genova, 2017, pp. 177-180. doi: 10.1109/NGCAS.2017.5.

Journals

2019-2020: IEEE Transaction on Haptics

Lucia Seminara, Hoda Fares, Marta Franceschi, Maurizio Valle, Matija Štrbac, Strahinja Dosen, Dario Farina," Dual-parameter modulation improves localization in multichannel electrotactile stimulation," 2019 IEEE Transaction on Haptic, doi: 10.1109/TOH.2019.2950625

Activities

2019: Special Session at 26th IEEE International Conference on Electronics, Circuits and Systems, ICECS2019 Genoa, Italy.

-Organizing and chairing the Special Session entitled "Session entitled ""Advanced Circuits and Systems for enabling Closed- Control in Prosthetic Limbs""" in the 26th IEEE International Conference on Electronics, Circuits and Systems, to be held in Genoa, Italy

2019: Summer school on Neurorehabilitation Symposium "SSNR2019", Baiona, Spain.

- Participating and presenting the contribution entitled "Compensatory Tracking Delay Tractability in Closed-loop Dynamic Task based on Visual and Electrotactile Feedback"

2018, 2019: Research fellowship at the Center for Sensory-Motor Interaction, Department of Health Science and Technology, The Faculty of Medical Science, Aalborg University, Aalborg, Denmark

- Working on the design and testing of different stimulation paradigms for transmitting tactile information from an artificial skin to the human subject.

2019: Workshop in Innovation in Rehabilitation Technologies Workshop (IRT workshop), Genoa, Italy

- Participating and presenting the contribution entitled:"A new concept of haptic interface for the reconstruction of the sense of touch".

2018:International Summer School of Neuroengineering "Massimo Grattarola" ,Department of Informatics, Bioengineering, Robotics, and Systems Engineering (DiBRiS), University of Genoa-Italy.

- Study the Neurotechnologies and computational methods to interact with the brain.

2017: Special Session at New Generation of Circuits and Systems Conference, NGCAS 2017-Genoa-Italy

- Organizing and chairing the Special Session entitled "Sensors and Systems for the Restoration of the Sense of Touch in Prosthetics" in the First New Generation of Circuits and Systems Conference NGCAS 2017, Genoa, Italy.

Awards

- Bronze Leaf Award from the 14th Conference on Ph.D. Research in Microelectronics and Electronics (PRIME), Prague, 2018 for the paper entitled "Multi-Channel Electrotactile Stimulation System for Touch Substitution: A Case Study".
- Bronze Leaf Award from the New Generation of Circuits and Systems Conference, NGCAS 2017-Genoa-Italy for the paper entitled "Distributed Sensing and Stimulation Systems for Sense of Touch Restoration in Prosthetics".

Research Interests

- Closed loop rehabilitation and assistive wearable/wireless systems including myoelectric prosthesis
- Coding and processing restoration of artificial tactile information
- Human-machine interface
- Functional electrical stimulation
- Distributed sensing systems
- Sensory feedback

Linguistic English, French, Italian, Arabic

References

- Maurizio Valle, IEEE Senior Member, Associate professor in Electronics –DITEN-University of Genoa-Italy maurizio.valle@unige.it
- Strahinja Dosen, Associate professor in the Department of Health science and technology, Faculty of Medicine, Integrative Neuroscience, University of Aalborg, Denmark. sdosen@hst.aau.dk